Module identification in dynamic networks: parametric and empirical Bayes methods

NIKLAS EVERITT

Doctoral Thesis
Stockholm, Sweden 2017

KTH Royal Institute of Technology
School of Electrical Engineering
Department of Automatic Control
SE-100 44 Stockholm
Sweden

TRITA-EE 2017:064
ISSN 1653-5146
ISBN 978-91-7729-467-2

Akademisk avhandling som med tillstånd av Kungliga Tekniska högskolan framlägges till offentlig granskning för avläggande av teknologie doktorsexamen i elektro- och systemteknik fredagen den 1 september 2017 klockan 10.00 i F3, Kungliga Tekniska högskolan, Lindstedtsvägen 26, Stockholm .

© Niklas Everitt, september 2017

Tryck: Universitetsservice US AB

Abstract

The purpose of system identification is to construct mathematical models of dynamical system from experimental data. With the current trend of dynamical systems encountered in engineering growing ever more complex, an important task is to efficiently build models of these systems. Modelling the complete dynamics of these systems is in general not possible or even desired. However, often, these systems can be modelled as simpler linear systems interconnected in a dynamic network. Then, the task of estimating the whole network or a subset of the network can be broken down into subproblems of estimating one simple system, called module, embedded within the dynamic network. The prediction error method (PEM) is a benchmark in parametric system identification. The main advantage with PEM is that for Gaussian noise, it corresponds to the so called maximum likelihood (ML) estimator and is asymptotically efficient. One drawback is that the cost function is in general nonconvex and a gradient based search over the parameters has to be carried out, rendering a good starting point crucial. Therefore, other methods such as subspace or instrumental variable methods are required to initialize the search. In this thesis, an alternative method, called model order reduction Steiglitz-McBride (MORSM) is proposed. As MORSM is also motivated by ML arguments, it may also be used on its own and will in some cases provide asymptotically efficient estimates. The method is computationally attractive since it is composed of a sequence of least squares steps. It also treats the part of the network of no direct interest nonparametrically, simplifying model order selection for the user. A different approach is taken in the second proposed method to identify a module embedded in a dynamic network. Here, the impulse response of the part of the network of no direct interest is modelled as a realization of a Gaussian process. The mean and covariance of the Gaussian process is parameterized by a set of parameters called hyperparameters that needs to be estimated together with the parameters of the module of interest. Using an empirical Bayes approach, all parameters are estimated by maximizing the marginal likelihood of the data. The maximization is carried out by using an iterative expectation/conditional-maximization scheme, which alternates so called expectation steps with a series of conditional-maximization steps. When only the module input and output sensors are used, the expectation step admits an analytical expression. The conditional-maximization steps reduces to solving smaller optimization problems, which either admit a closed form solution, or can be efficiently solved by using gradient descent strategies. Therefore, the overall optimization turns out computationally efficient. Using markov chain monte carlo techniques, the method is extended to incorporate additional sensors. Apart from the choice of identification method, the set of chosen signals to use in the identification will determine the covariance of the estimated modules. To chose these signals, well known expressions for the covariance matrix could, together with signal constraints, be formulated as an optimization problem and solved. However, this approach does neither tell us why a certain choice of signals is optimal nor what will happen if some properties change. The expressions developed in this part of the thesis have a different flavor in that they aim to reformulate the covariance expressions into a form amenable for interpretation. These expressions illustrate how different properties of the identification problem affects the achievable accuracy. In particular, how the power of the input and noise signals, as well as model structure, affect the covariance.

Sammanfattning

Systemidentifiering används för att skatta en modell av ett dynamiskt system genom att anpassa modellens parametrar utifrån experimentell mätdata inhämtad från systemet som ska modelleras. Systemen som modelleras tenderar att växa sig så omfattande i skala och så komplexa att direkt modellering varken är genomförbar eller önskad. I många fall går det komplexa systemet att beskriva som en komposition av enklare linära system (moduler) sammakopplade i något vi kallar dynamiska nätverk. Uppgiften att modellera hela eller delar av nätverket kan därmed brytas ner till deluppgiften att modellera en modul i det dynamiska nätverket. Det vanligaste sättet att skatta parametrarna hos en model är genom att minimera det så kallade prediktionsfelet. Den här typen av metod har nyligen anpassats för att identifiera moduler i dynamiska nätverk. Metoden åtnjuter goda egenskaper vad det gäller det modelfel som härrör från stokastisk störningar under experimentet och i de fall där störningarna är normalfördelade sammanfaller metoden med maximum likelihood-metoden. En nackdel med metoden är att functionen som minimeras vanligen är inte är konvex och därmed riskerar metoden att fastna i ett lokalt minimum. Det är därför essentiellt med en bra startpunkt. Andra metoder krävs därmed för att hitta en startpunkt, till exempel kan instrumentvariabelmetoder användas. I den här avhandlingen föreslås en alternativ metod kallad MORSM. MORSM är motiverad med argument hämtade från maximum likelihood och är också asymptotiskt effektiv i vissa fall. MORSM består av steg som kan lösas med minstakvadratmetoden och är därmed beräkningsmässigt attraktiv. Den del av nätverket som är utan intresse skattas enbart ickeparametriskt vilket underlättar valet av modellordning för användaren. En annan utgångspunkt tas i den andra metoden som föreslås för att skatta en modul inbäddad i ett dynamiskt nätverk. Impulssvaret från den del av nätverket som är utan intresse modelleras som realisation av en Gaussisk process. Medelvärdet och kovariansen hos den Gaussiska processen parametriseras av en mängd parametrar kallade hyperparametrar vilka skattas tillsammans med parametrarna för modulen. Parametrarna skattas genom att maximera den marginella likelihood funktionen. Optimeringen utförs iterativt med ECM, en variant av förväntan och maximering algoritmen (EM). Algoritmen har två steg. E-steget har en analytisk lösning medan CM-steget reduceras till delproblem som antingen har analytisk lösning eller har låg dimensionalitet och därmed kan lösas med gradientbaserade metoder. Den övergripande optimeringen är därmed beräkningsmässigt attraktiv. Med hjälp av MCMC tekniker generaliseras metoden till att inkludera ytterligare sensorer vars impulssvar också modelleras som Gaussiska processer. Förutom valet av metod så påverkar valet av signaler vilken nogrannhet eller kovarians den skattade modulen har. Klassiska uttryck för kovariansmatrisen kan användas för att optimera valet av signaler. Dock så ger dessa uttryck ingen insikt i varför valet av vissa signaler är optimalt eller vad som skulle hända om förutsättningarna vore annorlunda. Uttrycken som framställs i den här delen av avhandlingen har ett annat syfte. De försöker i stället uttrycka kovariansen i termer som kan ge insikt i vad som påverkar den nogrannhet som kan uppnås. Mer specifikt uttrycks kovariansen med bland annat avseende på insignalernas spektra, brussignalernas spektra samt modellstruktur.

ACKNOWLEDGEMENTS

First and foremost, I express my sincere gratitude to my supervisor Håkan Hjalmarsson for taking me on as a PhD student, providing me guidance and support. Thanks to you, I have learned a lot about every aspect of research. It has been a great experience. To my co-supervisor Cristian Rojas, thank you for your continuous support, knowledge and advice along the way. Many thanks go to Giulio Bottegal for our succesful collaborations, all the things you have taught me, as well as proofreading parts of this thesis. I also wish to thank my collaborators and co-authors, whom I had the pleasure to meet and collaborate with; Giulio Bottegal, Afrooz Ebadat, Miguel Galrinho, Jonas Mårtensson and Patricio Valenzuela, I have enjoyed our discussions immensely.

Many thanks to former and present colleagues at the departement of Automatic control at KTH for providing a friendly and collaborative environment. I would like to thank the administrators Silvia Cárdenas Svensson, Gerd Franzon, Kristina Gustafsson, Hanna Holmqvist, Karin Karlsson, and Anneli Ström for taking care of all things that make the department run smoothly. I would like to give special thanks to the Julia group, Mikael Johansson, Cristian Rojas and Arda Aytekin. It has been a pleasure developing software tools with you. Martin Andreasson, thank you for all the great times in and out of the office. Arda Aytekin, thanks for being a great friend, besides teaching me about all amazing software tools.

I thank all my friends for providing me with meaning to life outside work and all my dancing friends who gave me the energy to complete this thesis. Finally, I would like to thank my parents, my brother and Elin for your love, encouragement and support over the years.

Niklas Everitt
Stockholm, June 2017

CONTENTS

NOTATION

$\delta(\cdot)$	Dirac delta
$(\cdot)^*$	conjugate transpose
$\overline{(\cdot)}$	conjugation operator
$:=$	definition
$\det\{\cdot\}$	determinant operator
$\mathrm{diag}\{v\}$	matrix with the entries of the vector v in the main diagonal
$\mathbf{E}\{\cdot\}$	expectation
$\nabla f\left(x_0\right)$	gradient of f with respect to its argument evaluated at x_0
$\langle f, g\rangle$	inner product between f and g: $\langle f, g\rangle := \frac{1}{2\pi}\int_{-\pi}^{\pi} f\left(\mathrm{e}^{\mathrm{j}\omega}\right) g^*\left(\mathrm{e}^{\mathrm{j}\omega}\right) d\omega$
$\otimes$	Kronecker product
$\|f\|$	$\mathcal{L}_2$-norm of f: $\|f\| := \sqrt{\mathrm{Tr}\{\langle f, f\rangle\}}$
$\mathcal{L}_2$	vector space of all functions with finite $\mathcal{L}_2$-norm
$\mathcal{H}_2$	vector space of all functions with finite $\mathcal{L}_2$-norm analytic on the unit disc
$\mathcal{N}(x, X)$	normal distribution with mean x and covariance matrix X
$\mathbf{Proj}_{\mathcal{S}_\mathcal{X}}\{Y\}$	projection of Y onto the subspace $\mathcal{S}_\mathcal{X}$
$X^\dagger$	Moore-Penrose pseudoinvers
q	time shift operator, $qu(t) = u(t+1)$
$\mathbb{C}$	set of complex numbers
$\mathbb{C}^{n\times q}$	set of $n \times q$ dimensional matrices with complex entries
$\mathbb{C}^n$	set of n-dimensional column vectors with complex entries
$\mathbb{Z}$	set of integers
$\mathbb{R}$	set of real numbers
$\mathbb{R}^{n\times q}$	set of $n \times q$ dimensional matrices with real entries

$\mathbb{R}_{\geq 0}$	set of non-negative real numbers, $\{x \in \mathbb{R} : x \geq 0\}$
$\mathbb{R}^n$	set of n-dimensional column vectors with real entries
$\mathbf{Span}\{\cdot\}$	subspace spanned by the rows of a vector or matrix
$\mathcal{S}_{\mathcal{X}}$	subspace spanned by the rows of $\mathcal{X}$, *i.e.* $\mathcal{S}_{\mathcal{X}} = \mathbf{Span}\{\mathcal{X}\}$
θ	model parameter vector
$\hat{\theta}$	estimated parameter vector
θ^o	true parameter vector
$\mathcal{T}_n\{v\}$	for $v \in \mathbb{R}^m$, $m \times n$ lower triangular Toeplitz matrix of the elements of v
$\mathrm{Tr}\{\cdot\}$	trace operator
$(\cdot)^\top$	transpose operator
$\mathrm{vec}\{\cdot\}$	vectorization operator
$\hat{y}(t\|t-1,\theta)$	mean square optimal one-step ahead predictor
$\mathbb{Z}_{\geq 0}$	set of non-negative integers

ABBREVIATIONS

AR	autoregressive
ARMA	autoregressive moving average
ARMAX	autoregressive moving average with exogenous input
ARX	autoregressive with exogenous input
BCLIV	basic closed-loop instrumental variable
BJ	Box-Jenkins
BJSM	Box-Jenkins Steiglitz-McBride
BL	band limited
DSF	dynamical structure function
EB	empirical Bayes
ECM	Expectation/Conditional Maximization
EIV	errors-in-variables
EM	Expectation Maximization
FIR	finite impulse response
IQML	iterative quadratic maximum likelihood
IV	instrumental variable
LDG	linear dynamical graph

LTI	linear time invariant
MCMC	Markov chain Monte Carlo
MIMO	multiple input multiple output
MISO	multiple input single output
ML	maximum likelihood
MMSE	minimum mean squared error
MORSM	model order reduction Steiglitz-McBride
NEB	network empirical Bayes
OE	output error
PEM	prediction error method
RIV	refined instrumental variable method
SIMO	single input multiple output
SISO	single input single output
SML	sample maximum likelihood method
WNSF	weighted null-space fitting
WTLS	weighted total least squares
ZOH	zero order hold

CHAPTER 1

INTRODUCTION

Many complex systems can at some level be analyzed or described by interconnections of simpler systems. Examples can be found in diverse disciplines, such as Biology (del Vecchio et al., 2008), Cognitive Sciences (Quinn et al., 2010), Economics (Materassi and Innocenti, 2009). Many complex systems that can be described as an interconnection of dynamical systems are systems which are spatially distributed, as is the case in for instance power systems (Chow and Kokotovic, 1985), autonomous vehicles (Ren and Beard, 2008) or Geology (Bailly et al., 2006). Models of these complex systems are vital in order to understand, analyze and control these systems.

1.0.1 Purpose of modelling

A model is an abstraction of the real world that tries to capture the behaviour of a system in some sense. As an abstraction, its aim is to accurately describe relevant behaviour and obscure uneccesary complexity. What is relevant and what is irrelevant is determined by the purpose of the model and the modelling effort should reflect the intended use of the model (Ljung, 1999). There are many differerent purposes for models and we will list a few here, and later, come back the purpose of also modelling the structure of a system.

Prediction: A model can be used to predict the future behaviour of a system, *e.g.*, a model can be used to predict the price of a stock or predict the weather in the (near) future.

Simulation: A model can be used to simulate the behaviour of a system under different conditions allowing experiments, which may be costly, to be performed on the model instead of the actual system. We may also train system operators on a model before handling the real system, for instance letting pilots land their aircrafts in simulation before attempting it in harsh weather.

System design: A model can be used for analyzis and design. From a model of a system, we can extract important features such as pole locations or nonminimum phase zeros and design controllers to effectively control the system behaviour. We could also

realize that controlling the system in its current form is hard and that it should be redesigned instead.

Measurement: A model can be used to estimate unmeasured variables of a system. For instance, in navigation, dead reckoning calculates ones current position from a previous position and velocity information. The same principle is applied when driving into a tunnel and the GPS signal is lost.

Diagnosis: A model can be used to track the behaviour of a system. By comparing the observed behaviour with what the model predicts, unexpected behaviour, *e.g.*, due to equipment malfunctioning, can be detected.

1.0.2 Motivating examples

As there are many purposes of models, there are also many types of models. We are concerned with a special type of model, one in which dynamical systems are interconnected in a structure. Many systems are naturally modelled as simpler systems interconnected in a structure. For example, neurons are the basic building block of the nervous system, each neuron is interconnected with other neurons and structured models are used to describe the causal relationship when neurons transmit (Quinn et al., 2010). Other eamples of systems that naturally can be modelled as networks include drainage networks (Bailly et al., 2006), power systems (Chow and Kokotovic, 1985), distributed control of multiagent systems (Dimarogonas et al., 2012; Olfati-Saber et al., 2007). We will look at a few examples in greater detail to exemplify how they can be modelled as networks of dynamical systems.

1.0.3 Water supply system

The water supply systems is an engineering system that nicely fits the description of systems interconnected in a structure. The water supply system is a network of components that together provide water to consumers (which may be residential, industrial, commercial or governmental institutions). We consider pressure control of the pipe network, which transfers water to the consumers from the set of supply nodes, which could be for example water purification facilities or water storage facilities. The goal of the pressure controller is to have enough pressure in each node of the network to supply sufficient amount of water to consumers in the network. At the same time, water is a scarce resource in many parts of the world, and high pressure increases the risk of pipes breaking and increases the amount of leaking water. Furthermore, considerable amount of energy can be saved with efficient pressure control. Thus, proper management of the pressure in the network is needed for safe and effective operation of the network. The system can be modeled as a set of pipes, storage tanks, consumer nodes and supply nodes. The pipes transport the water between different

nodes in the network. We can describe the dynamics of a tank in the network as

$$\dot{V}_i = \sum_{j \in \mathcal{N}_i} q_{ij}$$
$$q_{ij} = \left(\frac{p_i - p_j}{R_{ij}} \right)^{1/a},$$

where V_i is the volume in the tank located in node i, q_{ij} is the flow of water in the pipe between nodes i and j, p_i is the pressure at node i, $\mathcal{N}_i$ is the set of neighbors of node i, a is the flow exponent and R_{ij} is the resistance coefficient. If the pressure can be controlled in a node i, we consider the pressure p_i a control input, otherwise it is modeled as determined by the pressure at neighboring nodes.

1.0.4 Flotation plant

The second example of a dynamic network is concentration of ore, using froth flotation. Froth flotation is a process that is used to separate hydrophobic from hydrophilic materials and is common in processing industries. In the flotation plant, the objective is to separate the valuable mineral from ore, while minimizing the amount of undesired minerals in the extracted concentrate. At the same time, as much of the mineral as possible should be harvested. Thus, the residual tailings should mainly be composed of finely ground waste rock. In a flotation cell, froth flotation is done by adding certain chemical reagents to render the desired mineral hydrophobic, so that air bubbles lift the mineral. The resulting froth layer is then skimmed to produce the concentrate. Normally a flotation process consists of several flotation cells connected in cascade together with cyclones, mills, and mixing tanks as seen in the schematics of a typical plant in Figure 1.1. The plant can be described as a network composed of interconnected systems with simple dynamics.

Steam pressure control

Industrial power plants are often equipped with several parallel boilers with controlled and close to constant loads. Together they produce steam at high pressure that will be used in the plant. However, steam is consumed at intermediate and low pressure in one intermediate pressure (IP) header and one low pressure (LP) header respectively, with rapid and large variations in consumption (Majanne, 2005). In the middle a set of back pressure turbines feed the IP header and LP header appropriate amounts of steam respectively. In order to control the pressure in the IP header and LP header, it is necessary to accurately control the pressure in the high pressure (HP) header as well. The boilers should, for energy effectiveness, operate at close to constant loads. Therefore, an accumulator tank is used to handle the rapid fluctuations in load. When the demand for steam is low, the accumulator tank may store steam, as long as its internal pressure is less than the pressure in the IP header. When demand is high, the steam tank may discharge steam into the LP header as long as the

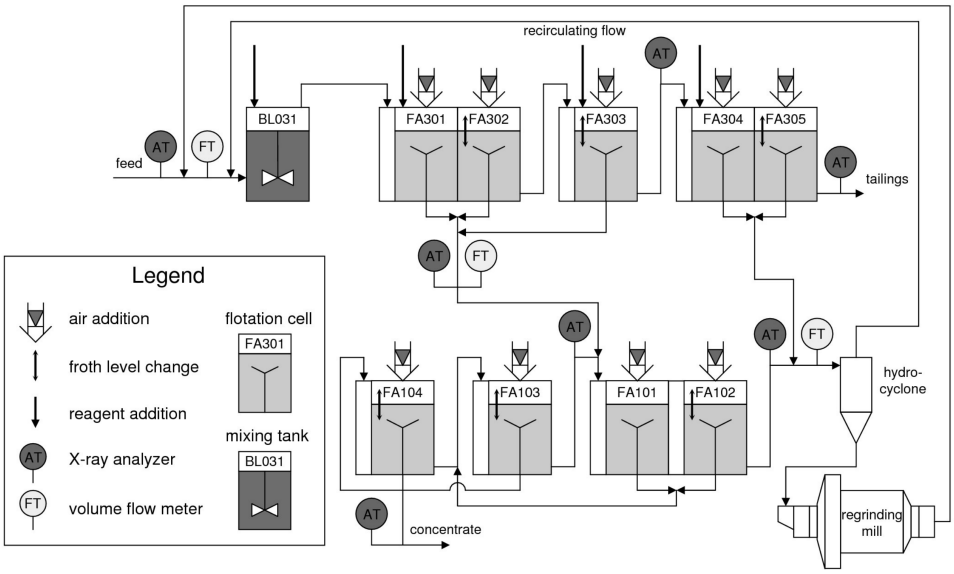

Figure 1.1: Schematic of a floatation plant with several cascades of flotation cells. (Image courtesy of ABB).

steam tanks internal pressure is higher than the pressure in the LP header. The plant can be modeled as in Figure 1.2, where neither the demand nor the feedback structure of the control system has been modeled.

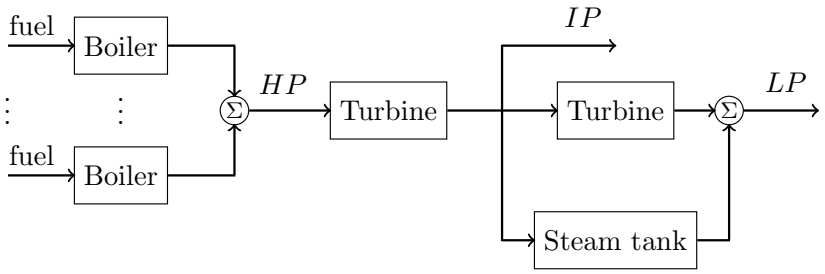

Figure 1.2: Steam pressure control model.

1.1 Motivation of structured models

The main point of this chapter is to motivate why we should care about representing the structure as well as the dynamics. What is it that makes it worthwile to take the structure into account? However, framing the question this way is socially biased. In systems theory we are used to abstract away the physical detail of the system under investigation and represent it in the most convenient representation, be it the impulse response, transfer function or states space representation. Each representation preserves the input to output relation and a rich theory and powerful toolset enables us to predict, analyze and design systems (see *e.g.* Kailath, 1979; Åström and Murray, 2008). An integral part of this theory is the ability to interconnection subsystems in intricate structures, and analyze the composition. Moreover, this toolset also includes tools that allow us to design feedback controllers of uncertain systems. Thus, from an estimated model of the system dynamics we can use the model for a wide range of purposes. From a system identification perspective, this means that, for many purposes, characterising the input output relationship is the end goal. Therefore, we will spend some time on the purpose of modelling and its relation to structure, different types of structure and what additional benefit we can achieve by taking structure into account. We start by mentioning a list of a few reasons of keeping the structure in mind.

Understandability: A network of simple systems can make for a truly complex system. Deconstructing the complex system as composed of interconnected simpler system can make the system easier to understand. Each of the individual simple systems can be understood, analyzed and verified. It is also possible to zoom out by bundling groups of highly connected systems together and thus focus on a higher level in a hierarchy of possible levels of detail. This enables vizualization of different aspects of the complex system.

Curse of dimensionality: When the size of the network increases, several types of constraints may render it unpractical or even infeasible to handle all the measurement data from the system all at once at one location. First of all, for many problems with large dimensions, usually referred to as *Big Data*, the amount of data may not easily fit on one computer. Secondly, if the system is distributed in space, *e.g.*, the power system, sending the data over long distances might be associated with a cost, introducing delay and vulnerabilities to the system. If we respect the structure of the system, we can use local models that only require part of the data and solve problems in a distributed and parallel manner.

Controller design: In control design, delays can often be of higher priority than model errors, since feedback can compensate for model errors, in many cases (Bakule, 2008). From the discussion on the curse of dimensionality, a decentralized controller which relies on local computations and local data will, in general, have less delays. How to design decentralized control laws has a rich theory (Siljak, 2011). Also approaches which design decentralized controllers based on the signal structure of a system has been proposed (Rai and Warnick, 2013).

Attack modelling: If an adversary would like to disrupte a system, he would naturally prefer to remain undetected. Any attacker, if he would like to remain undetected, need to respect the structure of the model of the system, *i.e.*, the attacker need to disrupt the normal operation of the system and at the same his attack should not conflict with what the model predicts of the system, because then the attack will be detected. Structural information in the model is providing constraints on how an attacker can affect the system without being detected. The assumption is that a coordinated attack involving several parts of the network is harder and more involved.

Vulnerability analysis: Engineered systems such as the power grid, communication systems and water transportation network provide essential service for our society and disturbances in these networks can have severe consequences. Ideally, a system should continue to operate close to normal operation in case some part of the network fails. The structural information of a system can be used to analyze how vulnerable the system is to individual failures. For example, how resilient is the power transmission system to power line failures (Holmgren, 2006).

Adaptability: The larger a system gets, the more likely it is that some part of it will change. Some equipment dynamics may change due to age, wear and tear, or due to being updated. In multi agent systems, agents may join and disconnect from the network at any time. Then, there is an advantage if minor local changes in the system can be captured by local updates of the model. Especially, if (re)-identification of the complete system is expensive.

1.1.1 Obeying the physics

From a physical modelling perspective, there is an argument to model interconnection of subsystem as variable sharing (Willems, 2007). For example, an elementary circuit of passive components can naturally be thought of as a network. We might remember Kirchoff's current law which states that the sum of the currents going into a node should be zero. There is a symmetry to this law; every current is treated equally. The law simply states that the variables (currents) related to the interconnected passive components are set equal. It is not apriori apropriate to say that any one of the currents is the cause of the others.

The argument made in Dankers (2014), is that, once a voltage source is connected to the circuit, the voltage source drives the currents of the circuit to be nonzero, then it is natural to think of the voltage of the voltage source as the input driving the currents which we choose to model as outputs. In essence it makes sense of thinking of the system as a transfer function mapping the input signal (voltage) to output signals (currents). Identifying the transfer function or any other representation of the relationship between input and output is the traditional focus of system identification and a rich litterature exist on different methods, how to design inputs as well as a theory on how accurate we can expect the models to be. While models relating the causal dependence between signals through transfer function are useful, care should be taken when making claims about the underlying physical system.

1.1.2 Subsystem structure representation

The closed loop transfer function is a compact and unique representation of the input output map and can serve many purposes. However, many different connections of subsystems may generate the same transfer function. In fact, there is no structural information of how subsystems are interconnected in the closed loop transfer function. The actual connection of subsystem that correctly models the mechanism which the system acheives its behaviour, denoted as the complete computational structure (Yeung et al., 2010), cannot be inferred from partial measurement of the states of the system. The naive solution would be to probe every state of the system, *i.e.*, measure everything and everywhere, to obtain the complete computational structure. This solution is certainly not practical, and in most cases not feasible.

1.1.3 Signal structure representation

The signal structure models the causal dependence between the measured signals available as a graph where each edge models the causal dependence between two signals and the signals are the nodes of the graph. One should not interpret the signal structure as the interconnection of subsystems. However it reveals the open loop casual depence among the measured variables. Identifying this structure is a lot easier than the correct subsystem structure. There are two main bodies of literature that study the causal dependence of signals, Granger causality and the Causal inference.

Granger causality informally says that X is causing Y if we are better able to predict the future of Y using all available information, than if we would not include the information in X (Granger, 1963). Causality is thus defined in terms of predictability; which naturally is not an acceptable definition of causation in most scientific fields. This conflict is also visible in the example in Section 1.1.1 and in the litteratur on Causal influnce (Pearl, 2000).

Models employed in Causal inference are based on Bayesian Networks (Pearl, 1988). One limitation in this framework is that there is no notion of time. Another limitation with Causal inference is that it only contains a comprehensive theory for acyclic models, *i.e.*, models without feedback loops (see *e.g.*, Pearl (2000)). However, there are recent efforts to extend the framework to the cyclic case (see *e.g.*, Mooij et al., 2011; Hyttinen et al., 2012; M. Schmidt and Murphy, 2009). While models based on causal inference currently lack a developed treatment of feedback loops and notion of time, the underlying Bayesian framework has been used in connection to modelling based on Granger causality (Chiuso and Pillonetto, 2010; Aravkin et al., 2011; Chiuso and Pillonetto, 2012). This thesis will work with Granger causality, and sometimes use the Bayesian framework.

Within the literature based on Granger causality there are many proposed model structures due to different assumptions on how the signals are generated, what signals are available and the presence of noise. We will try to give an overview of a few types of models, by no

means comprehensive, to try to give a flavor of the different formulations and try to connect them.

A Directed information graph is a graph relating signals through the concept of direct information (Marko, 1973; Massey, 1990), which is an information theoretic version of Granger causality. In a Directed information graph, nodes represent the signals as random processes and directed edges denotes wheter there is direct information from one process to another. Another related concept is that of Minimal generative model graphs, which are graphs of factorizations of the joint probability density of the signals of minimal degree. The Minimal generative model graph may be nonunique or not even exist. However, under some minor conditions on the joint distribution, the Minimal generative model graph is equivalent to the Directed information graph (Amblard and Michel, 2010; Quinn et al., 2011). The Directed information graph, on the other hand, always exists and is unique. When estimating the Directed information graph, the main challenges is the practical difficulty of estimating direct information and devising statistical tests for determining when there is direct information between two signals (Amblard and Michel, 2010).

There are also significant contributions that take a system theoretic framework. In this setting there are three different classes of models that differ mainly in the assumptions on the available signals, *i.e.*, the availability of known signals and assumptions on the noise affecting measured signals. Slight variations of these models appear in the literature. However, we will briefly relate these three models to each other. We have changed the notation compared to how they are presented in the literature to show their similarities. Hopefully, this will aid in putting the contributions made in the literature in context.

The first type of model, the linear dynamical graph (LDG) considers models without known reference signals, the model is thus completely driven by noise:

$$w(t) = \begin{bmatrix} 0 & G_{12}(q) & \dots & G_{1m}(q) \\ G_{21}(q) & 0 & \dots & G_{2m}(q) \\ \vdots & & \ddots & \vdots \\ G_{m1}(q) & G_{m2}(q) & \dots & G_{mm}(q) \end{bmatrix} w(t) + v(t).$$

The internal variables $w(t)$ are driven by the unknown noise process $v(t)$. The internal variables $w(t)$ are considered the nodes in the graph and nonzero modules $G_{ij}(q)$ represents edges. When all modules are causal (strictly proper) transfer functions, the LDG and the directed information graph are the same, *i.e.*, they share the same set of vertices (Etesami and Kiyavash, 2014). A module $G_{ij}(q)$ is identically zero if and only if there is no directed information, in other words, $G_{ij}(q) = 0$ if w_i is causally independent of w_j given the other internal variables.

The dynamical structure function (DSF), on the other hand, is developed in a nonstochastic setting (Goncalves et al., 2007; Yeung et al., 2010; Yeung et al., 2011). The DSF can be

described by the following set of equations,

$$w(t) = \begin{bmatrix} 0 & G_{12}(q) & \dots & G_{1m}(q) \\ G_{21}(q) & 0 & \dots & G_{2m}(q) \\ \vdots & & \ddots & \vdots \\ G_{m1}(q) & G_{m2}(q) & \dots & G_{mm}(q) \end{bmatrix} w(t) + R(q)r(t),$$

where $r(t)$ is a known reference signal. The DSF is defined as the set $(G(q), R(q))$, where $G(q)$ captures the causal dependencies between the internal variables $w(t)$. The closed loop transfer function from r to w is given by $(I - G(q))^{-1} R(q)$. In Goncalves and Warnick (2008) conditions were derived when it is possible to reconstruct $R(q)$ and $G(q)$ from knowledge of the closed loop transfer function, *e.g.*, when $R(q)$ is diagonal it is possible to reconstruct $(G(q), R(q))$ from $(I - G(q))^{-1} R(q)$. In Y. Yuan et al. (2015), a technique for retrieving a minimal state-space representation from a DSF were presented.

Lastly, the model structure that we will consider in this thesis is dynamic networks (Van den Hof et al., 2013; Dankers et al., 2016; Weerts et al., 2015). The dynamics for the internal variables $w(t)$ is the same as for the DSF with $R(q)$ often taken as the identity matrix. Similar to LDG, there is also a noise source $v(t)$ that excites the system. Measurements are collected as $\tilde{w}(t)$ with additive noise $e(t)$. The dynamics and measurements are thus described by

$$\begin{aligned} w(t) &= \begin{bmatrix} 0 & G_{12}(q) & \dots & G_{1m}(q) \\ G_{21}(q) & 0 & \dots & G_{2m}(q) \\ \vdots & & \ddots & \vdots \\ G_{m1}(q) & G_{m2}(q) & \dots & G_{mm}(q) \end{bmatrix} w(t) + R(q)r(t) + v(t), \\ \tilde{w}(t) &= w(t) + e(t) \end{aligned}$$

1.2 Identification in systems with structure

We will now review parts of the literature of identification in systems with structure. We consider the literature divided in three distinct topics; identification of the structure of the network, *i.e.*, the set of edges that are present; identification of the whole network; and identification of a specific module in the network. Here we will restrict the focus to the literature regarding the signal structure respresentation of a network. We will not cover the literature based on directed information to infer the topopoly because of the practical difficulty of estimating direct information and the contrbutions of this thesis is grounded in the system theoretic framework of dynamic networks. How to relate a physical system to some simpler model structure while still being able to identify some important physical properties is important, but will not be covered. One approach to this problem is Grey-box modelling; to give an example, in Linder (2014), a state space representation based on

physical modelling is carefully discretized and a tuned parametrization of the closed loop transfer function is identified. From the transfer function estimate a subset of the physical parameters can be estimated, and a multistep approach is suggested to increase the set of identfiable parameters.

1.2.1 Topology detection

Detecting the set of edges in the graph is a difficult problem for large networks, especially when there are no known reference signals, as is the case for LDGs. Many of the approaches to identify the topology of the netwok assumes some kind of sparsity, *i.e.*, that each internal variable only causally depends on a few other internal variables. Seneviratne and Solo (2012a) and Seneviratne and Solo (2012b) considers the l_0 norm using Laguerre basis function models. Adebayo et al. (2012) and Goncalves and Warnick (2008) derives conditions when the DSF can be reconstructed from knowledge of the closed loop transfer function. Based on this, Y. Yuan et al. (2011) proposes the l_0 norm to reconstruct the DSF. Convex relaxations such as the l_1 norm is used in Napoletani and Sauer (2008) and Timme (2007) to identify the complete network. In least absolute shrinkage and selection operator (LASSO) (Tibshirani, 1996) type of methods, the l_1 norm is used as a constraint on the connectivity, see *e.g.*, Julius et al. (2009) where finite impulse response (FIR) models are used. M. Yuan and Lin (2006) introduced the group LASSO (gLASSO) extension to Tibshirani's LASSO. While the LASSO penalizes the l_1 norm of the coefficient vector, the grouped Lasso divides the coefficient vector into predetermined sub-vectors and penalizes the sum of the l_2 norms of the sub-vectors. Using compressed sensing and modules modelled using FIR models, Sanandaji et al. (2012) and Sanandaji et al. (2011) presents a method to recover the topology of the network. A compressed sensing approach is also taken in Hayden et al. (2016) with a special focus on designing experiments to ensure reconstruction of the network. A nonparametric approach based on variations of Wiener filtering are presented in Innocenti and Materassi (2008), Materassi and Innocenti (2010), Materassi and Salapaka (2012), and Materassi et al. (2011). A compressed sensing approach, based on a sparse Wiener filter is presented in Materassi et al. (2013). In Torres (2014) and Torres et al. (2014), the modules of a directed acyclic network, *i.e.* without feedback, are modeled using states space models and the topology is identified using subspace methods. Also in a state space setting, Shahrampour and Preciado (2015) assumes that control can be applied to the network to drive internal variables to zero and the topology recovered from power spectral density estimates. Bottegal and Picci (2014), Bottegal and Picci (2015), and Bottegal and Pillonetto (2013) identifies a special type of complex system where a flocking component is present in the the description of the signals of the system. This flocking component can be viewed as a low-dimensional unmeasured input to the system.

1.2.2 Identification of the whole network

For very large networks there is a line of research that tries to identify the whole network when the interconnection structure is known. To do so, assumptions are often made on the network, either that it is composed of identical modules or that modules arise from discretizations of spatially distributed systems where the modules are only connected to a few neighbors. This structure is motivated by practical applications were partial differential equations have been discretized, for example heat conduction or flexible structures. Since the objective is to identify large networks, the focus is on algorithms that scale well with the number of modules, which traditional methods do not. The assumption that the modules are identical is made in Massioni and Verhaegen (2008) and Massioni and Verhaegen (2009). In M. Ali et al. (2009), M. Ali, A. Ali, Abbas, et al. (2011), M. Ali, A. Ali, Chughtai, et al. (2011), and M. Ali, Popov, et al. (2011), more complex noise structures, parameter varying modules, as well as the closed loop case are considered. Using a special type of matrices, called Sequentially Semi-separable matrices, a linear scaling in time complexity is achieved (van Wingerden and Torres, 2012; Torres, 2014). Any matrix can be written in this form; however, if the order of the Sequentially Semi-separable matrices grows large, the nice scaling in the number of modules is lost. Under the assumption that the systems only interact with spatially close neighbors, Haber and Verhaegen (2012) and Haber and Verhaegen (2014) propose a distributed algorithm to efficiently estimate all modules. An approach based on the Alternating Direction of Multipliers is presented in Hansson and Verhaegen (2014), which can be implemented in a distributed manner.

1.2.3 Identification of a module

The main interest in this work is to identify a module or a set of modules in the network. Recently, this topic has gained popularity (see *e.g.*, Chiuso and Pillonetto, 2012; Dankers, Van den Hof, Bombois, and P. S. Heuberger, 2013; Dankers, Van den Hof, and P. S. C. Heuberger, 2013; Dankers, Van den Hof, Bombois, and P. S. C. Heuberger, 2014; Gunes et al., 2014; Materassi and Salapaka, 2015; Van den Hof et al., 2013; Galrinho et al., 2015b). Also in this case the interconnection structure is assumed known. To estimate a transfer function in the network, a number of methods have been proposed. Some have been shown to give consistent estimates (Dankers, Van den Hof, Bombois, and P. S. Heuberger, 2013; Dankers, Van den Hof, and P. S. C. Heuberger, 2013), provided that a certain subset of signals is included in the identification process. In these methods, the user has the freedom to include additional signals. However, little is known about how these signals should be chosen, and how large the potential is for variance reduction. In Van den Hof et al. (2013), under the assumption that there is no measurement noise, the direct method and joint input-output method (Ljung, 1999) are generalized and conditions are given under which the methods give consistent estimates. The conditions are that the noise signals are mutually uncorrelated and uncorrelated with the reference signals. The spectral density of the measured internal variables should be positive definite (persistence of excitation) and

both the model set for the modules and noise models have to be flexible enough to capture the true system. The two-stage method and the instrumental variable (IV) method (Ljung, 1999) are also generalized in Van den Hof et al. (2013). However, in contrast, these methods rely more on the external reference signals. The persistence of excitation condition in this case concerns the spectral density of the measured internal variables projected onto the reference signals. The condition is that the spectral density of the projected internal variables needs to be positive definite. The benefit is that it is not necessary to include noise models. Some flexibility in how to choose the set of signals to use in the predictor is introduced for the direct method in Dankers, Van den Hof, and P. S. C. Heuberger (2013) and for the two-stage method in Dankers, Van den Hof, Bombois, and P. S. Heuberger (2013). Conditions are given on the set of signals in order to achieve consistency. Sensor noise is added to the framework in Dankers, Van den Hof, Bombois, and P. S. C. Heuberger (2014) and three generalizations of the basic closed-loop instrumental variable (BCLIV) method of Gilson and Van den Hof (2005) are presented. When there are no external signals available, *i.e.*, in the case of LDGs, (Dankers et al., 2015) generalizes error-in-variables techniques. In the same setting, (Materassi and Salapaka, 2015) derives conditions on the structure of the topology under which it is possible to recover the module dynamics from a Wiener filter. The method in Dankers et al. (2015) places some restrictions on the noise which may be restrictive. However, the noise restrictions may be loosened by high order noise modelling. A fully non-parametric approach has been proposed by Dankers and Van den Hof (2015); the method proposed by Pintelon et al. (2010a) and Pintelon et al. (2010b) can also be used in this scenario, where a semi-parametric approach is taken—the noise model is captured by a high order model and the plant model of interest is parametric.

Linder and Enqvist (2016) extends several of the mentioned methods by introducing a framework to handle inputs that are unknown and only indirectly measured by their effect on other signals in the system. Similar to what was done by Goncalves and Warnick (2008) for DSFs, Weerts et al. (2015) derives conditions how structural information, external signal properties and disturbance signal properties determines if topology and dynamics can be distinguished when the disturbance is full rank. Weerts et al. (2016) extends the results to non full-rank disturbances. The analysis of the accuracy of the presented methods is less developed than the consistency analysis. Before discussing what has been done in is this regard, we will take a step back, and discuss how the accuracy of a model can be analyzed. We will come back to this issue towards the end of this section.

1.3 Model accuracy

Depending on which method we use, we have to include some measurements and inputs to achieve consistent models. However, consistency is not the whole story. In order for us to trust a model that our identification algorithm gives us, we need some kind of guarantee that the model lies sufficiently close to the true module. To analyze the accuracy, mainly two approaches are possible, either the error sources are regarded as stochastic or they are

regarded as deterministic. Considering the errors as stochastic leads to confidence regions of the model error (see *e.g.*, Goodwin and Payne (1977), Söderström and Stoica (1989), and Ljung (1999)). In the deterministic case, hard bounds on the model error can be given in the frequency domain or in the time domain (see *e.g.*, Milanese and Vicino (1991), Milanese and Novara (2011), Wahlberg and Ljung (1992), and Ninness and Goodwin (1995)).

1.3.1 Confidence ellipsoids

This thesis takes the classical stochastic approach where we describe the accuracy of the estimated parameters $\hat{\theta}$ as confidence ellipsoids around the true system parameters θ^o. This is motivated by that, under reasonable assumptions (see Ljung (1999) for details), as the number of measurements N grows large, the random variable $\sqrt{N}\left(\hat{\theta} - \theta^o\right)$ converges in distribution to a Gaussian random variable with zero mean and covariance matrix P. For finite data, the covariance matrix is approximated as

$$\mathbf{Cov}\left\{\hat{\theta} - \theta^o\right\} \approx \frac{1}{N} P. \tag{1.1}$$

In some cases, we may not be interested in the model parameters themselves, but in some system theoretic property J, *e.g.*, the frequency response function or the poles of the system. Assuming sufficient smoothness of J (with respect to the parameters θ) and bounded moments of sufficiently high order of the noise, it follows that

$$\sqrt{N}(J\left(\hat{\theta}_N\right) - J(\theta^o)) \in \mathcal{N}\left(0, \mathbf{AsCov}\left\{J\left(\hat{\theta}_N\right)\right\}\right), \qquad \text{as } N \to \infty \tag{1.2}$$

where, using Gauss' approximation formula (also known as the delta method (Casella and R. Berger, 2002)) (Ljung, 1999), it can be shown that $\mathbf{AsCov}\left\{J\left(\hat{\theta}_N\right)\right\}$ in (1.2) is given by

$$\mathbf{AsCov}\left\{J\left(\hat{\theta}_N\right)\right\} = \nabla J^*(\theta^o) P \nabla J(\theta^o). \tag{1.3}$$

1.3.2 Motivation of asymptotic results

The asymptotic covariance is based on an assumption that the amount of input-output data available tends to infinity. The assumption is that for large enough N, (1.2) provides a reasonable approximation. In Garatti et al. (2004), some answers on when this is a reasonable assumption are given. Non-ellipsoidal confidence regions are considered in Bombois et al. (2009), which seem to give better approximations for small N, but are still based on a large number of samples. An interesting approach for non-asymptotic confidence regions has been developed in Campi and Weyer (2005), Campi and Weyer (2010), Csaji et al. (2012), Csáji et al. (2012), and Kolumbán et al. (2015). From this approach, promising methods based on hypothesis testing are emerging, which provide non-asymptotic confidence regions under mild assumptions on the noise distribution (Csaji et al., 2012; Csáji et al., 2012; Kolumbán et al., 2015). In Csaji et al. (2012) and Csáji et al. (2012), the noise terms are

assumed independent and symmetrically distributed around zero, and in Kolumbán et al. (2015) it is shown that the symmetry requirement may be replaced by exchangeability. The non-asymptotic case is also considered in (Douma, 2006; Hjalmarsson, 2005).

1.3.3 Parameter accuracy

The covariance matrix P in (1.3) has a long history of study. Early on, it was realized that some scalar measures of the covariance matrix P, *e.g.*, the determinant of P and weighted trace $\mathrm{Tr}\{WP\}$, grow with the model order, see for example Box and Jenkins (1976) and Gustavsson et al. (1977). Some more recent results can be found in Forssell and Ljung (1999), Agüero and Goodwin (2007), Bombois et al. (2005), and Agüero and Goodwin (2006). In these contributions, it is analyzed in which settings open loop or closed loop identification is optimal, *e.g.*, it is shown that under input constraints open loop identification is preferred (Agüero and Goodwin, 2006), while under output power constraints, typically closed loop is better (Agüero and Goodwin, 2006).

1.3.4 Frequency function estimate

Assuming that $\mathcal{S} \in \mathcal{M}$, the classical open loop variance approximation

$$\mathbf{AsCov}\left\{G\left(e^{j\omega}, \hat{\theta}_N\right)\right\} \approx \frac{n}{N}\frac{\Phi_v(\omega)}{\Phi_u(\omega)}, \tag{1.4}$$

was derived in Ljung (1985). This expression tells us that the variance of the estimated frequency response function $\hat{G}$, evaluated at the frequency ω, depends on the noise spectrum to signal spectrum ratio at that frequency. The variance increases linearly with the model order n. The result (1.4) is only valid when both n and N go to infinity. For finite model order, the expression can be quite misleading. Refinements of (1.4) can be found in Hildebrand and Gevers (2004), Hjalmarsson and Ninness (2006), Ninness and Hjalmarsson (2004), Xie and Ljung (2001), Xie and Ljung (2004), and Wahlberg et al. (2012). Variance expressions that are exact for finite model order are derived for some model structures in Xie and Ljung (2001), Xie and Ljung (2004), Ninness and Hjalmarsson (2004), and Hjalmarsson and Ninness (2006) and expressions for spectral estimates of AR Models are presented in Xie and Ljung (2004). For closed loop identification, variance expressions that are exact for finite model order are derived in Ninness and Hjalmarsson (2005a) and Ninness and Hjalmarsson (2005b). It is also known that the variance of the frequency response function satisfies a waterbed effect, similar to the Bode integral (Rojas et al., 2009).

1.3.5 Geometric approach

The geometric approach, the main analysis tool used in the second part of this thesis, was developed in Hjalmarsson et al. (2011), where the asymptotic variance of a smooth

function of the model parameters is expressed as an orthogonal projection onto the subspace spanned by the predictor error gradient (see also Mårtensson (2007)). The importance of this subspace, and the geometric properties of prediction error estimates were first recognized in a series of papers (Ninness and Hjalmarsson, 2004; Ninness and Hjalmarsson, 2005a; Ninness and Hjalmarsson, 2005b). The geometric analysis has since been applied to analyze different settings: In Mårtensson and Hjalmarsson (2009) the variance of identified poles and zeros are quantified and it is shown that non minimum phase zeroes and unstable poles can be estimated with finite variance, even when the model order tends to infinity; in Hjalmarsson et al. (2011) the difference in variance between the error-in-variables setting compared to when the input noise is zero is studied; when the minimum variance controller is the optimal experiment for closed loop identification is addressed in Mårtensson and Hjalmarsson (2011); some results on optimal and robust experiment design are presented in Mårtensson and Hjalmarsson (2011). The geometric approach has also been applied to MISO systems (Ramazi et al., 2014).

1.3.6 Multiple input multiple output (MIMO) results

There are far less results that consider the variance of MIMO system estimates. The paper Agüero et al. (2012) shows that the variance of the parameter estimates satisfies a waterbed effect. For fixed denominator models, it is not possible to simultaneously minimize both the bias error and the variance error at a particular frequency (Ninness and Gómez, 1996). In Bazanella et al. (2010), it is established that it is not necessary to excite all inputs in closed loop control of MIMO systems, provided the controller is sufficiently complex and the noise is sufficiently exciting. It is however preferable to excite all inputs at the same time in MIMO identification (Mišković et al., 2008).

1.3.7 Accuracy in identification of a module

There are but a few results that try to quantify the variance of different methods when a module in a network is estimated. In general, the available results are restricted to special cases of networks, in order to be able to say something meaningful. Cascaded modules are such a special case considered in Wahlberg et al. (2009). The main result is that measurements downstream do not improve the variance of the estimate of the first module, if the modules are identical and have the same parametrization. Cascaded modules are also considered in Chapter 6. In Hägg et al. (2011), a generalization of cascade modules is considered. Here, the effect of sensor placement, input spectrum, and common dynamics is considered. The same structure is considered in Chapter 7, where high order models are used for some of the modules. In a MISO system setting, the paper Gevers et al. (2006) studies which parameters are identified with decreased variance when an input signal is added (the added input is considered to be zero to start with). For MISO systems, it is shown in Ramazi et al. (2014) that the estimation accuracy decreases when inputs are correlated, and it is

shown how this effect depends on the correlation structure and the model structure. The above contributions all consider a direct approach. A technique to reduce the variance of a two stage method is presented in Gunes et al. (2014). The two step method first tries to obtain estimates of the inputs to the module of interest, and in a second step the module of interest is estimated (Van den Hof et al., 2013). The main idea in Gunes et al. (2014), is to simultaneously minimize the prediction error of the two steps in the two step method. This leads to a variance reduction compared to the two stage method, however, it is not clear how large the reduction will be. How to design identification experiments in dynamic networks is considered in Bombois et al. (2016).

1.4 Regularization and Bayesian system identification

Regularization is used extensively in several fields, *e.g.* in functional-approximation (Wahba, 1990), applied statistics, and machine learning (Hastie et al., 2009; Bishop, 2006). Regularization techniques have recently been introduced into the system identification field as a different approach to system identification (Nicolao and Pillonetto, 2008). Instead of searching for the true system within a finite model structure, *e.g.*, FIR models, regularization methods search for the system impulse response within an infinite-dimensional hypothesis space. The intrinsical ill-posedness of the problem is circumvented by imposing specific properties (*e.g.* smoothness or sparsity) on the estimated impulse response. The approach also admits a Bayesian interpretation (Rasmussen and Williams, 2006). Regularization has its mathematical foundation in reproducing kernel Hilbert spaces (Aronszajn, 1950). One of the key features of regularization is the definition of a so-called kernel which encodes prior information on the unknown system's impulse response. Special care has to be taken in system identification about which kernels to use since the kernels should encode that the impulse response is stable and possibly smooth (Pillonetto et al., 2014). Several different kernels for use in system identification has been proposed, *e.g.*, the *stable spline* kernels (Pillonetto and Nicolao, 2010) and the *tuned/correlated* kernel (Chen et al., 2012) as well as using multiple kernels (Chen et al., 2014). Chen and Ljung (2014) has proposed a method to construct kernels based on standard concepts of system theory. An overview of different kernels can be found in Dinuzzo (2015). The proposed kernels depend on some hyperparameters which may estimated from data, *e.g.*, using marginal likelihood maximization (see eg Aravkin et al. (2012). This procedure can be seen as an alternative to model selection (Pillonetto and Nicolao, 2010). Marginal likelihood maximization is also known as *empirical Bayes* (Maritz and Lwin, 1989), *type 2 maximum likelihood* (J. O. Berger, 1993), *generalized maximum likelihood* (Wahba, 1990), or *evidence approximation* (Bishop, 2006). It has been shown in Pillonetto and Chiuso (2015) that this procedure has some favorable robustness properties with respect to other hyperparameter selection techniques such as SURE (Stein, 1981). Regularization methods have recently been used for other problems in system identification, for example subspace identification (Chiuso et al., 2008), estimation of exponential signals (Pillonetto et al., 2010), correlation functions (Bottegal and Pillonetto, 2013), identification with data corrupted by outliers (Bottegal et al., 2016), and identification

with missing data (Risuleo et al., 2016).

1.5 Statement of contributions

The main contributions of this thesis are structured into two parts.

Part I: Identification methods

In the first main part of the thesis we introduce model order reduction Steiglitz-McBride (MORSM) which will be applied to dynamic networks in Chapter 4. We also introduce a Bayesian approach for identification in dynamic networks, network empirical Bayes (NEB).

Chapter 3. Model Order Reduction Steiglitz-McBride: In this chapter, we propose a method, MORSM, which is motivated by an aymptotic maximum likelihood (ML) criterion and bears a strong resemblence to the iterative method Box-Jenkins Steiglitz-McBride (BJSM). The asymptotic ML criterion of the ASYM method is reformulated in a way that techniques from BJSM can be used to minimize it. Second, we show that MORSM is asymptotically efficient in open loop with one iteration. We perform a simulation study, where we observe that MORSM has better finite sample convergence properties than BJSM, and that it is a viable alternative to prediction error method (PEM). The chapter is based on the publication:

N. Everitt and M. Galrinho and H. Hjalmarsson (2017b). "Optimal model order reduction with the Steiglitz-McBride method for open-loop data". *submitted to Automatica*.

Chapter 4. Model Order Reduction Steiglitz-McBride in dynamic networks: In this chapter, based on MORSM, we propose method to deal with the noise contribution when identifying a module in a dynamic network using a semi-parametric approach. First, we estimate a high order autoregressive with exogenous input (ARX) model of an appropriate part of the network. Second, we estimate the module of interest using signals simulated from the ARX model and the Steiglitz-McBride method. We motivate the method by an asymptotic ML criterion and argue that this will lead to an estimate with lower variance than existing time domain methods. We support this argument by simulations, where we observe that the method is most beneficial for colored noise. The chapter is based on the publication:

N. Everitt, M. Galrinho and H. Hjalmarsson (2017a). "Incorporating noise modeling in dynamic networks using non-parametric models". In: *Proceedings of the 20th IFAC World Congress*.

Chapter 5. An empirical Bayes approach: In this chapter, we explore ways to use regularization to reduce the variance of the estimated modules. The dynamic network is transformed into an acyclic structure, where any reference signal of the network is the input to a cascaded system. In this alternative system description, the first block captures the relation between the reference and the noisy input of the target module, the second block contains the target module. The blocks that do not contain the target module are modeled nonparametrically. An extension to include additional sensors downstream of the target module is also proposed. To keep the number of additional parameters to estimate low, we propose modeling as a Gaussian process also the impulse response of the path linking the target module to any additional sensor. In this case, however, the measured outputs and the unknown paths do not admit a joint Gaussian description. As a consequence, the E-step of the ECM method does not admit an analytical expression, as opposed to the one-sensor case. To overcome this issue, we use Markov chain Monte Carlo (MCMC) techniques to solve the integral associated with the E-step. In particular, we design an integration scheme based on the Gibbs sampler that, in combination with the ECM method, builds up a novel identification method for the target module. The chapter is based on the publications:

N. Everitt, G. Bottegal and H. Hjalmarsson (2017). "An empirical Bayes approach to identification of modules in dynamic networks". *submitted to Automatica*.

N. Everitt, G. Bottegal, C. R. Rojas and H. Hjalmarsson (2016). "Identification of modules in dynamic networks: An empirical Bayes approach". In: *Proceedings of the 55th IEEE Conference on Decision and Control*.

Part II: Covariance analysis

The second main contribution regards covariance analysis in mainly acyclic dynamic networks. Acyclic meaning that there is no feedback in the network. This may seem at first sight as a severe limitation to the applicability of the analys. However, a common way of dealing with networks with feedback is to reformulate the problem into forms analyzed in this part. In fact, the methods presented in Chapter 4 and Chapter 5, which are applicable to networks with feedback, use such reparametrizations.

Chapter 6. Cascade models: Cascaded modules are considered in this chapter. We quantify the accuracy improvement from additional sensors when estimating the first of a set of modules connected in a cascade structure. We present results on how the zeros of the first module affect the accuracy of the corresponding model. The results are illustrated on FIR systems. The chapter is based on the publications:

N. Everitt, C. R. Rojas and H. Hjalmarsson (2013). "A geometric approach to variance analysis of cascaded systems". In: *Proceedings of the 52nd IEEE Conference on Decision and Control*.

N. Everitt (2015). “Identification of Modules in Acyclic Dynamic Networks A Geometric Analysis of Stochastic Model Errors”. Licentiate thesis. KTH Royal Institute of Technology.

Chapter 7. Generalized parallel cascade models: Two types of generalized cascaded modules are considered in this chapter. The first structure may represent a system where several actuators with unknown dynamics are used to excite a system. Upper and lower bounds are provided for the variance of the estimated plant dynamics. The second structure may represent a sensor network where additional sensors are used to increase the accuracy of the estimated plant dynamics. Again, upper and lower bounds are provided for the variance of the estimated plant dynamics. The results are illustrated on FIR systems. The chapter is based on the publications:

N. Everitt, C. R. Rojas and H. Hjalmarsson (2014). "Variance Results for Parallel Cascade Serial Systems". In: *Proceedings of the 19th IFAC World Congress*.

N. Everitt (2015). “Identification of Modules in Acyclic Dynamic Networks A Geometric Analysis of Stochastic Model Errors”. Licentiate thesis. KTH Royal Institute of Technology.

Chapter 8. SIMO models with spatially correlated noise: In this chapter the effect of the noise correlation structure is examined in single input multiple output (SIMO) models. It is shown how the estimation accuracy depends on the correlation structure of the noise, model structure and model order. A formula for the asymptotic covariance of the frequency response function estimates and the model parameters is developed for the case of temporally white, but possibly spatially correlated additive noise. It is shown that when parts of the noise can be linearly estimated from measurements of other blocks with less estimated parameters, the variance decreases. The expressions reveal how the order of the different blocks and the correlation of the noise affects the variance of one block. In particular, it is shown that the variance of the block of interest levels off when the number of estimated parameters in another block reaches the number of estimated parameters of the block of interest. We show that the effect of the input spectrum is less significant than expected. The optimal correlation structure for the noise is determined for the case when one block has one parameter less than the other blocks. The chapter is based on the publications:

N. Everitt, G. Bottegal, C. R. Rojas and H. Hjalmarsson (2017). "Variance analysis of linear SIMO models with spatially correlated noise". *Automatica*. 77: 66–81.

N. Everitt, G. Bottegal, C. R. Rojas and H. Hjalmarsson (2015b). "On the Effect of Noise Correlation in Parameter Identification of SIMO Systems". In: *Proceedings of the 17th IFAC Symposium on System Identification*.

N. Everitt (2015). “Identification of Modules in Acyclic Dynamic Networks A Geometric Analysis of Stochastic Model Errors”. Licentiate thesis. KTH Royal Institute of Technology.

Chapter 9. MIMO models with correlated input and noise: In this chapter the effect of the noise correlation structure is examined in MIMO models. It is shown how the estimation accuracy depends on the correlation structure of the noise, correlation structure of the input, model structure and model order. A formula for the asymptotic covariance of the frequency response function estimates and the model parameters is developed for the case of temporally white, but possibly spatially correlated additive noise and similar assumptions on the input. The developed covariance formulas for MIMO systems are valid for finite model orders. We illustrate the connections with results for SIMO and MISO models discussed in Chapter 8. The interplay of model structure, input correlation and noise orrelation is exemplified by numerical simulations. The chapter is based on the publication:

N. Everitt, G. Bottegal, C. R. Rojas and H. Hjalmarsson (2015a). "On the variance analysis of identified linear MIMO models". In: *Proceedings of the 54th IEEE Conference on Decision and Control*.

1.5.1 Authors contributions

The orders of the authors reflects their contribution. The co-authors have contributed with discussion and normal supervision. The articles written together with Miguel Galrinho are to be considered shared equally.

1.6 Other publications

M. Galrinho, N. Everitt and H. Hjalmarsson (2017). "ARX modeling of unstable linear systems". *Automatica*. 75: 167–171.

J. Mårtensson, N. Everitt and H. Hjalmarsson (2017). "Covariance analysis in SISO linear systems identification". *Automatica*. 77: 82–92.

CHAPTER 2

BACKGROUND

This thesis concerns, first, methods for identifying dynamical systems interconnected in networks from experimental data, and second, the analysis of the accuracy of the obtained models. The objective of this chapter is to provide a theoretical background for the results presented in this thesis. The system identification method considered is mainly the prediction error method. However, since Bayesian estimation forms the basis for the methods presented in Chapter 5, an introduction to Bayesian estimation is given. The geometric analysis that is instrumental for the second part of this thesis is based on Hilbert space theory and a brief background is provided towards the end of this chapter.

2.1 System identification

System identification concerns building mathematical models from observed data from the system. The mathematical model should provide a good approximation of the behavior of the system relevant to the intended use of the model, *e.g.*, simulation, prediction or control. We consider linear time invariant (LTI) dynamic systems with m inputs collected in a column vector $u_c(t)$ and p outputs collected in a column vector $y_c(t)$ (the subscript c denotes continuous time, which we will drop when we move to discrete time). The output of the system can be described by the relation

$$y_c(t) = \int_{-\infty}^{\infty} g(t-\tau)u_c(\tau)\,d\tau$$

where $g(t)$ is the impulse response. We collect measurements of the output of the system at equidistant samples with sample time T_s. We thus have samples $y(t) = y(kT_s)$, $k = 1, \dots,$ according to

$$y(t) = y(kT_s) = \int_{-\infty}^{\infty} g(kT_s - \tau)u(\tau)\,d\tau. \tag{2.1}$$

We assume that we also have access to the control signal at these samples, *i.e.*, $u_k = u(kT_s)$. The inter sample behavior of the input signal is assumed to satisfy a zero order hold (ZOH)

assumption. Under this assumption the signal u is assumed to be constant in between sample instances, *i.e.*,

$$u(t) = u(kT_s), \qquad (k-1)T_s \leq t \leq kT_s. \tag{2.2}$$

For convenience, we let t enumerate the sampling instances. Under the ZOH assumption, the output samples $y(t)$ given by (2.1) can be written as

$$y(t) = \sum_{l=0}^{\infty} g_l u(l)(t-l), \qquad t = 0, 1, \ldots \tag{2.3}$$

where

$$g_l = \int_{(l-1)T_s}^{lT_S} g(\tau)\, d\tau.$$

Introducing the time shift operator q, defined by

$$qy(t) = y(t+1),$$

(2.3) can be written as

$$y(t) = G_o(q)u(t),$$

where $G_o(q)$ is the transfer function $G_o(q) = \sum_{l=1}^{\infty} g_l q^{-l}$. However, in practice, we cannot measure the output of the system exactly. There are always measurement noise and disturbances acting on the system. These are modeled as a zero mean white noise signal $e(t)$ with variance Λ, filtered through an inversely stable filter $H_o(q)$, so that our basic description of a (discrete) linear system is

$$y(t) = G_o(q)u(t) + H_o(q)e(t). \tag{2.4}$$

2.2 Prediction error identification

We model the system (2.4) as

$$y(t) = G(q,\theta)u(t) + H(q,\theta)e(t),$$

where $G(q,\theta)$ and $H(q,\theta)$ are rational functions which are parametrized with the parameter vector $\theta \in \mathbb{R}^n$. Thus, (2.5) describes a set of models. For a given θ, (2.5) can be used to predict the future output of the system given past samples of the output and input. The mean square optimal one-step ahead predictor is the conditional expectation, denoted by $\hat{y}(t|t-1,\theta)$ and is given by

$$\hat{y}(t|t-1,\theta) = H^{-1}(q,\theta)G(q,\theta)u(t) + \left[I - H^{-1}(q,\theta)\right]y(t). \tag{2.5}$$

The prediction error is

$$\varepsilon(t,\theta) = y(t) - \hat{y}(t|t-1,\theta). \tag{2.6}$$

The objective is to find the model within the set of models that most accurately describes the system. In PEM, the most accurate model is the one that minimizes a cost function $V_N(\theta)$ based on the prediction errors of the observed inputs and outputs. The cost function is a sum of some scalar norm l of the prediction error, *i.e.*,

$$V_N(\theta) = \frac{1}{N}\sum_{t=1}^{N} l(\varepsilon(t,\theta)). \tag{2.7}$$

In this work, a quadratic norm will be used with the noise variance as weighting matrix Λ^{-1}, *i.e.*,

$$l(\varepsilon(t,\theta)) = \frac{1}{2}\varepsilon^{\top}(t,\theta)\Lambda^{-1}\varepsilon(t,\theta). \tag{2.8}$$

This norm uses the (usually) unknown noise (co)-variance. However, this covariance can be estimated from the data. Since we are interested in the asymptotic properties of the estimates $\hat{\theta}$, it is interesting to note that minimizing the cost function

$$\det\left\{\frac{1}{N}\sum_{t=1}^{N}\varepsilon(t,\theta)\varepsilon(t,\theta)^{\top}\right\} \tag{2.9}$$

gives the same asymptotic covariance matrix as minimizing (2.7) with the norm (2.8) based on the true noise covariance.

PEM is a general purpose method that can be used under fairly genereal circumstances. However, in general it is required to solve a nonlinear optimization problem. For models where the predictor is linear in the parameters, PEM becomes numerically attractive. One such case is the ARX model. We now consider a single input single output (SISO) system. Note that the system (2.5) can be represented as

$$A^o(q)y(t) = B^o(q)u(t) + e(t), \tag{2.10}$$

where

$$A^o(q) := \frac{1}{H^o(q)} =: 1 + \sum_{k=1}^{\infty} a_k^o q^{-k},$$
$$B^o(q) := \frac{G^o(q)}{H^o(q)} =: \sum_{k=1}^{\infty} b_k^o q^{-k}$$

are stable transfer functions. Let us consider the finite truncation of the model (2.10)

$$A(q,\eta^n)y(t) = B(q,\eta^n)u(t) + e(t),$$

where

$$A(q,\eta^n) = 1 + \sum_{k=1}^{n} a_k q^{-k}, \qquad B(q,\eta^n) = \sum_{k=1}^{n} b_k q^{-k}, \tag{2.11}$$

and

$$\eta^n = \begin{bmatrix} a_1 & \dots & a_n & b_1 & \dots & b_n \end{bmatrix}^\top.$$

Here, $A(q)$ and $B(q)$ are both modeled with n coefficients. Note that (2.10) is in general not in the model set defined by (2.11) due to the truncation by n coefficients. Nevertheless, $\{a_k^o\}$ and $\{b_k^o\}$ are sequences converging to zero. Thus, if n is chosen large enough, (2.11) can model (2.10) with good accuracy.

An advantage of ARX models is that they are linear in the model parameters. In particular, the PEM estimate of η^n is obtained by minimizing the cost function

$$V_N(\eta^n) = \frac{1}{N}\sum_{t=1}^{N}\left[A(q,\eta^n)y(t) - B(q,\eta^n)u(t)\right]^2, \tag{2.12}$$

which can be done by linear least squares. Write (2.11) as

$$y(t) = (\varphi^n(t))^\top \eta^n + e(t),$$

where

$$\varphi^n(t) = \begin{bmatrix} -y(t-1) & \dots & -y(t-n) & u(t-1)\dots & u(t-n) \end{bmatrix}^\top. \tag{2.13}$$

Then, the least squares estimate of η^n is given by

$$\hat{\eta}_N^n := \left[R_N^n\right]^{-1} r_N^n, \tag{2.14}$$

where

$$R_N^n = \frac{1}{N}\sum_{t=1}^{N}\varphi^n(t)\left[\varphi^n(t)\right]^\top, \qquad r_N^n = \frac{1}{N}\sum_{t=1}^{N}\varphi^n(t)y(t).$$

2.2.1 High order modelling

Despite the simplicity of ARX models, they are not appropriate to model (2.4) for most practical uses. As the order n is required to be arbitrarily large, the estimated model will have unacceptably high variance.

Nevertheless, the high order ARX model estimate can be used to obtain a model of low order, reducing the variance. This can be done efficiently without re-using the data. The

reason is that the estimate $\hat{\eta}_N^n$ and its covariance, asymptotically, are a sufficient statistic for our problem. To observe this, consider the infinite order ARX model

$$y(t) = \varphi^\top(t)\eta + e(t), \tag{2.15}$$

where

$$\varphi(t) := \begin{bmatrix} -y(t-1) \\ -y(t-2) \\ \vdots \\ u(t-1) \\ u(t-2) \\ \vdots \end{bmatrix}, \qquad \eta := \begin{bmatrix} a_1 \\ a_2 \\ \vdots \\ b_1 \\ b_2 \\ \vdots \end{bmatrix}.$$

Then, the probability density function of $y^N := \{y(t)\}_{t=1}^N$ given η is

$$\begin{aligned} p\left(y^N \middle| \eta\right) &= \prod_{t=1}^N \frac{1}{\sqrt{2\pi\lambda_o}} \mathrm{e}^{-\frac{\left[y(t)-\varphi^\top(t)\eta\right]^2}{2\lambda_o}} \\ &= C\mathrm{e}^{-\frac{1}{2\lambda_o}\left(\eta^\top \sum_{t=1}^N \varphi(t)\varphi^\top(t)\eta + 2\sum_{t=1}^N \varphi^\top(t)y(t)\eta\right)} \mathrm{e}^{-\frac{1}{2\lambda_o}\sum_{t=1}^N y(t)^2}, \end{aligned}$$

where we treat λ_o as a known constant (in this case, because it is a scalar, it does not influence the estimation of the parameters of interest). Then, it follows from Lehmann and Casella (1998) that $R_N := \sum_{t=1}^N \varphi(t)\varphi^\top(t)$ and $r_N := \sum_{t=1}^N \varphi^\top(t)y(t)$ form a sufficient statistic for the data y^N. Alternatively, since $\hat{\eta}_N = R_N^{-1} r_N$, we can say that $\hat{\eta}_N$ and R_N are the sufficient statistic. However, when n is finite, there is a bias error induced by the truncation of the parameter sequences $\{a_k\}$ and $\{b_k\}$. If that error is assumed to be small, the estimate $\hat{\eta}_N^n$ will contain practically the same information about the system dynamics as the data. Thus, the data could in principle be disregarded, and $\hat{\eta}_N$ alone be used to obtain an estimate of a lower order model that is asymptotically efficient. This idea will be explored in Chapter 3, where the high order arx model will be reduced by least squares estimation on data pre-filtered by the high-order model.

2.3 Maximum likelihood

Assume now that the true system is of FIR type and we model it as such, *i.e.*, the true system is given by

$$y(t) = g_1 u(t-1) + g_2 u(t-2) + \cdots + g_n u(t-n) + e(t) \tag{2.16}$$

and the model is given by

$$y(t) = \varphi^\top(t)g + e(t),$$

where

$$\varphi(t) := \begin{bmatrix} u(t-1) \\ u(t-2) \\ \vdots \\ u(t-n) \end{bmatrix}, \qquad g := \begin{bmatrix} g_1 \\ g_2 \\ \vdots \\ g_n \end{bmatrix}.$$

The prediction errors for this model is given by (2.6) with

$$\hat{y}(t|t-1, g) = \varphi^\top(t) g.$$

If we assume that the noise is Gaussian, in addition to being independent, the *likelihood function*, *i.e.* the probability density function of the measurements as predicted by our model, is given by

$$L(g) := p\left(y^N \middle| g\right) = \prod_{t=1}^{N} \frac{1}{2\lambda_o} \mathrm{e}^{-\frac{\left[y(t)-\varphi^\top(t)g\right]^2}{2\lambda_o}}.$$

The ML estimate is the argument that maximizes the likelihood function. Since the logarithm is an increasing function we may instead, for convenience, maximize the log likelihood:

$$g^{\mathrm{ML}} = \arg\max_g \log L(g).$$

Writing out this expression, we get

$$g^{\mathrm{ML}} = \arg\max_g -\frac{1}{\sqrt{2\pi\lambda_o}} \sum_{t=1}^{N} \left[y(t) - \varphi^\top(t) g\right]^2 - \frac{N}{2} \log \lambda_o.$$

We observe that the first term corresponds to the PEM cost function. For Gaussian measurement noise, the PEM estimate and the ML estimate are the same, implying that PEM is optimal in a maximum likelihood sense. The PEM estimate is given by

$$\hat{g}^{\mathrm{PEM}} = \left[\sum_{t=1}^{N} \varphi(t)\varphi^\top(t)\right]^{-1} \left[\sum_{t=1}^{N} \varphi^\top(t) y(t)\right],$$

which can be written succinctly as

$$\hat{g}^{\mathrm{PEM}} = \left[\boldsymbol{\Phi}^\top \boldsymbol{\Phi}\right]^{-1} \boldsymbol{\Phi}^\top y,$$

where

$$\boldsymbol{\Phi} = \begin{bmatrix} \varphi^\top(1) \\ \varphi^\top(2) \\ \vdots \\ \varphi^\top(N) \end{bmatrix}, \qquad y = \begin{bmatrix} y(1) \\ y(2) \\ \vdots \\ y(N) \end{bmatrix}. \tag{2.17}$$

We can calculate the bias of the estimate, *i.e.*, the difference between the expected value of the estimate and the true paramters, as

$$\mathbf{E}\left\{\hat{g}^{\mathrm{PEM}} - g^o\right\} = \mathbf{E}\left\{ g^o + \left[\boldsymbol{\Phi}^\top \boldsymbol{\Phi}\right]^{-1} \boldsymbol{\Phi}^\top e - g^o \right\} = 0,$$

where e is the collection of measurement noise, stacked similar to (2.17). The covariance of the estimate is given by

$$\mathbf{E}\left\{ \left(\hat{g}^{\mathrm{PEM}} - g^o\right)\left(\hat{g}^{\mathrm{PEM}} - g^o\right)^\top \right\} = \lambda \left[\boldsymbol{\Phi}^\top \boldsymbol{\Phi}\right]^{-1},$$

In the next section we will try to reduce the covariance of the estimate by allowing some bias. The goal is to reduce the mean squared error by this trade-off.

2.4 Bayesian estimation and regularization

In this section, we will take a Bayesian perspective and introduce a prior ditribution for the coeffiecients, in order to encode our prior belief about the system, for example that the system is stable. We take as a prior for the impulse response g a zero-mean Gaussian distribution, *i.e.*

$$p\left(g; \nu, K_\beta\right) \sim \mathcal{N}\left(0, \nu K_\beta\right). \tag{2.18}$$

In this thesis, we will fix the structure of the covariance matrix so as to correspond to the *first-order stable spline kernel* (Pillonetto and Nicolao, 2010):

$$\left\{K_\beta\right\}_{i,j} = \beta^{\max(i,j)}, \quad \beta \in [0, 1). \tag{2.19}$$

The hyperparameter β regulates the decay velocity of the realizations from (2.18), whereas, ν tunes their amplitude. In this context, K_β is usually called a *kernel* (due to the connection between Gaussian process regression and the theory of reproducing kernel Hilbert space, see *e.g.* Rasmussen and Williams (2006) for details) and determines the properties of the realizations of g. In particular, the stable spline kernel enforces smooth and BIBO stable realizations (Pillonetto and Nicolao, 2010). However, there are many other kernels that may be used to do system identification, see Section 1.4. Our posterior belief about g, after taking the observed measurements into account, can be updated using Bayes' rule

$$p(g \mid y) = \frac{p(y \mid g) p(g)}{p(y)}. \tag{2.20}$$

where p(y|g) is the likelihood of the data y and, under Gaussian noise assumptions, is Gaussian ditributed, *i.e.*

$$p(y \mid g) \sim \mathcal{N}\left(\boldsymbol{\Phi} g, \lambda I_N\right). \tag{2.21}$$

The posterior is also Gaussian since the prior is chosen as a so called conjugate prior. The conjugate-prior property is an important property in Bayesian estimation which states that the posterior has the same distribution as the likelihood if the prior is chosen as a conjugate prior (see *e.g.* Bishop (2006) for details). The posterior distribution is available in closed form (Anderson and Moore, 1979)

$$p(g \mid y) \sim \mathcal{N}\left(\left[\frac{\Phi^\top \Phi}{\lambda} + \nu^{-1} K_\beta^{-1} \right]^{-1} \lambda^{-1} \Phi^\top y, \left[\frac{\Phi^\top \Phi}{\lambda} + \nu^{-1} K_\beta^{-1} \right]^{-1} \right).$$

The minimum mean squared error (MMSE) estimate is given by $\mathbf{E}\{g \mid y\}$ (Casella and Lehmann, 2003)

$$\hat{g}^{\text{MMSE}} = \left[\frac{\Phi^\top \Phi}{\lambda} + \nu^{-1} K_\beta^{-1} \right]^{-1} \lambda^{-1} \Phi^\top y$$

The mean of this estimate is

$$\mathbf{E}\left\{ \hat{g}^{\text{MMSE}} \right\} = \left[\frac{\Phi^\top \Phi}{\lambda} + \nu^{-1} K_\beta^{-1} \right]^{-1} \lambda^{-1} \Phi^\top \Phi g^o$$

and we see that the estimate is biased

$$\mathbf{E}\left\{ \hat{g}^{\text{MMSE}} - g^o \right\} = -\left[\frac{\Phi^\top \Phi}{\lambda} + \nu^{-1} K_\beta^{-1} \right]^{-1} \nu^{-1} K_\beta^{-1} g^o,$$

and has the covariance matrix

$$\mathbf{Cov}\left\{ \hat{g}^{\text{MMSE}} \right\} = \lambda \left[\Phi^\top \Phi + \frac{\lambda}{\nu} K_\beta^{-1} \right]^{-1} \Phi^\top \Phi \left[\Phi^\top \Phi + \frac{\lambda}{\nu} K_\beta^{-1} \right]^{-1}$$

From the expressions for the bias and variance, we see that the parameter ν tunes the bias and covariance. Large values of ν corresponds to a prior with large covariance and will give an estimate close to $\hat{g}^{\text{PEM}}$ with similar covariance and small bias. Small values of ν corresponds to a prior with small covariance and will give an estimate closer to zero with a small covariance and large bias.

2.4.1 Statistical properties of the PEM estimates

We assume that the model is in the model set, *i.e.*, there exists a θ^o such that $G_o(q) = G(q, \theta^o)$ and $H_o(q) = H(q, \theta^o)$. Under mild regularity conditions (see Ljung (1999) for details), as N goes to infinity, the parameter error $\sqrt{N}\left(\hat{\theta}_N - \theta^o\right)$ converges in distribution to the normal distribution with zero mean and covariance matrix $\mathbf{AsCov}\left\{\hat{\theta}_N\right\}$, which we conveniently denote by

$$\sqrt{N}(\hat{\theta}_N - \theta^o) \in \mathcal{N}\left(0, \mathbf{AsCov}\left\{\hat{\theta}_N\right\}\right) \qquad \text{as } N \to \infty. \tag{2.22}$$

where

$$\mathbf{AsCov}\{\hat{\theta}_N\} := \left(\mathbf{E}\{\psi(t,\theta^o)\Lambda^{-1}\psi^\top(t,\theta^o)\}\right)^{-1}, \tag{2.23}$$

$$\psi(t,\theta^o) := \frac{d}{d\theta}\varepsilon(t,\theta)\Big|_{\theta=\theta^o}. \tag{2.24}$$

In following chapters we will express (2.23) as

$$\mathbf{AsCov}\{\hat{\theta}_N\} = \langle \Psi, \Psi\rangle^{-1}, \tag{2.25}$$

where Ψ will depend on the problem at hand and the inner product of two functions $f, g : \mathbb{T} \to \mathbb{C}^{1\times m}$ is defined as

$$\langle f, g\rangle := \frac{1}{2\pi}\int_{-\pi}^{\pi} f\left(e^{i\omega}\right) g^*\left(e^{i\omega}\right) d\omega. \tag{2.26}$$

Often, we are not interested in the covariance of the parameters themselves, but in some "system theoretic" quantity. Let $J : \mathbb{R}^n \to \mathbb{C}^{1\times q}$ be a differentiable function of θ such that $J(\theta^o)$ is the quantity of interest. Assuming sufficient smoothness of J (with respect to θ), bounded noise moments of sufficiently high order, and using (2.22), it follows that

$$\sqrt{N}\left(J\left(\hat{\theta}_N\right) - J(\theta^o)\right) \in \mathcal{N}\left(0, \mathbf{AsCov}\left\{J\left(\hat{\theta}_N\right)\right\}\right) \qquad \text{as } N \to \infty. \tag{2.27}$$

where, using Gauss' approximation formula (or the delta method (Casella and R. Berger, 2002)) (Ljung, 1999) and (2.22), it can be shown that[1]

$$\begin{aligned}\mathbf{AsCov}\left\{J\left(\hat{\theta}_N\right)\right\} &:= \lim_{N\to\infty} N \cdot \mathbf{E}\left\{\left(J\left(\hat{\theta}_N\right) - J(\theta^o)\right)^*\left(J\left(\hat{\theta}_N\right) - J(\theta^o)\right)\right\} \\ &= \nabla J^*(\theta^o)\langle \Psi, \Psi\rangle^{-1}\nabla J(\theta^o),\end{aligned}$$

where $\nabla J(\theta) \in \mathbb{C}^{n\times q}$ is the gradient of J with respect to θ.

2.5 Dynamic networks

In this thesis we will work with networks of dynamic systems. We will spend some time in this section to formalize the different quantities in the network and the network structures we consider. Consider as an example the dynamic network given in Figure 2.1. In the network we have a set of internal variables $\{w_k\}$ which encode the states of the network. Their dynamics can be described by

$$w(t) = G(q)w(t) + r(t). \tag{2.28}$$

[1] This definition is slightly non-standard in that the second term is usually conjugated. For the standard definition, all results in the thesis have to be transposed.

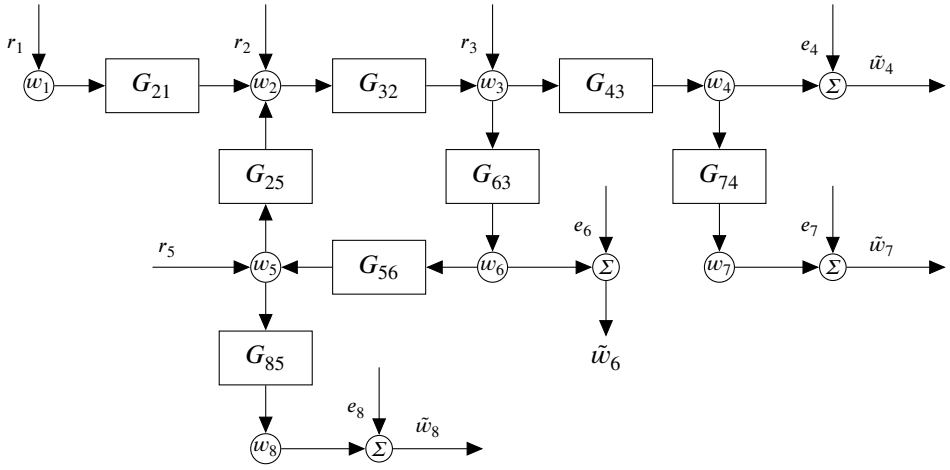

Figure 2.1: An example of a dynamic network. The internal variables $\{w_k\}$ are described by the dynamics (2.28), where $\{r_k\}$ is the set of reference signals. The set of measurements $\{y_k\}$ are described by (2.30), where $\{e_k\}$ is the measurement noise.

The example network of Figure 2.1 is described by

$$\begin{bmatrix} w_1 \\ w_2 \\ w_3 \\ w_4 \\ w_5 \\ w_6 \\ w_7 \\ w_8 \end{bmatrix} = \begin{bmatrix} 0 & 0 & 0 & 0 & 0 & 0 & 0 & 0 \\ G_{21} & 0 & 0 & 0 & G_{25} & 0 & 0 & 0 \\ 0 & G_{32} & 0 & 0 & 0 & G_{36} & 0 & 0 \\ 0 & 0 & G_{43} & 0 & 0 & 0 & 0 & 0 \\ 0 & 0 & 0 & 0 & 0 & G_{56} & 0 & 0 \\ 0 & 0 & G_{63} & 0 & 0 & 0 & 0 & 0 \\ 0 & 0 & 0 & G_{74} & 0 & 0 & 0 & 0 \\ 0 & 0 & 0 & 0 & G_{85} & 0 & 0 & 0 \end{bmatrix} \begin{bmatrix} w_1 \\ w_2 \\ w_3 \\ w_4 \\ w_5 \\ w_6 \\ w_7 \\ w_8 \end{bmatrix} + \begin{bmatrix} r_1 \\ r_2 \\ r_3 \\ 0 \\ r_5 \\ 0 \\ 0 \\ 0 \end{bmatrix}.$$

We will, in parts of the thesis, be adding process noise v so that the system dynamics is described by

$$w(t) = G(q)w(t) + r(t) + v(t). \tag{2.29}$$

The *internal variables* are measured with additive white noise e, *i.e.*,

$$\tilde{w}(t) = w(t) + e(t) = (I - G(q))^{-1}[r(t) + v(t)] + e(t), \tag{2.30}$$

where the inverse $(I - G(q))^{-1}$ is assumed to exist. In the example only $\{w_4(t), w_6(t), w_7(t), w_8(t)\}$ are measured so that

$$\begin{bmatrix} \tilde{w}_4(t) \\ \tilde{w}_6(t) \\ \tilde{w}_7(t) \\ \tilde{w}_8(t) \end{bmatrix} = \begin{bmatrix} w_4(t) \\ w_6(t) \\ w_7(t) \\ w_8(t) \end{bmatrix} + \begin{bmatrix} e_4(t) \\ e_6(t) \\ e_7(t) \\ e_8(t) \end{bmatrix} = G_{cl}(q) \begin{bmatrix} r_1(t) \\ r_2(t) \\ r_3(t) \\ r_5(t) \end{bmatrix} + \begin{bmatrix} e_4(t) \\ e_6(t) \\ e_7(t) \\ e_8(t) \end{bmatrix},$$

for some $G_{cl}(q)$ that depends on the dynamics of the modules in G.

The dynamic networks that we consider in this thesis consist of m scalar *internal variables* $w_j(t)$, $j = 1, \dots, m$ and m scalar external *reference signals* $r_l(t)$, $l = 1, \dots, m$, that can be manipulated by the user. Some of the reference signal may not be present, *i.e.*, they may be identically zero. Define $\mathcal{R}$ as the set of indices of reference signals that are present. In the dynamic network, the internal variables are considered nodes and transfer functions are the edges. Introducing the vector notation $w(t) := [\, w_1(t) \ \dots \ w_m(t) \,]^\top$, $r(t) := [\, r_1(t) \ \dots \ r_m(t) \,]^\top$, the dynamics of the network are defined by the equation

$$w(t) = G(q)w(t) + r(t) + v(t), \tag{2.31}$$

where

$$G(q) = \begin{bmatrix} 0 & G_{12}(q) & \cdots & G_{1m}(q) \\ G_{21}(q) & 0 & \ddots & \vdots \\ \vdots & \ddots & \ddots & G_{(m-1)m}(q) \\ G_{m1}(q) & \cdots & G_{m(m-1)}(q) & 0 \end{bmatrix},$$

$G_{ji}(q)$ is a proper rational transfer function for $j = 1, \dots, m$, $i = 1, \dots, m$ and the reference signal is a zero mean processes with finite moments of all orders and has power spectrum $\Phi_r(\omega)$. The internal variables $w(t)$ are measured with additive white noise, that is

$$\tilde{w}(t) = w(t) + e(t),$$

where $e(t) \in \mathbb{R}^m$ is a measurement noise sequences obtained by unknown stable filters driven by Gaussian white noise with noise covariance matrix Λ. To ensure stability and causality of the network the following assumption hold for the networks considered.

Assumption 2.1. The network is well posed in the sense that all principal minors of $\lim_{q\to\infty}(I - G(q))$ are non-zero (Van den Hof et al., 2013).

In the second part of the thesis, systems with acyclic structure without process noise will be consider. There, to stress that these systems may not only be the result of special parametrizations of dynamic networks, the measurements will be denoted by $y(t)$ instead of $\tilde{w}(t)$.

2.5.1 Zero order hold assumption

As discussed above, any modeling effort should take into account the intended use of the model. The assumption in this work is that we have access to one or several discrete control signals and samples of the outputs. In general, we would like to be able to model networks of continuous time systems. Each of the modules are modeled under the ZOH assumption. The inter sample behavior of signals in the network will however not (in general) satisfy this assumption. For this to hold at least approximately, all systems need to have low pass behavior and we need to sample at a high rate. Thus, in general, discrete time models of the modules will not be good approximations of their continuous time counterparts. The models will still be able to predict the sampled input output behavior of the modules, but the accuracy of a particular model is intrinsically linked to the other modules in the network. Even the network structure may be different from the continuous time network (Dankers, Van den Hof, and Bombois, 2014). If the network changes, the model will change too. As discussed in Pintelon and Schoukens (2012, Chapter 13), if the objective is to accurately model the module, it would be preferable to take another route using a band limited (BL) assumption on the signal and continuous time models. If the goal of the identification is continuous time models, the IV based method of Dankers, Van den Hof, and Bombois (2014) can be used. A signal $u(t)$ with power spectrum $\Phi(\omega)$ is considered BL if $\Phi(\omega) = 0$ for all $\omega > \omega_{\max}$ for some $\omega_{\max}$. If the physical interpretation of the parameters is not the main concern, then the sensor could be equipped with anti aliasing filters (to realize a BL setup), which would violate the ZOH assumption. However, discrete time models would accurately capture the dynamics of the modules, even though the dynamics of the anti-aliasing filters would be part of the models. From a control perspective, this is not that bad. If we are only interested in accurately modeling the behavior of the system up to some frequency, and we sample fast, the error will be small. For a further discussion on these issue we refer to Pintelon and Schoukens (2012, Chapter 13).

2.6 Hilbert space fundamentals

Many of the results derived in this thesis has its foundation on Hilbert space theory. In this section we introduce some notation and review a few fundamental results from this theory.

2.6.1 Inner product

We will mainly be concerned with functions $f : \mathbb{T} \to \mathbb{C}^{n\times m}$ that arise as the restrictions of $f : \mathbb{C} \to \mathbb{C}^{n\times m}$ to the domain $z = e^{j\omega}, \omega \in [0, 2\pi]$. This thesis will alternate between the notation $f(\omega)$, $f(e^{j\omega})$, and $f(z)$ as is convenient. We will consider vector valued complex functions as row vectors and the inner product of two such functions $f, g : \mathbb{T} \to \mathbb{C}^{1\times m}$ is

defined as

$$\langle f, g\rangle := \frac{1}{2\pi}\int_{-\pi}^{\pi} f\left(\mathrm{e}^{\mathrm{j}\omega}\right) g^*\left(\mathrm{e}^{\mathrm{j}\omega}\right) d\omega \tag{2.32}$$

When f and g are matrix-valued functions, we will still use the notation $\langle f, g\rangle$ to denote $\int_{-\pi}^{\pi} f\left(\mathrm{e}^{\mathrm{j}\omega}\right) g^*\left(\mathrm{e}^{\mathrm{j}\omega}\right) d\omega$, whenever the dimensions of f and g are compatible. In particular, $\langle f, f\rangle$ is the Gramian matrix of the rows of f.

2.6.2 Orthonormal functions

When $W : \mathbb{T} \to \mathbb{C}^{m\times m}$ is such that $W(z)$ is a positive definite hermitian matrix for all z, the $\mathcal{L}_2^W$-norm of $f : \mathbb{T} \to \mathbb{C}^{n\times m}$ is given by

$$\|f\|_W = \sqrt{\mathrm{Tr}\{\langle fW, f\rangle\}} \tag{2.33}$$

where $\mathrm{Tr}\{\cdot\}$ denotes the Trace operator. When $W \equiv I$ (the identity), we write $\|f\|$ and denote this the $\mathcal{L}_2$-norm of f.

We call two functions f, g orthogonal if $\langle f, g\rangle = 0$; if f, g are matrix valued, they are considered orthogonal if every entry of the resulting matrix is zero. A set of functions $\{\mathcal{B}_k\}_{k=1}^n$ is said to be orthonormal if they are mutually orthogonal with unit $\mathcal{L}_2$-norm.

2.6.3 The spaces $\mathcal{L}_2$ and $\mathcal{H}_2$

The space $\mathcal{L}_2^{n\times m}$ consists of all functions $f : \mathbb{T} \to \mathbb{C}^{n\times m}$, such that $\|f\| < \infty$. When $n = 1$, the notation is simplified to $\mathcal{L}_2^m$. For $f : \mathbb{T} \to \mathbb{C}^{n\times m}$, $f_i : \mathbb{T} \to \mathbb{C}^{1\times m}$ denotes the ith row of f. $\mathcal{H}_2^m$ is defined as the $\mathcal{L}_2^m$-functions that are analytic in $\mathbb{E}$. If $\Psi \in \mathcal{L}_2^{n\times m}$ for some positive integers n and m, then $\mathcal{S}_\Psi$ denotes the span of the rows of Ψ.

2.6.4 Subspaces

For an $\mathcal{L}_2$-function $\Psi \in \mathcal{L}_2^{n\times m}$, we denote by $\mathcal{S}_\Psi \subset \mathcal{L}_2^m$ the r-dimensional subspace spanned by the rows of Ψ, $r \le n$. An orthonormal basis of $\mathcal{S}_\Psi$ consists of a set of r orthonormal functions that span $\mathcal{S}_\Psi$, where r also corresponds to the dimension of the subspace $\mathcal{S}_\Psi$. Given an $\mathcal{L}_2$-function $\Psi \in \mathcal{L}_2^{n\times m}$, it is straightforward to construct an orthonormal basis of $\mathcal{S}_\Psi$ as a linear combination of the rows of Ψ, *e.g.*, by using the Gram-Schmidt orthogonalization.

2.6.5 Takenaka-Malmquist functions

In some cases it is possible to derive explicit expressions for a set of orthonormal basis functions that span a given subspace. A well known case (Ninness and Gustafsson, 1997) is

when

$$\mathbf{Span}\left\{ \frac{\Gamma_n}{A(q)} \right\} = \mathbf{Span}\left\{ \frac{q^{-1}}{A(q)}, \frac{q^{-2}}{A(q)}, \dots, \frac{q^{-n}}{A(q)} \right\}, \tag{2.34}$$

where $A(q) = \prod_{k=1}^{n_a}\left(1 - \xi_k q^{-1}\right)$, $|\xi_k| < 1$ for some set of specified poles $\{\xi_1, \dots, \xi_{n_a}\}$, $n \geq n_a$, and where

$$\Gamma_n = \begin{bmatrix} q^{-1} \\ q^{-2} \\ \vdots \\ q^{-n} \end{bmatrix}.$$

Then, it holds that (Ninness and Gustafsson, 1997)

$$\mathbf{Span}\left\{ \frac{\Gamma_n}{A(q)} \right\} = \mathbf{Span}\left\{ \mathcal{B}_1, \dots, \mathcal{B}_n \right\}$$

where $\{\mathcal{B}_k\}$ are the Takenaka-Malmquist functions given by

$$\mathcal{B}_k(q) := \frac{\sqrt{1 - |\xi_k|^2}}{q - \xi_k}\phi_{k-1}(q), \qquad k = 1, \dots, n \tag{2.35}$$

$$\phi_k(q) := \prod_{i=1}^{k} \frac{1 - \overline{\xi}_i q}{q - \xi_i}, \qquad \phi_0(q) := 1, \tag{2.36}$$

and with $\xi_k = 0$ for $k = n_a + 1, \dots, n$. Notice that the system zeros do not affect the basis functions above.

2.6.6 Orthogonal projections

We denote the orthogonal projection of f onto the space $\mathcal{S}_\Psi$ by $\mathbf{Proj}_{\mathcal{S}_\Psi}\{f\}$, *i.e.*, $\mathbf{Proj}_{\mathcal{S}_\Psi}\{f\}$ is the unique solution to

$$\min_{g \in \mathcal{S}_\Psi} \|g - f\|.$$

Given an orthonormal basis $\{\mathcal{B}_k\}_{k=1}^r$ of $\mathcal{S}_\Psi$, the projection is readily calculated as

$$\mathbf{Proj}_{\mathcal{S}_\Psi}\{f\} = \sum_{k=1}^{r} \langle f, \mathcal{B}_k \rangle \mathcal{B}_k. \tag{2.37}$$

It can alternatively be expressed as

$$\mathbf{Proj}_{\mathcal{S}_\Psi}\{f\} = \langle f, \Psi \rangle \langle \Psi, \Psi \rangle^{-1} \Psi. \tag{2.38}$$

2.7 Geometric tools for variance analysis

Many results in this thesis are based on the following results from Hjalmarsson and Mårtensson (2011), restated here for completeness.

Lemma 2.1. *(Lemma II.3 in Hjalmarsson and Mårtensson (2011)) Suppose that $J : \mathbb{R}^n \to \mathbb{C}^{1\times q}$ is differentiable and let the asymptotic covariance matrix $\boldsymbol{AsCov}\{J(\hat{\theta}_N)\}$ be defined by* (2.28) *where $\Psi \in \mathcal{L}_2^{n\times m}$. Suppose that $\gamma \in \mathcal{L}_2^{q\times m}$ is such that*

$$\nabla J(\theta^o) = \langle \Psi, \gamma \rangle, \tag{2.39}$$

then

$$\begin{aligned} \boldsymbol{AsCov}\{J(\hat{\theta}_N)\} &= \langle \gamma, \Psi \rangle \langle \Psi, \Psi \rangle^{-1} \langle \Psi, \gamma \rangle \\ &= \left\langle \boldsymbol{Proj}_{\mathcal{S}_\Psi}\{\gamma\}, \boldsymbol{Proj}_{\mathcal{S}_\Psi}\{\gamma\} \right\rangle. \end{aligned} \tag{2.40}$$

Finally it holds that

$$\boldsymbol{AsCov}\{J(\hat{\theta}_N)\} = \sum_{k=1}^{r} \langle \gamma, \mathcal{B}_k \rangle \langle \mathcal{B}_k, \gamma \rangle, \tag{2.41}$$

where $\mathcal{S}_\Psi$ is the subspace of $\mathcal{L}_2^m$ spanned by the rows of Ψ, and $\{\mathcal{B}_k\}_{k=1}^r$ is any orthonormal basis for this space.

Proof. Taking the inner product of (2.38) with itself, (2.40) follows. Similarly, (2.41) follows from taking the inner product of (2.37) with itself. ■

Since there are many functions γ for which (2.39) holds, there is a large degree of freedom in the choice of γ. In Hjalmarsson and Mårtensson (2011, Lemma II.8) it is shown that all solutions $\gamma \in \mathcal{L}_2^{q\times m}$ to the equation $\nabla J(\theta^o) = \langle \Psi, \gamma \rangle$ are given by

$$\gamma = \nabla J(\theta^o)^* \langle \Psi, \Psi \rangle^\dagger \Psi + s^\perp, \tag{2.42}$$

where $s^\perp$ is any $\mathcal{L}_2^{q\times m}$-function orthogonal to $\mathcal{S}_\Psi$ and $\Psi^\dagger$ denotes the $X^\dagger$ of Ψ. We will explore this degree of freedom in the next lemma, where a re-parametrization of $J(\theta)$ is used to find an expression for a γ that fulfills the condition (2.42).

Lemma 2.2. *(Lemma II.9 in Hjalmarsson and Mårtensson (2011)) Let J, Ψ, and $\mathcal{S}_\Psi$ be as in Lemma 2.1 and suppose that $\nabla J(\theta^o) = \Psi(z_o)L$ for some $z_o \in \mathbb{C}$ and $L \in \mathbb{C}^{m\times q}$. Let $\{\mathcal{B}_k\}_{k=1}^r$, $r \le n$, be an orthonormal basis for $\mathcal{S}_\Psi$. Then*

$$\boldsymbol{AsCov}\{J(\hat{\theta}_N)\} = L^* \sum_{k=1}^{r} \mathcal{B}_k^*(z_o)\mathcal{B}_k(z_o)L.$$

Proof. Let $\Gamma = \begin{bmatrix} \mathcal{B}_1^\top & \cdots & \mathcal{B}_r^\top \end{bmatrix}^\top$. Then there exists a full (column) rank $T \in \mathbb{C}^{n \times r}$ such that $\Psi = T\Gamma$. Inserting this in (2.40) and some straightforward algebra gives the result. ■

The next lemma will be useful to derive upper bounds for (2.28). For two two closed subspaces of $\mathcal{L}_2^m$, $\mathcal{X}$ and $\mathcal{Y}$, we use $\mathcal{X} + \mathcal{Y}$ to denote the subspace $\{x + y : x \in \mathcal{X}, y \in \mathcal{Y}\}$ and $\mathcal{Z} = \mathcal{X} \oplus \mathcal{Y}$ to denote that $\mathcal{Z}$ is the *direct sum* of $\mathcal{X}$ and $\mathcal{Y}$ which means that $\mathcal{Y}$ is the orthogonal complement of $\mathcal{X}$ in $\mathcal{Z}$. Furthermore, we define $\mathcal{Y} \ominus \mathcal{X}$ to be the orthogonal complement of $\mathcal{X}$ in $\mathcal{X} + \mathcal{Y}$, *i.e.*, $\mathcal{X} + \mathcal{Y} = \mathcal{X} \oplus (\mathcal{Y} \ominus \mathcal{X})$.

Lemma 2.3. *(Lemma II.6 in Hjalmarsson and Mårtensson (2011)) Let $\mathcal{X}$ and $\mathcal{Y}$ be two closed subspaces of $\mathcal{L}_2^m$ such that $\mathcal{X} \subseteq \mathcal{Y} \subseteq \mathcal{L}_2^m$ and let $\gamma \in \mathcal{L}_2^{q \times m}$. It holds that*

$$\left\langle \boldsymbol{Proj}_{\mathcal{Y}}\{\gamma\}, \boldsymbol{Proj}_{\mathcal{Y}}\{\gamma\} \right\rangle - \langle \boldsymbol{Proj}_{\mathcal{X}}\{\gamma\}, \boldsymbol{Proj}_{\mathcal{X}}\{\gamma\} \rangle = \left\langle \boldsymbol{Proj}_{\mathcal{Y} \ominus \mathcal{X}}\{\gamma\}, \boldsymbol{Proj}_{\mathcal{Y} \ominus \mathcal{X}}\{\gamma\} \right\rangle. \quad (2.43)$$

Proof. By definition it follows that $\mathcal{X} + \mathcal{Y} = \mathcal{X} \oplus (\mathcal{Y} \ominus \mathcal{X})$ and since $\mathcal{X} \subseteq \mathcal{Y}$ we have $\mathcal{X} + \mathcal{Y} = \mathcal{Y}$. Thus, $\mathbf{Proj}_{\mathcal{Y}}\{\gamma\} = \mathbf{Proj}_{\mathcal{X}}\{\gamma\} + \mathbf{Proj}_{\mathcal{Y} \ominus \mathcal{X}}\{\gamma\}$ and by taking the inner product of each side of the equation with itself, the result (2.43) follows. ■

Upper bounds for (2.40) can now be constructed by taking $\mathcal{X} = \Psi$ and $\mathcal{Y} = \mathcal{L}_2^m$ for example. It is immediate from (2.43) that

$$\left\langle \mathbf{Proj}_{\mathcal{Y}}\{\gamma\}, \mathbf{Proj}_{\mathcal{Y}}\{\gamma\} \right\rangle - \langle \mathbf{Proj}_{\mathcal{X}}\{\gamma\}, \mathbf{Proj}_{\mathcal{X}}\{\gamma\} \rangle \geq 0.$$

Lemma 2.3 will prove useful when deriving upper bounds for the asymptotic covariance in dynamics networks.

Part I

Identification methods

CHAPTER 3

MODEL ORDER REDUCTION STEIGLITZ-MCBRIDE

In this chapter, we introduce model order reduction Steiglitz-McBride (MORSM), which is motivated by an aymptotic ML criterion and bears a strong resemblence to the iterative method Box-Jenkins Steiglitz-McBride (BJSM). The setting of this chapter is SISO system identification and MORSM will be shown to be asymptotically efficient for open loop data. The method of this chapter will, in the following chapter, be shown to be particularly suited for identification in dynamic networks.

3.1 Introduction

The prediction error method (PEM) is a well-know approach for estimation of parametric models (Ljung, 1999). If the model orders are chosen correctly, a quadratic cost function provides asymptotically efficient estimates when the noise is Gaussian. The drawback is that, in general, PEM requires solving a non-convex optimization problem, which can converge to minima that are only local. Alternative methods, such as subspace (van Overschee and de Moor, 1996) or instrumental variable (Söderström and Stoica, 1983) methods, do not suffer from non-convexity, being useful to provide initialization points for PEM.

Other methods first estimate a high order model. In general, this is an ARX model, for which the global minimum of the prediction error cost function can be found by least squares. Because it is high order, this estimate will have high variance. However, it can be reduced to a parametric model description of low order. If the model reduction step is performed according to an exact maximum likelihood (ML) criterion, the low order estimates are asymptotically efficient (Wahlberg, 1989). This approach still requires, in general, solving a non-convex optimization problem.

Another possibility to perform model order reduction from a high order model is with the weighted null-space fitting (WNSF) method (Galrinho et al., 2014). Although it can be motivated by an exact ML criterion, this criterion is not minimized explicitly. Rather, it is interpreted as a weighted least squares problem by fixing the parameters in the weighting.

One problem with estimation of parametric models is the choice of model orders. Model order selection and estimation based on ML has a long history (see *e.g.* Whittle, 1951; Box and Jenkins, 1976; E. Hannan and Deistler, 1988). One classical approach to model order selection is to estimate the model orders from data. For autoregressive moving average with exogenous input (ARMAX) models, one iterative procedure is the Hannan-Rissanen-Kavalieris type methods (E. J. Hannan and Kavalieris, 1984; E. J. Hannan and Rissanen, 1982) (see *e.g.* E. Hannan and Deistler (1988) for an in-depth statistical analysis), which, at each iteration, estimates the innovations and selects new model orders according to an information criterion.

While the plant model order can sometimes be based on physical intuition, the noise model order is usually a more abstract concept. This has been observed in Schoukens et al. (2011), where a frequency domain method is proposed to estimate a parametric model of the plant and a high order noise model. Because this approach does not require a noise model order selection, it can be seen as more user friendly.

If the data are obtained in open loop, the asymptotic properties of the plant and noise model estimates obtained with PEM are uncorrelated, if the two transfer functions are independently parametrized (Ljung, 1999). Therefore, when a parametric noise model estimate is not of interest, asymptotically efficient estimates of the plant can be obtained as long as the noise model order is chosen high enough for the system to be in the model set. The limitation of choosing the noise model order arbitrarily large with PEM is that, as more parameters are estimated, the complexity of the problem increases, and it is more difficult to find the global minimum.

However, if a high order ARX model is estimated, there are no issues with local minima, while the order is arbitrarily large. Then, for the model reduction step, an approximate asymptotic ML criterion allows separating the estimation of the plant and noise model (Wahlberg, 1989). This allows obtaining asymptotically efficient estimates of the plant in open loop without the high order structure of the noise model affecting the difficulty of the problem. Nevertheless, the model reduction step still requires solving a non-convex optimization problem. The ASYM method (Zhu, 2001) is based on this approach.

Another approach that does not require a parametric noise model is the BJSM method (Zhu and Hjalmarsson, 2016). This method uses a high order ARX model estimate to pre-filter the input and output data, creating a pre-filtered data set for which the output noise is approximately white. Then, a noise model is no longer required when estimating the plant based on the pre-filtered data set. Instead of explicitly minimizing a non-convex function, BJSM applies the Steiglitz-McBride to the pre-filtered data set. In Zhu and Hjalmarsson (2016), it is shown that this procedure is asymptotically efficient in open loop. However, there are two limitations. First, even if the true noise model is known exactly, a high order estimate is still required to achieve efficiency. Second, although the method does not apply local non-linear optimization techniques, the number of Steiglitz-McBride iterations needs to tend to infinity to obtain a consistent estimate.

Our contributions are the following. First, we make a connection between ASYM and BJSM, and propose a method—termed model order reduction Steiglitz-McBride (MORSM)—connecting ideas from both. More specifically, the asymptotic ML criterion of the ASYM method is reformulated in a way that techniques from BJSM can be used to minimize it. Second, we show that MORSM is asymptotically efficient in open loop with one iteration. Third, we perform a simulation study, where we observe that MORSM has better finite sample convergence properties than BJSM, and that it is a viable alternative to PEM.

3.2 Problem formulation

Assumption 3.1 (True system)**.** The system has scalar input $u(t)$, scalar output $y(t)$ and is subject to scalar noise $e(t)$. The relationship between these signals is given by

$$y(t) = G^o(q)u(t) + H^o(q)e(t), \tag{3.1}$$

where $G^o(q)$ and $H^o(q)$ are rational functions

$$G^o(q) = \frac{L^o(q)}{F^o(q)} = \frac{l_1^o q^{-1} + \cdots + l_{m_l}^o q^{-m_l^o}}{1 + f_1^o q^{-1} + \cdots + f_{m_f}^o q^{-m_f^o}},$$
$$H^o(q) = \frac{C^o(q)}{D^o(q)} = \frac{1 + c_1^o q^{-1} + \cdots + c_{m_c}^o q^{-m_c^o}}{1 + d_1^o q^{-1} + \cdots + d_{m_d}^o q^{-m_d^o}}.$$

The transfer functions G^o, H^o, and $1/H^o$ are assumed to be stable. The polynomials L^o and F^o—as well as C^o and D^o—do not share common factors.

Let the input sequence $\{u(t)\}$ be a realization of a stochastic process generated by a random sequence $\{w(t)\}$. Also, let $\mathcal{F}_{t-1}$ be the σ-algebra generated by $\{e_s, w_s, s \leq t-1\}$. Then, the following assumption applies for the input signal.

Assumption 3.2 (Input)**.** The sequence $\{u(t)\}$ is defined by

$$u(t) = F_u(q)w(t),$$

where $F_u(q)$ is a stable and inversely stable finite dimensional filter, where $\{w(t)\}$ is independent of $\{e(t)\}$, satisfying

$$\mathbf{E}\{w(t)|\mathcal{F}_{t-1}\} = 0, \qquad \mathbf{E}\{w^2(t)|\mathcal{F}_{t-1}\} = \sigma_o^2, \qquad |w(t)| \leq C, \forall t$$

for some finite positive finite constant C.

Assumption 3.2 implies that the system is operating in open loop. Also, F_u can be interpreted as the stable minimum phase spectral factor of the input spectrum.

For the noise, the following assumption applies.

Assumption 3.3 (Noise)**.** $\{e(t)\}$ is a stochastic process that satisfies

$$\mathbf{E}\{e(t)|\,\mathcal{F}(t-1)\} = 0, \qquad \mathbf{E}\left\{ e^2(t) \middle|\, \mathcal{F}(t-1) \right\} = \sigma_o^2, \qquad \mathbf{E}\left\{ |e(t)|^{10} \right\} \leq C, \forall t$$

for some positive finite constant C.

3.3 The Prediction Error Method

The idea of PEM is to minimize a cost function of the prediction errors. In this section, we discuss how PEM can be used to estimate a model of the system (3.1). First, we consider a Box-Jenkins (BJ) model, and then a high order ARX model.

3.3.1 Box-Jenkins model

In a Box-Jenkins model, $G(q)$ and $H(q)$ are rational transfer functions parameterized independently, according to

$$y(t) = G(q,\theta)u(t) + H(q,\alpha)e(t), \tag{3.2}$$

where

$$G(q,\theta) = \frac{L(q,\theta)}{F(q,\theta)} = \frac{l_1 q^{-1} + \cdots + l_{m_l} q^{-m_l}}{1 + f_1 q^{-1} + \cdots + f_{m_f} q^{-m_f}},$$
$$H(q,\alpha) = \frac{C(q,\alpha)}{D(q,\alpha)} = \frac{1 + c_1 q^{-1} + \cdots + c_{m_c} q^{-m_c}}{1 + d_1 q^{-1} + \cdots + d_{m_d} q^{-m_d}},$$

and

$$\theta = \begin{bmatrix} f_1 \\ \vdots \\ f_{m_f} \\ l_1 \\ \vdots \\ l_{m_l} \end{bmatrix}, \qquad \alpha = \begin{bmatrix} c_1 \\ \vdots \\ c_{m_c} \\ d_1 \\ \vdots \\ d_{m_d} \end{bmatrix}. \tag{3.3}$$

We assume that $H^o(q)$ is in the model set defined by $H(q,\alpha)$ (*i.e.*, $m_c \geq m_c^o$ and $m_d \geq m_d^o$). Moreover, the order of the polynomials of $G^o(q)$ are assumed to be known (*i.e.*, $m_f = m_f^o$ and $m_l = m_l^o$). For simplicity of notation only, we also assume that $m := m_f = m_l$.

The one step ahead prediction errors of the Box-Jenkins (BJ) model (3.2) are given by

$$\varepsilon(t,\theta,\alpha) = \frac{D(q,\alpha)}{C(q,\alpha)}\left[y(t) - \frac{L(q,\theta)}{F(q,\theta)}u(t)\right].$$

The parameter estimates using PEM with a quadratic cost function are determined by minimizing the loss function

$$V_N(\theta,\alpha) = \frac{1}{N}\sum_{t=1}^{N}\varepsilon^2(t,\theta,\alpha), \tag{3.4}$$

where N is the number of data samples. We denote by $\hat{\theta}_N^{\text{PEM}}$ the estimate of θ obtained by minimizing (3.4). Moreover, θ_o corresponds to the vector θ evaluated at the coefficients of $F^o(q)$ and $L^o(q)$.

Since the system operates in open loop (Assumption 3.2), it is well known that, when PEM is applied to the model (3.2), under weak conditions, the (normalized) error of the estimated parameters $\hat{\theta}_N^{\text{PEM}}$ converges to the Gaussian distribution (Ljung, 1999)

$$\sqrt{N}\big(\hat{\theta}_N^{\text{PEM}} - \theta_o\big) \in \mathcal{N}\big(0, \sigma_o^2 M_{\text{CR}}^{-1}\big), \qquad \text{as } N \to \infty,$$

where the asymptotic covariance matrix (we omit the argument of the transfer functions for brevity)

$$M_{\text{CR}} = \frac{1}{2\pi\sigma_o^2}\int_{-\pi}^{\pi}\begin{bmatrix} -\frac{G^o}{F^oH^o}\Gamma_m \\ \frac{1}{F^oH^o}\Gamma_m \end{bmatrix}\begin{bmatrix} -\frac{G^o}{F^oH^o}\Gamma_m \\ \frac{1}{F^oH^o}\Gamma_m \end{bmatrix}^{*}\Phi_u\, d\omega,$$

with $\Gamma_m(q) = [\, q^{-1} \;\ldots\; q^{-m}\,]^\top$ and Φ_u the spectrum of the input $\{u(t)\}$.

When $\{e(t)\}$ is Gaussian, PEM with a quadratic cost function is asymptotically efficient, meaning that M_{CR}^{-1} corresponds to the Cramér-Rao lower bound—the smallest possible asymptotic covariance matrix for a consistent estimator(Ljung, 1999). Again, we recall that only the orders of $G^o(q)$ need to be chosen correctly to achieve efficiency, while $H(q,\alpha)$ only needs to include $H^o(q)$. Thus, if only a model for $G^o(q)$ is of interest, and the order of $H^o(q)$ is unknown, m_c and m_d can be let grow to infinity (guaranteeing that $H^o(q)$ is in the model set) without asymptotically affecting the estimate of θ.

An important remark is that minimizing the loss function (3.4) is a non-convex optimization problem. Therefore, a good initialization point is required to converge to the global minimum. For Box-Jenkins models, an initialization point that is sufficiently close to the global minimum is particularly challenging to obtain. Moreover, the problem becomes yet more challenging if we want to let the order of the noise model $H(q,\alpha)$ be arbitrarily large, as PEM will have increased problems with local minima.

3.3.2 High order ARX model

To circumvent the limitations of solving a non-convex optimization problem, we consider the following approach. Note that the system (3.1) can be represented as

$$A^o(q)y(t) = B^o(q)u(t) + e(t), \tag{3.5}$$

where

$$A^o(q) := \frac{1}{H^o(q)} =: 1 + \sum_{k=1}^{\infty} a_k^o q^{-k},$$
$$B^o(q) := \frac{G^o(q)}{H^o(q)} =: \sum_{k=1}^{\infty} b_k^o q^{-k}$$

are stable transfer functions (by Assumption 3.1).

Consider also the ARX model

$$A(q,\eta^n)y(t) = B(q,\eta^n)u(t) + e(t),$$

where

$$A(q,\eta^n) = 1 + \sum_{k=1}^{n} a_k q^{-k}, \qquad B(q,\eta^n) = \sum_{k=1}^{n} b_k q^{-k}, \tag{3.6}$$

and

$$\eta^n = \begin{bmatrix} a_1 & \dots & a_n & b_1 & \dots & b_n \end{bmatrix}^\top.$$

Here, we assumed, without loss of generality, that $A(q)$ and $B(q)$ are both modeled with n coefficients. Note that (3.5) is not in the model set defined by (3.6) due to the truncation by n coefficients. Nevertheless, the stability assumption on $G^o(q)$ and $1/H^o(q)$ implies that $\{a_k^o\}$ and $\{b_k^o\}$ are sequences converging to zero. Thus, if n is chosen large enough, (3.6) can model (3.5) with good accuracy.

An advantage of ARX models is that they are linear in the model parameters. In particular, the PEM estimate of η^n is obtained by minimizing the cost function

$$V_N(\eta^n) = \frac{1}{N}\sum_{t=1}^{N}\left[A(q,\eta^n)y(t) - B(q,\eta^n)u(t)\right]^2, \tag{3.7}$$

which can be done by linear least squares. Thus, it can be solved as follows. Write (3.6) as

$$y(t) = \left[\varphi^n(t)\right]^\top \eta^n + e(t),$$

where

$$\varphi^n(t) = \begin{bmatrix} -y_{t-1} & \dots & -y_{t-n} & u_{t-1} \dots & u_{t-n} \end{bmatrix}^\top. \tag{3.8}$$

Then, the least squares estimate of η^n is given by

$$\hat{\eta}_N^{n,ls} := \left(R_N^n\right)^{-1} r_N^n, \tag{3.9}$$

where

$$R_N^n = \frac{1}{N}\sum_{t=1}^{N} \varphi^n(t)(\varphi^n(t))^\top, \qquad r_N^n = \frac{1}{N}\sum_{t=1}^{N} \varphi^n(t)y(t).$$

In the analysis, we will use the slightly modified estimate

$$\hat{\eta}_N^n := \left(R_{N,\mathrm{reg}}^n\right)^{-1} r_N^n, \tag{3.10}$$

where

$$R_{N,\mathrm{reg}}^n = \begin{cases} R_N^n & \text{if} \left\| [R_N^n]^{-1} \right\|_2 < 2/\delta \\ R_N^n + \frac{\delta}{2} I_{2n} & \text{otherwise} \end{cases},$$

for some small $\delta > 0$. The reason is that $\hat{\eta}_N^n$ is easier to analyze statistically, while the first and second order statistical properties of $\hat{\eta}_N^{n,ls}$ and $\hat{\eta}_N^n$ are asymptotically identical (Ljung and Wahlberg, 1992).

It follows from Assumption 3.2 and Assumption 3.3 (see Ljung and Wahlberg (1992) for details),

$$\hat{\eta}_N^n \to \bar{\eta}^n := \left[\bar{R}^n\right]^{-1} \bar{r}^n,$$

where $\bar{R}^n$ and $\bar{r}^n$ are the limits of R_N^n and r_N^n w.p.1, respectively.

To guarantee that the true system (3.5) is asymptotically in the model set defined by the ARX model (3.6), n should be allowed to grow to infinity. Accordingly, we let the model order depend on the sample size N. For our theoretical results, we use the following assumption.

Assumption 3.4 (Model order)**.** It holds that

$$\begin{aligned} n(N) &\to \infty, \quad \text{as} \quad N \to \infty, \\ n(N)^{4+\delta}/N &\to 0, \quad \text{as} \quad N \to \infty, \end{aligned}$$

for some $\delta > 0$.

Introduce the notation $\hat{\eta}_N := \hat{\eta}_N^{n(N)}$ and, for future reference,

$$\eta_o^n := \begin{bmatrix} a_1^o & \dots & a_n^o & b_1^o & \dots & b_n^o \end{bmatrix}^\top, \tag{3.11}$$

$$\eta_o := \begin{bmatrix} a_1^o & a_2^o & \dots & b_1^o & b_2^o & \dots \end{bmatrix}^\top. \tag{3.12}$$

The asymptotic properties of $\hat{\eta}_N$ have been established in Ljung and Wahlberg (1992). We will need the following result on the rate of convergence of the ARX model.

Lemma 3.1. *Assume that Assumptions 3.1, 3.2, 3.3 and 3.4 hold. Then with probability 1,*

$$\sup_{\omega} \left\| \begin{bmatrix} A\left(\mathrm{e}^{\mathrm{j}\omega}, \hat{\eta}_N\right) - A^o\left(\mathrm{e}^{\mathrm{j}\omega}\right) \\ B\left(\mathrm{e}^{\mathrm{j}\omega}, \hat{\eta}_N\right) - B^o\left(\mathrm{e}^{\mathrm{j}\omega}\right) \end{bmatrix} \right\|_2 = \mathcal{O}(m(N)),$$

where

$$m(N) = n(N)\sqrt{\log N / N}(1 + d(N)) + d(N)$$

and

$$d(N) := \sum_{k=n(N)+1}^{\infty} \left|a_k^o\right| + \left|b_k^o\right| \leq \bar{C}\rho^{n(N)}, \tag{3.13}$$

for some $\bar{C} < \infty$ and $\rho < 1$.

Proof. See Appendix 3.A.1. ■

Lemma 3.1 implies that, as N tends to infinity, the coefficients of $A\left(q, \hat{\eta}_N\right)$ converge to those of $A^o(q) = 1/H^o(q)$, and the coefficients of $B\left(q, \hat{\eta}_N\right)$ converge to those of $B^o(q) = G^o(q)/H^o(q)$. Therefore, $B\left(q, \hat{\eta}_N\right)/A\left(q, \hat{\eta}_N\right)$ can be used as a high order estimate of $G^o(q)$, and $1/A\left(q, \hat{\eta}_N\right)$ as a high order estimate of $H^o(q)$. We thus define these high order estimates by

$$G\left(q, \hat{\eta}_N\right) := \frac{B\left(q, \hat{\eta}_N\right)}{A\left(q, \hat{\eta}_N\right)}, \qquad H\left(q, \hat{\eta}_N\right) := \frac{1}{A\left(q, \hat{\eta}_N\right)}. \tag{3.14}$$

Despite the simplicity of ARX models, they are not appropriate to model (3.1) for most practical uses. As the order n is required to be arbitrarily large, the estimated model will have unacceptably high variance.

Nevertheless, the high order ARX model estimate can be used to obtain a model of low order, reducing the variance. This can be done efficiently without re-using the data. The reason is that the estimate $\hat{\eta}_N$ and its covariance are asymptotically a sufficient statistic for our problem as we saw in Section 2.2.1.

3.4 Model reduction

Having estimated a high order ARX model, we are interested in using this estimate to obtain a low order estimate $G(q, \theta)$. In this section, we discuss available approaches to do so.

3.4.1 Exact Maximum Likelihood

Being a sufficient statistic, $\hat{\eta}_N$ and its covariance can be used to obtain an estimate of θ that is asymptotically efficient. This can be done using an exact ML criterion (Wahlberg, 1989). Let $\eta^n(\theta, \alpha)$ be the parameter vector η^n obtained from θ and α, satisfying the relations

$$A(q, \eta) = \frac{1}{H(q, \alpha)}, \qquad B(q, \eta) = \frac{G(q, \theta)}{H(q, \alpha)}.$$

This procedure consists in minimizing

$$\left[\hat{\eta}_N - \eta^n(\theta, \alpha)\right]^\top \left[\mathbf{Cov}\left\{\hat{\eta}_N\right\}\right]^{-1} \left[\hat{\eta}_N - \eta^n(\theta, \alpha)\right],$$

where $\mathbf{Cov}\left\{\hat{\eta}_N\right\}$ denotes the covariance of the estimated vector $\hat{\eta}_N$. Since this covariance matrix is in general unknown, in practice the cost function (3.15) requires an approximation. We consider two possibilities that do not affect the asymptotic properties of the obtained estimates.

One possibility consists in replacing $\left[\mathbf{Cov}\left\{\hat{\eta}_N\right\}\right]^{-1}$ by a consistent estimate—for example, R_N^n (Wahlberg, 1989). In this case, we minimize

$$\left[\hat{\eta}_N - \eta^n(\theta, \alpha)\right]^\top R_N^n \left[\hat{\eta}_N - \eta^n(\theta, \alpha)\right], \tag{3.15}$$

which yields asymptotically efficient estimates of $G(q, \theta)$ and $H(q, \alpha)$. Because $\eta^n(\theta, \alpha)$ is nonlinear in general, minimizing (3.15) is a non-convex optimization problem.

Another possibility is to write the covariance matrix as function of the low order parameters θ and α—denoted $R^n(\theta, \alpha)$ (see Wahlberg (1989) for details). In this case, we minimize the criterion

$$\left[\hat{\eta}_N - \eta^n(\theta, \alpha)\right]^\top R^n(\theta, \alpha) \left[\hat{\eta}_N - \eta^n(\theta, \alpha)\right], \tag{3.16}$$

Although minimizing (3.16) seems, at first sight, more complicated than minimizing (3.15), it is observed in Wahlberg (1989) that the cost function (3.16) can be approximated by an asymptotic ML criterion that allows separating the estimation of $G(q, \theta)$ and $H(q, \alpha)$, while still providing asymptotically efficient estimates.

3.4.2 Asymptotic Maximum Likelihood (ASYM)

As shown in Wahlberg (1989), minimizing (3.16) is asymptotically the same as minimizing

$$\frac{1}{2\pi} \int_{-\pi}^{\pi} \left| G\left(e^{j\omega}, \hat{\eta}_N\right) - G\left(e^{j\omega}, \theta\right) \right|^2 \frac{\boldsymbol{\Phi}_u\left(e^{j\omega}\right)}{\left| H\left(e^{j\omega}, \hat{\eta}_N\right) \right|^2} \, d\omega$$

$$+ \frac{\hat{\sigma}^2}{2\pi} \int_{-\pi}^{\pi} \frac{\left| H\left(e^{j\omega}, \hat{\eta}_N\right) - H\left(e^{j\omega}, \alpha\right) \right|^2}{\left| H\left(e^{j\omega}, \hat{\eta}_N\right) \right|^2} \, d\omega, \tag{3.17}$$

where $\hat{\sigma}^2$ is a consistent estimate of σ_o^2. Because the first term in (3.17) is only dependent on $G(q,\theta)$ and the second term on $H(q,\alpha)$, $G(q,\theta)$ can be estimated by minimizing the first term. The minimization problem we are interested in becomes

$$V_N(\theta) = \int_{-\pi}^{\pi} \left| G\left(e^{j\omega}, \hat{\eta}_N^n\right) - G\left(e^{j\omega}, \theta\right) \right|^2 \frac{\Phi_u\left(e^{j\omega}\right)}{\left| H\left(e^{j\omega}, \hat{\eta}_N\right) \right|^2} \, d\omega. \tag{3.18}$$

The idea of the ASYM method (Zhu, 2001) is to minimize the time domain equivalent to (3.18) for finite sample size:

$$V_N(\theta) = \frac{1}{N} \sum_{t=1}^{N} \left(\left[\frac{B\left(q, \hat{\eta}_N\right)}{A\left(q, \hat{\eta}_N\right)} - G(q,\theta) \right] A\left(q, \hat{\eta}_N\right) u(t) \right)^2. \tag{3.19}$$

Minimizing (3.19) is still a non-convex optimization problem. However, it is pointed out in Zhu (2001) that this minimization problem has an advantage over directly estimating $G(q,\theta)$ using PEM, which makes the method numerically more reliable. Because the output is not used explicitly in (3.19), and the noise contribution is only present indirectly through the high order estimates, the influence of the disturbance is reduced.

3.4.3 BJSM method

In alternative to using local non-linear optimization techniques, the BJSM method uses the Steiglitz-McBride iterations. The idea of BJSM is to first estimate a high order ARX model and then apply the Steiglitz-McBride method (Steiglitz and McBride, 1965) to a data set pre-filtered by the ARX model estimate. The estimates obtained are asymptotically efficient in open loop. Because BJSM uses the Steiglitz-McBride, we start by reviewing the latter.

Steiglitz-McBride

The setting for the Steiglitz-McBride algorithm is when the transfer function $H^o(q)$ equals one (*i.e.* $C^o(q) = D^o(q) = 1$). The objective is to estimate $L(q,\theta)$ and $F(q,\theta)$.

Consider the following three steps. First, an ARX model

$$F(q,\theta)y(t) = L(q,\theta)u(t) + e(t)$$

is estimated using least squares, providing an initialization estimate $\hat{\theta}_N^0$. Second, the output and input are filtered by

$$y^f(t) = \frac{1}{F\left(q, \hat{\theta}_N^1\right)} y(t), \qquad u^f(t) = \frac{1}{F\left(q, \hat{\theta}_N^1\right)} u(t).$$

Third, least squares is applied to the ARX model

$$F(q,\theta)y^f(t) = L(q,\theta)u^f(t) + e(t),$$

providing a new estimate—$\hat{\theta}_N^1$. Then, we can continue to iterate by repeating Steps 2 and 3. We define the estimate obtained at iteration k by $\hat{\theta}_N^k$.

Notice that, since the true system has an output error (OE) structure, and we are estimating an ARX model, we are actually minimizing, in Step 1, the function

$$V_N(\theta) = \frac{1}{N}\sum_{t=1}^{N}[F(q,\theta)y(t) - L(q,\theta)u(t)]^2, \tag{3.20}$$

which, evaluated at the true parameter θ_o, equals

$$V_N(\theta_o) = \frac{1}{N}\sum_{t=1}^{N}\left[F(q,\theta_o)e(t)\right]^2. \tag{3.21}$$

From (3.21), we observe that the true parameter θ_o does not correspond to the cost function of a white sequence. Consequently, the initialization estimate $\hat{\theta}_N^0$ is not consistent. However, at iteration k we have, evaluated at $\theta = \theta_o$,

$$V_N(\theta_o) = \frac{1}{N}\sum_{t=1}^{N}\left[\frac{F(q,\theta_o)}{F(q,\hat{\theta}_N^k)}e(t)\right]^2. \tag{3.22}$$

So, assuming convergence to the true parameters (*i.e.*, $\hat{\theta}_N^k \to \theta_o$, as $k \to \infty$ and $N \to \infty$), (3.22) asymptotically corresponds to (3.4) for an OE model structure.

Convergence of the Steiglitz-McBride has been studied in Stoica and Söderström (1981), where it is shown that the method is locally convergent when the additive output noise is white. Moreover, it will be globally convergent if the signal-to-noise ratio is sufficiently large. Assuming convergence, the estimates are asymptotically Gaussian distributed. However, in general, the covariance of the estimated parameters does not asymptotically attain M_{CR}^{-1}.

The Steiglitz-McBride is thus an attempt to minimize (3.4), but it only does so consistently with additive white noise, and even then it is not asymptotically efficient.

BJSM

In Zhu and Hjalmarsson (2016), the BJSM algorithm is introduced. This algorithm copes with two limitations of the Steiglitz-McBride. First, it is consistent for systems with BJ structure, instead of only OE. Second, it is asymptotically efficient for open loop data.

The method uses the following procedure. First, an ARX model (3.6) is estimated with least squares. Second, the original data set is pre-filtered by $A(q,\hat{\eta}_N)$. Third, the Steiglitz-McBride algorithm is applied to the pre-filtered data set.

Recall that, to be convergent, the Steiglitz-McBride algorithm requires that $H^o(q) = 1$. The main idea of BJSM is thus to use $A\left(q, \hat{\eta}_N\right)$ as an estimate of $[H^o(q)]^{-1}$ and pre-filter the data according to

$$y^{\text{pf}}(t) = A\left(q, \hat{\eta}_N\right) y(t), \qquad u^{\text{pf}}(t) = A\left(q, \hat{\eta}_N\right) u(t).$$

Then, the pre-filtered data satisfies

$$y^{\text{pf}}(t) = \frac{L^o(q)}{F^o(q)} u^{\text{pf}}(t) + A\left(q, \hat{\eta}_N\right) H^o(q) e(t), \tag{3.23}$$

which asymptotically is according to, due to Lemma 3.1,

$$y^{\text{pf}}(t) \approx \frac{L^o(q)}{F^o(q)} u^{\text{pf}}(t) + e(t). \tag{3.24}$$

Since (3.24) is of OE structure, the Steiglitz-McBride algorithm can be applied to the data set $\{y^{\text{pf}}(t), u^{\text{pf}}(t)\}$.

Notice that, if we were to apply PEM to the pre-filtered data set, we would minimize, motivated by (3.24),

$$V_N(\theta) = \frac{1}{N} \sum_{t=1}^{N} \left(y^{\text{pf}}(t) - \frac{L(q,\theta)}{F(q,\theta)} u^{\text{pf}}(t) \right)^2. \tag{3.25}$$

To avoid an explicit non-convex minimization problem, we use the Steiglitz-McBride method instead. Although the Steiglitz-McBride is not asymptotically efficient, the BJSM method is when used with open loop data (Zhu and Hjalmarsson, 2016).

However, not all the information in $\hat{\eta}_N$ is being used, as the filtering (3.23) only uses $A\left(q, \hat{\eta}_N\right)$. In other words, the ARX model is not used as a sufficient statistic for this problem. For the method to still be asymptotically efficient, the output data are used when constructing the pre-filtering. This leads to two limitations.

The first is a counter-intuitive result. Suppose that $H^o(q) = 1$ (*i.e.*, the true system is already of OE structure). Then, we have that $A^o(q) = 1$, and estimating a FIR model would suffice to asymptotically model the true system. However, this would maintain the data set unchanged when applying the filtering (3.23), and BJSM would simply be reduced to the Steiglitz-McBride method, which is not asymptotically efficient. If, on the other hand, it is not assumed that $A^o(q) = 1$ and an estimate $A\left(q, \hat{\eta}_N\right)$ is still computed, BJSM will be asymptotically efficient. Thus, although an FIR model is asymptotically a sufficient statistic for a system of OE structure (like the ARX model is for BJ structures) it is not possible to make use of this information when applying the BJSM method, since it does not exploit the full statistical properties of the high order model.

As for the second limitation, we observe that although BJSM avoids solving a non-convex optimization problem by applying the Steiglitz-McBride algorithm, it has the disadvantage

of requiring the number of iterations of the Steiglitz-McBride to tend to infinity in order to provide consistent and asymptotically efficient estimates (Zhu and Hjalmarsson, 2016). To bypass this problem but still avoid a non-convex minimization procedure, we use the Steiglitz-McBride with the ASYM method. This will allow us to obtain an asymptotically efficient estimate in one iteration.

3.5 Model Order Reduction Steiglitz-McBride

The objective of our approach is to minimize (3.19) without using a non-convex optimization method. To do so, we use an approach that combines ideas from ASYM and BJSM.

First, we write (3.19) as

$$V_N(\theta) = \frac{1}{N}\sum_{t=1}^{N}\left[B\big(q,\hat{\eta}_N\big)u(t) - \frac{L(q,\theta)}{F(q,\theta)}A\big(q,\hat{\eta}_N\big)u(t)\right]^2. \tag{3.26}$$

Then, we notice that (3.26) has the same form as (3.25) if we define

$$y^{\text{pf}}(t) := B\big(q,\hat{\eta}_N\big)u(t), \qquad u^{\text{pf}}(t) := A\big(q,\hat{\eta}_N\big)u(t), \tag{3.27}$$

and thus the same idea (*i.e.* applying the Steiglitz-McBride to $\{y^{\text{pf}}(t), u^{\text{pf}}(t)\}$) can be used.

The only difference between this approach and BJSM is in the pre-filtered output. Comparing (3.27) and (3.23), we observe that $u^{\text{pf}}(t)$ are defined similarly, but $y^{\text{pf}}(t)$ are different. The difference lies in the true output not being used to construct the new pre-filtered data set. Rather, it is simulated from the input and the ARX model estimate. Indeed, we can simulate the output with

$$y^{s}(t) := \frac{B\big(q,\hat{\eta}_N\big)}{A\big(q,\hat{\eta}_N\big)}u(t), \tag{3.28}$$

and then apply the same filter as in (3.23), but on the simulated output, according to

$$y^{\text{pf}}(t) = A\big(q,\hat{\eta}_N\big)y^{s}(t) = B\big(q,\hat{\eta}_N\big)u(t), \tag{3.29}$$

obtaining the proposed pre-filter (3.27).

In summary, the proposed method is as follows:

1. estimate an ARX model using the input-output data $\{u(t), y(t)\}$, $t = 1, \dots, N$, according to (3.9);
2. construct the pre-filtered data $\{u^{\text{pf}}(t), y^{\text{pf}}(t)\}$, according to (3.27);
3. apply the Steiglitz-McBride method with $\{u^{\text{pf}}(t), y^{\text{pf}}(t)\}$ to obtain estimates $L(q,\hat{\theta}_N)$ and $F(q,\hat{\theta}_N)$ of $L^o(q)$ and $F^o(q)$, respectively.

Note that the pre-filtered data set (3.27) only depends on the original output data $\{y(t)\}$ through the least squares estimate $\hat{\eta}_N$. With this method, we treat the high order ARX model as if it was a sufficient statistic for our problem, and disregard the data without loss of information (asymptotically). Indeed, as will be shown in the next section, this procedure is asymptotically efficient for open loop data.

Moreover, there are two advantages for disregarding the data after the high order ARX model has been estimated. Although these are formally shown in the next section, we observe them here, supported by intuitive explanations.

First, the pre-filter (3.27) uses the complete statistical information contained in the estimate $\hat{\eta}_N$. So, if the noise contribution affecting the true system (3.1) is white, a high-order FIR model can be estimated instead of an ARX. In this case, $A\left(q, \hat{\eta}_N\right) = 1$.

Second, this procedure asymptotically (in N) only requires one iteration. To intuitively understand why this is the case, we recall why the Steiglitz-McBride is an iterative method. Note that the initialization step of the Steiglitz-McBride minimizes (3.20), which, when evaluated at the true parameters, as in (3.21), does not correspond to a cost function of a white sequence. Therefore, the initialization estimate $\hat{\theta}_N^0$ is biased. Then, we start iterating. At the first iteration, the cost function evaluated at θ_o is given by (3.22) with $F(q, \hat{\theta}_N^0)$. Because $F(q, \hat{\theta}_N^0)$ is biased, the true parameter will still not correspond to the cost function of a white sequence. Therefore, the new estimate $\hat{\theta}_N^1$ will not be consistent either. However, by continuing to iterate, it can be shown that, under the conditions observed in Stoica and Jansson (2000), $\hat{\theta}_N^k \to \theta_o$, as $k \to \infty$ and $N \to \infty$. Concerning the original BJSM method, since the pre-filtered data is according to (3.23), it is asymptotically approximately an OE model structure, and a similar procedure takes place.

On the other hand, the alternative pre-filtering, which disregards the original data, satisfies

$$y^{\mathrm{pf}}(t) = \frac{L^o(q)}{F^o(q)} u^{\mathrm{pf}}(t) + \left(\frac{B\left(q, \hat{\eta}_N\right)}{A\left(q, \hat{\eta}_N\right)} - \frac{L^o(q)}{F^o(q)} \right) u^{\mathrm{pf}}(t). \tag{3.30}$$

This is a noise-free equation, except for the noisy parameters in the ARX model. However, from Lemma 3.1, the second term in (3.30) tends to zero asymptotically. As consequence, the variance of the error sequence being minimized by the Steiglitz-McBride iterations disappears asymptotically, and only one iteration is required.

We observe that the proposed method essentially consists of applying the Steiglitz-McBride algorithm to perform model order reduction based on an asymptotic ML criterion. We will thus refer to the method as model order reduction Steiglitz-McBride (MORSM).

The idea of using the Steiglitz-McBride to, in some sense, perform model order reduction, is not new. Variants of the Steiglitz-McBride method have been applied to estimate rational filters from an impulse response estimate, instead of applying the method directly to data (see, *e.g.* Evans and Fischl, 1973; McClellan and Lee, 1991; Shaw, 1994). However, although some of these procedures are in some sense optimal under specific conditions, we consider

a quite general system identification problem and motivate the application of the method based on an ML criterion. This, as we proceed to show, not only provides asymptotically efficient estimates under a quite general class of systems and external signals, but also does so in one iteration.

3.5.1 Noise Model

One of the advantages of MORSM is that it does not requires a noise-model order selection. However, if a low-order noise model is wanted, it can be estimated independently of the plant model using a similar procedure, starting from the second term in(3.17). Minimizing this term is the same as minimizing, in the time domain,

$$V_N^H(\alpha) = \frac{1}{N}\sum_{t=1}^{N}\left[\frac{1}{D(q,\alpha)}\big(D(q,\alpha)e(t) - C(q,\alpha)A\big(q,\hat{\eta}_N\big)e(t)\big)\right]^2. \tag{3.31}$$

We recognize that the Steiglitz-McBride can be applied to (3.31) with (assuming $\{e(t)\}$ is available)

$$y^k(t) := \frac{1}{D\big(q,\hat{\alpha}_N^{k-1}\big)}e(t), \qquad u^k(t) := \frac{A\big(q,\hat{\eta}_N\big)}{D\big(q,\hat{\alpha}_N^{k-1}\big)}e(t). \tag{3.32}$$

Then, the estimate $\hat{\alpha}_N^{k+1}$ is given by

$$\hat{\alpha}_N^{k+1} = \left[\frac{1}{N}\sum_{t=1}^{N}\varphi^k(t)\big[\varphi^k(t)\big]^\top\right]^{-1}\frac{1}{N}\sum_{t=1}^{N}\varphi^k(t)y^k(t). \tag{3.33}$$

Although $\{e(t)\}$ is not available, the terms $\varphi^k(t)\big(\varphi^k(t)\big)^\top$ and $\varphi^k(t)y^k(t)$ contain products $e(i)e(j)$, which may be replaced by a scaling of the respective expected value (*i.e.*, $\mathbf{E}\{e(i)e(j)\} = 0$ if $i \neq j$ and $\mathbf{E}\{e(i)e(j)\} = 1$ if $i = j$).

3.6 Asymptotic properties

In this section, we analyze both the convergence and asymptotic covariance of MORSM. To derive these results, we will need a formal expression for the estimate of θ at iteration $k+1$ of the MORSM algorithm. Define

$$y(t,\eta,\theta) = \frac{B(q,\eta)}{F(q,\theta)}u(t), \qquad y\big(t,\eta_o,\theta\big) = \frac{B^o(q)}{F(q,\theta)}u(t),$$
$$u(t,\eta,\theta) = \frac{A(q,\eta)}{F(q,\theta)}u(t), \qquad y\big(t,\eta_o,\theta\big) = \frac{A^o(q)}{F(q,\theta)}u(t),$$

and

$$\xi(t,\eta,\theta) = \frac{L^o(q)}{F^o(q)}\frac{B(q,\eta)-B^o(q)}{B^o(q)}u(t,\eta,\theta) - \frac{A(q,\eta)-A^o(q)}{A^o(q)}y(t,\eta,\theta).$$

The same definition also applies to vector valued signals, such as (3.8).

Using that the pre-filtered data set consists of filtered versions of $u(t)$ and that $G(q)$ can be represented both using $L^o(q)$ and $F^o(q)$ as well as using $B^o(q)$ and $A^o(q)$, we have that

$$u(t) = \frac{1}{B\big(q,\hat{\eta}_N\big)}y^{\mathrm{pf}}(t) = \frac{L^o(q)A^o(q)}{F^o(q)B^o(q)}\frac{1}{A\big(q,\hat{\eta}_N\big)}u^{\mathrm{pf}}(t). \tag{3.34}$$

Filtering (3.34) by

$$F^o(q)\frac{A\big(q,\hat{\eta}_N\big)B\big(q,\hat{\eta}_N\big)}{A^o(q)F\big(q,\hat{\eta}_N\big)},$$

we arrive at the noise-free equation

$$F^o(q)\frac{A\big(q,\hat{\eta}_N\big)}{A^o(q)}y\big(t,\hat{\eta}_N,\hat{\theta}_N^k\big) = L^o(q)\frac{B\big(q,\hat{\eta}_N\big)}{B^o(q)}u\big(t,\hat{\eta}_N,\hat{\theta}_N^k\big)$$

relating the pre-filtered data. Equivalently,

$$F^o(q)y\big(t,\hat{\eta}_N,\hat{\theta}_N^k\big) = L^o(q)u\big(t,\hat{\eta}_N,\hat{\theta}_N^k\big) + F^o(q)\xi\big(t,\hat{\eta}_N,\hat{\theta}_N^k\big),$$

which can be written in regression form as

$$y\big(t,\hat{\eta}_N,\hat{\theta}_N^k\big) = \big[\varphi^m\big(t,\hat{\eta}_N,\hat{\theta}_N^k\big)\big]^\top\theta_o + F^o(q)\xi\big(t,\hat{\eta}_N,\hat{\theta}_N^k\big). \tag{3.35}$$

Given $\hat{\theta}_N^k$, the next parameter estimate in the Steiglitz-McBride iterations $\hat{\theta}_N^{k+1}$, is defined as the least squares estimate of θ_o in the linear regression (3.35):

$$\hat{\theta}_N^{k+1} = \big[R^m\big(\hat{\eta}_N,\hat{\theta}_N^k\big)\big]^{-1}r^m\big(\hat{\eta}_N,\hat{\theta}_N^k\big), \tag{3.36}$$

where

$$R^m(\eta^n,\theta) = \frac{1}{N}\sum_{t=m+1}^{N}\varphi^m(t,\eta^n,\theta)\big[\varphi^m(t,\eta^n,\theta)\big]^\top,$$

$$r^m(\eta^n,\theta) = \frac{1}{N}\sum_{t=m+1}^{N}\varphi^m(t,\eta^n,\theta)y(t,\eta^n,\theta).$$

Notice that (3.35) is a linear regression form of (3.30) with the notable difference that the error made in the ARX model enters linearly into $\xi(t,\hat{\eta}_N,\hat{\theta}_N^k)$. The initialization step of the

Steiglitz-McBride algorithm in MORSM, estimating an ARX model, corresponds to the second and third step of the algorithm without pre-filtering, *i.e.*, with $F(q, \hat{\theta}_N^{-1}) \equiv 1$. Thus, the initialization step $\hat{\theta}_N^0$ is contained in the analysis of the iterations. As before, the ARX model error tends to zero asymptotically. This is, in essence, what enables the following results.

Theorem 3.2. *Let Assumptions 3.1, 3.2, 3.3, and 3.4 hold. Then,*

$$\hat{\theta}_N^k \to \theta_o \quad as \quad N \to \infty, \text{ w.p. } 1, \quad \text{for all } k \geq 0$$

Proof. See Appendix 3.A.2. ■

Theorem 3.2 implies that the proposed algorithm achieves consistency in the initialization estimate—that is, $\hat{\theta}_N^0$ is a consistent estimate of θ_o.

For the asymptotic covariance, we have the following theorem.

Theorem 3.3. *Let Assumptions 3.1, 3.2, 3.3, and 3.4 hold. Then,*

$$\lim_{N\to\infty} N \boldsymbol{E}\left\{ \left(\hat{\theta}_N^k - \theta_o\right)\left(\hat{\theta}_N^k - \theta_o\right)^\top \right\} = \sigma_o^2 \boldsymbol{M}_{CR}^{-1},$$

and $\sqrt{N}\left(\hat{\theta}_N^k - \theta_o\right) \sim \mathcal{N}\left(0, \sigma_o^2 \boldsymbol{M}_{CR}^{-1}\right)$, *as* $N \to \infty$, *for* $k \geq 1$.

Proof. See Appendix 3.A.4. ■

From Theorem 3.3, we observe that the proposed method has the same asymptotic covariance as PEM with Gaussian noise (3.5). Therefore, it is asymptotically efficient with open loop data. Moreover, it is obtained in one iteration, *i.e.*, for $k = 1$.

3.7 Numerical simulations

In this section, we perform Monte Carlo simulations to study the performance of the method. First, we illustrate the advantages with respect to the BJSM algorithm, with which is bears similarities, and how it may be an appropriate method to initialize PEM. Second, we perform comparisons to other methods using systems where PEM can have difficulties with local minima.

3.7.1 Advantages with respect to BJSM

Although using different motivations, the algorithms for MORSM and BJSM have close similarities. In Zhu and Hjalmarsson (2016), simulation studies have been performed with examples where BJSM can be an alternative to PEM when PEM has convergence problems. Here, we illustrate how BJSM and MORSM typically perform similarly given that the algorithms converge, but that MORSM converges much faster. First, we illustrate how MORSM only requires one iteration for an asymptotically efficient estimate, while this is not sufficient for BJSM. Second, we illustrate how even when (for finite sample size) MORSM requires more than one iteration for convergence, it is still a much faster converging method than BJSM.

One iteration scheme

In the first simulation, we illustrate that MORSM, unlike BJSM, gives an asymptotically efficient estimate in one iteration.

For the simulation, the data are generated by

$$y(t) = \frac{q^{-1} + 0.1q^{-2}}{1 - 1.2q^{-1} + 0.6q^{-2}}u(t) + \frac{1 + 0.7q^{-1}}{1 - 0.9q^{-1}}e(t). \tag{3.37}$$

One hundred Monte Carlo simulations are performed with eight sample sizes logarithmically spaced between $N = 200$ and $N = 20000$. The sequence $\{u(t)\}$ is obtained by

$$u(t) = \frac{1}{1 - q^{-1} + 0.89q^{-2}}w(t), \tag{3.38}$$

where $\{w(t)\}$ and $\{e(t)\}$ are independent Gaussian white sequences with unit variance.

We compare PEM, BJSM (one and 100 iterations), and MORSM (one and 100 iterations). All methods estimate a plant parameterized with the correct orders, and PEM also estimates a correctly parameterized noise model. For BJSM and MORSM, an ARX model of order 50 is estimated in the first step. In the iterative versions, the estimate obtained in the last iteration is the one used. As the objective of this simulation is to observe convergence and asymptotic variance properties, PEM is started at the true parameters, and all methods assume known initial conditions.

The results are presented in Figure 3.1, where the average root mean square error (RMSE) of the impulse response from 1000 Monte Carlo runs is presented for each sample size. The RMSE is given by

$$\text{RMSE} = \|g^o - \hat{g}\|_2, \tag{3.39}$$

where g^o is the impulse response of $G^o(q)$ and $\hat{g}$ is the impulse response of the estimated plant model. In Figure 3.1, we observe that MORSM and BJSM perform similarly with

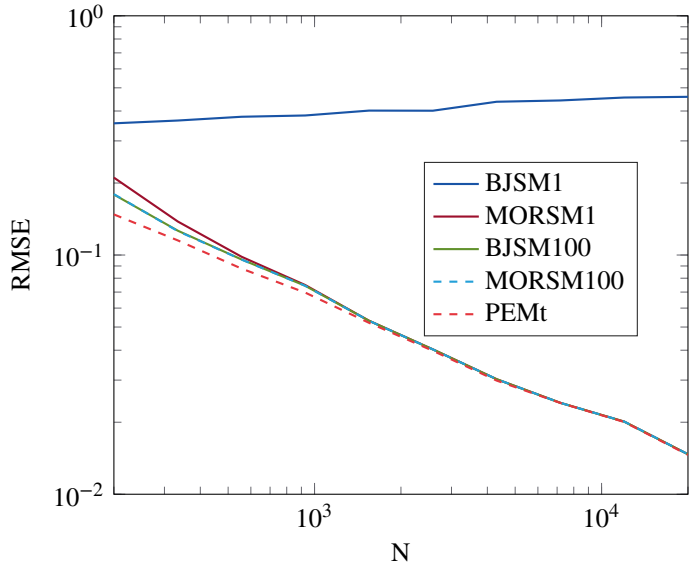

Figure 3.1: Average RMSE as function of sample size for several methods, obtained from 200 Monte Carlo runs with a fixed system.

100 iterations for all the sample size range used. MORSM performs slightly worse with one iteration than with 100 for small sample sizes, but they have the same performance for larger N. However, the same is not true for BJSM with one iteration, for which the RMSE does not even decrease with increasing sample size.

In conclusion, if a sufficiently amount of iterations are performed, both MORSM and BJSM attain the asymptotic covariance of PEM. However, BJSM theoretically needs the Steiglitz-McBride iterations to tend to infinity, while MORSM only needs one iteration.

Convergence Speed

In the following simulation, we will compare the performance of PEM and the proposed method with randomly generated systems, with structure

$$y(t) = \frac{l_1^o q^{-1} + l_2^o q^{-2} + l_3^o q^{-3} + l_4^o q^{-4}}{1 + f_1^o q^{-1} + f_2^o q^{-2} + f_3^o q^{-3} + f_4^o q^{-4}} u(t) \tag{3.40}$$

$$+ \frac{1 + c_1^o q^{-1} + c_2^o q^{-2} + c_3^o q^{-3} + c_4^o q^{-4}}{1 + d_1^o q^{-1} + d_2^o q^{-2} + d_3^o q^{-3} + d_4^o q^{-4}} e(t), \tag{3.41}$$

Table 3.1: Sample mean, sample standard deviation and theoretical standard deviation for MORSM with 100 iterations.

N	True values	-1.200	0.600	1.000	0.100
200	Sample mean	-1.195	0.594	1.000	0.109
	Sample σ	0.043	0.039	0.063	0.105
	Theoretical σ	0.033	0.031	0.050	0.080
20000	Sample mean	-1.200	0.600	1.000	0.100
	Sample σ	0.003	0.003	0.005	0.008
	Theoretical σ	0.003	0.003	0.005	0.008

where $\{u(t)\}$ is given as in the previous simulation, and $\{e(t)\}$ is Gaussian white noise with variance chosen to obtain a signal-to-noise ratio

$$\text{SNR} = \frac{\sum_{t=1}^{N}[G^o(q)u(t)]^2}{\sum_{t=1}^{N}[H^o(q)e(t)]^2} = 5. \tag{3.42}$$

The coefficients of $L^o(q)$ are generated from a uniform distribution, with values between -1 and 1. The coefficients of the remaining polynomials are generated such that $F^o(q)$, $C^o(q)$, and $D^o(q)$ have all roots inside a half-ring in the unit disc with a radius between 0.7 and 0.9, with positive real part. We do this with the objective of studying a particular class of systems: namely, the systems are effectively of fourth order (*i.e.*, no poles are extremely dominant over others), they can be approximated by ARX models roughly of orders between 30 and 100, and they resemble physical systems.

An important practical aspect in implementing the proposed method is how to choose the ARX model order, in case we do not previously have information of an appropriate order to choose. As we have seen, theoretically the ARX model order should tend to infinity as function of the sample size. However, for practical purposes it is sufficient to choose an order that can correctly capture the dynamics of the true system. We then propose the following procedure to choose the order of the ARX model. Since our objective is to minimize the loss function (3.4) using an indirect approach, we repeat the estimation for a grid of ARX model orders, and choose the low order model that minimizes (3.4). Because with MORSM we do not need to compute a low-order model $H(q, \alpha)$, we may use the highest order ARX polynomial $A\left(q, \hat{\eta}_N\right)$ instead when computing the loss function (3.4). Although this is a very noisy estimate, the error induced will be the same for every computation. For the class of systems we consider, we choose the ARX model order from a grid of values between 25 and 125, spaced with intervals of 25.

Moreover, when more than one iteration is used, the same criterion can be applied to optimize over the number of iterations—that is, we choose the model obtained at the iteration that minimizes the cost function (3.4).

We consider the following methods:

- the prediction error method, initialized at the true parameters (PEMt);
- the Box-Jenkins Steiglitz-McBride (BJSM).
- the iterative model order reduction Steiglitz-McBride (MORSM);
- the iterative Model Order Reduction Steiglitz-McBride method, estimating also a noise model (MORSMh);
- the one-iteration Model Order Reduction Steiglitz-McBride, estimating also a low-order noise model (MORSM1h).

All the iterative methods perform a maximum of 10000 iterations. MORSM and BJSM have a stopping criterion of 10^{-4} as tolerance for normalized norm of the last iteration, and PEM uses the default 10^{-2}. With PEM, we estimate initial conditions, and with MORSM and BJSM we truncate them. Although a procedure to estimate initial conditions for this type of methods has been proposed in Galrinho et al. (2015a), it is only applicable if the plant and noise model share the same poles (*e.g.*, autoregressive moving average (ARMA), ARMAX) or if the noise model poles are known (*e.g.*, OE), which is not the case of BJ models.

The performance of each method is evaluated by calculating the FIT of the impulse response of the plant, given by, in percent,

$$\text{FIT} = 100\left(1 - \frac{\text{RMSE}}{\|g^o - \bar{g}^o\|}\right), \tag{3.43}$$

where $\bar{g}^o$ is the average of g^o.

The results are presented in Figure 3.2, with the average FIT as function of sample size. Unlike in Figure (3.1), this more challenging scenario and for the range of sample sizes does not allow to observe that one iteration of MORSM provides an asymptotically efficient estimate. If we continue to iterate, there is an improvement in the obtained model estimate, and both MORSM (without low-order noise-model estimate) and BJSM perform similarly, attaining the performance of PEM (initialized at the true parameters) for this range of sample sizes.

The performance of MORSM also improves for small sample size if a noise model is estimated in the iterative version. The estimation of $H(q, \alpha)$, as pointed out in Section 3.5.1, is independent of the estimation of $G(q, \theta)$. The improvement observed in the model estimate is because having an estimate of $H(q, \alpha)$ allows for a more accurate computation of (3.4) when choosing the best model over all the iterations.

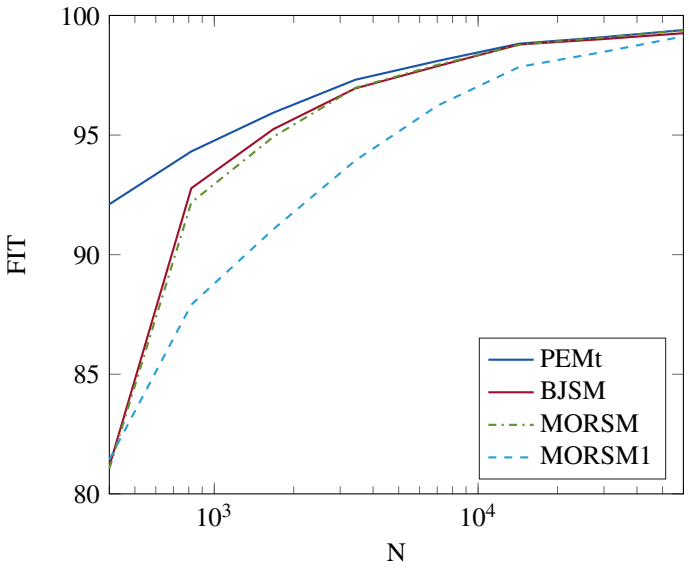

Figure 3.2: Average FIT for several methods, obtained from 100 Monte Carlo runs with random systems.

The fact that, for finite sample size, both MORSM and BJSM require more than one iteration for convergence does not render MORSM useless with respect to BJSM. In Table 3.2, we indicate the average number of iterations required for MORSM and BJSM to converge, for the difference sample sizes used. From here, we conclude that, even when MORSM needs more than one iteration to converge, it still converges faster than BJSM. Moreover, BJSM needs approximately the same amount of iterations independently of sample size, while the number of iterations required for MORSM decreases with sample size. This is in accordance with our theoretical result that, asymptotically, MORSM gives an efficient estimate in one iteration.

Initialization for PEM

Here, we illustrate how MORSM can be an appropriate method to initialize PEM. For that, we repeat the simulation in the previous section with the following methods:

- the prediction error method, with default MATLAB initialization (PEMd);
- the prediction error method, with MORSM1h as initialization (PEMm1);
- the prediction error method, with MORSMh as initialization (PEMm).

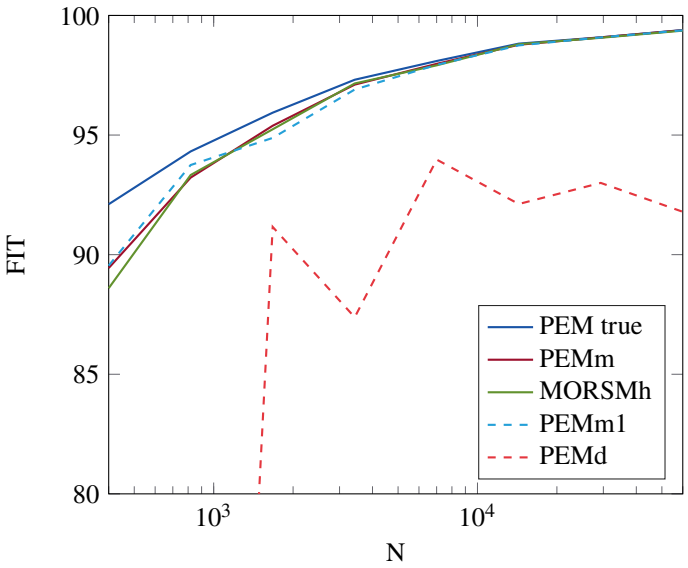

Figure 3.3: Average FIT for several methods, obtained from 100 Monte Carlo runs with random systems.

The results are presented in Figure 3.3, where we can compare how PEM performs with the default MATLAB initialization and with the MORSM initialization, as well as how much PEM can improve the MORSM estimate. For reference, we also include PEMt and MORSMh from the previous simulation.

In Figure 3.3, we see that the standard MATLAB initialization for PEM is not always accurate enough to find the global minimum: for all the sample sizes used, there are cases when PEM does not converge to the same parameters as PEMt, which decreases the average FIT. On the other hand, there is a considerable improvement for PEM if it is initialized with MORSM, performing close to PEM initialized at the true parameters for the smallest sample sizes and identically otherwise. However, initializing with one iteration of MORSM or with the iterative version gives identical performance. Therefore, if MORSM is used to initialize PEM, it may not be needed to wait for MORSM to converge. Alternatively, the iterative version of MORSM with low-order noise model estimate also performs similar to these: in this case, using it to initialize PEM showed no improvement. As initialization for PEM, a few iterations of MORSM might be a good compromise as the number of PEM iterations decreases with iterative MORSM compared to only one MORSM iteration (*cf.* Table 3.2).

Table 3.2: Average number of iterations until convergence for several methods and different sample sizes. For PEM with different initializations, only the PEM iterations are counted.

Method\N	400	818	3425	7007	29328	60000
BJSM	46	54	116	111	119	117
MORSM	23	13	8	6	4	3
PEM	18	18	15	16	12	18
PEMt	7	5	3	2	2	2
PEMm	7	4	2	1	1	1
PEMm1	10	6	4	3	2	1

3.7.2 Comparison with other methods

In this section, we perform a simulation study with two systems for which PEM has difficulty finding the global minimum. We point out to settings where MORSM is a good alternative to PEM and other competitive methods.

The following methods will be compared:

- the prediction error method, with default MATLAB initialization (PEMd);
- subspace method with CVA weighting (SS);
- refined instrumental variable method (RIV);
- the iterative model order reduction Steiglitz-McBride (MORSM);
- the prediction error method, initialized at the true parameters (PEMt).

PEMd, SS and PEMt are according to the implementation in MATLAB2016b with default settings. RIV is according to the implementation in the CAPTAIN toolbox v7.5:11 with default settings. With PEM and RIV, the plant and noise models always have the correct order. With SS, the state-space model order is chosen as the maximum order of the plant and noise model. With MORSM, the plant is estimated with the correct order, and the noise model is of high order.

Here, we do not initialize PEM with MORSM, as we want to make use of the feature that MORSM does not require estimating a low-order noise model. However, we include PEM initialized at the true parameters as benchmark.

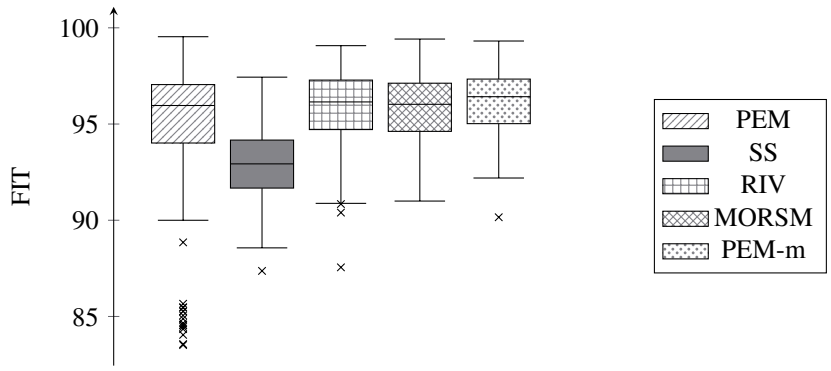

Figure 3.4: Boxplot of FIT for several methods, obtained from 100 Monte Carlo runs of System 1.

System 1: widely separated eigenvalues

The first system we consider is given by

$$G_o(q) = \frac{0.016 + 0.026q^{-1} - 0.0375q^{-2}}{1 - 1.6252q^{-1} + 0.642q^{-2}}. \tag{3.44}$$

This system, with its widely separated eigenvalues, is problematic for PEM in some conditions if the initial conditions are not very close to the true parameter values (Young, 2008). Here, we begin by repeating the simulation in Young (2008), for which RIV does not have the same convergence problems as PEM. In the considered scenario,

$$H_o(q) = \frac{1 + 0.5q^{-1}}{1 - 0.85q^{-1}}, \tag{3.45}$$

$\{u_t\}$ and $\{e_t\}$ are zero-mean Gaussian white-noise sequences with variances 8.8 and 0.0009, respectively, and the sample size is $N = 1700$. We perform 100 Monte Carlo simulations.

The obtained FITs are shown in Figure 3.4. Confirming the results in Young (2008), there is probably a local minimum for the PEM cost function giving a FIT around 85, where the optimization procedure often converges to with the default initialization in MATLAB. In this simulation, the subspace method CVA is an appropriate approach to avoid the local-minimum issue with PEM; however, the median performance is inferior to PEM. Also RIV avoids the problematic local minimum of PEM, but has a median performance superior to subspace. Finally, MORSM performs similarly to RIV and to PEM initialized at the true parameters.

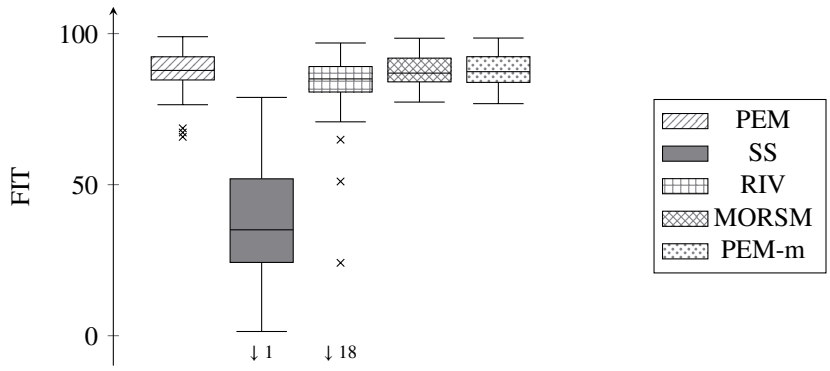

Figure 3.5: Boxplot of FIT for several methods, obtained from 100 Monte Carlo runs of System 1 with the more complicated noise model.

We now consider the same simulation settings except for the noise model, now given by

$$H_o(q) = \frac{1 + 0.23q^{-1} + 0.07q^{-2} + 0.05q^{-3} + 0.014q^{-4}}{1 - 3.04q^{-1} + 3.85q^{-2} - 2.36q^{-3} + 0.616q^{-4}}. \tag{3.46}$$

In this case, the results are given in Figure 3.5. PEM with the default MATLAB initialization has less instances of significantly lower performance than in the previous scenario; however, the optimization did not converge at all in two cases. Subspace CVA is not competitive, having poor median performance. Although RIV has a median performance similar to PEM, it has a considerable amount of instances of significantly lower performance. Finally, MORSM has a median performance similar to RIV and PEM, but with no instances of significantly lower performance. In this case, there could still be margin to improve the MORSM estimate, as PEM when initialized at the true parameters has a slightly better median performance.

System 2: resonance peaks

The second system we consider is a 6th order system with three resonance peaks, given by

$$G_o(q) = \frac{0.08q^{-1} + 0.53q^{-2} - 0.29q^{-3} + }{1 - 1.89q^{-1} + 2.26q^{-2} - 1.78q^{-3} + } \\ \frac{\cdots - 0.51q^{-4} + 0.23q^{-5} + 0.04q^{-6}}{\cdots + 1.63q^{-4} - 1.09q^{-5} + 0.56q^{-6}}. \tag{3.47}$$

Also here, we consider two scenarios. In both scenarios, the noise model is given by

$$H_o(q) = \frac{1 + 0.8q^{-1}}{1 - 0.9q^{-1}}, \tag{3.48}$$

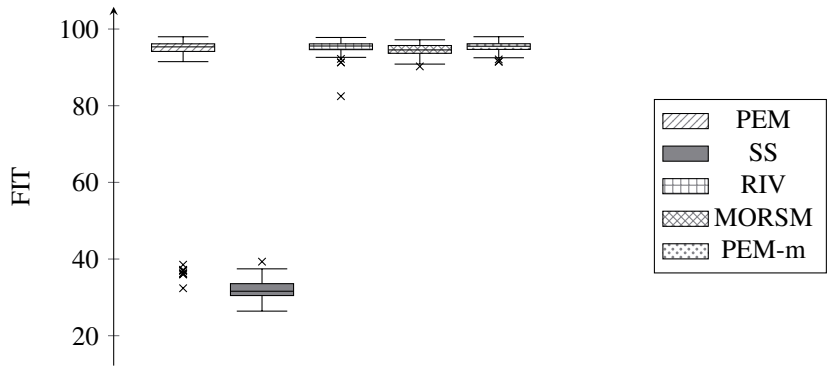

Figure 3.6: Boxplot of FIT for several methods, obtained from 100 Monte Carlo runs of System 2.

$\{e_t\}$ is a Gaussian white-noise sequence with unit variance, and the sample size is $N = 2600$. The input will be different in each scenario. In the first, $\{u_t\}$ is a Gaussian white-noise sequence with unit variance.

The FITs obtained from 100 Monte Carlo simulations are shown in Figure 3.6. Like the case in Figure 3.4, there is a local minimum in the PEM cost function corresponding to FIT between 30 and 40%, to where the optimization procedure often converges with the standard MATLAB initialization. The subspace method also provides a model that gives a FIT around 30–40%. Also like in Figure 3.4, RIV and MORSM always avoid the non-global minimum that PEM sometimes converges to, and both perform close to PEM initialized at the true parameters.

In the following, we show a scenario where MORSM is considerably advantageous with respect to the remaining methods. The setting is the same as before, except for the input. In this case, the input is given by

$$u(t) = \frac{\sqrt{0.05}}{1 - 1.85q^{-1} + 0.87q^{-2}} w(t), \tag{3.49}$$

where $\{w(t)\}$ is the input from the previous simulation.

The FITs obtained from 100 Monte Carlo simulations are shown in Figure 3.7. Here, PEM with the default MATLAB initialization also has a considerable amount of instances of significantly lower performance. The subspace methods is favored with this setting compared to the previous one, but the median performance is still worse than PEM. Here, the median performance of RIV is only slightly inferior to that of PEM, and it also has a considerable amount of instances of significantly lower performance. On the other hand, MORSM has no instances of significantly lower performance, while the median performance is only slightly inferior to that of PEM and RIV. Despite the robust performance of MORSM, it does not

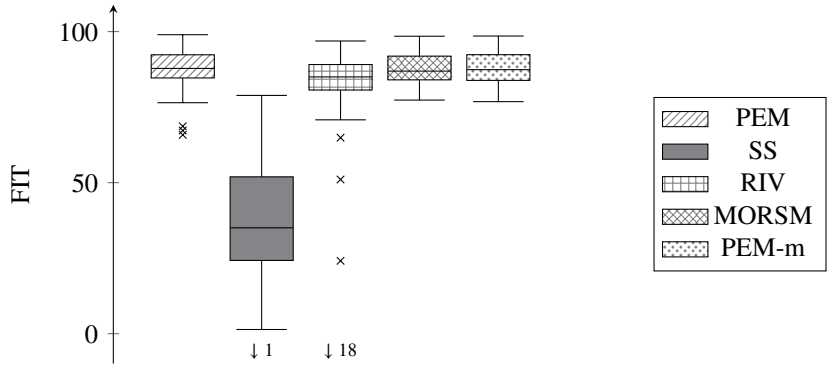

Figure 3.7: Boxplot of FIT for several methods, obtained from 100 Monte Carlo runs of System 2 with colored input signal.

attain the performance of PEM initialized with the true parameters, meaning that MORSM is not converging to the global minimum of PEM, but still always finds a model with good performance.

3.8 Summary

In this chapter, we proposed a least squares method for estimation of models with a plant parameterized by a rational transfer function and a high order noise model. The method was shown to provide consistent and asymptotically efficient estimates of the plant if data are obtained in open loop.

Essentially, the method performs model order reduction based on an asymptotic ML criterion using the Steiglitz-McBride method. We thus name it model order reduction Steiglitz-McBride (MORSM). The method uses ideas from the ASYM and BJSM methods. However, unlike ASYM, we avoid a non-convex optimization procedure by applying Steiglitz-McBride; unlike BJSM, we propose a procedure that only requires one iteration to provide asymptotically efficient estimates.

Finally, we performed two simulation studies to analyze the performance of the method, from which the following are observed. First, MORSM is asymptotically efficient in one iteration, while BJSM is not. Second, even when extra iterations are required for convergence with finite sample sizes, MORSM still converges in less iterations than BJSM. Third, MORSM may be a viable alternative to PEM, specially when PEM has difficulty in finding the global minimum.

3.A Proofs and auxilliary lemmas

3.A.1 Proof of Lemma 3.1

The result follows from Theorem 3.1 in Ljung and Wahlberg (1992). Next, we verify the conditions of that theorem. Assumption 3.1 and the finite dimensionality of G^o and H^o implies that

$$\max\big(|a_k|, |b_k|\big) \leq C\rho^k \tag{3.50}$$

for some $C < \infty$ and $0 < \rho < 1$. This implies that Condition S1 holds. Furthermore, the bound (3.50) implies the inequality in (3.13) for some $\bar{C} < infty$. Assumption 3.3 clearly implies Condition S2 (for any $p \leq 5$). Assumption 3.4 implies Conditions D1 and D3. Thus all conditions in Theorem 3.1 of Ljung and Wahlberg (1992) have been verified and the result in the lemma follows from this theorem.

3.A.2 Proof of Theorem 3.2

Using Parseval's formula, we have

$$\bar{R}(\theta) = \frac{1}{2\pi}\int_{-\pi}^{\pi} \begin{bmatrix} -B^o\Gamma_m \\ A^o\Gamma_m \end{bmatrix} \begin{bmatrix} -B^o\Gamma_m \\ A^o\Gamma_m \end{bmatrix}^* \frac{\Phi_u}{|F(\theta)|^2}\, d\omega \tag{3.51}$$

We notice that $\bar{R}(\theta) > 0$ whenever θ is in the stability region for the coefficients of polynomials of degree m

$$\bar{S} := \big\{\theta \in \mathbb{R}^{2m} \;:\; F(z,\theta) = 0 \Rightarrow |z| < 1\big\}. \tag{3.52}$$

We introduce the notation

$$f(N) = \mathcal{O}(g(N))$$

to mean that $f(N)$ decays to zero with the rate $g(N)$, *i.e.*, that there exists some positive constants C and N_0 such that for all $N \geq N_0$,

$$\|f(N)\| \leq C|g(N)| \;\text{ as }\; N \to \infty.$$

From Lemma 3.1 it follows that

$$R^m\big(\hat{\eta}_N, \theta\big) - \bar{R}(\theta) = \mathcal{O}(m(N)). \tag{3.53}$$

By standard continuity arguments, with probability 1

$$R^m\big(\hat{\eta}_N, \theta\big) > 0$$

for large enough N. Hence, for N large enough, using (3.35) in (3.36)

$$\hat{\theta}_N^{k+1} = \theta_o + \left[R^m\left(\hat{\eta}_N, \theta_N^k\right)\right]^{-1} \frac{1}{N} \sum_{t=m+1}^{N} \varphi^m\left(t, \eta^n, \theta_N^k\right) F^o(q)\xi\left(t, \hat{\eta}_N, \hat{\theta}_N^k\right). \quad (3.54)$$

Now, since $\{u(t)\}$ is uniformly bounded and $1/F(q,\theta)$ is uniformly stable, it follows that

$$\left\|\varphi^m\left(t, \hat{\eta}_N, \theta_N^k\right)\right\| \leq C_1,$$

for some $C_1 < \infty$, and furthermore, by Lemma 3.1, it follows that

$$F^o(q)\xi\left(t, \hat{\eta}_N, \hat{\theta}_N^k\right) = \mathcal{O}(m(N)).$$

It thus follows that

$$\hat{\theta}_N^{k+1} - \theta_o = \mathcal{O}(m(N)), \quad (3.55)$$

for any $k \geq 0$ and

$$\left\|\hat{\theta}_N^{k+1} - \theta_o\right\| \to 0, \quad \text{as N} \to \infty, \text{ w.p. 1.}$$

3.A.3 Auxiliary lemmas

This section includes a few results needed for the proof of Theorem 3.3 in Section 3.A.4.

Lemma 3.4. *Assume that $X(q) = \sum_{k=1}^{n} x_k q^{-k}$ and $Z(q) = \sum_{l=1}^{n} z_l q^{-l}$ are stable filters and let $v(t)$ be quasi-stationary. Then,*

$$\left\|\frac{1}{N} \sum_{t=m+1}^{N} X(q)v(t)Z(q)v(t)\right\|_2 \leq \|X\|_2 \|Z\|_2 C$$

for some $C < \infty$.

Proof.

$$\begin{aligned}
\left\|\frac{1}{N} \sum_{t=m+1}^{N} X(q)v(t)Z(q)v(t)\right\|^2 &= \left\|\frac{1}{N} \sum_{t=m+1}^{N} \sum_{k=1}^{n} x_k v_{t-k} \sum_{l=1}^{n} z_l v_{t-l}\right\|^2 \\
&= \left\|\sum_{k=1}^{n} x_k \sum_{l=1}^{n} z_l \frac{1}{N} \sum_{t=m+1}^{N} v_{t-k}v_{t-l}\right\|^2 \\
&\leq \sum_{k=1}^{n} |x_k|^2 \sum_{l=1}^{n} |z_l|^2 \left|\frac{1}{N} \sum_{t=m+1}^{N} v_{t-k}v_{t-l}\right|^2 \\
&\leq \sum_{k=1}^{n} |x_k|^2 \sum_{l=1}^{n} |z_l|^2 \left|R_{vv}^N(k-l)\right|^2 \\
&\leq \|X\|_2^2 \|Z\|_2^2 C^2,
\end{aligned}$$

where the last equality is due to the quasi stationarity of $v(t)$. ■

Lemma 3.5. *Let Assumptions 3.1, 3.2, 3.3, and 3.4 be in force. Let Y^n be an $m \times 2n$ deterministic matrix, with m fixed. Then, we have that*

$$\sqrt{N} Y^n \left[\hat{\eta}_N - \bar{\eta}^n\right] \sim \mathcal{N}(0, P), \quad \text{as } N \to \infty, \tag{3.56}$$

where

$$P = \sigma_o^2 \lim_{n\to\infty} Y^n \left[\bar{R}^n\right]^{-1} \left[Y^n\right]^\top, \tag{3.57}$$

if the limit exists.

Proof. See Ljung and Wahlberg (1992, Theorem 7.3). ■

Lemma 3.6. *Let $\{x_n\}$ be a sequence of random variables that is asymptotically Gaussian distributed—$\{x_n\} \sim \mathcal{N}(0, P)$ as $N \to \infty$. Let $\{M_n\}$ be a sequence of random square matrices that converge in probability to a non-singular matrix M, and $\{b_n\}$ be a sequence of random vectors that converges in probability to b. Also, let*

$$y_n = M_n x_n + b_n. \tag{3.58}$$

Then, y_n converges in distribution to $\mathcal{N}\left(b, MPM^\top\right)$.

Proof. See Söderström and Stoica (1989, Lemma B.4). ■

Lemma 3.7. *Let S_n be the subspace of $\mathcal{L}_2^2$ spanned by the rows of*

$$\begin{bmatrix} -F_1 F_2 \Gamma_n & F_3 \Gamma_n \\ F_2 \Gamma_n & 0 \end{bmatrix}, \tag{3.59}$$

where

$$\Gamma_n(q) = \begin{bmatrix} q^{-1} & \dots & q^{-n} \end{bmatrix}^\top, \tag{3.60}$$

$$F_i(q) = \sum_{k=0}^{\infty} f_k^i q^{-k}. \tag{3.61}$$

Suppose that F_1, F_2 and F_3 are exponentially stable, i.e.*, for an exponentially stable F_i*

$$|f_k^i| \le C\lambda^k, \qquad \text{for some } C < \infty, \qquad \lambda < 1, \tag{3.62}$$

and that there is a causal exponentially stable inverse

$$\tilde{F}_2(q) = \sum_{k=0}^{\infty} \tilde{f}_k^2 q^{-k}, \quad |\tilde{f}_k|^2 < C\lambda^k. \tag{3.63}$$

Let $\gamma = \left[\sum_{k=1}^{\infty} d_k q^{-k} \; 0\right]$ be exponentially stable. Then

$$\left\|\gamma - \boldsymbol{Proj}_{S_n}\{\gamma\}\right\|_2 \le C\lambda^n, \qquad \text{for some } C < \infty, \qquad \lambda < 1. \tag{3.64}$$

Proof. We will construct an explicit approximation to γ that belongs to S_n. Let

$$\tilde{F}_2\gamma = \begin{bmatrix} \sum_{l=1}^{\infty} \beta_l z^{-l} & 0 \end{bmatrix},$$

which is exponentially stable since both γ and $\tilde{F}_2$ are exponentially stable. Take as approximation for γ

$$\hat{\gamma_n} = \begin{bmatrix} \sum_{l=1}^{n} \beta_l F_2(z) z^{-l} & 0 \end{bmatrix},$$

which by construction belongs to S_Ψ. Introduce the notation $\gamma = [\,\gamma_1 \;\gamma_2\,]$. Hence

$$\begin{aligned} \left\| \gamma_k - \mathbf{Proj}_{S_{\tilde{\Psi}}}\{\gamma\} \right\|_2 &\le \left\| \gamma - \hat{\gamma}_n \right\|_2 \\ &= \left\| \gamma_1 - \sum_{l=1}^{n} \beta_l F_2(z) z^{-l} \right\|_2 \\ &= \left\| F_2(z) \left[\tilde{F}_2(z)\gamma_1 - \sum_{l=1}^{n} \beta_l z^{-l} \right] \right\|_2 \\ &\le \left\| F_2(z) \right\|_2 \left\| \sum_{l=n+1}^{\infty} \beta_l z^{-l} \right\|_2 \\ &\le C\lambda^n, \end{aligned}$$

for some $C < \infty$ and $\lambda < 1$ since F_2 and $\tilde{F}_2\gamma$ are exponentially stable. ∎

3.A.4 Proof of Theorem 7.3

We start by using (3.54) to write

$$\sqrt{N}\left(\hat{\theta}_N^{k+1} - \theta_o\right) = M_N^{-1} x_N,$$

where

$$\begin{aligned} M_N &= R^m\left(\hat{\eta}_N, \theta_N^k\right) \\ x_N &= \frac{1}{\sqrt{N}} \sum_{t=m+1}^{N} \varphi^m\left(t, \hat{\eta}_N, \theta_N^k\right) F^o(q) \xi\left(t, \hat{\eta}_N, \hat{\theta}_N^k\right). \end{aligned}$$

From (3.53) and Theorem 3.2, for $k \ge 1$, we have that

$$M_N \to M_{CR}, \quad \text{as } N \to \infty, \quad \text{w.p. } 1.$$

Assume for now (we will prove it later) that

$$x_N \sim \mathcal{N}(0, P), \quad \text{as } N \to \infty.$$

Then, using Lemma 3.6, we have that

$$\sqrt{N}\left(\hat{\theta}_N^{k+1} - \theta_o\right) \sim \mathcal{N}\left(0, M_{CR}^{-1} P M_{CR}^{-1}\right), \quad \text{as } N \to \infty. \tag{3.65}$$

3.A.5 x_N

We will now establish the asymptotic distribution and covariance of x_N. To this end, we first define

$$\begin{aligned}\boldsymbol{\Phi}^m(\eta^n,\theta) &:= \frac{1}{F(q,\theta)}\begin{bmatrix}-B(q,\eta^n)\Gamma_m\\ A(q,\eta^n)\Gamma_m\end{bmatrix},\\ \Xi^m(\eta^n,\theta) &:= \frac{F^o(q)}{A^o(q)F(q,\theta)}\begin{bmatrix}-B^o(q) & A^o(q)\end{bmatrix}\begin{bmatrix}A(q,\eta^n)-A^o(q)\\ B(q,\eta^n)-B^o(q)\end{bmatrix}.\end{aligned}$$

Then we rewrite $\xi\big(t,\hat{\eta}_N,\theta_N^k\big)$ as

$$\begin{aligned}\xi\big(t,\hat{\eta}_N,\theta_N^k\big) &= -\frac{B\big(q,\hat{\eta}_N\big)}{A^o(q)F\big(q,\theta_N^k\big)}\big[A\big(q,\hat{\eta}_N\big)-A^o(q)\big]u(t)\\ &\quad+\frac{A\big(q,\hat{\eta}_N\big)}{A^o(q)F\big(q,\theta_N^k\big)}\big[B\big(q,\hat{\eta}_N\big)-B^o(q)\big]u(t)\\ &= -\frac{B^o(q)}{A^o(q)F\big(q,\theta_N^k\big)}\big[A\big(q,\hat{\eta}_N\big)-A^o(q)\big]u(t)\\ &\quad+\frac{A^o(q)}{A^o(q)F\big(q,\theta_N^k\big)}\big[B\big(q,\hat{\eta}_N\big)-B^o(q)\big]u(t)\\ &= \frac{1}{F^o(q)}\Xi^m\big(\hat{\eta}_N,\theta_N^k\big)u(t).\end{aligned}$$

We can thus express x_N as

$$x_N = \frac{1}{\sqrt{N}}\sum_{t=m+1}^{N}\boldsymbol{\Phi}^m\big(\hat{\eta}_N,\theta_N^k\big)u(t)\Xi^m\big(\hat{\eta}_N,\theta_N^k\big)u(t).$$

We will in the remainder of the proof need some properties regarding the filters $\boldsymbol{\Phi}^m$ and Ξ^m that are easily established using Lemma 3.1:

$$\left\|\Xi^m(\hat{\eta}_N,\theta_N^k)\right\| = \mathcal{O}(m(N)) \tag{3.66}$$

$$\left\|\boldsymbol{\Phi}^m\big(\hat{\eta}_N,\theta_N^k\big)-\boldsymbol{\Phi}^m\big(\hat{\eta}_N,\theta^o\big)\right\| = \mathcal{O}(m(N)) \tag{3.67}$$

$$\left\|\boldsymbol{\Phi}^m\big(\hat{\eta}_N,\theta^o\big)-\boldsymbol{\Phi}^m(\eta^o,\theta^o)\right\| = \mathcal{O}(m(N)) \tag{3.68}$$

$$\left\|\Xi^m\big(\hat{\eta}_N,\theta_N^k\big)-\Xi^m\big(\hat{\eta}_N,\theta^o\big)\right\| = \mathcal{O}\big(m^2(N)\big) \tag{3.69}$$

$$\|\boldsymbol{\Phi}^m(\eta^o,\theta^o)\| = \mathcal{O}(1) \tag{3.70}$$

For future reference, we will establish the limit of $\sqrt{N}m^2(N)$. The dominating term in $m(N)$ is $n(N)\sqrt{\log N/N}$ and terms with $d(N)$ will be neglected. For N large enough, we

have

$$\lim_{N\to\infty} \sqrt{N} m^2(N) = \lim_{N\to\infty} \sqrt{N} n(N)^2 \frac{\log N}{N}$$
$$= \lim_{N\to\infty} \left[\frac{n(N)^{4+\delta}}{N}\right]^{\frac{2}{4+\delta}} \frac{\log N}{N^{\frac{\delta}{4+\delta}}} = 0,$$

where the first term goes to zero by Assumption 3.4.

Using Lemma 3.4 and Lemma 3.6 with (3.66) and (3.67), it follows that difference between x_N and

$$\frac{1}{\sqrt{N}} \sum_{t=m+1}^{N} \boldsymbol{\Phi}^m\big(\hat{\eta}_N, \theta_o\big) u(t) \Xi^m\big(\hat{\eta}_N, \theta_N^k\big) u(t) \tag{3.71}$$

tend to zero as $N \to \infty$ w.p.1, and therefore they have the same asymptotic distribution and the same asymptotic covariance. We will analyze (3.71) instead. Similarly, using Lemma 3.4 and Lemma 3.6 with (3.66) and (3.68), it follows that difference between (3.71) and

$$\frac{1}{\sqrt{N}} \sum_{t=m+1}^{N} \boldsymbol{\Phi}^m\big(\eta^o, \theta_o\big) u(t) \Xi^m\big(\hat{\eta}_N, \theta_N^k\big) u(t) \tag{3.72}$$

tend to zero as $N \to \infty$ w.p.1, and we will analyze (3.72) instead. Similarly, using Lemma 3.4 and Lemma 3.6 with (3.69) and (3.70), the difference between (3.72) and

$$\frac{1}{\sqrt{N}} \sum_{t=m+1}^{N} \boldsymbol{\Phi}^m\big(\eta^o, \theta_o\big) u(t) \Xi^m\big(\hat{\eta}_N, \theta^o\big) u(t) \tag{3.73}$$

tend to zero as $N \to \infty$ w.p.1, and we will analyze (3.73) instead.

We rewrite $\Xi^m(\hat{\eta}_N, \theta^o)u(t)$ as

$$\Xi^m\big(\hat{\eta}_N, \theta^o\big) u(t) = \frac{1}{A^o(q)} \begin{bmatrix} -B^o(q)u(t)\Gamma_n \\ A^o(q)u(t)\Gamma_n \end{bmatrix}^\top \big[\hat{\eta}_N - \bar{\eta}^n\big]$$
$$= \frac{1}{A^o(q)} \big[\varphi^n\big(t, \eta_o, \theta^o\big)\big]^\top \big[\hat{\eta}_N - \bar{\eta}^n\big]. \tag{3.74}$$

Thus, we have shown that x_N has the same distribution and covariance as

$$T_N := Z^n \sqrt{N} \big[\hat{\eta}_N - \bar{\eta}^n\big], \tag{3.75}$$

where

$$Z^n = \sum_{t=m+1}^{N} \varphi^m\big(t, \eta_o, \theta_o\big) \frac{F^o(q)}{A^o(q)} \big[\varphi^n\big(t, \eta_o, \theta_o\big)\big]^\top, \tag{3.76}$$

and we will analyze T_N instead.

3.A.6 Asymptotic covariance of T_N

Using Lemma 3.5, we have that

$$T_N \sim \mathcal{N}(0, Q), \quad \text{as } N \to \infty,$$

where

$$Q = \sigma_o^2 \lim_{n\to\infty} Z^n \left[\bar{R}^n\right]^{-1} \left[Z^n\right]^\top,$$

provided the right hand side limit exists. This will be shown next. We start by analyzing $\bar{R}^n$.

$$\begin{aligned}\bar{R}^n &= \mathbf{E}\left\{ \varphi^n(t)\left[\varphi^n(t)\right]^\top \right\} \\ &= \langle \Psi, \Psi \rangle,\end{aligned}$$

where Ψ is given by

$$\Psi = \begin{bmatrix} -G^o\Gamma_n & H^o\Gamma_n \\ \Gamma_n & 0_{n\times 1} \end{bmatrix} U_o$$

and U_o is a spectral factor of the the covariance matrix of the input $u(t)$ and the noise $e(t)$, given by

$$U_o = \begin{bmatrix} F_u & 0 \\ 0 & \sigma_o \end{bmatrix}.$$

For (3.76), we have that

$$\begin{aligned} Z^n &= \mathbf{E}\left\{ \varphi^m\left(t, \eta_o, \theta_o\right) \frac{F^o(q)}{A^o(q)} \left[\varphi^n\left(t, \eta_o, \theta_o\right)\right]^\top \right\} \\ &= \mathbf{E}\left\{ \begin{bmatrix} -\frac{B^o}{F^o}\Gamma_m u(t) \\ \frac{A^o}{F^o}\Gamma_m u(t) \end{bmatrix} \begin{bmatrix} -G^o\Gamma_n u(t) \\ \Gamma_n u(t) \end{bmatrix}^\top \right\} \\ &= \left\langle \begin{bmatrix} -\frac{G^o}{F^oH^o}\Gamma_m & 0_{n\times 1} \\ \frac{1}{F^oH^o}\Gamma_m & 0_{n\times 1} \end{bmatrix} F_u, \begin{bmatrix} -G^o\Gamma_n & 0_{n\times 1} \\ \Gamma_n & 0_{n\times 1} \end{bmatrix} F_u \right\rangle \\ &= \langle \gamma, \Psi \rangle, \end{aligned} \tag{3.77}$$

with

$$\gamma = \begin{bmatrix} -\frac{G^o}{F^oH^o}\Gamma_m & 0_{m\times 1} \\ \frac{1}{F^oH^o}\Gamma_m & 0_{m\times 1} \end{bmatrix} F_u,$$

where the last equality is due to the fact that the added column in the right argument of the inner product is multiplied by the zero column in γ when the inner product is taken. Hence, we can write the asymptotic covariance matrix of T_N as

$$\begin{aligned}\lim_{N\to\infty} \mathbf{E}\{T_N T_N^\top\} &= \sigma_o^2 \langle \gamma, \Psi\rangle \langle \Psi, \Psi\rangle^{-1} \langle \Psi, \gamma\rangle \\ &= \sigma_o^2 \Big\langle \mathbf{Proj}_{\mathcal{S}_\Psi}\{\gamma\}, \mathbf{Proj}_{\mathcal{S}_\Psi}\{\gamma\}\Big\rangle, \end{aligned} \tag{3.78}$$

where $\mathcal{S}_\Psi$ is the subspace in $\mathcal{L}_2^{1\times 2}$ spanned by the rows of Ψ. Lemma 3.7 gives that, as $n \to \infty$, $\mathcal{S}_\gamma \subseteq \mathcal{S}_\Psi$ and

$$\lim_{N\to\infty} \mathbf{E}\{T_N T_N^\top\} = \sigma_o^2 \langle \gamma, \gamma\rangle = \sigma_o^2 M_{CR}.$$

3.A.7 Summing up

Consider T_N defined in (3.75). As observed in Section 3.A.6, it follows from Lemma 3.5 that

$$T_N \sim \mathcal{N}\big(0, \sigma_o^2 M_{CR}\big), \quad \text{as } N \to \infty. \tag{3.79}$$

The asymptotic normality of $\sqrt{N}\big(\hat\theta_N - \hat\theta_o\big)$ follows from (3.65) and (3.79), together with that $\sqrt{N}\big(\hat\theta_N - \hat\theta_o\big)$ has the same asymptotic distribution as T_N. From (3.65) and (3.79), it now follows that

$$\sqrt{N}(\hat\theta_N^k - \theta_o) \sim \mathcal{N}\big(0, \sigma_o^2 M_{CR}^{-1}\big), \quad \text{as } N \to \infty. \tag{3.80}$$

CHAPTER 4

MODEL ORDER REDUCTION STEIGLITZ-MCBRIDE IN DYNAMIC NETWORKS

In this chapter, model order reduction Steiglitz-McBride (MORSM) will be generalized to dynamic networks. In this setting, the method will resemble standard two-stage methods, but use high order noise modelling. Like for the SISO case, we motivate the method using asymptotic ML arguments. We argue that this should decrease the estimation error compared with standard two-stage and IV methods.

4.1 Introduction

Dynamic networks are often too complex to be estimated as a whole using the prediction error method (Ljung, 1999). Estimating a chosen part of the network is computationally more appealing. However, using internal signals as inputs to the identification problem and applying a direct prediction error method (PEM) is often problematic: with feedback loops, the noise must be correctly modeled to obtain consistent estimates; with sensor noise, we have an errors-in-variables (EIV) setting, for which PEM is biased. Approaches to obtain consistent estimates of network modules have been studied by among others Dankers et al. (2016), Dankers et al. (2015), Dankers and Van den Hof (2015), Gunes et al. (2014), and Van den Hof et al. (2013).

In an errors-in-variables (EIV) setting and without estimating a noise model, possible approaches include instrumental variable (IV) methods (Dankers et al., 2015) and two-stage methods (Van den Hof et al., 2013). In the latter, noiseless inputs are simulated from a high order estimate of an appropriate part of the network. Although these methods are consistent, disregarding noise modeling may come at a cost in estimation error. Some frequency-domain methods deal with this issue: a fully non-parametric approach has been proposed by Dankers and Van den Hof (2015); the method proposed in Pintelon et al. (2010a) and Pintelon et al. (2010b) can also be used in this scenario, where a semi-parametric approach is taken—the noise model is captured by a high order model and the plant model of interest is parametric.

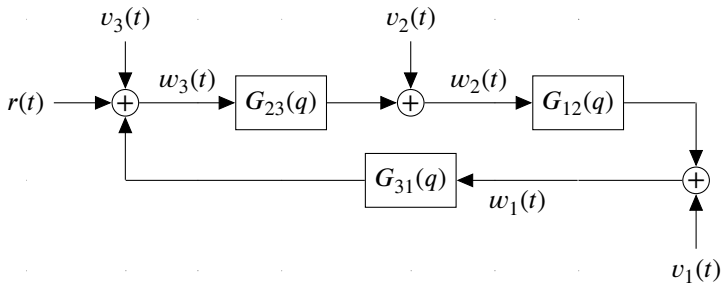

Figure 4.1: Example of a dynamic network.

In this chapter, we propose a time-domain method to deal with the noise contribution also using a high order model. The proposed method is based on model order reduction Steiglitz-McBride introduced in Chapter 3 for SISO systems. Here, we extend this approach to estimate a module in a dynamic network. First, we estimate a high order ARX model of an appropriate part of the network. Second, we estimate the module of interest using signals simulated from the ARX model and the Steiglitz-McBride method.

Although the basic idea resembles two-stage methods, the main contribution is that we use an asymptotic ML criterion (Wahlberg, 1989) to derive the filters that simulate the signals. Because of the theoretical support on an ML criterion, we argue that the method may provide lower estimation error than alternative approaches. We support this argument by simulations, where we observe that the method is most beneficial for colored noise.

4.2 Problem formulation

Consider the dynamic network in Fig. 4.1, written as

$$\begin{bmatrix} w_1(t) \\ w_2(t) \\ w_3(t) \end{bmatrix} = \begin{bmatrix} 0 & G_{12}(q) & 0 \\ 0 & 0 & G_{23}(q) \\ G_{31}(q) & 0 & 0 \end{bmatrix} \begin{bmatrix} w_1(t) \\ w_2(t) \\ w_3(t) \end{bmatrix} + \begin{bmatrix} v_1(t) \\ v_2(t) \\ v_3(t) \end{bmatrix} + \begin{bmatrix} 0 \\ 0 \\ r(t) \end{bmatrix}. \tag{4.1}$$

We have the following assumptions:

- $G_{12}(q)$, $G_{23}(q)$, and $G_{31}(q)$ are rational transfer functions in the delay operator q^{-1}, with at least one containing a delay;
- $\{v_1(t)\}$, $\{v_2(t)\}$, and $\{v_3(t)\}$ are unknown process noise sequences given by Gaussian white noise sequences with finite variance filtered by unknown stable filters;

- $\{w_1(t)\}$, $\{w_2(t)\}$, and $\{w_3(t)\}$ are measurable signals, whose measurements are given by

$$\tilde{w}_k(t) = w_k(t) + e_k(t), \tag{4.2}$$

  $k = \{1, 2, 3\}$, where $\{e_1(t)\}$, $\{e_2(t)\}$, and $\{e_3(t)\}$ are measurement noise sequences obtained by unknown stable filters driven by Gaussian white noise;

- $\{r(t)\}$ is a known bounded reference signal, uncorrelated with the noise signals.

We will use this network throughout the chapter to review available methods and to explain the proposed method. The objective is to estimate $G_{12}(q)$, parametrized as

$$G_{12}(q, \theta) = \frac{L_{12}(q, \theta)}{F_{12}(q, \theta)} = \frac{l_1 q^{-1} + \cdots + l_m q^{-m}}{1 + f_1 q^{-1} + \cdots + f_m q^{-m}}, \tag{4.3}$$

where $\theta = [\, f_1 \ \cdots \ f_m \ l_1 \ \cdots \ l_m \,]^\top$ are the parameters to estimate. We assume that there is unique $\theta = \theta^o$ such that $G_{12}(q) = G_{12}(q, \theta^o)$.

Alternatively to the recursive description in (4.1), the network can also be described by the relation from its external input signals to the measured output signals (4.2):

$$\begin{bmatrix} \tilde{w}_1(t) \\ \tilde{w}_2(t) \\ \tilde{w}_3(t) \end{bmatrix} = S(q) \begin{bmatrix} G_{12}(q)G_{23}(q) \\ G_{23}(q) \\ 1 \end{bmatrix} r(t) + H_v(q) \begin{bmatrix} v_1(t) \\ v_2(t) \\ v_3(t) \end{bmatrix} + \begin{bmatrix} s_1(t) \\ s_2(t) \\ s_3(t) \end{bmatrix}, \tag{4.4}$$

with $S(q) = [1 - G_{12}(q)G_{23}(q)G_{31}(q)]^{-1}$ and

$$H_v(q) = S(q) \begin{bmatrix} 1 & G_{12}(q) & G_{12}(q)G_{23}(q) \\ G_{23}(q)G_{31}(q) & 1 & G_{23}(q) \\ G_{31}(q) & G_{12}(q)G_{31}(q) & 1 \end{bmatrix}. \tag{4.5}$$

Estimating the individual network modules with PEM using the complete network description can be problematic in several aspects. For this reason, identification in dynamic networks concerns estimating particular modules of interest. In our example, we are interested in $G_{12}(q)$. If the signals $\{w_1(t), w_2(t)\}$ were known, the perhaps most natural approach to estimate $G_{12}(q)$ would be to use these signals as output and input to PEM. This is known as the direct approach (Van den Hof et al., 2013). Because there is feedback in the network, this approach has a disadvantage that the noise contribution $\{v_1(t)\}$ must be correctly modeled to achieve a consistent estimate of $G_{12}(q)$. Nevertheless, the direct approach is not applicable in our setting: because $\{w_1(t), w_2(t)\}$ are not known, but measured with noise according to (4.2), we need to use $\{\tilde{w}_1(t), \tilde{w}_2(t)\}$ as output and input to the identification problem. This creates an errors-in-variables (EIV) problem, for which PEM provides biased estimates. We proceed to review two possible time-domain methods to consistently identify $G_{12}(q)$: the two-stage (or indirect) method and the instrumental variable IV method.

4.2.1 The Two-Stage Method

The two-stage method was proposed by Van den Hof and Schrama (1993) to obtain consistent estimates of a plant from closed-loop data without having to estimate a noise model. However, it can also be applied in the network case to simulate the desired input signal as follows (Van den Hof et al., 2013).

For the first stage, the measured input to $G_{12}(q)$ is (4.4)

$$\tilde{w}_2(t) = S(q)G_{23}(q)r(t) + S(q)[G_{23}(q)G_{31}(q)v_1(t) + v_2(t) + G_{23}(q)v_3(t)] + e_2(t). \quad (4.6)$$

Because $\{r(t)\}$ is uncorrelated with the noise signals, estimating a high-order FIR model (without loss of generality, one delay is assumed in G_{23})

$$\tilde{w}_2(t) = \sum_{k=1}^{n} \eta_k q^{-k} r(t) + e(t), \quad (4.7)$$

where n is the model order and $\{\eta_k\}_{k=1}^{n}$ are the parameters to estimate, provides a high order estimate of $S(q)G_{23}(q)$ that is arbitrarily close to a consistent estimate as n increases. This stage provides estimates $\{\hat{\eta}_k\}_{k=1}^{n}$ of $\{\eta_k\}_{k=1}^{n}$, by solving the least-squares problem

$$\hat{\eta} = \left[\frac{1}{N}\sum_{t=1}^{N} \varphi(t)^\top \varphi(t)\right]^{-1} \left[\frac{1}{N}\sum_{t=1}^{N} \varphi(t)\tilde{w}_2(t)\right], \quad (4.8)$$

where N is the sample size, $\eta = [\,\eta_1 \cdots \eta_n\,]^\top$, and $\varphi(t) = [\,r(t-1) \cdots r(t-n)\,]^\top$.

For the second stage, we simulate a noiseless input to $G_{12}(q)$ by

$$\hat{w}_2(t) := \sum_{t=1}^{n} \hat{\eta}_k q^{-k} r(t). \quad (4.9)$$

Then, PEM can be applied to the output error (OE) model

$$\tilde{w}_1(t) = G_{12}(q,\theta)\hat{w}_2(t) + e(t), \quad (4.10)$$

which provides a consistent estimate of $G_{12}(q)$.

4.2.2 The Instrumental Variable Method

Instrumental variable methods (Söderström and Stoica, 1983) can provide consistent estimates of a plant without estimating a noise model and in an EIV setting (Thil et al., 2008). Thus, they are appropriate to estimate systems in dynamic networks (Dankers et al., 2015).

IV methods are a generalization of the least-squares method. To explain the idea, we start by using (4.1) and (4.2) to write

$$\tilde{w}_1(t) = \varphi(t)^\top \theta + F_{12}(q)v_2(t) + F_{12}(q)e_1(t) - L_{12}(q)e_2(t), \quad (4.11)$$

where $\varphi(t) = [\, -\tilde{w}_1(t-1) \cdots -\tilde{w}_1(t-m)\ \tilde{w}_2(t-1) \cdots \tilde{w}_2(t-m)\,]^\top$. With an IV method, θ is estimated by solving

$$\hat{\theta} = \left[\frac{1}{N}\sum_{t=1}^{N} z(t)^\top \varphi(t)\right]^{-1}\left[\frac{1}{N}\sum_{t=1}^{N} z(t)\tilde{w}_2(t)\right], \tag{4.12}$$

where $z(t)$ is a vector containing an appropriate set of variables called instruments. If $z(t) \equiv \varphi(t)$, (4.12) reduces to the least-squares method, which provides biased estimates because the residual term

$$\tilde{w}_1(t) - \varphi(t)^\top\theta = F_{12}(q)v_2(t) + F_{12}(q)e_1(t) - L_{12}(q)e_2(t) \tag{4.13}$$

is not white. Using (4.12) provides a consistent estimate if $z(t)$ is correlated with $\varphi(t)$ and uncorrelated with the residual term (4.13). Here, the reference signal $\{r(t)\}$ may be used to construct the instruments because it is correlated with $\{\tilde{w}_1(t), \tilde{w}_1(t)\}$ and uncorrelated with $\{v_2(t), e_1(t), e_2(t)\}$. On the other hand, $\{\tilde{w}_3(t)\}$ is not a candidate instrument because it is correlated with $\{v_2(t)\}$. Although a generalized IV approach allows other instruments to be used (Dankers et al., 2015), we consider it outside the scope of this chapter because it requires estimating a parametric noise model.

4.2.3 Summary and potential improvement

The reviewed approaches to estimate systems in dynamic networks focus on obtaining consistent estimates of particular modules, but they do not attempt to reduce the variance of the estimates. The latter problem has been considered, for example, in the two-stage method extension by Gunes et al. (2014). However, none of these approaches considers the noise signal properties when estimating a particular module. While we want to avoid estimating a parametric noise model, not taking the noise properties into account potentially increases the estimation error.

For SISO systems, there are approaches that capture the noise model with a high order model and the plant with a parametric model: for example, the method by Schoukens et al. (2011) in the frequency domain and the method by Everitt, Galrinho, et al. (2017b) in the time domain. To estimate a module in a dynamic network with a similar semi-parametric approach, the frequency domain method in Pintelon et al. (2010a) and Pintelon et al. (2010b) can be applied. This method consists of two steps. In the first step, the parts of the noisy input and output signals to the module of interest that are correlated with the reference signal are estimated with the noise covariance, using the local polynomial method. In the second step, the non-parametric estimates of these signals and of the noise covariance are used as starting point to estimate a parametric plant model using the sample maximum likelihood method (SML) estimator.

In this chapter, we address the problem of noise modeling in dynamic networks in the time domain, by extending the model order reduction Steiglitz-McBride (MORSM) method

by Everitt, Galrinho, et al. (2017b) to this scenario. With this method, the parametric estimate of the plant is obtained from a high order estimate, where the reduction is motivated by an asymptotic ML criterion. We proceed to review the SISO version of this method and the theoretical background that motivates it, which will be essential for the generalization to estimate modules in dynamic networks.

4.3 The Model Order Reduction Steiglitz-McBride Method

Consider the SISO system

$$y(t) = G(q)u(t) + H(q)e(t), \tag{4.14}$$

where $G(q)$ and $H(q)$ can be described by rational transfer functions. We parametrize the plant by $G(q, \theta)$, similarly to (4.3). MORSM allows us to obtain an asymptotically efficient estimate of $G(q)$ without estimating a parametric model for $H(q)$ and without explicitly solving a non-convex optimization problem.

If PEM is used with data obtained in open loop, $H(q)$ can be over-parametrized without affecting the asymptotic properties of the estimated $G(q, \theta)$. However, choosing the noise-model order arbitrarily large will make the problem computationally more difficult for PEM. The exception is if an ARX model structure is used, in which case the global minimum of the prediction error criterion can be found by least squares. This consists in estimating the model

$$A(q, \eta)y(t) = B(q, \eta)u(t) + e(t), \tag{4.15}$$

where

$$A(q, \eta) = 1 + \sum_{k=1}^{n} a_k q^{-k}, \qquad B(q, \eta) = \sum_{k=1}^{n} b_k q^{-k}, \tag{4.16}$$

and $\eta = [\, a_1 \ \cdots \ a_n \ b_1 \ \cdots \ b_n \,]^\top$, providing estimates $\hat{\eta}$.

If the ARX-model order n is allowed to be arbitrarily large, (4.15) models (4.14) with arbitrary accuracy (Ljung and Wahlberg, 1992). Then, asymptotically in model order, the ARX-model estimate can be used to obtain high order estimates of $G(q)$ and $H(q)$ by

$$\hat{G}(q) = \frac{B(q, \hat{\eta})}{A(q, \hat{\eta})}, \qquad \hat{H}(q) = \frac{1}{A(q, \hat{\eta})}. \tag{4.17}$$

The asymptotic distribution of the high order estimate $G(q, \hat{\eta})$ can be characterized in the frequency domain by (Wahlberg, 1989)

$$\hat{G}\left(\mathrm{e}^{\mathrm{j}\omega}\right) - G\left(\mathrm{e}^{\mathrm{j}\omega}\right) \sim \mathcal{N}\left(0, \frac{n}{N} \frac{\boldsymbol{\Phi}_v\left(\mathrm{e}^{\mathrm{j}\omega}\right)}{\boldsymbol{\Phi}_u\left(\mathrm{e}^{\mathrm{j}\omega}\right)}\right), \tag{4.18}$$

where $\Phi_u\left(e^{j\omega}\right)$ is the spectrum of the input and $\Phi_v\left(e^{j\omega}\right)$ is the spectrum of the noise term $v := H(q)e(t)$. This motivates that the reduction from the high order estimate $\hat{G}(q)$ to a low order one—$G(q,\theta)$—be performed by minimizing the asymptotic maximum likelihood criterion

$$V_N(\theta) = \int_{-\pi}^{\pi} |\hat{G}\left(e^{j\omega}\right) - G\left(e^{j\omega},\theta\right)|^2 \frac{\Phi_u\left(e^{j\omega}\right)}{\Phi_v\left(e^{j\omega}\right)}\, d\omega. \tag{4.19}$$

Because $\Phi_v\left(e^{j\omega}\right)$ is typically unknown, we need to replace it by an estimate. As shown by Wahlberg (1989), $\Phi_v\left(e^{j\omega}\right)$ may be replaced by its high order (scaled) estimate $|\hat{H}(q)|^2$ without affecting the asymptotic properties of the estimate of $G(q,\theta)$. Thus, minimizing

$$V_N(\theta) = \int_{-\pi}^{\pi} |\hat{G}\left(e^{j\omega}\right) - G\left(e^{j\omega},\theta\right)|^2 \frac{\Phi_u\left(e^{j\omega}\right)}{|\hat{H}\left(e^{j\omega}\right)|^2}\, d\omega \tag{4.20}$$

provides an asymptotic efficient estimate of θ.

In the time domain, a consistent estimate of (4.20) for finite sample size is given by

$$V_N(\theta) = \frac{1}{N}\sum_{t=1}^{N}\left[\frac{\hat{G}(q) - G(q,\theta)}{\hat{H}(q)}u(t)\right]^2. \tag{4.21}$$

In turn, using (4.17), we can re-write (4.21) as

$$V_N(\theta) = \frac{1}{N}\sum_{t=1}^{N}[B(q,\hat{\eta})u(t) - G(q,\theta)A(q,\hat{\eta})u(t)]^2. \tag{4.22}$$

The ASYM method (Zhu, 2001) consists in minimizing (4.22), which is an OE problem with a simulated output and filtered input, defined by

$$\hat{y}(t) := B(q,\hat{\eta})u(t), \qquad \hat{u}(t) := A(q,\hat{\eta})u(t). \tag{4.23}$$

Using PEM, a non-convex optimization routine is required to minimize (4.22). An alternative is to use the Steiglitz-McBride method (Stoica and Söderström, 1981), which uses least squares iteratively (we refer to it as *Steiglitz-McBride*). This method is not asymptotically efficient when applied to the measured data (Stoica and Söderström, 1981); however, when applied to the simulated data set (4.23), Steiglitz-McBride provides asymptotically efficient estimates in one iteration (Everitt, Galrinho, et al., 2017b).

Motivated by this, the Model Order Reduction Steiglitz-McBride method consists of the following two steps: first, estimate a high-order ARX model, using least squares; second, apply Steiglitz-McBride to the data set (4.23), which is motivated by an asymptotic ML criterion.

We identify three advantages compared to a direct PEM estimation. First, we transform a Box-Jenkins problem into an OE one, which is computationally simpler. Second, the user

does not need to choose a parametrization for the noise model. Third, we avoid a non-convex optimization routine by applying Steiglitz-McBride. These properties make MORSM an appealing method to estimate systems in dynamic networks.

4.4 MORSM for Dynamic Networks

To generalize MORSM to dynamic networks, consider the SIMO ARX model from $r(t)$ to the input and output signals of $G_{12}(q)$ (the module of interest), $w_2(t)$ and $w_1(t)$, respectively:

$$A(q,\eta)\begin{bmatrix} w_2(t) \\ w_1(t) \end{bmatrix} = B(q,\eta)r(t) + \begin{bmatrix} e_1(t) \\ e_2(t) \end{bmatrix} \tag{4.24}$$

where $A(q,\eta)$ is 2×2, $B(q,\eta)$ is 2×1, and the parameter vector η contains all the polynomials in these transfer matrices. An estimate $\hat{\eta}$ can then be obtained by least squares, which allows us to obtain high order estimates

$$\begin{bmatrix} \hat{T}_{23}(q) \\ \hat{T}_{13}(q) \end{bmatrix} = A^{-1}(q,\hat{\eta})B(q,\hat{\eta}), \tag{4.25}$$

where

$$\begin{bmatrix} T_{23}(q) \\ T_{13}(q) \end{bmatrix} := S(q)\begin{bmatrix} G_{23}(q) \\ G_{12}(q)G_{23}(q) \end{bmatrix}. \tag{4.26}$$

Having estimates of $T_{13}(q)$ and $T_{23}(q)$, the asymptotic ML estimate of $G_{12}(q)$ can be derived from these estimates, using that they are related by $T_{13}(q) - G_{12}(q)T_{23}(q) = 0$. To do this, we start by writing the asymptotic distribution

$$\hat{T}_{13}\left(e^{j\omega}\right) - G_{12}\left(e^{j\omega}\right)\hat{T}_{23}\left(e^{j\omega}\right) \sim \mathcal{N}\left(0, \frac{n}{N}\frac{P\left(e^{j\omega},\theta^o\right)}{\Phi_r\left(e^{j\omega}\right)}\right), \tag{4.27}$$

where $\Phi_r\left(e^{j\omega}\right)$ the spectrum of the reference signal $r(t)$ and

$$P\left(e^{j\omega},\theta\right) = \begin{bmatrix} -G_{12}\left(e^{j\omega},\theta\right) & 1 \end{bmatrix}\Phi_{\bar{v}}\left(e^{j\omega}\right)\begin{bmatrix} -G_{12}\left(e^{-j\omega},\theta\right) \\ 1 \end{bmatrix}, \tag{4.28}$$

where $\Phi_{\bar{v}}\left(e^{j\omega}\right)$ is the spectrum of the noise signal

$$\bar{v}(t) := \begin{bmatrix} \tilde{w}_2(t) \\ \tilde{w}_1(t) \end{bmatrix} - \begin{bmatrix} T_{23}(q) \\ T_{13}(q) \end{bmatrix} r(t). \tag{4.29}$$

This suggests that the model reduction step should be according to the cost function

$$V_N(\theta) = \int_{-\pi}^{\pi} |\hat{T}_{13}(e^{j\omega}) - G_{12}(e^{j\omega}, \theta)\hat{T}_{23}(e^{j\omega})|^2 \frac{\Phi_r(e^{j\omega})}{P(e^{j\omega}, \theta^o)}\, d\omega. \tag{4.30}$$

As with MORSM, we replace $\Phi_{\tilde{v}}(e^{j\omega})$ in (4.28) by a high order estimate—that is, the spectrum of the signal

$$\hat{\tilde{v}}(t) = \begin{bmatrix} \tilde{w}_2(t) \\ \tilde{w}_1(t) \end{bmatrix} - \begin{bmatrix} \hat{T}_{23}(q) \\ \hat{T}_{13}(q) \end{bmatrix} r(t) \tag{4.31}$$

instead of (4.29)—and apply Steiglitz-McBride to perform the model reduction. However, we have two problems to address. First, the term $P(e^{j\omega}, \theta^o)$ depends on the true parameters θ^o. Second, a spectral factor of this term is not available in closed form to simulate the signals.

Concerning the first problem, we replace θ^o by a consistent estimate. Because it is an ML criterion, this can be done without affecting the asymptotic properties of the ML estimate (Wahlberg, 1989). To obtain a consistent estimate, we may set $P(e^{j\omega}, \theta^o)$ in (4.30) to one and minimize the time-domain cost function

$$V_N^0(\theta) = \frac{1}{N} \sum_{t=1}^{N} \left(\left[\hat{T}_{13}(e^{j\omega}) - G_{12}(e^{j\omega}, \theta)\hat{T}_{23}(e^{j\omega}) \right] r(t) \right)^2. \tag{4.32}$$

To do this, we apply Steiglitz-McBride with the data set

$$\hat{y}^0(t) = \hat{T}_{13}(q)r(t), \qquad \hat{u}^0(t) = \hat{T}_{23}(q)r(t), \tag{4.33}$$

which provides a consistent estimate $\hat{\theta}$ that we use to replace θ^o in (4.30).

Concerning the second problem, a standard approach to obtain a spectral factorization of $P(e^{j\omega}, \hat{\theta})$ is to write the state-space form of the signal $\begin{bmatrix} G_{12}(q,\hat{\theta}) & 1 \end{bmatrix} \hat{\tilde{v}}(t)$ and compute the Kalman filter. However, numerical problems might occur when solving the Riccati equation because of the potential high order of the model. Because we only need a high order estimate of the spectral factor, we instead fit an autoregressive (AR) model $D(q)\hat{x}(t) = e(t)$ using least squares, where

$$D(q) = 1 + \sum_{k=1}^{n} d_k q^{-k}, \qquad \hat{x}(t) := \begin{bmatrix} -G_{12}(q, \hat{\theta}) & 1 \end{bmatrix} \hat{\tilde{v}}(t). \tag{4.34}$$

Then, if $\hat{D}(q)$ is the AR-model estimate, we have that $|\hat{D}(q)|^2 \approx P^{-1}(e^{j\omega}, \hat{\theta})$. Finally, minimizing (4.30) with this estimate of $P^{-1}(e^{j\omega}, \hat{\theta})$ corresponds to minimizing

$$V_N(\theta) = \frac{1}{N} \sum_{t=1}^{N} \left(\left[\hat{T}_{13}(e^{j\omega}) - G_{12}(e^{j\omega}, \theta)\hat{T}_{23}(e^{j\omega}) \right] \hat{D}(q) r(t) \right)^2, \tag{4.35}$$

which provides the final data set for the Steiglitz-McBride:

$$\hat{y}(t) := \hat{T}_{13}(q)\hat{D}(q)r(t), \qquad \hat{u}(t) := \hat{T}_{23}(q)\hat{D}(q)r(t). \tag{4.36}$$

In summary, the MORSM algorithm for networks consists of the following steps:

1. estimate an ARX model and construct estimates $\hat{T}_{13}(q)$ and $\hat{T}_{23}(q)$, according to (4.25);
2. apply the Steglitz McBride method to the simulated data set (4.33), providing a consistent estimate $\hat{\theta}$;
3. estimate an AR model from the signal $\hat{x}(t)$, defined by (4.34) and (4.31);
4. apply the Steglitz-McBride method to the simulated data set (4.36), with $\hat{D}(q)$ obtained in Step 3.

4.5 Numerical simulations

In this section, we perform a simulation study covering three cases with different noise signal spectra. For all cases, the transfer function we are interested in estimating is

$$G_{12}(q) = \frac{q^{-1}}{1 - 0.8q^{-1}}, \tag{4.37}$$

while the remaining modules in the network are

$$G_{23}(q) = \frac{0.2q^{-1}}{1 - 0.5q^{-1}}, \qquad G_{31}(q) = \frac{-0.1q^{-1}}{1 - 0.4q^{-1}}. \tag{4.38}$$

We generate the reference signal by $r(t) = [1 - 0.7q^{-1}]^{-1}e^r(t)$, where $\{e^r(t)\}$ is Gaussian white noise with unit variance. The sample size is $N = 5000$.

We compare the following methods:

- two-stage method (2-Stage), estimating an FIR model of order $n = 30$ (first stage) according to (4.7) and (4.8), and estimating an OE model using PEM (second stage) with (4.10) and simulated input (4.9);
- instrumental variable method (IV), estimating (4.12) with $z(t) = [\, r_{t-3} \; r_{t-4} \; r_{t-5} \,]^\top$;
- the SML, according to the implementation in the MATLAB toolbox (version October 2011) complementing the book Pintelon and Schoukens (2012), with 50 degrees of freedom for the covariance estimate and order 1 for the local polynomial approximation;

- the proposed method (MORSM), estimating an ARX model of order $n = 15$ (first step), an AR model of order $n = 30$ (third step), and using 5 Steiglitz-McBride iterations (second and fourth steps).

For SML, the MIMO local polynomial method is first used with $\{r(t)\}$ as input and $\{\tilde{w}_1(t), \tilde{w}_2(t)\}$ as outputs; then, the obtained non-parametric frequency-domain estimates of the latter signals and of the noise covariance are used with the sample maximum likelihood method. We obtain the initial estimate for the optimization problem by applying iterative quadratic maximum likelihood (IQML), which, in turn, is initialized by weighted total least squares (WTLS)—functions that are available in the toolbox. A maximum number of 100 iterations (default) is used.

The settings for all the methods were chosen based on a few empirical observations regarding performance. In a more extensive simulation study, a data-based selection of these settings should be used instead. However, we do not consider it for the purpose of this preliminary simulation.

For illustrative purposes, it would be interesting to observe how much is gained from Step 2 to Step 4 of the proposed method, as well as how much is lost by not using θ^o when obtaining the spectral factor. With this purpose, the following estimates are also included for comparison:

- Step 2 of the proposed method (naive MORSM);
- the proposed method with $G_{12}(q, \theta^o)$ used in Step 3 when constructing (4.34) (oracle MORSM).

We evaluate the performance using the FIT of the estimated impulse response of $G_{12}(q)$, given in percent by

$$\text{FIT} = 100\left(1 - \frac{\|g_{12} - \hat{g}_{12}\|_2}{\|g_{12} - \text{mean}(g_{12})\|_2}\right), \tag{4.39}$$

where g_{12} and $\hat{g}_{12}$ are vectors with the impulse coefficients of $G_{12}(q)$ and $G_{12}\left(q, \hat{\theta}\right)$ (for a particular method), respectively. We perform 100 Monte Carlo runs.

The three cases we study are:

I the process and sensor noises are uncorrelated Gaussian white noise sequences with unit variance;

II the process noise sequences are low-pass signals generated by $v_k(t) = H(q)e_{v_k}(t)$, $k = \{1, 2, 3\}$, where $H(q) = \left[1 - 0.95q^{-1}\right]^{-1}$, and $\{e_{v_k}(t)\}$ are mutually uncorrelated white Gaussian noise sequences with unit variance, and the sensor noise sequences are as in Case I).

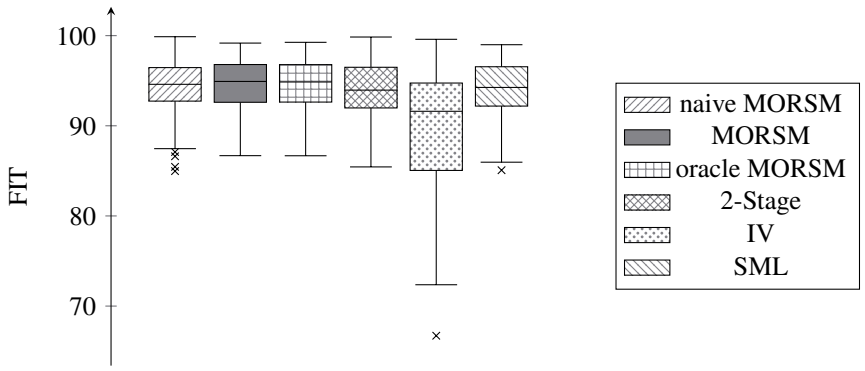

Figure 4.2: Simulation studies with white process and sensor noise signals (Case I).

III the process noise sequences are as in Case II), and the sensor noise sequences are generated to have the same spectra, by $s_k(t) = H(q)e_{s_k}(t)$, $k = \{1, 2, 3\}$, where $\{e_{s_k}(t)\}$ are mutually uncorrelated white Gaussian noise sequences with unit variance.

Although correlation between signals should not affect the methods, we consider the uncorrelated case for simplicity.

Case I)

The results for the case where all noise contributions are white are presented in the left plot of Fig. 4.2. In this case, there is hardly any improvement from Step 2 of the proposed method (naive MORSM) to the complete method (MORSM), which also has little advantage over the two-stage method (2-Stage). The reason is that the total noise contribution when driven by white noise signals does not have a considerable influence, and may be disregarded at almost no cost in performance. Moreover, there is no observable difference between the proposed method and using knowledge of the true system to filter the signals in Step 3 (oracle MORSM), meaning that our proposal of replacing the true system in Step 3 by the estimate obtained in Step 2 is acceptable in this case. The IV method we use is not competitive with the remaining methods here. Finally, SML and MORSM have similar performance.

Case II)

The results for the case where the process noise signals are low pass are presented in the middle plot of Fig. 4.3. In this case, there is a clear improvement from naive MORSM to MORSM, while the 2-Stage is not competitive. Thus, when the noise contributions are

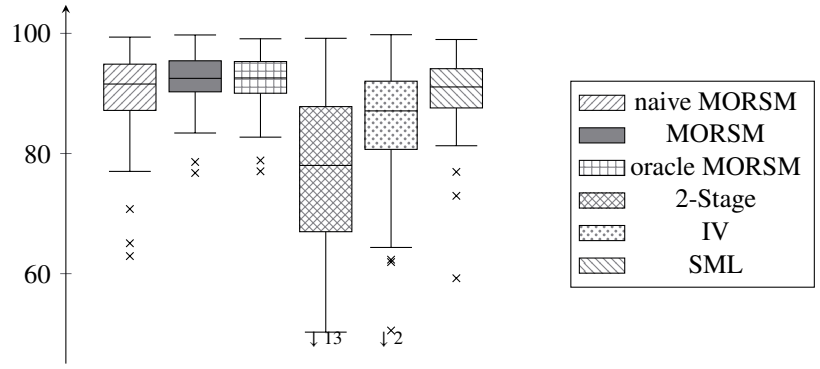

Figure 4.3: Simulation studies with low-pass process noise signals and white sensor noise signals (Case II).

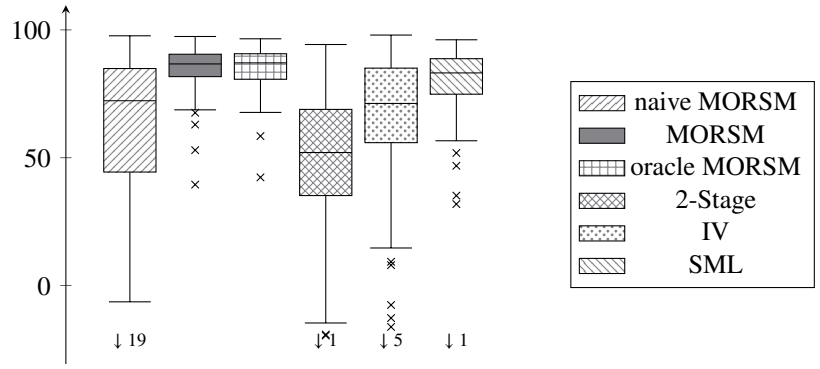

Figure 4.4: Simulation studies with low-pass process and sensor noise signals (Case III).

sufficiently correlated in time, performing the filtering derived from the asymptotic ML approach is beneficial. Moreover, replacing the true system with a consistent estimate in the ML weighting does not deteriorate our approach here either, as MORSM and the oracle version have identical performance. The IV method we use has better performance than in the previous case, because it benefits from additional correlations in the internal network signals. Like MORSM, the SML method is also capable of handling the colored noise signals used.

Case III)

The results for the case where both the process and sensor noise signals are low-pass signals are presented in the right plot of Fig. 4.4. In this case, the estimate naive MORSM is very poor, but the improvement to the complete method is considerable. Also here, MORSM performs similarly to the case that the true system is used in Step 3 (oracle MORSM), even if the true system is replaced by a poor estimate (the one obtained by naive MORSM). The SML and MORSM are competitive in this simulation, but 2-Stage and IV are not.

In summary, our simulations suggest that the proposed method can provide a smaller estimation error than standard two-stage and IV methods. If the noise contributions are not sufficiently colored, the two-stage method performs very similar to the proposed method. With increasingly colored process noise, IV methods may benefit from additional correlations in the internal network signals, but performance of the two-stage method deteriorates. If also the sensor noise is highly colored, performance of both IV and two-stage is affected. Meanwhile, the proposed method showed good performance in all the cases studied, and is competitive with the SML method. More extensive simulation studies are required to test the robustness and limitations of the method.

4.6 Summary

In this chapter, we proposed a method for estimation of systems in dynamic networks. The method resembles standard two-stage methods, but we motivate the simulated signals using asymptotic ML. We argue that this should decrease the estimation error compared with two-stage and IV methods, and support this argument with simulations.

The proposed method showed also competitive performance with the frequency-domain sample maximum likelihood method. These methods are conceptually similar, although using different approaches. Besides the time- and frequency-domain difference, MORSM uses a high order ARX model to capture the dynamics of the system, while SML uses the local polynomial method to obtain a high order estimate of the noise and the frequency response function. In both cases, the parametric estimate is motivated by an ML criterion. A more in-depth comparison between these methods—both theoretical and experimental—is considered for future work.

CHAPTER 5

AN EMPIRICAL BAYES APPROACH

In this chapter, we explore ways to use regularization to reduce the variance of the estimated modules. Simular to the two-stage method and MORSM in dynamic networks, the dynamic network is transformed into an acyclic structure, where any reference signal of the network is the input to a cascaded system. This system is modeled following a Bayesian kernel-based approach, which enables the identification of the target module using empirical Bayes arguments. In particular, the target module is estimated using a marginal likelihood criterion, whose solution is obtained by a novel iterative scheme designed through the Expectation/Conditional Maximization (ECM) algorithm. In the second part of this chapter, an extension to include additional sensors downstream of the target module is proposed.

5.1 Introduction

As observed in Van den Hof et al. (2013), dynamic networks with known topology can be seen as a generalization of simple compositions, such as systems in cascade, series or feedback connection. Therefore, identification techniques for dynamic networks may be derived by extending methods already developed for simple structures. This is the idea underlying the method presented in Van den Hof et al. (2013), which generalizes the two-stage method, originally developed for closed-loop systems, to dynamic networks (Forssell and Ljung, 1999). Instrumental variable methods for closed-loop systems (Gilson and Van den Hof, 2005) are adapted to networks in Dankers et al. (2015). Similarly, the methodology proposed in Wahlberg et al. (2009) for the identification of cascaded systems is generalized to the context of dynamic networks in Gunes et al. (2014). In that work, the underlying idea is that a dynamic network can be transformed into an acyclic structure, where any reference signal of the network is the input to a cascaded system consisting of two LTI blocks. In this alternative system description, the first block captures the relation between the reference and the noisy input of the target module, the second block contains the target module. The two LTI blocks are identified simultaneously using PEM (Ljung, 1999). In this setup, determining the model structure of the first block of the cascaded structure may be complicated, due to the possibly large number of interconnections in the dynamic network.

Furthermore, it requires knowledge of the model structure of essentially all modules in the feedback loop. Therefore, in Gunes et al. (2014), the first block is modeled by an unstructured FIR model of high order. The major drawback of this approach is that, as is usually the case with estimated models of high order, the variance of the estimated FIR model is high. The uncertainty in the estimate of the FIR model of the first block will in turn decrease the accuracy of the estimated target module.

The objective of this chapter is to propose a method for the identification of a module in dynamic networks that circumvents the high variance that is due to the high order model of the first block. The main contributions of this chapter are two-fold. First, we discuss the case where only the sensors directly measuring the input and the output of the target module are used in the identification process. Following a recent trend in system identification, we use regularization to control the variance (Chen et al., 2012). In particular, by exploiting the equivalence between regularization and Gaussian process regression (Pillonetto et al., 2014), we model the impulse response of the first block as a zero-mean stochastic process. The covariance matrix is given by the recently introduced *first-order stable spline kernel* (Pillonetto and Nicolao, 2010), whose structure is parametrized by two *hyperparameters*. An estimate of the target module is then obtained by empirical Bayes (EB) arguments, that is, by maximization of the marginal likelihood of the available measurements (Pillonetto et al., 2014). This likelihood depends not only on the parameter of the target module, but also on the kernel hyperparameters and the variance of the measurement noise. Therefore, it is required to estimate all these quantities. This is done by designing a novel iterative solution scheme based on an Expectation Maximization (EM)-type algorithm (Dempster et al., 1977), known as the Expectation/Conditional Maximization (ECM) algorithm (Meng and Rubin, 1993), which alternates the so called expectation step (E-step) with a series of conditional-maximization steps (CM-steps). When only the module input and output sensors are used, the E-step admits an analytical expression, because the joint likelihood of the module output and the sensitivity function is Gaussian. As for the CM-steps, one has to solve relatively simple optimization problems, which either admit a closed form solution, or can be efficiently solved using gradient descent strategies. Therefore, the overall optimization scheme for solving the marginal likelihood problem turns out computationally efficient.

The second main contribution of this chapter deals with the case where more sensors spread in the network are used in the identification of the target module. Adding information through addition of measurements used in the identification process has the potential to further reduce the variance of the estimated module (Everitt, Bottegal, Rojas, et al., 2017). The downside is that an additional measurement comes with another module to estimate, also increasing the number of parameters to estimate. To keep the number of additional parameters to estimate low, we propose a method that exploits regularization, modeling as a Gaussian process also the impulse response of the path linking the target module to any additional sensor. In this case, however, the measured outputs and the unknown paths do not admit a joint Gaussian description. As a consequence, the E-step of the ECM method does not admit an analytical expression, as opposed to the one-sensor case described above.

To overcome this issue, we use MCMC techniques (Gilks et al., 1995) to solve the integral associated with the E-step. In particular, we design an integration scheme based on the Gibbs sampler (S. Geman and D. Geman, 1984) that, in combination with the ECM method, builds up a novel identification method for the target module reminiscent of the so called empirical Bayes Gibbs sampling (Casella, 2001).

The effectiveness of the proposed methods is demonstrated through numerical experiments. The methods proposed in this chapter are close in spirit to some recently proposed kernel-based techniques for blind system identification (Bottegal and Picci, 2015) and Hammerstein system identification (Risuleo et al., 2015).

5.2 Problem formulation

We consider dynamic networks that consist of L scalar *internal variables* $w_j(t)$, $j = 1, \dots, L$ and L scalar external *reference signals* $r_l(t)$, $l = 1, \dots, L$, that can be manipulated by the user. Some of the reference signal may not be present, *i.e.*, they may be identically zero. Define $\mathcal{R}$ as the set of indices of reference signals that are present. In the dynamic network, the internal variables are considered nodes and transfer functions are the edges. Introducing the vector notation $w(t) := [\, w_1(t) \ \dots \ w_L(t) \,]^\top$, $r(t) := [\, r_1(t) \ \dots \ r_L(t) \,]^\top$, the dynamics of the network are defined by the equation

$$w(t) = G(q)w(t) + r(t), \tag{5.1}$$

where

$$G(q) = \begin{bmatrix} 0 & G_{12}(q) & \cdots & G_{1L}(q) \\ G_{21}(q) & 0 & \ddots & \vdots \\ \vdots & \ddots & \ddots & G_{(L-1)L}(q) \\ G_{L1}(q) & \cdots & G_{L(L-1)}(q) & 0 \end{bmatrix},$$

where $G_{ji}(q)$ is a proper rational transfer function for $j = 1, \dots, L$, $i = 1, \dots, L$. The internal variables $w(t)$ are measured with additive white noise, that is

$$\tilde{w}(t) = w(t) + e(t),$$

where $e(t) \in \mathbb{R}^L$ is a stationary zero-mean Gaussian white-noise process with diagonal noise covariance matrix $\Sigma_e = \operatorname{diag}\{\lambda_1, \dots, \lambda_L\}$. We assume that the λ_i are unknown. To ensure stability and causality of the network the following assumptions hold for all networks considered in this chapter.

Assumption 5.1. The network is well posed in the sense that all principal minors of $\lim_{q\to\infty}(I - G(q))$ are non-zero (Van den Hof et al., 2013).

Assumption 5.2. The sensitivity path

$$S(q) := (I - G(q))^{-1}$$

is stable.

Assumption 5.3. The reference variables $\{r_l(t)\}$ are mutually uncorrelated and uncorrelated with the measurement noise $e(t)$.

Thus, we can write

$$\tilde{w}(t) = S(q)r(t) + e(t). \tag{5.2}$$

We define a $\mathcal{N}_j$ as the set of indices of internal variables that have a direct causal connection to w_j, *i.e.*, $i \in \mathcal{N}_j$ if and only if $G_{ji}(q) \neq 0$. Without loss of generality, we assume that $\mathcal{N}_j = 1, 2, \ldots, p$, where p is the number of direct causal connections to w_j (we may always rename the nodes so that this holds). The goal is to identify module $G_{j1}(q)$ given N measurements of the reference $r(t)$, the "output" $\tilde{w}_j(t)$ and the set of p neighbor signals in $\mathcal{N}_j$. To this end, we express $\tilde{w}_j$, the measured output of module $G_{j1}(q)$ as

$$\tilde{w}_j(t) = \sum_{i \in \mathcal{N}_j} G_{ji}(q)w_i(t) + r_j(t) + e_j(t). \tag{5.3}$$

The above equation depends on the internal variables $w_i(t)$, $i \in \mathcal{N}_j$, which we we only have noisy measurement of; these can be expressed as

$$\tilde{w}_i(t) = w_i(t) + e_i(t) = \sum_{l \in \mathcal{R}} S_{il}(q)r_l(t) + e_i(t). \tag{5.4}$$

where $S_{il}(q)$ is the transfer function path from reference $r_l(t)$ to output $\tilde{w}_i(t)$. Together, (5.3) and (5.4) allow us to express the relevant part of the network, possibly containing feedback loops, as a direct acyclic graph with two blocks connected in cascade. Note that, in general, the first block depends on all other blocks in the network. Therefore, accurate low order parametrization of this block depends on global knowledge of the network.

Example 5.1. As an example consider the network depicted in Figure 5.1, where, using (5.3) and (5.4), the acyclic graph of Figure 5.2 can describe the relevant dynamics, when $w_j = w_3$ is the output and we wish to identify $G_{31}(q)$.

In the following, we briefly review two standard methods for closed-loop identification that we will use as a starting point to derive the methodology described in the chapter.

5.2.1 A two stage method

The first stage of the two-stage method (Van den Hof et al., 2013), proceeds by finding a consistent estimate $\hat{w}_i(t)$ of all nodes $w_i(t)$ in $\mathcal{N}_j$. This is done by high-order modeling of

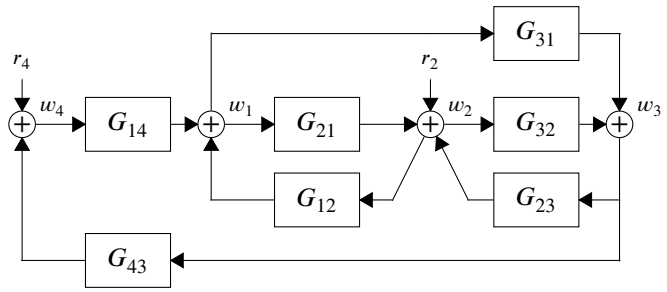

Figure 5.1: Network example of 4 internal variables and 2 reference signals.

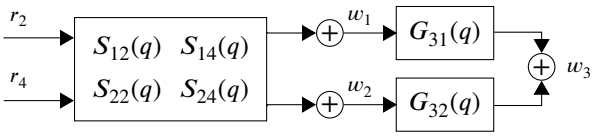

Figure 5.2: Direct acyclic graph of part of the network in Figure 5.1.

$\{S_{il}\}$ and estimating it from (5.4) using the prediction error method. The prediction errors are constructed as

$$\varepsilon_i(t,\alpha) = \tilde{w}_i(t) - \sum_{l\in\mathcal{R}} S_{il}(q,\alpha) r_l(t), \tag{5.5}$$

where α is a parameter vector. The resulting estimate $S_{il}(q,\hat{\alpha})$ is then used to obtain the node estimate as

$$\hat{w}_i(t) = \sum_{l\in\mathcal{R}} S_{il}(q,\hat{\alpha}) r_l(t). \tag{5.6}$$

In a second stage, the module of interest $G_{j1}(q)$ (and the other modules in $\mathcal{N}_j$) is parameterized by θ and estimated from (5.3), again using the prediction error method. The prediction errors are now constructed as

$$\varepsilon_j(t,\theta) = \tilde{w}_j(t) - r_j(t) - \sum_{i\in\mathcal{N}_j} G_{ji}(q,\theta)\hat{w}_i(t).$$

5.2.2 Simultaneous minimization of prediction errors

It is useful to briefly introduce the simultaneous minimization of prediction error method (SMPE) (Gunes et al., 2014). The main idea underlying SMPE is that if the two prediction errors (5.5) and (5.7) are simultaneously minimized, the variance will be decreased

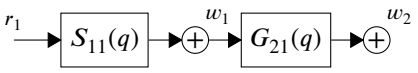

Figure 5.3: Basic network of 1 reference signal and 2 internal variables.

(Wahlberg et al., 2009). In the SMPE method, the prediction error of the measurement $\tilde{w}_j$ depends explicitly on α and is given by

$$\varepsilon_j(t,\theta,\alpha) = \tilde{w}_j(t) - \sum_{i\in\mathcal{N}_j} G_{ji}(q,\theta) \sum_{l\in\mathcal{R}} S_{il}(q,\alpha) r_l(t). \tag{5.7}$$

The method proceeds to minimize

$$V_N(\theta,\alpha) = \frac{1}{N}\sum_{t=1}^{N}\left[\frac{\varepsilon_j^2(t,\theta,\alpha)}{\lambda_j} + \sum_{i\in\mathcal{N}_j}\frac{\varepsilon_i^2(t,\alpha)}{\lambda_i}\right]. \tag{5.8}$$

In (Gunes et al., 2014), the noise variances are assumed known, and how to estimate the noise variances is not analyzed. As an initial estimate of the parameters θ and α, the minimizers of the two-stage method can be taken.

The main drawback is that the least-squares estimation of S may still induce high variance in the estimates. Additionally, if each of the n_s estimated transfer functions in S is estimated by the first n impulse response coefficients, the number of estimated parameters in S alone is $n_s \cdot n$. Already for relatively small dimensions of S the SMPE method is prohibitively expensive. To handle this, a frequency domain approach is taken in Dankers and Van den Hof (2015). In this chapter, we will instead use regularization to reduce the variance and the complexity.

5.3 An empirical Bayes method

In this section we derive our approach to the identification of a specific module based on EB. For ease of exposition, we give a detailed derivation in the one-reference-one-module case. The extension to general dynamic networks follows along similar arguments.

We consider a dynamic network with one non-zero reference signal $r_1(t)$. Without loss of generality, we assume that the module of interest is $G_{21}(q)$, and hence $G_{22}(q), \dots, G_{2L}(q)$ are assumed zero (We can always rename the signals such that this holds). The setting we consider has been illustrated in Figure 5.3. We parametrize the target module by means of a parameter vector $\theta \in \mathbb{R}^{n_\theta}$. Using the vector notation introduced in the previous section, we denote by $\tilde{w}_1$ the stacked measurements $\tilde{w}_1(t)$ before the module of interest $G_{21}(q,\theta)$, and by $\tilde{w}_2$ the stacked output of this module $\tilde{w}_2(t)$. We define the impulse response coefficients

of $G_{21}(q,\theta)$ by the inverse discrete-time Fourier transform

$$g_\theta(t) := \frac{1}{2\pi}\int_{-\pi}^{\pi} G_{21}(e^{j\omega},\theta)e^{j\omega t}\,d\omega. \tag{5.9}$$

Similarly we define s_{11} as the impulse response coefficients of $S_{11}(q)$, where $S_{11}(q)$ is, as before, the sensitivity path from $r_1(t)$ to $w_1(t)$, and $e_1(t)$ and $e_2(t)$ are the measurement noise sources (which we have assumed white and Gaussian). Their variance is denoted by λ_1 and λ_2, respectively. We rewrite the dynamics as

$$\begin{aligned} \tilde{w}_1 &= \quad S_{11}r_1 + e_1, \\ \tilde{w}_2 &= G_\theta S_{11} r_1 + e_2, \end{aligned} \tag{5.10}$$

where G_θ is the $N \times N$ lower triangular Toeplitz matrix of the N first impulse response samples g_θ. The same notation holds for the impulse response s_{11} and its Toeplitz-matrix version $S_{11} = \mathcal{T}_N\{s_{11}\}$. In general, given a vector $a \in \mathbb{R}^m$, we define by $\mathcal{T}_n\{a\}$ the $m \times n$ lower triangular Toeplitz matrix whose elements are the entries of a. Lower case letters indicate, in general, column vectors and, when there is no confusion, capital letters indicate their Toeplitz form, so given $a \in \mathbb{R}^m$, we have that $A = \mathcal{T}_n\{a\}$, where the number of columns n is consistent with the rest of the formula. We further rewrite (5.10) as

$$\begin{aligned} \tilde{w}_1 &= \quad R_1 s_{11} + e_1, \\ \tilde{w}_2 &= G_\theta R_1 s_{11} + e_2. \end{aligned} \tag{5.11}$$

where $R_1 = \mathcal{T}_N\{r_1\}$. For computational purposes, we only consider the first n samples of s_{11}, where n is large enough such that the truncation captures the dynamics of the sensitivity $S_{11}(q)$ well enough. Let $Z := \left[\tilde{w}_1^\top \; \tilde{w}_2^\top\right]^\top$; we rewrite (5.11) as

$$Z = W_\theta s_{11} + e, \qquad W_\theta = \begin{bmatrix} R_1 \\ G_\theta R_1 \end{bmatrix} \qquad e = \begin{bmatrix} e_1 \\ e_2 \end{bmatrix} \tag{5.12}$$

Note that e is a random vector such that

$$\Sigma_e := \mathbf{E}\{ee^\top\} = \begin{bmatrix} \lambda_1 I & 0 \\ 0 & \lambda_2 I \end{bmatrix}. \tag{5.13}$$

5.3.1 Bayesian model of the sensitivity path

To reduce the variance in the sensitivity estimate (and also reduce the number of estimated parameters), we cast our problem in a Bayesian framework and model the sensitivity function as a zero-mean Gaussian stochastic vector (Rasmussen and Williams, 2006), *i.e.*

$$p(s_{11}; \nu, K_\beta) \sim \mathcal{N}(0, \nu K_\beta). \tag{5.14}$$

The structure of the covariance matrix is given by the *first-order stable spline kernel* (Pillonetto and Nicolao, 2010):

$$\left\{K_\beta\right\}_{i,j} = \beta^{\max(i,j)}, \quad \beta \in [0,1). \tag{5.15}$$

The parameter β regulates the decay velocity of the realizations from (5.14), whereas, ν tunes their amplitude. In this context, K_β is usually called a *kernel* (due to the connection between Gaussian process regression and the theory of reproducing kernel Hilbert space, see *e.g.* Rasmussen and Williams (2006) for details) and determines the properties of the realizations of s. In particular, the stable spline kernel enforces smooth and BIBO stable realizations (Pillonetto and Nicolao, 2010).

5.3.2 The marginal likelihood estimator

Since s_{11} is assumed stochastic, it admits a probabilistic description jointly with the vector of observations Z, parametrized by the vector

$$\eta = \begin{bmatrix} \lambda_1 & \lambda_2 & \nu & \beta & \theta \end{bmatrix}. \tag{5.16}$$

In particular, having assumed a Gaussian distribution of the noise, the joint description is also Gaussian, that is,

$$p\left(\begin{bmatrix} Z \\ s_{11} \end{bmatrix}; \eta\right) \sim \mathcal{N}\left(\begin{bmatrix} 0 \\ 0 \end{bmatrix}, \begin{bmatrix} \Sigma_z & \Sigma_{zs} \\ \Sigma_{sz} & \nu K_\beta \end{bmatrix}\right), \tag{5.17}$$

where $\Sigma_z = W_\theta \nu K_\beta W_\theta^\top + \Sigma_e$, and $\Sigma_{zs} = \Sigma_{sz}^\top = W_\theta \nu K_\beta$. It is instrumental to derive the posterior distribution of s_{11} given the measurement vector Z. It is given by (Anderson and Moore, 1979)

$$p\left(s_{11}|Z;\eta\right) \sim \mathcal{N}\left(PW_\theta^\top \Sigma_e^{-1} Z, P\right), \tag{5.18}$$

$$P = (W_\theta^\top \Sigma_e^{-1} W_\theta + (\nu K_\beta)^{-1})^{-1}, \tag{5.19}$$

and it is also parametrized by the vector η.

The module identification strategy we propose in this chapter relies on an empirical Bayes approach. We introduce the marginal probability density function (pdf) of the measurements

$$p(Z;\eta) = \int p\left(Z, s_{11}\right) \mathrm{d}s_{11} \sim \mathcal{N}\left(0, \Sigma_z\right), \tag{5.20}$$

that is, the pdf of the measurements after having integrating out the dependence on the sensitivity path s_{11}. Then, we can define the (log) marginal likelihood (ML) criterion as the maximum of the marginal pdf defined above

$$\begin{aligned} \hat{\eta} &= \arg\max_\eta p(Z;\eta) \\ &= \arg\min_\eta \left\{\log\det\left\{\Sigma_z\right\} + Z^\top \Sigma_z^{-1} Z\right\}, \end{aligned} \tag{5.21}$$

whose solution provides also an estimate of θ and thus of the module of interest.

5.3.3 Computation of the solution of the marginal likelihood criterion

Problem (5.21) is nonlinear and may involve a large number of decision variables, if n_θ is large. In this section, we derive an iterative solution scheme based on the ECM algorithm (Meng and Rubin, 1993), which is a generalization of the standard Expectation Maximization (EM) algorithm. In order to employ EM-type algorithms, one has to define a *latent variable*; in our problem, a natural choice is s_{11}. Then, a (local) solution to (5.21) is achieved by iterating over the following steps:

(E-step). Given an estimate $\hat{\eta}^{(k)}$ (computed at the k-th iteration of the algorithm), compute

$$Q^{(k)}(\eta) := \mathbf{E}\left\{\log p\left(Z, s_{11}; \eta\right)\right\}, \tag{5.22}$$

where the expectation is taken with respect to the posterior of s_{11} when the estimate $\eta^{(k)}$ is used, *i.e.*, $p\left(s_{11}|Z, \hat{\eta}^{(k)}\right)$;

(M-step). Solve the problem

$$\hat{\eta}^{(k+1)} = \arg\max_{\eta} Q^{(k)}(\eta). \tag{5.23}$$

First, we turn our attention on the computation of the E-step, *i.e.*, the derivation of (5.22). Let $\hat{s}_{11}^{(k)}$ and $\hat{P}^{(k)}$ be the posterior mean and covariance matrix of s_{11}, computed from (5.18) using $\hat{\eta}^{(k)}$. Define $\hat{S}_{11}^{(k)} := \hat{P}^{(k)} + \hat{s}_{11}^{(k)}\hat{s}_{11}^{(k)T}$. The following lemma provides an expression for the function $Q^{(k)}(\eta)$.

Lemma 5.1. *Let* $\hat{\eta}^{(k)} = \left[\begin{smallmatrix}\hat{\lambda}_1^{(k)} & \hat{\lambda}_2^{(k)} & \hat{\nu}^{(k)} & \hat{\beta}^{(k)} & \hat{\theta}^{(k)}\end{smallmatrix}\right]$ *be an estimate of* η *after the* k*-th iteration of the EM method. Then*

$$Q^{(k)}(\eta) = -\frac{1}{2}Q_0^{(k)}(\lambda_1, \lambda_2, \theta) - \frac{1}{2}Q_s^{(k)}(\nu, \beta), \tag{5.24}$$

where

$$\begin{aligned} Q_0^{(k)}(\lambda_1, \lambda_2, \theta) = \Big(&\log\det\left\{\Sigma_e\right\} + Z^\top \Sigma_e^{-1} Z - 2Z^\top W_\theta \hat{s}_{11}^{(k)} \\ &+ \mathrm{Tr}\left\{W_\theta^\top \Sigma_e^{-1} W_\theta \hat{S}_{11}^{(k)}\right\}\Big), \end{aligned} \tag{5.25}$$

$$Q_s^{(k)}(\nu, \beta) = \log\det\left\{\nu K_\beta\right\} + \mathrm{Tr}\left\{\left(\nu K_\beta\right)^{-1}\hat{S}_{11}^{(k)}\right\}. \tag{5.26}$$

Having computed the function $Q^{(k)}(\eta)$, we now focus on its maximization. We first note that the decomposition (5.24) shows that the kernel hyperparameters can be updated independently of the rest of the parameters:

Theorem 5.2. *Define*

$$Q_\beta(\beta) = \log\det\left\{K_\beta\right\} + n\log\mathrm{Tr}\left\{K_\beta^{-1}\hat{S}_{11}^{(k)}\right\}. \tag{5.27}$$

Then

$$\hat{\beta}^{(k+1)} = \arg\min_{\beta\in[0,1)} Q_\beta(\beta), \tag{5.28}$$

$$\hat{v}^{(k+1)} = \frac{1}{n}\mathrm{Tr}\left\{K_{\hat{\beta}^{(k+1)}}^{-1}\hat{S}_{11}^{(k)}\right\}. \tag{5.29}$$

Therefore, the update of the scaling hyperparameter is available in closed-form, while the update of β requires the solution of a scalar optimization problem in the domain $[0, 1]$, an operation that requires little computational effort, see Bottegal et al. (2016) for details.

We are left with the maximization of the function $Q_0^{(k)}(\lambda_1, \lambda_2, \theta)$. In order to simplify this step, we split the optimization problem into constrained subproblems that involve fewer decision variables. This operation is justified by the ECM paradigm, which, under mild conditions (Meng and Rubin, 1993), guarantees the same convergence properties of the EM algorithm even when the optimization of $Q^{(k)}(\eta)$ is split into a series of constrained subproblems. In our case, we decouple the update of the noise variances from the update of θ. By means of the ECM paradigm, we split the maximization of $Q_0^{(k)}(\lambda_1, \lambda_2, \theta)$ in a sequence of two constrained optimization subproblems:

$$\hat{\theta}^{(k+1)} = \arg\max_{\theta} Q_0^{(k)}(\lambda_1, \lambda_2, \theta) \tag{5.30}$$
$$\text{subject to } \lambda_1 = \hat{\lambda}_1^{(k)}, \quad \lambda_2 = \hat{\lambda}_2^{(k)},$$

$$\hat{\lambda}_1^{(k+1)},\ \hat{\lambda}_2^{(k+1)} = \arg\max_{\lambda_1,\,\lambda_2} Q_0^{(k)}(\lambda_1, \lambda_1, \theta) \tag{5.31}$$
$$\text{subject to } \theta = \hat{\theta}^{(k+1)}.$$

The following result provides the solution of the above problems.

Theorem 5.3. *Introduce the matrix $D \in \mathbb{R}^{N^2\times N}$ such that $Da = \mathrm{vec}\left\{\mathcal{T}_N\{a\}\right\}$, for any $a \in \mathbb{R}^N$. Define*

$$\hat{A}^{(k)} = D^\top\left(R_1\hat{S}_{11}^{(k)}R_1^\top \otimes I_N\right)D \tag{5.32}$$

$$\left(\hat{b}^{(k)}\right)^\top = \tilde{u}_2^\top\,\mathcal{T}_N\left\{R_1\hat{s}_{11}^{(k)}\right\}, \tag{5.33}$$

where $\otimes$ denotes the standard Kronecker product. Then

$$\hat{\theta}^{(k+1)} = \arg\min_{\theta} g_\theta^\top\hat{A}^{(k)}g_\theta - 2\left(\hat{b}^{(k)}\right)^\top g_\theta. \tag{5.34}$$

The closed form updates of the noise variance estimates are as follows

$$\hat{\lambda}_1^{(k+1)} = \frac{1}{N}\left(\left\|\tilde{w}_1 - R_1 \hat{s}_{11}^{(k)}\right\|_2^2 + \operatorname{Tr}\left\{R_1 \hat{P}^{(k)} R_1^\top\right\}\right),$$
$$\hat{\lambda}_2^{(k+1)} = \frac{1}{N}\left(\left\|\tilde{w}_2 - G_{\hat{\theta}^{(k+1)}} R_1 \hat{s}_{11}^{(k)}\right\|_2^2 + \operatorname{Tr}\left\{G_{\hat{\theta}^{(k+1)}} R_1 \hat{P}^{(k)} R_1^\top G_{\hat{\theta}^{(k+1)}}^\top\right\}\right). \tag{5.35}$$

Each variance is the result of the sum of one term that measures the adherence of the identified systems to the data and one term that compensates for the bias in the estimates introduced by the Bayesian approach. The update of the parameter θ involves a (generally) nonlinear least-squares problem, which can be solved using gradient descent strategies. Note that, in case the impulse response g_θ is linearly parametrized (*e.g.*, it is an FIR system or orthonormal basis functions are used (Wahlberg, 1991)), then the update of θ is also available in closed-form.

Example 5.2. Assume that the linear parametrization $g_\theta = L\theta$, $L \in \mathbb{R}^{N \times n_\theta}$, is used, then

$$\hat{\theta}^{(k+1)} = \left(L^\top \hat{A}^{(k)} L\right)^{-1} L^\top \hat{b}^{(k)}. \tag{5.36}$$

5.3.4 Identification algorithm

The proposed method for module identification can be summarized in the following steps.

Algorithm 1: Identification algorithm for dynamic network

Input : Measurement data Z, reference signal r.
Initialization: An initial estimate of $\hat{\eta}^{(0)}$, set $k = 0$.

repeat
- Compute $\hat{s}_{11}^{(k)}$ and $\hat{P}^{(k)}$ from (5.18).
- Update kernel hyperparameters $\nu^{(k+1)}$ and $\beta^{(k+1)}$ using (5.29)–(5.28).
- Update the vector $\theta^{(k+1)}$ solving (5.34).
- Update the noise variances $\lambda_1^{(k+1)}$ and $\lambda_2^{(k+1)}$ using (5.35).
- Set $\eta^{(k+1)} = \left[\lambda_1^{(k+1)} \ \lambda_2^{(k+1)} \ \nu^{(k+1)} \ \beta^{(k+1)} \ \theta^{(k+1)}\right]$.
- Set $k = k + 1$.

until η *has converged*

The method can be initialized in several ways. One option is to first estimate $\hat{S}_{11}(q)$ by an empirical Bayes method using only r_1 and $\tilde{w}_1$. Then, $\hat{w}_1$ is constructed from (5.6), using the obtained $\hat{S}_{11}(q)$. Finally, G is estimated using the prediction error method, using $\hat{w}_1$ as input and $\tilde{w}_2$ as output.

5.3.5 Extension to general structures

In this section, we generalize the previous algorithm to a general network structure with $m \leq L$ reference signals $\{r_{l_1}(t), \dots, r_{l_m}(t)\}$, and $p \leq L$ modules $\{G_{j1}(q), \dots, G_{jp}(q)\}$ sharing the same output $\tilde{w}_j(t)$ as the module of interest, and modeled in time domain as $\{g_{\theta_1}, \dots, g_{\theta_p}\}$. For any $i = 1, \dots, p$, we can write

$$\tilde{w}_i = R_{l_1} s_{il_1} + \dots + R_{l_m} s_{il_m} + e_{k_i} = \mathbf{R} s_i + e_{k_i}, \tag{5.37}$$

where $\mathbf{R} := [R_{l_1} \dots R_{l_m}]$ and $s_i = \begin{bmatrix} s_{il_1}^\top & \cdots & s_{il_m}^\top \end{bmatrix}^\top$. Using these definitions we can also write (*cf.* (5.3))

$$\tilde{w}_j = r_j + G_{\theta_1} \mathbf{R} s_1 + \dots + G_{\theta_p} \mathbf{R} s_p + e_j. \tag{5.38}$$

Defining also

$$\mathbf{w} = \begin{bmatrix} \tilde{w}_1 \\ \vdots \\ \tilde{w}_p \end{bmatrix}, \quad \mathbf{s} = \begin{bmatrix} s_1 \\ \vdots \\ s_p \end{bmatrix}, \quad G_\theta = \begin{bmatrix} G_{\theta_1} & \dots & G_{\theta_p} \end{bmatrix}, \quad \mathbf{e}_\mathbf{w} = \begin{bmatrix} e_1 \\ \vdots \\ e_p \end{bmatrix},$$

we obtain the following expression for the network dynamics

$$\begin{aligned} \mathbf{w} &= \big(I_p \otimes \mathbf{R}\big)\mathbf{s} + \mathbf{e}_\mathbf{w} \\ \tilde{w}_j - r_j &= G_\theta \big(I_p \otimes \mathbf{R}\big)\mathbf{s} + e_j, \end{aligned} \tag{5.39}$$

or, with

$$\mathbf{Z} = \begin{bmatrix} \mathbf{w} \\ \big(\tilde{w}_j - r_j\big) \end{bmatrix},$$

i.e., the measurements related to the input of the module of interest stacked on top of the measurement related to the output of the module of interest. Then we have the compact notation

$$\mathbf{Z} = \mathbf{W}_\theta \mathbf{s} + \mathbf{e}, \qquad \mathbf{W}_\theta = \begin{bmatrix} \big(I_p \otimes \mathbf{R}\big) \\ G_\theta \big(I_p \otimes \mathbf{R}\big) \end{bmatrix}, \qquad \mathbf{e} = \begin{bmatrix} \mathbf{e}_\mathbf{w} \\ e_j \end{bmatrix}. \tag{5.40}$$

Each sensitivity path s_{il} is given a prior of the form (5.14), with hyperparameters ν_{il} and β_{il}, assuming mutual independence between the sensitivity paths. Although it may appear more sensible to incorporate some correlation among the sensitivity paths, at present, it is not clear how this can be done using Gaussian priors. Some recent work suggests to enrich the stable spline kernel with a component enforcing low McMillan degree (Prando et al., 2014). Furthermore, as we will see, assuming independent priors allows the kernel hyperparameters to be updated independently. Introducing Λ as the diagonal matrix with elements corresponding to $\{\nu_{il}\}$, and similarly, defining $\mathbf{K}_\beta$ with diagonal elements $\{K_{\beta_{il}}\}$, we have

$$p\big(\mathbf{s}; \Lambda, \mathbf{K}_\beta\big) \sim \mathcal{N}\big(0, \big(\Lambda \otimes I_n\big)\mathbf{K}_\beta\big). \tag{5.41}$$

We collect all the parameters characterizing the model into the vector η. It follows that

$$p(\mathbf{Z};\eta) \sim \mathcal{N}\big(0, \Sigma_{\mathbf{z}}\big), \tag{5.42}$$

where $\Sigma_{\mathbf{z}} = \mathbf{W}_\theta(\Lambda \otimes I_n)\mathbf{K}_\beta\mathbf{W}_\theta^\top + \Sigma_{\mathbf{e}}$, and

$$\Sigma_{\mathbf{e}} = \operatorname{diag}\big\{\lambda_1, \dots, \lambda_p, \lambda_j\big\} \otimes I_N. \tag{5.43}$$

Therefore, we can define the following ML criterion

$$\hat{\eta} = \arg\max_{\eta} \log p(\mathbf{Z};\eta). \tag{5.44}$$

Having set the notation, we outline the ECM algorithm for this general setting below. To this end, note that

$$p(\mathbf{s}|\mathbf{Z};\eta) = \mathcal{N}(\hat{\mathbf{s}}, \mathbf{P}), \tag{5.45}$$

where

$$\hat{\mathbf{s}} = \mathbf{P}\mathbf{W}_\theta^\top \Sigma_{\mathbf{e}}^{-1}\mathbf{Z}, \tag{5.46}$$

$$\mathbf{P} = \Big(\mathbf{W}_\theta^\top \Sigma_{\mathbf{e}}^{-1}\mathbf{W}_\theta + \big((\Lambda \otimes I_n)\mathbf{K}_\beta\big)^{-1}\Big)^{-1}. \tag{5.47}$$

We use again the notation $\hat{\mathbf{s}}^{(k)}, \hat{\mathbf{P}}^{(k)}, \hat{\mathbf{S}}^{(k)}$ to mean the estimates of the corresponding quantities at iteration k.

Theorem 5.4. *Let η collect all the parameters characterizing* (5.44)*, and let $\eta^{(k)}$ be its estimate after the k-th iteration of the ECM method. Then the estimate $\eta^{(k+1)}$ is obtained by means of the following updates:*

Hyperparameters. *Define*

$$Q_{\beta_{ij}}(\beta) = \log\det\big\{K_\beta\big\} + n\log\operatorname{Tr}\Big\{K_\beta^{-1}\hat{S}_{ij}^{(k)}\Big\}, \tag{5.48}$$

where $\hat{S}_{ij}^{(k)}$ is the $n \times n$ diagonal block of $\hat{S}^{(k)}$ corresponding to the path s_{ij}. Then ν_{ij} and β_{ij} are updated as in Theorem 5.2, for any i, j.

Module parameters. *Define*

$$\hat{\mathbf{A}}^{(k)} := \big(I_p \otimes D\big)^\top\Big(\bar{\mathbf{R}}\hat{\mathbf{S}}^{(k)}\bar{\mathbf{R}}^\top \otimes I_N\Big)\big(I_p \otimes D\big), \tag{5.49}$$

$$\Big(\hat{\mathbf{b}}^{(k)}\Big)^\top := \big(\tilde{w}_j - r_j\big)^\top\Big[\mathcal{T}_N\Big\{\mathbf{R}\hat{s}_1^{(k)}\Big\} \quad \dots \quad \mathcal{T}_N\Big\{\mathbf{R}\hat{s}_p^{(k)}\Big\}\Big], \tag{5.50}$$

where D is as in Theorem 5.3 and $\bar{\mathbf{R}} = I_p \otimes \mathbf{R}$. Then

$$\hat{\theta}^{(k+1)} = \arg\min_{\theta} \mathbf{g}_\theta^\top\hat{\mathbf{A}}^{(k)}\mathbf{g}_\theta - 2\Big(\hat{\mathbf{b}}^{(k)}\Big)^\top\mathbf{g}_\theta, \tag{5.51}$$

where

$$\mathbf{g}_\theta := \begin{bmatrix} g_{\theta_1} \\ \vdots \\ g_{\theta_p} \end{bmatrix}.$$

Noise variances.

$$\begin{aligned} \hat{\lambda}_i^{(k+1)} &= \frac{1}{N}\left(\|i\tilde{w}_i - \mathbf{R}\hat{s}_i^{(k)}\|_2^2 + \mathrm{Tr}\left\{ \mathbf{R}\hat{\mathbf{P}}_i^{(k)}\mathbf{R}^\top \right\} \right) \\ \hat{\lambda}_j^{(k+1)} &= \frac{1}{N}\big(\|i\tilde{w}_j - r_j - G_{\hat{\theta}^{(k+1)}}(I \otimes \mathbf{R})\hat{\mathbf{s}}^{(k)}\|_2^2 \\ &\quad + \mathrm{Tr}\left\{ G_{\hat{\theta}^{(k+1)}}\bar{\mathbf{R}}\hat{\mathbf{P}}^{(k)}\bar{\mathbf{R}}^\top G_{\hat{\theta}^{(k+1)}}^\top \right\} \big), \end{aligned} \tag{5.52}$$

where $\mathbf{P}_i^{(k)}$ *is the* $nm \times nm$ *diagonal block of* $\mathbf{P}^{(k)}$*, corresponding to the covariance matrix of* $\hat{s}_i^{(k)}$.

5.4 Including additional sensors

By using the kernel-based approach adopted above, the sensitivity paths could be modeled with only a few hyperparameters while still keeping the module of interest parametric. One potential benefit with this approach is that including another reference signal will not increase the number of estimated parameters significantly. Although the complexity of the problem increases slightly, only a few extra hyperparameters need to be estimated and the dimensions of (5.34) remain the same in the update of θ.

As reference signals can be added with little effort, a natural question is if also output measurements "downstream" of the module of interest can be added with little effort. In Example 5.1 the measurement w_4 is such a measurement that, with the same strategy as before, can be expressed as

$$w_4(t) = G_{43}(q)w_3(t) + r_4(t). \tag{5.53}$$

Using this measurement for the purpose of identification would require the identification of $G_{43}(q)$ in addition to the previously considered modules. The signal $w_4(t)$ contains information about $w_3(t)$, and thus information about the module of interest. The price we have to pay for this information is the additional parameters to estimate and, as we will see, another layer of complexity.

To extend the previous framework to include additional measurements after the module of interest, let us consider the case where we would like to include only one additional measurement, in this context denoted by $\tilde{w}_3(t)$; the generalization to more sensors is straightforward but notationally heavy. Let the path linking the target module to the additional sensor be denoted by $F(q)$, with impulse response f. Furthermore, let us for simplicity consider the

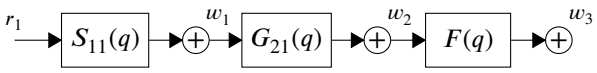

Figure 5.4: Basic network of 1 reference signal and 3 internal variables.

one-reference-signal-one-input case again, *i.e.*, (5.10), (5.11). The setting we consider has been illustrated in Figure 5.4. We model also this module using a Bayesian framework by interpreting f as a zero-mean Gaussian stochastic vector, *i.e.*,

$$p\Big(f; \nu_f, K_{\beta_f}\Big) \sim \mathcal{N}\Big(0, \nu_f K_{\beta_f}\Big), \tag{5.54}$$

where again K_{β_f} is the first-order stable spline kernel (5.15). We introduce the following variables

$$\lambda = \begin{bmatrix}\lambda_1 & \lambda_2 & \lambda_3\end{bmatrix}, \tag{5.55}$$

$$Z = \begin{bmatrix}\tilde{w}_1 \\ \tilde{w}_2 \\ \tilde{w}_3\end{bmatrix}, \tag{5.56}$$

$$Z_f = \tilde{w}_3. \tag{5.57}$$

For given vales of θ, s and f, we construct

$$W_s = \begin{bmatrix} R \\ G_\theta R \\ F G_\theta R \end{bmatrix}, \tag{5.58}$$

$$W_f = \mathcal{T}_N\big\{G_\theta R s\big\}, \tag{5.59}$$

$$\Lambda = \mathrm{diag}\{\lambda\} \otimes I_N. \tag{5.60}$$

Notice that the last internal variable w_3 can be expressed as

$$\begin{aligned} w_3 &= F G_\theta S r \\ &= G_\theta F S r \\ &= G_\theta F R s \\ &= G_\theta R F s \\ &= G_\theta R v, \end{aligned} \tag{5.61}$$

where commutation of the matrices follows from the fact that they are lower-triangular Toeplitz matrices, and $v := Fs$. For ease of exposition, we will also use the notation $v = f * s$.

The key difficulty in this setup is that the description of the measurements and the system description with both s and f no longer admit a jointly Gaussian probabilistic model, because v in (5.61) is the result of the convolution of two Gaussian vectors. In fact, a closed-form expression is not available. This fact has a detrimental effect in our empirical Bayes approach, because the marginal likelihood estimator of

$$\eta = \begin{bmatrix} \lambda & \nu_s & \beta_s & \nu_f & \beta_f & \theta \end{bmatrix}, \tag{5.62}$$

where ν_s, β_s are the hyperparameters of the prior of s, that is

$$\hat{\eta} = \arg\max_{\eta} p(Z;\eta) \tag{5.63}$$

$$= \arg\max_{\eta} \int p(Z, s, f;\eta)\mathrm{d}s\mathrm{d}f, \tag{5.64}$$

does not admit an analytical expression, since the integral (5.63) is intractable. To treat this problem, again we resort to EM-type methods. In this case, the latent variables to add to the problem are both s and f, so that the EM method has to alternate between the following steps:

(E-step). Given an estimate $\hat{\eta}^{(k)}$ (computed at the k-th iteration of the algorithm), compute

$$Q^{(k)}(\eta) := \mathbf{E}\left\{\log p(Z, s, f;\eta)\right\}, \tag{5.65}$$

where the expectation is taken with respect to the target distribution when the estimate $\eta^{(k)}$ is used, *i.e.*, $p\left(s, f \,|\, Z, \hat{\eta}^{(k)}\right)$;

(M-step). Solve the problem

$$\hat{\eta}^{(k+1)} = \arg\max_{\eta} Q^{(k)}(\eta). \tag{5.66}$$

While the M-Step remains substantially unchanged, the E-step requires more attention. Now, it requires the computation of the integral

$$\mathbf{E}\left\{\log p(Z, s, f;\eta)\right\} = \int \log p(Z, s, f;\eta) p\left(s, f \,|\, Z, \hat{\eta}^{(k)}\right)\mathrm{d}s\mathrm{d}f,$$

which does not admit an analytical solution, because the posterior distribution $p\left(s, f \,|\, Z, \hat{\eta}^{(k)}\right)$ is non-Gaussian (it does not have an analytical form, in fact). However, using Markov Chain Monte Carlo (MCMC) techniques, we can compute an approximation of the integral by sampling from the joint posterior density (also called a target distribution)

$$p(s, f \,|\, Z;\eta). \tag{5.67}$$

As pointed out before, (5.67) does not admit a closed-form expression and hence direct sampling is a hard task. However, if it is easy to draw samples from the conditional probability

distributions, samples of (5.67) can be easily drawn using the Gibbs sampler. In Gibbs sampling, each conditional is considered the state of a Markov chain; by iteratively drawing samples from the conditionals, the Markov chain will converge to its stationary distribution, which corresponds to the target distribution. In our problem, the conditionals of (5.67) are as follows:

$p(s|f, Z; \eta)$. Using (5.58), we write the linear model

$$Z = W_s s + e, \tag{5.68}$$

where $e = \begin{bmatrix} e_1^\top & e_2^\top & e_3^\top \end{bmatrix}^\top$. Then, given f, the vectors s and Z are jointly Gaussian, so that

$$p(s|f, Z; \eta) \sim \mathcal{N}\left(m_s, P_s\right), \tag{5.69}$$

with

$$\begin{aligned} P_s &= \left(W_s^\top \Sigma^{-1} W_s + \left(\nu_s K_{\beta_s} \right)^{-1} \right)^{-1} \\ m_s &= P_s W_s^\top \Sigma^{-1} Z. \end{aligned}$$

$p(f|s, Z; \eta)$. Given s and r, all sensors but the last becomes redundant. Using (5.59) we write the linear model

$$Z_f = W_f f + e_3, \tag{5.70}$$

which shows that

$$p(f|s, Z; \eta) \sim \mathcal{N}\left(m_f, P_f\right), \tag{5.71}$$

with

$$\begin{aligned} P_f &= \left(\frac{W_f^\top W_f}{\lambda_3} + (\nu_f K_{\beta_f})^{-1} \right)^{-1} \\ m_f &= P_f \frac{W_f^\top}{\lambda_3} Z_f. \end{aligned}$$

The following algorithm summarizes the Gibbs sampler used for dynamic network identification. In this algorithm, M_0 is the number of initial samples that are discarded, which is also known as the *burn-in* (Meyn and Tweedie, 2009). These samples are discarded since the Markov chain needs a certain number of samples to converge to its stationary distribution.

5.4.1 The ECM method with additional sensor

We now discuss the computation of the E-step and the CM-steps using the Gibbs sampler scheme introduce above.

Algorithm 2: Gibbs sampler for a dynamic network

Input : A parameter vector η
Output : Samples from the target distribution $p(s, f \mid Z; \eta)$
Initialization: compute initial value of s^0 and f^0.

for $k \leftarrow 1$ **to** $M + M_0$ **do**
  Draw the sample s^k from $p\big(s \mid f^{k-1}, Z; \eta\big)$
  Draw the sample f^k from $p\big(f \mid s^k, Z; \eta\big)$
end

Theorem 5.5. *Introduce the mean and covariance quantities*

$$s_s^M = \frac{1}{M} \sum_{k=M_0+1}^{M_0+M} s^k, \tag{5.72}$$

$$f_s^M = \frac{1}{M} \sum_{k=M_0+1}^{M_0+M} f^k, \tag{5.73}$$

$$v_s^M = \frac{1}{M} \sum_{k=M_0+1}^{M_0+M} v^k, \tag{5.74}$$

$$P_s^M = \frac{1}{M} \sum_{k=M_0+1}^{M_0+M} (s^k - s_s^M)(s^k - s_s^M)^\top, \tag{5.75}$$

$$P_f^M = \frac{1}{M} \sum_{k=M_0+1}^{M_0+M} (f^k - f_s^M)(f^k - f_s^M)^\top, \tag{5.76}$$

$$P_v^M = \frac{1}{M} \sum_{k=M_0+1}^{M_0+M} (v^k - v_s^M)(v^k - v_s^M)^\top, \tag{5.77}$$

where s^k, f^k and $v^k = s^k * f^k$ are samples drawn using Algorithm 2.

Define

$$\begin{aligned}
\tilde{Q}_s(\nu, \beta, x, X) &:= \log\det\{\nu K_\beta\} + \operatorname{Tr}\Big\{ \big(\nu K_\beta\big)^{-1} (xx^\top + X) \Big\}, \\
\tilde{Q}_z(\lambda, Z, x, X) &:= N \log\lambda + \frac{1}{\lambda} \|Z - Rx\|_2^2 + \frac{1}{\lambda} \operatorname{Tr}\big\{RXR^\top\big\}, \\
\tilde{Q}_f(\lambda, Z, \theta, x, X) &:= N \log\lambda + \frac{1}{\lambda} \big\|Z - G_\theta Rx\big\|_2^2 + \frac{1}{\lambda} \operatorname{Tr}\big\{G_\theta RXR^\top G_\theta^\top\big\}.
\end{aligned}$$

Then

$$\begin{aligned}
-2Q^{(k)}(\eta) = \lim_{M\to\infty} &\tilde{Q}_s(\nu_s, \beta_s, s_s^M, P_s^M) + \tilde{Q}_s(\nu_f, \beta_f, f_s^M, P_f^M) + \tilde{Q}_z(\lambda_1, \tilde{w}_1, s_s^M, P_s^M) \\
&+ \tilde{Q}_f(\lambda_2, \tilde{w}_2, \theta, s_s^M, P_s^M) + \tilde{Q}_f(\lambda_3, \tilde{w}_3, \theta, v_s^M, P_v^M).
\end{aligned} \tag{5.78}$$

The CM-steps are now very similar to the previous method and follows by similar reasoning as in the proof of Theorem 5.3.

Theorem 5.6. *Let $\hat{\eta}^{(k)}$ be the parameter estimate obtained at the k:th iteration. Define $S_s^M = s_s^M \left(s_s^M\right)^\top + P_s^M$, $S_v^M = v_s^M \left(v_s^M\right)^\top + P_v^M$,*

$$\begin{aligned} \hat{A}_s &= D^\top (R S_s^M R^\top \otimes I_N) D, & \hat{b}_s^\top &= \tilde{w}_2^\top \mathcal{T}_N\left\{R s_s^M\right\}, \\ \hat{A}_v &= D^\top (R S_v^M R^\top \otimes I_N) D, & \hat{b}_v^\top &= \tilde{w}_3^\top \mathcal{T}_N\left\{R v_s^M\right\}. \end{aligned}$$

Then the updated parameter vector $\hat{\eta}^{(k+1)}$ is obtained as follows

$$\hat{\theta}^{(k+1)} = \arg\min_\theta g_\theta^\top \left(\frac{1}{\lambda_2}\hat{A}_s + \frac{1}{\lambda_3}\hat{A}_v\right) g_\theta - 2\left(\frac{1}{\lambda_2}\hat{b}_s^\top + \frac{1}{\lambda_3}\hat{b}_v^\top\right) g_\theta. \tag{5.79}$$

The closed form updates of the noise variances are

$$\begin{aligned} \hat{\lambda}_1^{(k+1)} &= \frac{1}{N}\left(\|\tilde{w}_1 - R s_s^M\|_2^2 + \mathrm{Tr}\left\{R P_s^M R^\top\right\}\right), \\ \hat{\lambda}_2^{(k+1)} &= \frac{1}{N}\left(\left\|\tilde{w}_2 - G_{\hat{\theta}^{(k+1)}} R s_s^M\right\|_2^2 + \mathrm{Tr}\left\{G_{\hat{\theta}^{(k+1)}} R P_s^M R^\top G_{\hat{\theta}^{(k+1)}}^\top\right\}\right), \\ \hat{\lambda}_3^{(k+1)} &= \frac{1}{N}\left(\left\|\tilde{w}_3 - G_{\hat{\theta}^{(k+1)}} R v_s^M\right\|_2^2 + \mathrm{Tr}\left\{G_{\hat{\theta}^{(k+1)}} R P_v^M R^\top G_{\hat{\theta}^{(k+1)}}^\top\right\}\right). \end{aligned} \tag{5.80}$$

The kernel hyperparameters are updated through (5.28) *and* (5.29) *for both s and f.*

5.4.2 Identification algorithm

The proposed method for module identification can be summarized in the following steps.

Algorithm 3: Identification algorithm for dynamic network

Input : Measurement data Z, reference signal r.
Initialization: An initial estimate of $\hat{\eta}^{(0)}$, set $k = 0$.

repeat

- Compute the quantities (5.72)–(5.77) using samples generated from Algorithm 2.
- Update kernel hyperparameters $\nu_s^{(k+1)}$, $\beta_s^{(k+1)}$, $\nu_f^{(k+1)}$ and $\beta_f^{(k+1)}$ using (5.29)–(5.28).
- Update the vector $\theta^{(k+1)}$ solving (5.79).
- Update the noise variances $\lambda_1^{(k+1)}$, $\lambda_2^{(k+1)}$ and $\lambda_3^{(k+1)}$ using (5.80).
- Set $\eta^{(k+1)} = \left[\lambda_1^{(k+1)}\ \lambda_2^{(k+1)}\ \lambda_3^{(k+1)}\ \nu_s^{(k+1)}\ \beta_s^{(k+1)}\ \nu_f^{(k+1)}\ \beta_f^{(k+1)}\ \theta^{(k+1)}\right]$.
- Set $k = k + 1$.

until η *has converged*

As can be seen, the main difference with the one-input-one-sensor algorithm (see Section 5.3.4) is that the first steo of the algorithm requires a heavier computational burden, because of the integration via Gibbs sampling. Nevertheless, as will be seen in the next section, this pays off in terms of performance in identifying the target module.

5.5 Numerical simulations

In this section, we present results from two Monte Carlo simulations to illustrate the performance of the proposed method, which we abbreviate as *Network Empirical Bayes* (NEB) and its extension NEBX outlined in Section 5.4, and we compare with SMPE (see Section 5.2.2). We consider the network case of Example 5.1 and a simple closed loop network. The reference signals used are zero-mean unit-variance Gaussian white noise. The noise signals e_k are zero-mean Gaussian white noise with variances such that noise to signal ratios $\mathbf{Var}\{w\}_k / \mathbf{Var}\{e\}_k$ are constant. The setting of the compared methods are provided in some more details below, where the model order of the plant $G(q)$ is known for both the SMPE method and the proposed NEB method.

NEB: The method is initialized by the two-stage method. First, $\hat{S}(q)$ is estimated by least-squares. Second, G is estimated using MORSM (Everitt, Galrinho, et al., 2017b) from the simulated signal $\hat{w}$ obtained from (5.6) and $\tilde{w}_j$. MORSM is an iterative method that is asymptotically efficient for open loop data presented in Chapter 3. Then, the iterative method outlined in Section 5.3.4 is employed with the stopping criteria $\left\|\hat{\eta}^{(k+1)} - \hat{\eta}^{(k)}\right\| / \left\|\hat{\eta}^{(k)}\right\| < 10^{-10}$.

NEBX: The method is initialized by NEB. f^0 is obtained by an empirical Bayes method using simulated input and measured output of f. Then, the iterative method outlined in Section 5.4 is employed with the stopping criteria $\left\|\hat{\eta}^{(k+1)} - \hat{\eta}^{(k)}\right\| / \left\|\hat{\eta}^{(k)}\right\| < 10^{-10}$, or a maximum of 50 iterations.

SMPE: The method is initialized by the two-stage method, exactly as NEB. Then, the cost function (5.8), with a slight modification, is minimized. The modification of the cost function comes from that, as mentioned before, the SMPE method assumes that the noise variances are known. To make the comparison fair, also the noise variances need to be estimated. By maximum likelihood arguments, the logarithm of the determinant of the complete noise covariance matrix is added to the cost function (5.8) and the noise variances are included in θ, the vector of parameters to estimate. The tolerance is set to $\left\|\hat{\theta}^{(k+1)} - \hat{\theta}^{(k)}\right\| / \left\|\hat{\theta}^{(k)}\right\| < 10^{-10}$.

The simulations were run in Julia, a high-level, high-performance dynamic programming language for technical computing (Bezanson et al., 2017).

5.5.1 Closed-loop identification

The first Monte Carlo simulation is from a system operating in closed loop with an unknown low order controller with $N = 200$ data samples. This setting is slightly different to the standard closed-loop setting in that the measurement noise of $\tilde{w}_2$ is not fed back in the loop, and that the signals w_1 and w_2 are treated completely symmetric. The noise to signal ratio are all set to 1. The true plant and true controller are chosen such that the sensitivity function $S(q^{-1})$ has an impulse response that can be well approximated by $n = 100$ impulse response coefficients. The closed loop is depicted in Figure 5.5, where

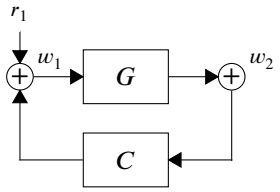

Figure 5.5: Closed loop network of first Monte Carlo simulation.

$$G(q,\theta) = \frac{b_1 q^{-1} + b_2 q^{-2}}{1 + a_1 q^{-1} + a_2 q^{-2}}, \tag{5.81}$$

The controller C is given by

$$C(q,\theta) = \frac{0.8 + 0.4q^{-1} - 0.5q^{-2}}{1 + 0.5q^{-1} + 0.2q^{-2}}, \tag{5.82}$$

with the parameter vector $\theta = [b_1, b_2, a_1, a_2]$, and true parameters $\theta^0 = [0.4, 0.5, -0.4, 0.3]$.

The two methods are compared using the fit of the impulse response coefficients of g according to

$$FIT = 1 - \frac{\left\| g^0 - \hat{g} \right\|_2}{\left\| g^0 \right\|_2} \tag{5.83}$$

For this example, the proposed NEB method achieves a higher fit, on average, than the SMPE method, cf. the box plot of Figure 5.6. Comparing the fits obtained at each Monte Carlo run (see Figure 5.7), it can be seen that NEB consistently performs at least as good as SMPE for almost every Monte Carlo run and in some runs considerably better. From the sample means and variance reported in Table 5.1, it can be seen that, in general, the estimates produced by NEB have smaller variance than SMPE while their mean values are similar.

Table 5.1: Sample mean and sample variance of the parameters estimates for $\hat{G}$ for compared methods.

	$b_1^0 = 0.2$		$b_2^0 = 0.3$		$a_1^0 = 0.4$		$a_2^0 = 0.5$	
Method	$\mathbf{E}_s\,\hat{b}_1$	$N\,\mathbf{Var}_s\,b_1$	$\mathbf{E}_s\,\hat{b}_2$	$N\,\mathbf{Var}_s\,b_2$	$\mathbf{E}_s\,\hat{a}_1$	$N\,\mathbf{Var}_s\,a_1$	$\mathbf{E}_s\,\hat{a}_2$	$N\,\mathbf{Var}_s\,a_2$
SMPE	0.21	0.43	0.31	0.93	0.50	3.4	0.16	2.8
NEB	0.20	0.22	0.31	0.26	0.68	2.9	0.23	2.0

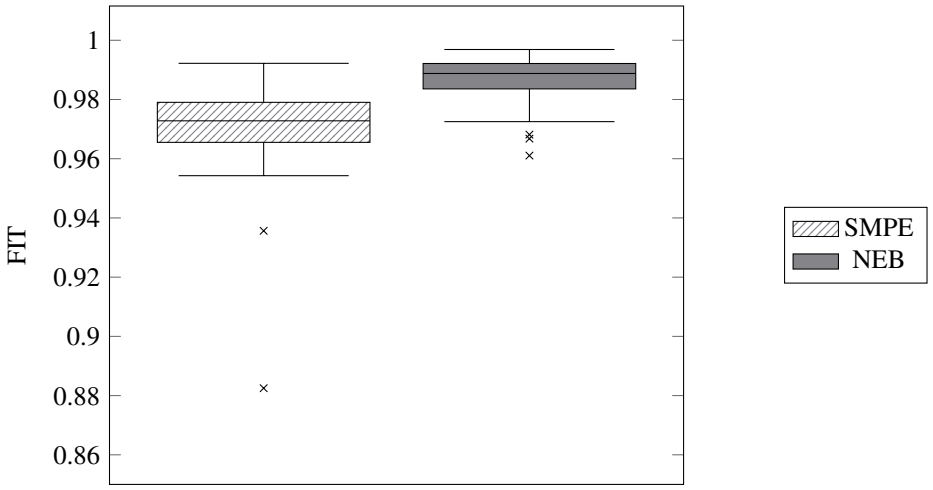

Figure 5.6: Box plot of the fit of the impulse response of G obtained by the SMPE, and NEB methods respectively.

5.5.2 Dynamic network example

This Monte Carlo simulation compares the NEB method and NEBX with the SMPE method on data from the network of Example 5.1, illustrated in Figure 5.1, where each of the modules are of second order, *i.e.*

$$G_{ij}(q) = \frac{b_1 q^{-1} + b_2 q^{-2}}{1 + a_1 q^{-1} + a_2 q^{-2}},$$

for a set of parameters that were chosen such that all modules are stable and all sensitivities $\{S_{12}(q), S_{24}(q), S_{22}(q), S_{24}(q)\}$ are stable and can be well approximated with 70 impulse response coefficients. Two reference signals, $r_2(t)$ and $r_4(t)$ are available and $N = 200$ data samples are used with the goal to estimate $G_{31}(q)$ and G_{32}. In total 6 transfer functions are estimated, $\{S_{12}(q), S_{24}(q), S_{22}(q), S_{24}(q), G_{31}(q)$ and $G_{32}(q)\}$, where

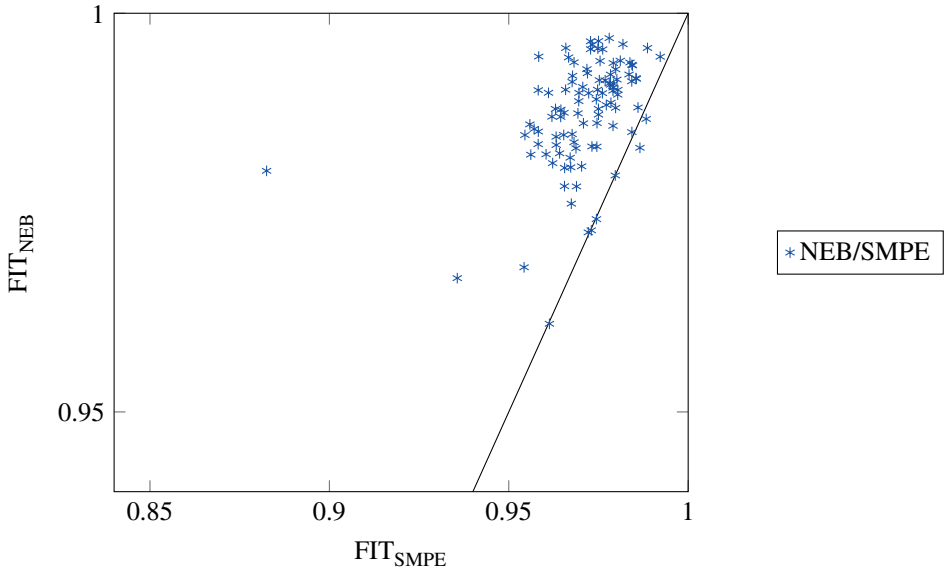

Figure 5.7: Each fit of the impulse response coefficients of G for NEB compared with SMPE for 100 Monte Carlo simulations. The black line represents $y = x$, *i.e.*, when SMPE performs equally good as NEB. Note the scaling of the x-axis of this figure.

Table 5.2: Sample mean and sample variance of the parameters estimates for $\hat{G}_{31}$ for the three compared methods.

	$b_1^0 = 0.2$		$b_2^0 = 0.3$		$a_1^0 = 0.4$		$a_2^0 = 0.5$	
Method	$\mathbf{E}_s\,\hat{b}_1$	$N\,\mathbf{Var}_s\,b_1$	$\mathbf{E}_s\,\hat{b}_2$	$N\,\mathbf{Var}_s\,b_2$	$\mathbf{E}_s\,\hat{a}_1$	$N\,\mathbf{Var}_s\,a_1$	$\mathbf{E}_s\,\hat{a}_2$	$N\,\mathbf{Var}_s\,a_2$
SMPE	0.20	0.088	0.28	0.075	0.36	1.6	0.53	0.85
NEB	0.21	0.049	0.29	0.070	0.36	0.94	0.52	0.62
NEBX	0.20	0.024	0.29	0.036	0.40	0.60	0.50	0.52

$\{S_{12}(q), S_{24}(q), S_{22}(q), S_{24}(q)\}$ are each parameterized by $n = 75$ impulse response coefficients in all methods. For NEBX also $G_{43}(q)$ is estimated by $n = 75$ impulse response coefficients. The noise to signal ratio at each measurement is set to $\mathbf{Var}\{w\}_k / \mathbf{Var}\{e\}_k = 0.1$ and the additional measurement used in NEBX has a lower noise to signal ratio of $\mathbf{Var}\{w\}_4 / \mathbf{Var}\{e\}_4 = 0.01$.

The fits of the impulse responses of G_{31} and G_{32} for the experiment are shown as a boxplot

Table 5.3: Sample mean and sample variance of the parameters estimates for $\hat{G}_{32}$ for the three compared methods.

	$b_1^0 = 0.4$		$b_2^0 = 0.5$		$a_1^0 = 0.5$		$a_2^0 = 0.15$	
Method	$\mathbf{E}_s\, \hat{b}_1$	$N\, \mathbf{Var}_s\, b_1$	$\mathbf{E}_s\, \hat{b}_2$	$N\, \mathbf{Var}_s\, b_2$	$\mathbf{E}_s\, \hat{a}_1$	$N\, \mathbf{Var}_s\, a_1$	$\mathbf{E}_s\, \hat{a}_2$	$N\, \mathbf{Var}_s\, a_2$
SMPE	0.34	1.9	0.44	2.1	0.60	5.0	0.23	3.0
NEB	0.34	0.30	0.44	0.30	0.65	1.0	0.26	0.84
NEBX	0.36	0.11	0.45	0.16	0.63	0.68	0.25	0.55

in Figure 5.8 and Figure 5.10 respectively. Comparing the fits obtained at each Monte Carlo run (see Figure 5.11 and Figure 5.11), the proposed NEB and NEBX methods are competitive with the SMPE method for this network. In many cases, the SMPE method failed to produce a reasonable estimate as 10 percent of the Monte Carlo runs gave a negative fit and were removed before the impulse response fits, boxplots and parameter sample means and variances were computed. From the sample means and variance reported in Table 5.2 and Table 5.3, it can be seen that, in general, the estimates produced by NEB and NEBX have, in general, significantly smaller variance than SMPE, while the mean values are roughly the same. Recalling that one of the motivations of the proposed methods was to reduced the variance induced by the high order modeling of the sensitivity paths, both the closed-loop example and network example gives some support for this motivation.

In almost all of the Monte Carlo runs, NEBX outperformed NEB in this simulation. However, NEBX is significantly more computationally expensive than NEB.

5.6 Summary

In this chapter, we have addressed the identification of a module in dynamic networks with known topology. The problem is cast as the identification of a set of systems in series connection. The second system corresponds to the target module, while the first represents the dynamic relation between exogenous signals and the input and the target module. This system is modeled following a Bayesian kernel-based approach, which enables the identification of the target module using empirical Bayes arguments. In particular, the target module is estimated using a marginal likelihood criterion, whose solution is obtained by a novel iterative scheme designed through the ECM algorithm. The method is extended to incorporate measurements downstream of the target module, which numerical experiments suggest increases performance.

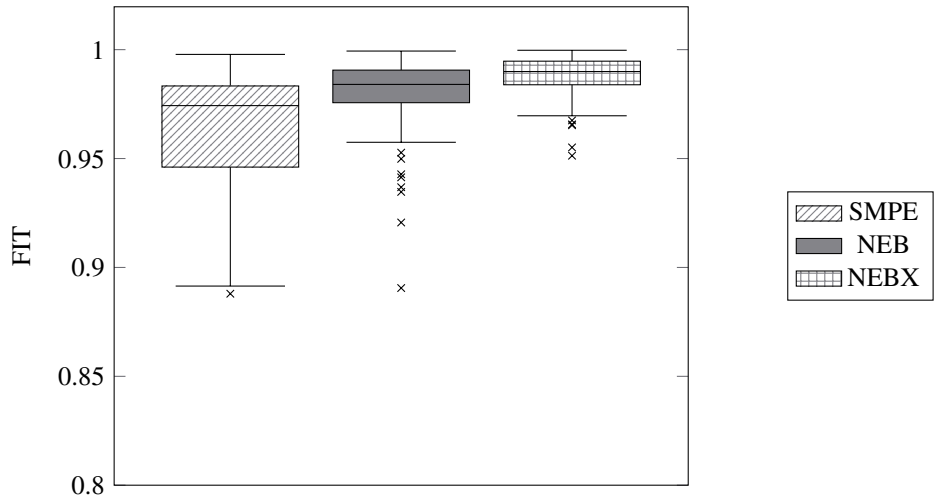

Figure 5.8: Box plot of the fit of the impulse response of G_{31} obtained by the methods SMPE, NEB and NEBX respectively.

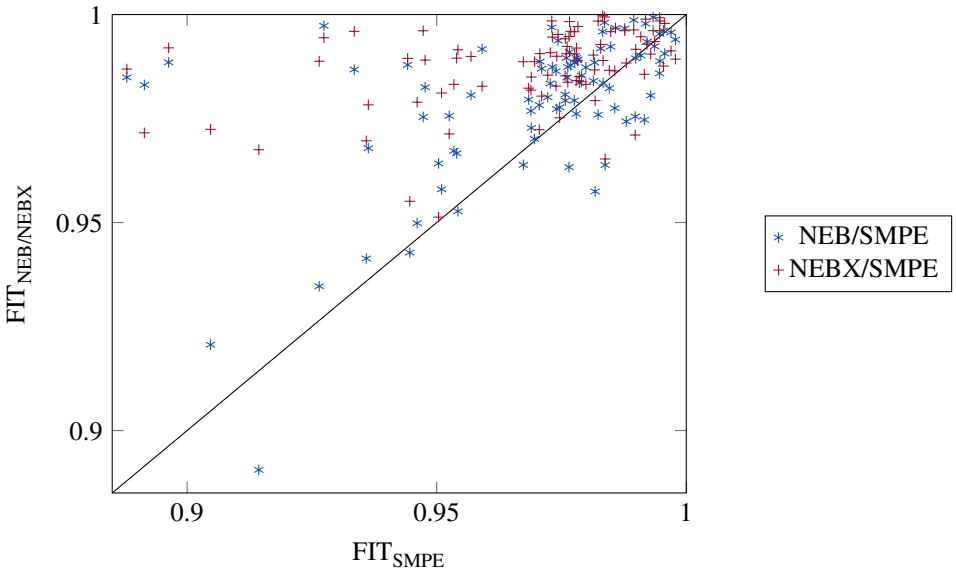

Figure 5.9: Fit of impulse response coefficients of G_{31} for SMPE compared with NEB and NEBX respectively for 100 Monte Carlo simulations. The black line represents $y = x$, *i.e.*, when SMPE performs equally good as NEB and NEBX.

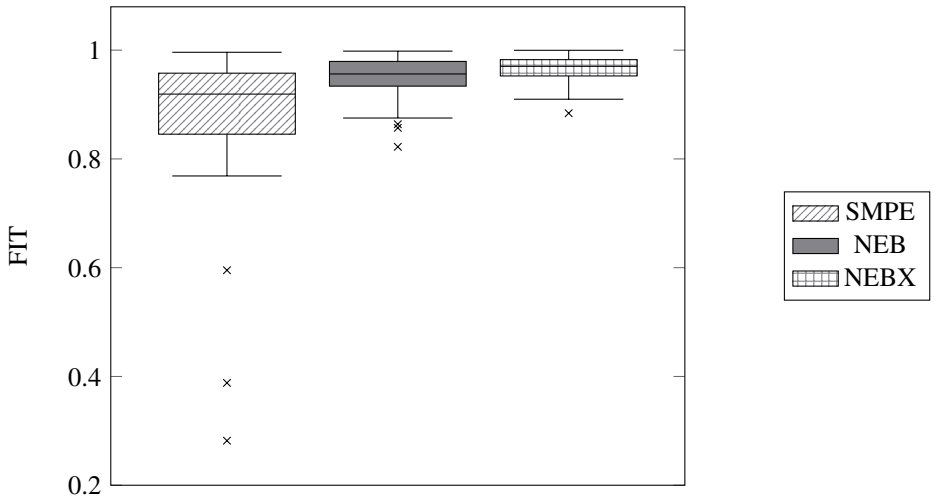

Figure 5.10: Box plot of the fit of the impulse response of G_{32} obtained by the methods SMPE, NEB and NEBX respectively.

5.A Proofs

Proof of Lemma 5.1

From Bayes' rule it follows that

$$\log p\big(Z, s_{11}; \hat{\eta}^{(k)}\big) = \log p\big(Z|s_{11}, \hat{\eta}^{(k)}\big) + \log p\big(s_{11}; \hat{\eta}^{(k)}\big), \tag{5.84}$$

with (neglecting constant terms)

$$\begin{aligned}\log p\big(Z|s_{11}, \eta\big) &\propto -\frac{1}{2}\log\det\big\{\Sigma_e\big\} - \frac{1}{2}\|Z - W_\theta s_{11}\|^2_{\Sigma_e^{-1}}\\ \log p\big(s_{11}; \eta\big) &\propto -\frac{1}{2}\log\det\big\{\nu K_\beta\big\} - \frac{1}{2}s_{11}^\top(\nu K_\beta)^{-1}s_{11}\,.\end{aligned}$$

Now we have to take the expectation w.r.t. the posterior $p\big(s_{11}|\tilde{w}_2; \hat{\eta}^{(k)}\big)$. Developing the second term in the first equation above and recalling that

$$\mathbf{E}_{p(s_{11}|\tilde{w}_2;\hat{\eta}^{(k)})}\big\{s_{11}^\top A s_{11}\big\} = \mathrm{Tr}\Big\{A\hat{S}_{11}^{(k)}\Big\}, \tag{5.85}$$

the statement of the lemma readily follows.

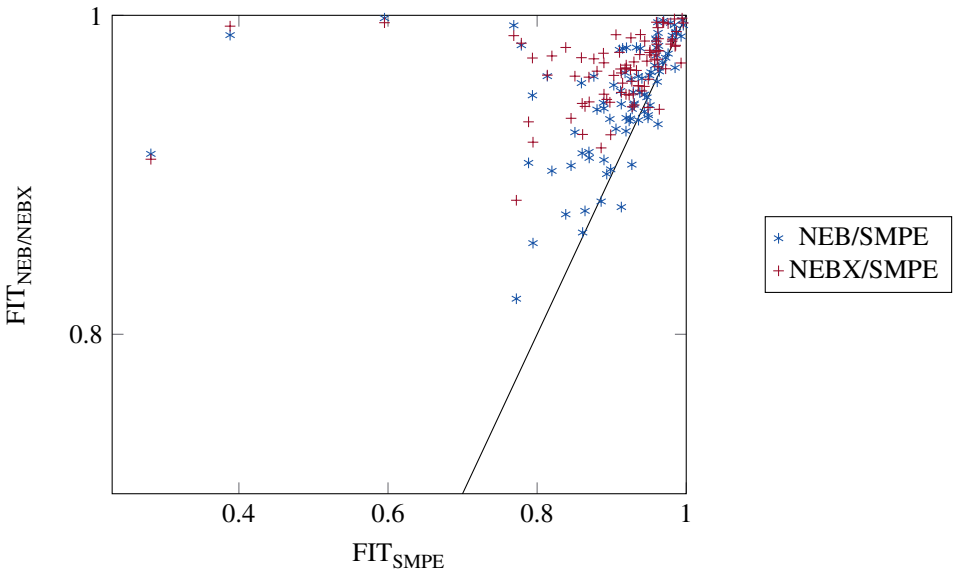

Figure 5.11: Fit of impulse response coefficients of G_{32} for SMPE compared with NEB and NEBX respectively for 100 Monte Carlo simulations. The black line represents $y = x$, *i.e.*, when SMPE performs equally good as NEB and NEBX. Note the scaling of the x-axis of this figure.

Proof of Theorem 5.3

In (5.25), fix Σ_e to the value $\hat{\Sigma}_e^{(k)}$ (computed inserting $\lambda_1^{(k)}$ and $\lambda_2^{(k)}$). After multiplication by a factor -2, we obtain the θ-dependent terms

$$-2Z^\top \big(\hat{\Sigma}_e^{(k)}\big)^{(-1)} W_\theta \hat{s}_{11}^{(k)} = -\frac{2}{\lambda_2^{(k)}} y^\top G_\theta R_1 \hat{s}_{11}^{(k)} + k_1 \tag{5.86}$$

$$= -\frac{2}{\lambda_2^{(k)}} y^\top \mathcal{T}_N \Big\{ R_1 \hat{s}_{11}^{(k)} \Big\} g_\theta + k_1, \tag{5.87}$$

$$\mathrm{Tr}\Big\{ W_\theta^\top \big(\Sigma_e^{(k)}\big)^{-1} W_\theta \hat{S}_{11}^{(k)} \Big\} = \frac{1}{\lambda_2^{(k)}} \mathrm{Tr}\Big\{ G_\theta R_1 \hat{S}_{11}^{(k)} R_1^\top G_\theta^\top \Big\} + k_2 \tag{5.88}$$

$$= \frac{1}{\lambda_2^{(k)}} \mathrm{vec}\big\{G_\theta\big\}^\top \Big(R_1 \hat{S}_{11}^{(k)} R_1^\top \otimes I_N \Big) \mathrm{vec}\big\{G_\theta\big\} + k_2$$

$$= \frac{1}{\lambda_2^{(k)}} g_\theta^\top D^\top \Big(R_1 \hat{S}_{11}^{(k)} R_1^\top \otimes I_N \Big) D g_\theta + k_2, \tag{5.89}$$

where k_1 and k_2 contain terms independent of θ. Recalling the definitions of $\hat{A}^{(k)}$ and $\hat{b}^{(k)}$, (5.34) readily follows.

Now, let θ be fixed at the value $\hat{\theta}^{(k+1)}$. After multiplication by a factor -2, the function (5.25) can be rewritten as

$$\begin{aligned} Q_0^{(k)}(\lambda_1, \lambda_2, \hat{\theta}^{(k+1)}) = N(\log\lambda_1 + \log\lambda_2) + \frac{\|\tilde{w}_1\|_2^2}{\lambda_1} + \frac{\|\tilde{w}_2\|_2^2}{\lambda_2} \\ - \frac{2\tilde{w}_1^\top}{\lambda_1} R_1 \hat{s}_{11}^{(k)} - \frac{2\tilde{w}_2^\top}{\lambda_2} G_{\hat{\theta}^{(k+1)}} R_1 \hat{s}_{11}^{(k)} \\ + \frac{1}{\lambda_1}\operatorname{Tr}\Big\{ R_1^\top R_1 \hat{S}_{11}^{(k)} \Big\} + \frac{1}{\lambda_2}\operatorname{Tr}\Big\{ R_1^\top G_{\hat{\theta}^{(k+1)}}^\top G_{\hat{\theta}^{(k+1)}} R_1 \hat{S}_{11}^{(k)} \Big\}. \end{aligned} \quad (5.90)$$

The results (5.35) follow by minimizing (5.90) with respect to λ_1 and λ_2. Differentiating w.r.t. λ_1 and λ_2 and calculating the zeros.

Proof of Theorem 5.5

Using Bayes' rule we can decompose the complete likelihood as

$$\log p\big(Z, s_{11}, f; \eta\big) = \log p\big(Z | s_{11}, f; \eta\big) + \log p\big(s_{11}; \eta\big) + \log p(f; \eta),$$

and we will analyze each term in turn. First, note that

$$\begin{aligned} -2\log p\big(s_{11}|\eta\big) &= \log\det\Big\{ \nu_s K_{\beta_s} \Big\} + s_{11}^\top \Big(\nu_s K_{\beta_s} \Big)^{-1} s_{11} \\ &= \log\det\Big\{ \nu_s K_{\beta_s} \Big\} + \operatorname{Tr}\Big\{ \Big(\nu_s K_{\beta_s} \Big)^{-1} s_{11} s_{11}^\top \Big\} \end{aligned}$$

Replacing $s_{11}s_{11}^\top$ with its sample estimate yields the first term in (5.78). Similarly,

$$-2\log p(f|\eta) = \log\det\Big\{ \nu_f K_{\beta_f} \Big\} + \operatorname{Tr}\Big\{ \Big(\nu_f K_{\beta_f} \Big)^{-1} f f^\top \Big\}.$$

Replacing $f f^\top$ with its sample estimate yields the second term in (5.78). Finally,

$$-2\log p\big(Z|t, s_{11}; \eta\big) = \log\det\{\Sigma\} + \big(Z - \hat{Z}\big)^\top \Sigma^{-1} \big(Z - \hat{Z}\big), \quad (5.91)$$

with

$$\hat{Z} := \begin{bmatrix} Rs \\ G_\theta Rs \\ G_\theta Rv \end{bmatrix}.$$

The first term of (5.91) is N times the sum of the logarithms of the noise variances squared. The second term of (5.91) decomposes into a sum of the (weighted) error of each signal. Then, the first weighted error is given by

$$\lambda_1 \left\| \tilde{w}_1 - Rs \right\|_2^2 = \left\| \tilde{w}_1 \right\|_2^2 - 2\tilde{w}_1^\top Rs + \mathrm{Tr}\left\{ Rss^\top R^\top \right\}.$$

Replacing s and $ss^\top$ with their respective expected values gives the third term in (5.78), with the corresponding noise variance term of (5.91) added. Similar calculations on the remaining two weighted errors in (5.91) gives the last two terms in (5.78). This concludes the proof.

Part II

Covariance analysis

CHAPTER 6

CASCADE MODELS

In the second and final part of the thesis, the covariance of modules embedded in different networks is analyzed. The aim is to illustrate how different properties of the identification problem affects the achievable accuracy. In particular, we quantify how the properties of the input and noise signals, as well as model structure, affect the covariance. The structures consider in this part will all be acyclic, *i.e.*, they will not contain feedback loops. However, identification in networks with feedback can be solved by converting the network to acyclic forms, as was examplified by the methods presented in the first main part of this thesis.

6.1 Introduction

We start by considering the relatively simple interconnection structure of modules connected in cascade. Cascaded modules are very common in applications; consider for example the flotation plant example in Chapter 1. Our concern in this chapter is the accuracy of the model of the first module, and we try to give some insight into how much the accuracy is improved by additional measurements. It turns out that the zero locations of the first module play an important role and we analyze how the zeros of the first module affect the accuracy. We quantify the contribution of each sensor to the accuracy, with focus on a frequency range dependent on the zeros of the transfer function of interest. This information might be useful in determining if we should use additional sensors. There is a trade-off to be made since additional sensors means more data have to be collected, and more parameters have to be identified. Hence, if the gain in accuracy is concentrated mainly in regions of little interest, the additional effort may not be worthwhile. For FIR systems, the results are illustrated by numerical simulations. A surprising special case occurs when the first module contains a zero on the unit circle; as the model orders of all modules grow large at the same rate, the variance of the frequency function estimate, evaluated at the corresponding frequency of the unit-circle zero, is shown to be the same as the case where the other modules are completely known.

6.2 Problem formulation

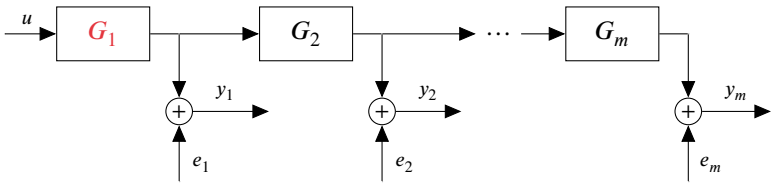

Figure 6.1: Cascaded structure.

Consider the SISO LTI systems connected in cascade as depicted in Figure 6.1, the output of which can be described by the following set of equations:

$$y_k(t) = \prod_{i=1}^{k} G_i(q)u(t) + e_k(t), \qquad k = 1, \dots, m. \tag{6.1}$$

Define

$$y(t) = \begin{bmatrix} y_1(t) \\ \vdots \\ y_m \end{bmatrix}, \qquad e(t) = \begin{bmatrix} e_1(t) \\ \vdots \\ e_m \end{bmatrix}, \tag{6.2}$$

and T as the row vector containing all frequency responses between u and $y(t)^\top$, *i.e.*,

$$T := \begin{bmatrix} G_1 & G_2G_1 & \dots & G_m \cdots G_1 \end{bmatrix}.$$

Then we can express the relationship between the input, noise and outputs as follows:

$$y(t)=T^\top u(t) + e(t).$$

We assume that the additive noise sequences, $\{e_i(t)\}$ are mutually independent zero mean white noise sequences, independent of the input $u(t)$, with variances $\lambda_i, i = 1, \dots, m$, *i.e.*,

$$\mathbf{Cov}\{e(t)\} = \Lambda,$$

where $\Lambda = \operatorname{diag}\{\lambda_1, \dots, \lambda_m\}$. The models of the modules are independently parameterized, module G_i is parameterized with $\theta_i \in \mathbb{R}^{d_i}$, $n_i \in \mathbb{R}$ for all $i = 1, \dots, m$, and let $\theta = \begin{bmatrix} \theta_1^\top & \dots & \theta_m^\top \end{bmatrix}^\top$ and $n = \sum_{i=1}^{m} n_i$. We assume the true system is in the model set and denote the true parameters by θ^o, *i.e.*,

$$G_k(q) = G_k\left(q, \theta_k^o\right), \qquad k = 1, \dots, m.$$

We are interested in estimating the first module G_1. The predictor of $y(t)$ based on θ is given by

$$\hat{y}(t) = T^\top(\theta)u(t).$$

The predictor error gradient defined in (2.23), of dimension $n \times m$, is then given by

$$\psi(t) = -T'(\theta)u(t),$$

where $T'(\theta) \in \mathcal{L}_2^{n\times m}$ is the gradient of T with respect to θ and is given by

$$T' = \begin{bmatrix} G_1' & G_2G_1' & \cdots & G_m \cdots G_2G_1' \\ 0 & G_2'G_1 & \ddots & G_m \cdots G_3G_2'G_1 \\ \vdots & \ddots & \ddots & \vdots \\ 0 & \cdots & 0 & G_m'G_{m-1} \cdots G_1 \end{bmatrix},$$

where G_i' is the gradient of G_i with respect to θ, for $i = 1, \ldots, m$. From (2.23) and Parseval's relation we can express the asymptotic covariance of the parameter estimate as

$$\begin{aligned} \mathbf{AsCov}\{\hat{\theta}_N\} &= \langle \Psi, \Psi \rangle^{-1} \\ \Psi &= T'(\theta^o)R\Lambda^{-1/2} \in \mathcal{L}_2^{n\times m}, \end{aligned}$$

where R is the spectral factor of the input power spectrum $\Phi_u(\omega)$. From this equation it is clear that we can rewrite

$$T'(\theta^o) = \Psi\Lambda^{1/2}R^{-1},$$

and hence, with $L = \Lambda^{1/2}R^{-1}$, we may use Lemma 2.2 to express the asymptotic covariance matrix for the estimate of the transfer functions from the input to the outputs as

$$\mathbf{AsCov}\{\hat{T}(e^{j\omega})\} = \frac{1}{\Phi_u(\omega)}\Lambda^{1/2}\sum_{k=1}^{l} \mathcal{B}_k^*(e^{j\omega})\mathcal{B}_k(e^{j\omega})\Lambda^{1/2}. \tag{6.3}$$

We are only interested in $\hat{G}_1$, so we only need to consider the top left corner of (6.3). To this end, without loss of generality, the basis functions can be expressed according to the following definition:

Definition 1. The basis functions $\{\mathcal{B}_k\}$ are expressed as

$$\mathcal{B}_k := \begin{bmatrix} c_k^1\mathcal{B}_k^1 & \ldots & c_k^m\mathcal{B}_k^m \end{bmatrix}, \tag{6.4}$$

where $c_k^j \in \mathbb{R}_{\geq 0}$. If $\mathcal{B}_k^j \neq 0$, then $\mathcal{B}_k^j$ has unit $\mathcal{L}_2$-norm for all j and k, *i.e.*, $\|\mathcal{B}_k^j\| = 1$ for all $k \leq l, j \leq m$. For each basis function $\mathcal{B}_k$, the coefficients $\{c_k^j\}_{j=1}^m$ satisfy $\left\| \begin{bmatrix} c_k^1 & \cdots & c_k^m \end{bmatrix} \right\|_2^2 = 1$, which ensures that $\|\mathcal{B}_k\| = 1$. If $\mathcal{B}_k^j = 0$ then c_k^j is defined to be zero.

With this notation, we obtain

$$\mathbf{AsVar}\{\hat{G}_1(e^{j\omega})\} = \frac{\lambda_1}{\Phi_u(\omega)}(c_k^1)^2 \sum_{k=1}^{l} \left|\mathcal{B}_k^1(e^{j\omega})\right|^2. \tag{6.5}$$

In the next section we will provide a specific basis function $\mathcal{B}_1$ that is used to obtain insights into (6.5), insight into how much $\mathbf{AsVar}\{\hat{G}_1(e^{j\omega})\}$ is reduced by additional measurements. The basis function will be determined by a zero of $G_1(e^{j\omega})$ and we will analyze $\mathbf{AsVar}\{\hat{G}_1(e^{j\omega})\}$ with focus on a frequency range dependent on this zero.

6.3 Variance results for one branch of cascaded systems

6.3.1 Basis functions and variance results

In this section we present a theorem that lets us determine one basis function, $\mathcal{B}_1$, of a set $\{\mathcal{B}_k\}_{k=1}^{l}$ that spans Ψ and satisfies

$$\left\langle \mathcal{B}_1^i, \mathcal{B}_j^i \right\rangle = 0, \qquad i = 1, \dots, l \qquad j = 2, \dots, m. \tag{6.6}$$

Not only is the first basis function $\mathcal{B}_1$ orthogonal to all other basis functions $\mathcal{B}_k$, $k = 2, \dots, l$, but also, every column of $\mathcal{B}_1$ is orthogonal the corresponding column in all other basis functions $\mathcal{B}_k$, $k = 2, \dots, l$. This allows us to compute the variance expression (6.5) at a specific frequency point.

Lemma 6.1. *Let G_1 have a zero in $\xi \in \mathbb{C}$ and none of $\{G_k\}_{k=1}^{m}$ have a pole in ξ,* i.e.*, there is no pole-zero cancellation of the zero ξ in Ψ. Let $\{\mathcal{A}_k^i\}_{k=1}^{l_i}$ be a basis (not necessarily orthonormal) for the space spanned by the rows of the i-th column of Ψ for $i = 1, \dots, m$. Then we can choose an orthonormal basis $\{\mathcal{B}_k\}_{k=1}^{l}$ for Ψ, in the form of* (6.4)*, such that*

$$\left\langle \mathcal{B}_1^i, \mathcal{B}_j^i \right\rangle = 0, \qquad i = 1, \dots, m \qquad j = 2, \dots, l, \tag{6.7}$$

where

$$c_1^1 = \frac{b_1}{\lambda_1^{1/2}} \left(\frac{b_1^2}{\lambda_1^{1/2}} + \frac{b_2}{\lambda_2^{1/2}} |G_2(\xi)|^2 + \cdots + \frac{b_m^2}{\lambda_m^{1/2}} |G_m(\xi) \cdots G_2(\xi)|^2 \right)^{-1/2}, \tag{6.7a}$$

$$\mathcal{B}_1^i = b_i \sum_{k=1}^{l_i} \overline{\mathcal{A}_k^i(\xi)} \mathcal{A}_k^i, \quad i = 1, \dots, m, \tag{6.7b}$$

and $\{b_i\}_{i=1}^{m}$ are normalization constants such that $\left\|\mathcal{B}_1^i\right\| = 1$, i.e.*,*

$$b_i^2 = \left(\sum_{k=1}^{l_i} \left|\mathcal{A}_k^i(\xi)\right|^2 \right)^{-1},$$

and $b_i^2 = l_i^{-1}$ *when* $\mathcal{A}_k^i$ *is an orthonormal basis,* e.g.*, the basis* $\{z^{-k}\}$.

Proof. See Appendix 6.A.2. ■

Notice that (6.7) does not follow from the orthogonality of the basis functions $\{\mathcal{B}_k\}$ as the next example illustrates.

Example 6.1. Consider

$$\Psi(z) = \begin{bmatrix} z^{-1} & z^{-2} \\ z^{-1} & -z^{-2} \end{bmatrix},$$

formed from $\{\mathcal{A}_k^1\}_{k=1}^1 = z^{-1}$ and $\{\mathcal{A}_k^2\}_{k=1}^1 = z^{-2}$. Recall that $\{z^{-k}\}_{k=0}^{\infty}$ forms a (complete) orthonormal set (Friedman, 1970). Then one choice of basis functions is

$$\mathcal{B}_1(z) = 2^{-1/2}\begin{bmatrix} z^{-1} & z^{-2} \end{bmatrix}, \qquad \mathcal{B}_2(z) = 2^{-1/2}\begin{bmatrix} z^{-1} & -z^{-2} \end{bmatrix}$$

and $\langle \mathcal{B}_1, \mathcal{B}_2 \rangle = 0$, even though $\langle \mathcal{B}_1^1, \mathcal{B}_2^1 \rangle = \langle z^{-1}, z^{-1} \rangle = 1$.

6.3.2 Variance results

The work invested in calculating a specific basis function will now be put to use. The covariance of the transfer function estimate will, at the frequency of the zero, be strongly linked to that specific basis function as the next theorem shows.

Theorem 6.2. *Assume that* G_1 *has a zero at* $\xi = re^{i\omega_\xi}$*, where* $r \in \mathbb{R}_{\geq 0}$ *and that the assumptions in Lemma 6.1 hold. Then*

$$\mathbf{AsVar}\{\hat{G}_1(e^{i\omega_\xi})\} \leq \frac{\lambda_1}{\Phi_u(\omega_\xi)}\|f_1\|^2\left(1 - \left(1 - (c_1^1)^2\right)\left\langle \mathcal{B}_1^1, \frac{f_1}{\|f_1\|}\right\rangle^2\right), \tag{6.8}$$

where c_1^1 *and* $\mathcal{B}_1^1$ *are chosen according to Lemma 6.7 and where*

$$f_1 = \sum_{k=1}^{l_1} \overline{\mathcal{A}_k^1(e^{i\omega_\xi})}\mathcal{A}_k^1.$$

If $r = 1$, i.e.*, the zero is lies on the unit circle, then*

$$\mathbf{AsVar}\{\hat{G}_1(e^{i\omega_\xi})\} = \frac{\lambda_1}{\Phi_u(\omega_\xi)}(c_1^1)^2 b_1^{-2}, \tag{6.9}$$

or equivalently

$$\mathbf{AsVar}\{\hat{G}_1(e^{i\omega_\xi})\} = Z^{-1}, \tag{6.10}$$

where

$$Z = b_1^2 \frac{\boldsymbol{\Phi}_u(\omega_\xi)}{\lambda_1} + b_2^2 \frac{\boldsymbol{\Phi}_u(\omega_\xi)}{\lambda_2} \left| G_2\left(\mathrm{e}^{\mathrm{j}\omega_\xi}\right) \right|^2 + \cdots + b_m^2 \frac{\boldsymbol{\Phi}_u(\omega_\xi)}{\lambda_m} \left| G_m\left(\mathrm{e}^{\mathrm{j}\omega_\xi}\right) \cdots G_2\left(\mathrm{e}^{\mathrm{j}\omega_\xi}\right) \right|^2.$$

Proof. Using Lemma 6.4 we can rewrite (6.5) as

$$\mathbf{AsVar}\left\{\hat{G}_1\left(r\mathrm{e}^{\mathrm{j}\omega_\xi}\right)\right\} = \frac{\lambda_1}{\boldsymbol{\Phi}_u(\omega_\xi)} \sum_{k=1}^{l} \left(c_k^1\right)^2 \left| \left\langle \mathcal{B}_k^1, f_1 \right\rangle \right|^2. \tag{6.11}$$

To arrive at (6.8) from (6.11), we notice that we can bound the contribution from the other basis functions through $c_k \leq 1$ and $\sum_{k=1}^{l} \left| \left\langle f_1, \mathcal{B}_k^1 \right\rangle \right|^2 = \left\| f_1 \right\|^2$, where the second equality is due to Lemma 6.4 in Appendix 6.A.1. We can form the upper bound

$$\begin{aligned}
\sum_{k=1}^{l} \left(c_k^1\right)^2 \left| \left\langle \frac{f_1}{\|f_1\|}, \mathcal{B}_k^1 \right\rangle \right|^2 &= \left(c_1^1\right)^2 \left| \left\langle \frac{f_1}{\|f_1\|}, \mathcal{B}_k^1 \right\rangle \right|^2 + \sum_{k=2}^{l} \left(c_k^1\right)^2 \left| \left\langle \frac{f_1}{\|f_1\|}, \mathcal{B}_k^1 \right\rangle \right|^2 \\
&\leq \left(c_1^1\right)^2 \left| \left\langle \frac{f_1}{\|f_1\|}, \mathcal{B}_k^1 \right\rangle \right|^2 + \sum_{k=2}^{l} \left| \left\langle \frac{f_1}{\|f_1\|}, \mathcal{B}_k^1 \right\rangle \right|^2 \\
&\leq \left(c_1^1\right)^2 \left| \left\langle \frac{f_1}{\|f_1\|}, \mathcal{B}_k^1 \right\rangle \right|^2 + \left(1 - \left| \left\langle \frac{f_1}{\|f_1\|}, \mathcal{B}_k^1 \right\rangle \right|^2 \right) \\
&= 1 - \left(1 - \left(c_1^1\right)^2 \right) \left| \left\langle \frac{f_1}{\|f_1\|}, \mathcal{B}_k^1 \right\rangle \right|^2.
\end{aligned}$$

Using this bound in (6.11) gives (6.8). If $r = 1$, *i.e.*, when the zero is on the unit circle, then $f_1 = b_1^{-1} \mathcal{B}_1^1$, *i.e.*, it is a scaled version of the first basis function. The orthogonality of $\left\{\mathcal{B}_k^1\right\}$ gives that (6.11) simplifies to

$$\mathbf{AsVar}\left\{\hat{G}_1\left(\mathrm{e}^{\mathrm{j}\omega_\xi}\right)\right\} = \frac{\lambda_1}{\boldsymbol{\Phi}_u(\omega_\xi)} \left(c_1^1\right)^2 b_1^{-2}.$$

By inserting the value of c_1^1 provided by Lemma 6.7, (6.9) and (6.10) follows. ∎

Remark 6.1. If G_1 has a unit circle zero in $\xi = r\mathrm{e}^{\mathrm{j}\omega_\xi}$, then (6.10) and (6.10) in Theorem 6.2 are exact expression for the asymptotic variance of the transfer function estimate $\mathbf{Var}\left\{\hat{G}_1\left(\mathrm{e}^{\mathrm{j}\omega}\right)\right\}$ at the frequency $\omega = \omega_\xi$. In (6.10), Z is a weighted sum of terms, where sensor k corresponds to a term

$$b_k^2 \frac{\boldsymbol{\Phi}_{SNR}^k(\omega)}{\left| G_1\left(\mathrm{e}^{\mathrm{j}\omega}\right) \right|^2},$$

where $\Phi^k_{SNR}(\omega)$ is the signal to noise ratio at sensor k, *i.e.*, for sensor k we have that

$$\Phi^k_{SNR}(\omega) = \frac{\Phi_u(\omega)\left|G_1\left(e^{j\omega}\right)\cdots G_k\left(e^{j\omega}\right)\right|^2}{\lambda_k}$$

This means that a higher ratio between the gain from the output of G_1 to a given sensor and the noise variance leads to better accuracy. The constants $\left\{b_j\right\}_{j=1}^m$, *i.e.*, the weights for the different signal to noise ratios in Z, provide a scaling that in some sense depends on the "size" of the corresponding spaces. This weighting gives that sensors far away from G_1 (sensors further to the right in Figure 6.1) contribute less to the accuracy of the model of G_1. If we only use the first measurement, we get

$$\mathbf{AsVar}\left\{\hat{G}_1\left(e^{j\omega_\xi}\right)\right\} = \frac{\lambda_k}{\Phi_u(\omega)}\frac{1}{b_k^2}$$

For fixed denominator models, *e.g.*, FIR models, this is exactly the high model order approximation 1.4, so this constant reflects the contribution to the model error from the model complexity. The expressions (6.10) and (6.10)) give insight into how much the variance of $\hat{G}_1\left(e^{j\omega_\xi}\right)$ would increase if we for example remove one sensor since this corresponds to removing the corresponding term in Z.

Similar observations can be made when $r \neq 1$ regarding the upper bound in (6.8). If we take a closer look at c_1^1, we see that a similar weighted sum of the signal to noise ratio $\Phi^k_{SNR}(\omega)$ of the sensors appears, almost the same as in Z. This means that a higher ratio between the gain from the output of G_1 to a given sensor and the noise variance leads to better accuracy. Again, $\left\{b_j\right\}_{j=1}^m$, *i.e.*,the weights for the different signal to noise ratios in c_1^1, provide a scaling that in some sense depends on the "size" of the corresponding spaces. This weighting gives that sensors far away from G_1 (more to the right in Figure 6.1) contribute less to the accuracy of the model of G_1.

Note that if one module is zero at $e^{j\omega_\xi}$, *i.e.*, $G_j\left(e^{j\omega_\xi}\right) = 0$, then sensors downstream of G_j will not reduce the variance of $G_1(e^{j\omega_\xi})$ regardless of their signal-to-noise ratio. This should come as no surprise since any measurement downstream of G_j will be zero, regardless of $G_1\left(e^{j\omega_\xi}\right)$. This generalizes to the following observation: if $G_j\left(e^{j\omega_\xi}\right)$ is small, then the benefit to the accuracy of $\hat{G}_1\left(e^{j\omega_\xi}\right)$ from sensors downstream of G_j is limited. These results are related to those found in Wahlberg et al., 2009, where, in the case of three modules, knowing y_2 and y_3 will not improve the quality of the estimate of θ_1, if $G_2\left(q,\theta_2^o\right)G_1'\left(q,\theta_1^o\right) = G_2'\left(q,\theta_2^o\right)G_1\left(q,\theta_1^o\right)$. Our results have a weaker condition and provide a weaker result, that is, if one zero is common between G_1 and G_2, then y_2 and y_3 will not considerably improve the quality of the estimate around the corresponding frequency.

The previous result is valid for $\hat{G}_1\left(e^{j\omega_\xi}\right)$, *i.e.*, at the same frequency as the zero. We will in the following corollary extend (6.8) to hold for all frequencies.

Corollary 6.3. *Let the assumptions of Theorem 6.2 hold, where G_1 has a zero at $\xi = re^{j\omega_\xi}$. Then*

$$\boldsymbol{AsVar}\{\hat{G}_1(e^{j\omega})\} \leq \frac{\lambda_1}{\boldsymbol{\Phi}_u(e^{j\omega})}\|f_1\|^2\left(1 - \left(1 - (c_1^1)^2\right)\left\langle \mathcal{B}_1^1, \frac{f_1}{\|f_1\|}\right\rangle^2\right), \qquad (6.12)$$

where

$$f_1 = \sum_{k=1}^{l_1} \overline{\mathcal{A}_k^1(e^{j\omega})}\mathcal{A}_k^1.$$

and where c_1^1 and $\mathcal{B}_1^1$ are chosen according to Lemma 6.7.

Proof. Follows from the proof of Theorem 6.2, by changing ω_ξ to ω in the definition of f_1, but keeping c_1^1 and $\mathcal{B}_1^1$ according to Lemma 6.7. ■

if $\omega \approx \omega_\xi$, we can expect $\mathcal{B}_1^1$ and f_1 to be similar and that (6.12) will provide a rather tight upper bound. However, if $f \perp \mathcal{B}_1$, *i.e.*, $\langle f, \mathcal{B}_1\rangle = 0$, then (6.12) gives the upper bound

$$\mathbf{AsVar}\{\hat{G}_1(e^{j\omega})\} \leq \frac{\lambda_1}{\boldsymbol{\Phi}_u(e^{j\omega})}\|f_1\|^2,$$

which is the same as if we would only use the first measurement to estimate $\hat{G}_1(e^{j\omega_\xi})$.

Theorem 6.2 and Corollary 6.3 only consider one basis function determined by one zero of G_1. If we know additional zeros, Theorem 6.2 provides different sets of basis functions for the different zeros and corresponding lower bounds for the variance at the corresponding frequencies. However, using Gram-Smith orthogonalization we can determine orthonormal basis functions of one set and refine the lower bounds in Theorem 6.2 and Corollary 6.3 accordingly.

6.4 Variance results for several branches of cascaded systems

In this section we generalize the previous result to an arbitrary number of branches. We only consider the case of one additional branch, even though the generalization to a tree structure is straightforward. We assume that we have an extra branch of m systems, which are connected in cascade, with the output of G_1 as input to the first additional system as depicted in Figure 6.2. The additional module G_i is parameterized with $\theta_i \in \mathbb{R}^{n_i}$, $n_i \in \mathbb{Z}_{\geq 0}$ for all $i = 1, \ldots, 2m$. The parameter vector is extended to $\theta_e = \left[\theta^\top, \theta_{m+1}^\top, \ldots, \theta_{2m}^\top\right]^\top$ and let $n_e = \sum_{i=1}^{2m} n_i$. The measured extra outputs can be described by the following set of equations:

$$y_k(t) = \left(\prod_{i=1}^{k} G_{m+i}(q)\right)G_1(q)u(t) + e_k(t), \qquad k = m+1, \ldots, 2m. \qquad (6.13)$$

The noise satisfies

$$\mathbf{Cov}\{e(t)\} = \Lambda_e,$$

where $\Lambda_e = \operatorname{diag}\{\lambda_1, \ldots, \lambda_{2m}\}$. Before we continue, we partition T and Ψ according to

$$T = \begin{bmatrix} G_1 & T_1 \end{bmatrix}.$$

We append T as follows:

$$T_e := \begin{bmatrix} G_1 & T_1 & T_2 \end{bmatrix}, \quad T_2 = \begin{bmatrix} G_{m+1}G_1 & G_{m+2}G_{m+1}G_1 & \cdots & G_{2m}\cdots G_{m+1}G_1 \end{bmatrix}.$$

The predictor error gradient is then of dimension $n_e \times 2m$, and is given by

$$\psi = -T_e'(\theta)u(t),$$

where $T'(\theta) \in \mathcal{L}_2^{n_e \times 2m}$ is the gradient of T_e with respect to θ, and is given by

$$T_e' = \begin{bmatrix} G_1' & G_1'T_1 & G_1'T_2 \\ 0 & T_1'G_1 & 0 \\ 0 & 0 & T_2'G_1 \end{bmatrix}.$$

The variance of the estimated parameters can also this time be expressed as

$$\begin{aligned} \mathbf{AsCov}\{\hat{\theta}_e\} &= \langle \Psi_e, \Psi_e \rangle^{-1} \\ \Psi_e &= T_e'(\theta^o) R \Lambda_e^{-1/2} \in \mathcal{L}_2^{n_e \times 2m}. \end{aligned}$$

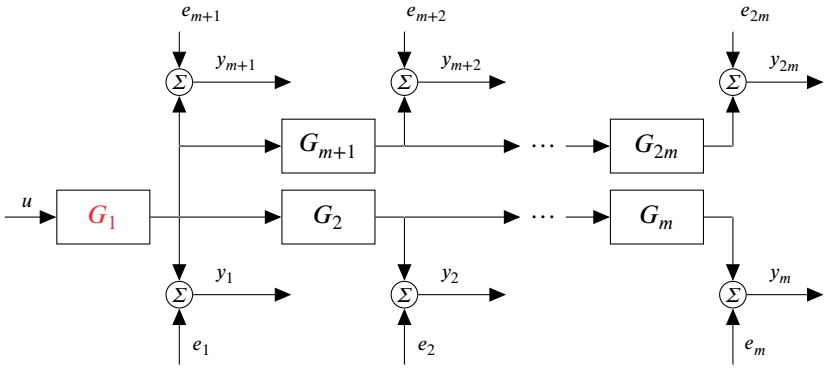

Figure 6.2: Cascaded structure with two branches.

It is straightforward to extend the previous results to this case. The only thing that is different is the constant c_1^1 in Lemma 6.1, Theorem 6.2 and corollary 6.3. The constant c_1^1 now becomes:

$$c_1^1 = b_1\lambda_1^{-1/2}\Big(b_1^2\lambda_1^{-1} + b_2^2\lambda_2^{-1}\big|G_2(\xi)\big|^2 + \cdots + b_l^2\lambda_m^{-1}\big|G_m(\xi)\cdots G_2(\xi)\big|^2 \\ b_{m+1}^2\lambda_{m+1}^{-1}\big|G_{m+1}(\xi)\big|^2 + \cdots + b_{2m}^2\lambda_{2m}^{-1}\big|G_{2m}(\xi)\cdots G_{m+1}(\xi)\big|^2\Big)^{-1/2} \quad (6.14)$$

and subsequently Z in (6.10) is changed accordingly. We get

$$Z = b_1^2\frac{\boldsymbol{\Phi}_u(\omega_\xi)}{\lambda_1} \\ +b_2^2\frac{\boldsymbol{\Phi}_u(\omega_\xi)}{\lambda_2}\Big|G_2\big(\mathrm{e}^{\mathrm{j}\omega_\xi}\big)\Big|^2 + \cdots + b_m^2\frac{\boldsymbol{\Phi}_u(\omega_\xi)}{\lambda_m}\Big|G_m\big(\mathrm{e}^{\mathrm{j}\omega_\xi}\big)\cdots G_2\big(\mathrm{e}^{\mathrm{j}\omega_\xi}\big)\Big|^2 \\ +b_{m+1}^2\frac{\boldsymbol{\Phi}_u(\omega_\xi)}{\lambda_{m+1}}\Big|G_{m+1}\big(\mathrm{e}^{\mathrm{j}\omega_\xi}\big)\Big|^2 + \cdots + b_{2m}^2\frac{\boldsymbol{\Phi}_u(\omega_\xi)}{\lambda_{2m}}\Big|G_{2m}\big(\mathrm{e}^{\mathrm{j}\omega_\xi}\big)\cdots G_{m+1}\big(\mathrm{e}^{\mathrm{j}\omega_\xi}\big)\Big|^2. \quad (6.15)$$

The remarks concerning Theorem 6.2 and corollary 6.3 also applies in this case. We see that a sensor k adds a term

$$b_k^2\frac{\boldsymbol{\Phi}_{SNR}^k(\omega)}{\Big|G_1\big(\mathrm{e}^{\mathrm{j}\omega}\big)\Big|^2},$$

where $\boldsymbol{\Phi}_{SNR}^k(\omega)$ is the signal to noise ratio at sensor k. We see that also in this case, the weighting b_k^2 gives that sensors far away from G_1 (more to the right in Figure 6.2) contribute less to the accuracy of $\hat{G}_1$. Also note that adding one branch, *i.e.*,adding modules $G_{m+1}, \ldots, G_{2m}$, do not reduce (nor increase) the weights b_k for $2 \le k \le m$; the contribution of the first branch stays the same.

6.5 Numerical simulations

In this section, we consider FIR systems, all with true order p. That is, module j can be expressed for some $\{g_{j,k}\}_{k=1}^p \in \mathbb{R}^p$ as

$$G_j(q) = \sum_{k=1}^{p} g_{j,k}q^{-k}.$$

The first system G_1 has a zero at $\xi = \mathrm{e}^{\mathrm{j}\omega_\xi}$, $\omega_\xi \in [0, 2\pi]$, $\boldsymbol{\Phi}_u \equiv 1$, and we estimate each transfer function with n_1 parameters. We only give the expressions for two modules to ease notation, but, the generalization to more sensors is straightforward. We assume that we

can take $\{\mathcal{A}_k^l\} = \{z^{-k}\}_{k=l}^{n_1+(l-1)p}$ as a basis for l-th column of Ψ. This assumption is a rank condition, based on that the l-th column will consist of the functions $\{z^{-k}\}_{k=l}^{n_1+(l-1)p}$. Thus, we exclude degenerate cases, *e.g.*, when $G_1 = G_2$. In the case we consider, $b_l^{-2} = n_1 + (l-1)p - (l-1)$ and (6.10) becomes

$$\mathbf{AsVar}\{\hat{G}_1(e^{i\omega_\xi})\} = \frac{n_1}{\lambda_1^{-1} + \frac{n_1}{n_1+p-1}\lambda_2^{-1}\left|G_2(e^{i\omega_\xi})\right|^2}. \tag{6.16}$$

We would expect that when we estimate both G_1 and G_2 with many parameters, the benefit of the second sensor would diminish. However, this is not the case when G_1 has a zero on the unit circle, as then, using (6.10) in Theorem 6.2,

$$\lim_{n_1\to\infty}\lim_{N\to\infty}\frac{N}{n}\mathbf{Var}\{\hat{G}_1(e^{i\omega_\xi})\} = \frac{1}{\frac{1}{\lambda_1} + \frac{1}{\lambda_2}\left|G_2(e^{i\omega_\xi})\right|^2}.$$

This is the same asymptotic variance as if the module G_2 was completely known (the noise signals are uncorrelated, so the optimal variance is the inverse of the sum of the information in each signal).

To us, this is a surprising result. However, it fits with the discussion on optimal input design of structured systems, where the input signal should be designed to hide unimportant system properties (see, *e.g.*, Hjalmarsson (2009)). Here, since $G_1(e^{i\omega_\xi}) = 0$, the output signal y_2 does not contain any information about $G_2(e^{i\omega_\xi})$ in the limit when the number of estimated parameters tends to infinity. However, what we measure in y_2 is 0 + noise, but the zero is the quantity$G_1(e^{i\omega_\xi})$ we try to identify, and hence y_2 can be used entirely to estimate this quantity.

In the following example and Example 6.3, (6.16) and its generalization are verified by MATLAB simulations.

Example 6.2. We consider a setup according to (6.1), with two FIR transfer functions: $G_1 = z^{-1} + z^{-2}$ and $G_2 = z^{-1}$, where $\lambda_1 = \lambda_2 = 1$. The first system, G_1, thus has a zero at $z = e^{j\pi}$. The input signal is white noise with variance $\sigma_u^2 = 1$. The variance at $\omega_\xi = \pi$ is estimated in 3 ways: from (6.10), directly from (2.23) and as the sample variance from 1,000 Monte-Carlo simulations. When estimating the given system with FIR models of order n_1, (6.10) reduces to

$$\mathbf{AsVar}\{\hat{G}_1(e^{i\omega_\xi})\} = \frac{1}{\frac{1}{n_1} + \frac{1}{n_1+1}}.$$

Each estimate in the Monte-Carlo simulations is the minimizer of the cost function

$$\sum_{i=1}^{N}\big(y_1(i) - G_1(q)u(i)\big)^2 + \big(y_2(i) - G_1(q)G_2(q)u(i)\big)^2,$$

Table 6.1: Comparison of the asymptotic variance of $\hat{G}_1\left(e^{j\pi}\right)$ with Monte-Carlo simulations.

$n_1^{-1}\,\mathbf{AsVar}\left\{\hat{G}_1\left(e^{j\pi}\right)\right\}$	(6.9)	Directly from (2.23)	Monte-Carlo
$n_1 = 2$	0.6000	0.6000	0.5913
$n_1 = 10$	0.5238	0.5238	0.5413

Table 6.2: Comparison of the asymptotic variance of $\hat{G}_1\left(e^{j\pi}\right)$ with Monte-Carlo simulations. The outputs y_1-y_4 are used here.

$n_1^{-1}\,\mathbf{AsVar}\left\{\hat{G}_1\left(e^{j\pi}\right)\right\}$	(6.9)	Directly from (2.23)	Monte-Carlo
$n_1 = 2$	0.3371	0.3309	0.3305
$n_1 = 10$	0.2336	0.2314	0.2561

with $N = 10^4$ data points. The minimization is solved with Matlab's built in function *lsqnonlin*, initialized at the true parameter values of the systems.

The Monte-Carlo simulations come close to what is predicted by (6.10) (*cf.* Table 6.1). The reduction in variance, compared to only using y_1, is centered around the frequency of the zero (see Figures 6.3 and 6.4). Note that if we only use y_1 then $N/n_1\,\mathbf{Var}\left\{\hat{G}_1\left(e^{i\omega_\xi}\right)\right\} = 1$ for all frequencies. The intuition is that the input to the second system is zero at the frequency $e^{i\omega_\xi}$ and therefore, with a slight abuse of notation, $y_2\left(e^{i\omega_\xi}\right)$ is a signal uncorrelated with the input $u\left(e^{i\omega_\xi}\right)$. Thus, $y_2(e^{i\omega_\xi})$ tells us that either $G_1\left(e^{i\omega_\xi}\right) = 0$, or $G_2\left(e^{i\omega_\xi}\right) = 0$ (or both). Furthermore, the transfer functions in our model set are all continuous, which implies that if G_2 is large around $e^{i\omega_\xi}$, it is unlikely to drop to zero at $e^{i\omega_\xi}$. Thereby, y_2 gives us information that $G_1(e^{i\omega_\xi})$ is small. A related aspect, not presented in the figures, is that the estimate of $G_2\left(e^{i\omega_\xi}\right)$ is poor because of the poor signal-to-noise ratio, as expected. When the number of estimated parameters increases, the reduction in variance becomes more focused around ω_ξ. This is due to the increased order of the basis functions (*cf.* Figures 6.3 and 6.4).

Example 6.3. Consider the case when two additional modules are appended to the setup of Example 6.2, still satisfying (6.1), with $G_3 = z^{-2}$, $G_4 = {}^{z^{-1}-z^{-2}}/\sqrt{2}$ and $\lambda_3 = \lambda_4 = 1$. Simulations are performed in the same way as in Example 6.2. Again, the Monte-Carlo simulations come close to what is predicted by (6.10) (*cf.* Table 6.3). Notice the similarities between the sets of Figures 6.3 and 6.4 compared to Figures 6.5 and 6.6; we get a variance reduction that is focused around the frequency of the unit circle zero, but, when we use more sensor the reduction is larger, and for both sets, as more parameters are estimated, the variance reduction becomes more focused.

The fit is significantly better in Figure 6.3 compared to Figures 6.4–6.6 because the ratio between number of samples and estimated parameters is larger. The difference between the Monte-Carlo simulations and the theory is smooth because only a relatively small number

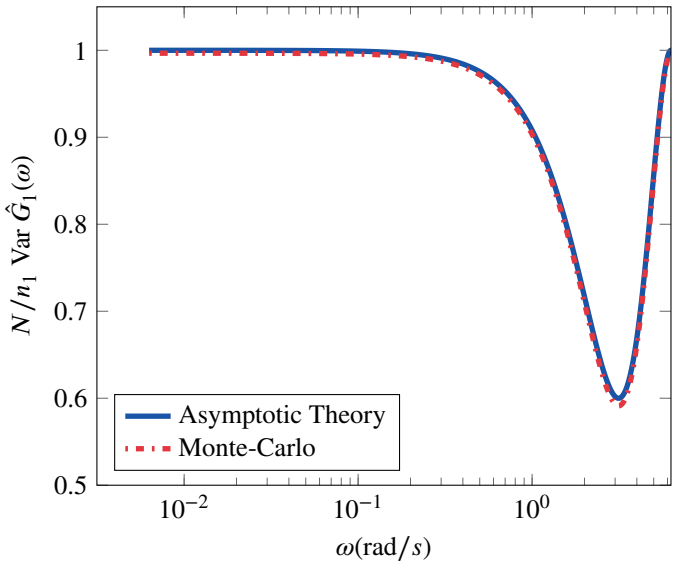

Figure 6.3: Asymptotic variance of $\hat{G}_1$ in Example 6.2, weighted by number of estimated parameters of $\hat{G}_1$ ($n_1 = 2$), and number of data points $N = 10^4$, at frequencies $[0, 2\pi]$. The variance is reduced around the frequency where G_1 is zero, when the output y_2 from G_2 is also used.

of parameters of $\hat{G}_1$ is estimated compared to the number of frequencies.

6.6 Summary

In this chapter we have analyzed the asymptotic variance of the first of a set of modules connected in a cascade structure. The main contribution is the result on how the zeros of the first module affect the accuracy of the corresponding model. The analysis has revealed a surprising result. When the first module contains a zero on the unit circle, as the model orders grow large, the variance at the corresponding frequency of the unit-circle zero is shown to be the same as if the other modules were completely known. Additionally, we have derived quantifications of the increase in accuracy for a broader frequency range, the extent of which depends on the number of estimated parameters and model structure.

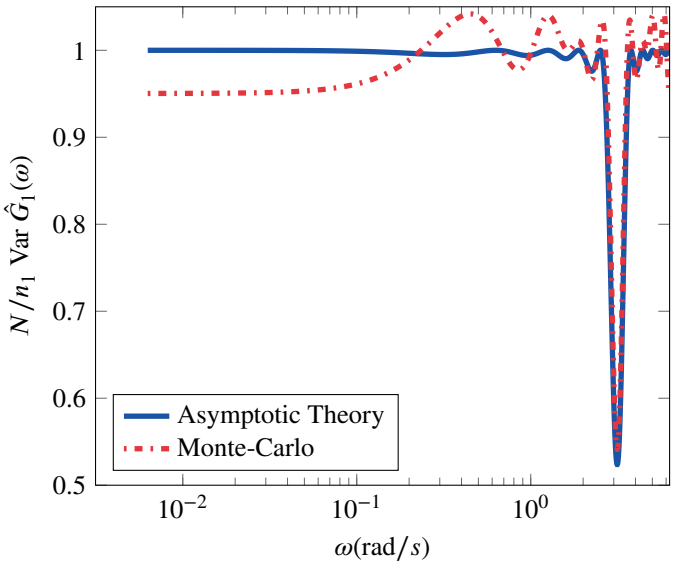

Figure 6.4: Asymptotic variance of $\hat{G}_1$ in Example 6.2, weighted by number of estimated parameters of $\hat{G}_1$ ($n_1 = 10$), and number of data points $N = 10^4$, at frequencies $[0, 2\pi]$. The reduction in variance is more focused around the frequency where G_1 is zero compared to Figure 6.3.

6.A Proofs and auxilliary lemmas

6.A.1 Auxilliary lemmas

Lemma 6.4. *Let $\mathcal{X}$ be a finite-dimensional subspace of $\mathcal{L}_2^m$, $\{\mathcal{A}_k\}_{k=1}^{\infty}$ be an orthonormal basis for $\mathcal{L}_2^m$ and $\{\mathcal{A}_k\}_{k=1}^{r}$ a basis for $\mathcal{X}$. If the function $f : \mathbb{C} \to \mathbb{C}^m$ is given by*

$$f(z) = \sum_{k=1}^{r} \overline{\mathcal{A}_k(\xi)}\mathcal{A}_k(z),$$

where $\xi \in \mathbb{C}$, then for any $G \in \mathcal{X}$

$$\langle G, f \rangle = G(\xi). \tag{6.17}$$

Proof. We can express G as

$$G = \sum_{j=1}^{r} G_j \mathcal{A}_j,$$

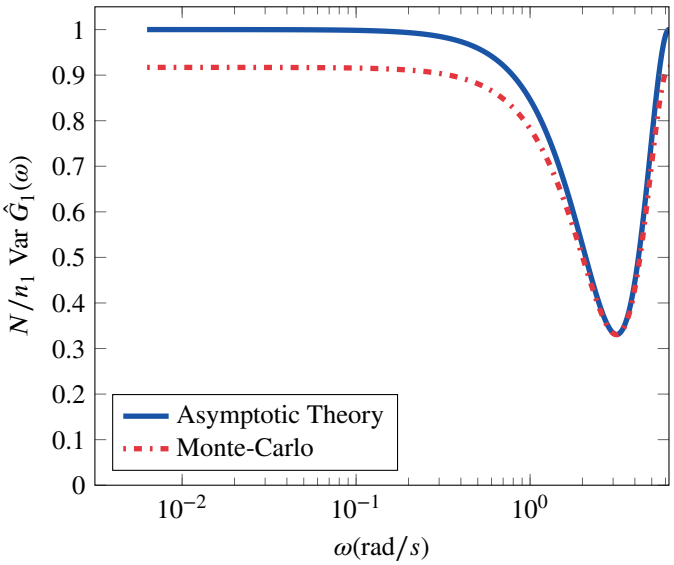

Figure 6.5: Asymptotic variance of $\hat{G}_1$ in Example 6.3, weighted by number of estimated parameters of $\hat{G}_1$ ($n_1 = 2$), and number of data points $N = 10^4$, at frequencies $[0, 2\pi]$. The variance is reduced more than in Figure 6.3, when also y_3 and y_4 are used.

for some scalars $\{G_j\}$. From the orthogonality of the basis functions we have that

$$\begin{aligned}\langle G, f\rangle &= \left\langle \sum_{j=1}^{r} G_j \mathcal{A}_j, \sum_{k=1}^{r} \overline{\mathcal{A}_k(\xi)}\mathcal{A}_k \right\rangle \\ &= \sum_{k=1}^{r} G_k \mathcal{A}_k(\xi) = G(\xi).\end{aligned}$$

■

Remark 6.2. The function f is strongly related to the so-called "reproducing kernel" for the space $\mathcal{X}$ (see Ninness and Hjalmarsson (2004) and the references therein).

Corollary 6.5. *Let $G \in \mathcal{X}$ and f be as in Lemma 6.17. Then*

$$\langle G, f\rangle = 0 \tag{6.18}$$

if and only if

$$G(\xi) = 0.$$

Proof. Follows directly from Lemma 6.4. ■

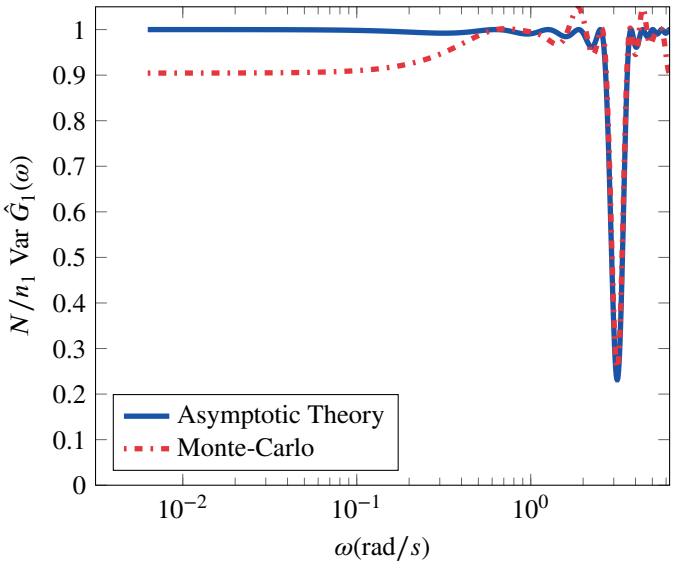

Figure 6.6: Asymptotic variance of $\hat{G}_1$ in Example 6.3, weighted by the number of estimated parameters of $\hat{G}_1$ ($n_1 = 10$), and number of data points $N = 10^4$, at frequencies $[0, 2\pi]$. The variance is reduced more than in Figure 6.4, when also y_3 and y_4 are used.

6.A.2 Proof of Lemma 4.2.1

For ease of notation we will assume that $\Phi_u\left(e^{j\omega}\right) = 1$ for $\omega \in [0, 2\pi]$ and $\lambda_1 = \cdots = \lambda_m = 1$; it is straightforward to adjust the derivations for the general setting. It is not obvious that $\mathcal{B}_1 = \begin{bmatrix} c_k^1 \mathcal{B}_k^1 & \cdots & c_k^m \mathcal{B}_k^m \end{bmatrix}$, as defined by (6.4), lies in the space spanned by the rows of Ψ; however, this will be clear from how we construct $\mathcal{B}_1$. To construct $\mathcal{B}_1$, we project Ψ onto the space $\mathcal{X}$, defined as the span of the m functions $\{\alpha_i\}$ that have $\mathcal{B}_1^i$ in the ith column and zeros in the other columns, *e.g.*, the first one being $\alpha_1 = \begin{bmatrix} \mathcal{B}_1^1 & 0 & \cdots \end{bmatrix}$. Here, $\mathcal{B}_1^k$ is defined as in (6.7b). The reason for this construction is that we can write (6.7) as

$$\left\langle \alpha_i, \mathcal{B}_j \right\rangle = 0, \qquad \text{for } i = 1, \ldots, m \qquad \text{for } j = 2, \ldots, m, \tag{6.19}$$

since $\left\langle \alpha_i, \mathcal{B}_j \right\rangle = 0$ if and only if $\left\langle \mathcal{B}_1^i, \mathcal{B}_j^i \right\rangle = 0$. Furthermore, the basis functions for Ψ, $\{\mathcal{B}_k\}_{k=1}^l$, satisfy (6.19) if and only if they are orthogonal to $\mathcal{X}$ for $k \geq 2$. Applying the projection of Ψ onto the space $\mathcal{X}$ according to (2.37), we obtain

$$\mathbf{Proj}_{\mathcal{X}}\{\Psi\} = \begin{bmatrix} \left\langle G_1', \mathcal{B}_1^1 \right\rangle \mathcal{B}_1^1 & \left\langle G_2 G_1', \mathcal{B}_1^2 \right\rangle \mathcal{B}_1^2 & \cdots & \left\langle G_m \cdots G_1', \mathcal{B}_1^m \right\rangle \mathcal{B}_1^m \\ 0 & 0 & 0 & 0 \\ \vdots & \vdots & \vdots & \vdots \end{bmatrix}, \tag{6.20}$$

where all rows are zero except the first because of Corollary 6.5. Furthermore, we have used the fact that $\mathcal{B}_1^k, k = 1, \ldots, l$ have unit norm. Applying Lemma 6.4 to (6.20) we obtain

$$\mathbf{Proj}_{\mathcal{X}}\{\Psi\} = \begin{bmatrix} G_1'(\xi) \\ 0 \\ \vdots \end{bmatrix} \begin{bmatrix} b_1\mathcal{B}_1^1 & b_2G_2(\xi)\mathcal{B}_1^2 & \cdots & b_mG_m(\xi)\cdots G_2(\xi)\mathcal{B}_1^m \end{bmatrix}.$$

Normalize the vector $\begin{bmatrix} b_1\mathcal{B}_1^1 & b_2G_2(\xi)\mathcal{B}_1^2 & \cdots & b_mG_m(\xi)\cdots G_2(\xi)\mathcal{B}_1^m \end{bmatrix}$ to form $\mathcal{B}_1$. Note that $\mathbf{Proj}_{\mathcal{X}}\{\Psi\} = [\, C \; 0 \,]^\top \mathcal{B}_1 = \mathbf{Proj}_{\mathcal{B}_1}\{\Psi\}$ for some constant vector C, *i.e.*, $\operatorname{rank}\{\mathbf{Proj}_{\mathcal{X}}\{\Psi\}\} = 1$ and $\mathcal{B}_1$ is a basis vector for the space spanned by the rows of $\mathbf{Proj}_{\mathcal{B}_1}\{\Psi\}$. Consequently, the part of Ψ that is orthogonal to $\mathcal{B}_1$ is also orthogonal to $\mathcal{X}$,

$$\Psi - \mathbf{Proj}_{\mathcal{B}_1}\{\Psi\} = \mathbf{Proj}_{\mathcal{X}^\perp}\{\Psi\} \perp \mathcal{X},$$

where $\mathcal{X}^\perp$ is the orthogonal complement of $\mathcal{X}$ in $\mathcal{L}_2$. However, for $2 \le k \le l$, $\mathcal{B}_k$ lies in the space spanned by the rows of $\Psi - \mathbf{Proj}_{\mathcal{B}_1}\{\Psi\}$, since this corresponds to he part of Ψ that is orthogonal to $\mathcal{B}_1$ ($\{\mathcal{B}_k\}_{k=1}^l$ is an orthonormal basis). As noted above, (6.7) is equivalent to (6.19), which only holds if $\mathcal{B}_k$, for $2 \le k \le l$, is orthogonal to $\mathcal{X}$. But, we know that $\mathcal{B}_k$, for $2 \le k \le l$, lies in $\Psi - \mathbf{Proj}_{\mathcal{B}_1}\{\Psi\}$ which we showed was orthogonal to $\mathcal{X}$ and the theorem follows.

CHAPTER 7

GENERALIZED PARALLEL CASCADE MODELS

In this chapter, we generalize the cascade models of the previous chapter to include parallel paths. We consider two forms of parallel serial structures, one multiple-input multiple-output structure and one single-input multiple-output structure. We derive lower and upper bounds on the asymptotic covariance of the frequency response function estimate and the model parameters for the case of temporally white noise.

7.1 Introduction

The first structure is an abstraction of the structure found in the motivating example on steam pressure control in Chapter 1. This structure has also been considered in Hägg et al. (2011), whose key results concern the case when there is common dynamics among the modules. The closed loop structure used in Chapter 4 and Chapter 5 can also fit in this formulation. The second structure can be an example of a network of spatially distributed sensors where the sensor dynamics are not completely known and therefore need to be estimated if these sensors are to be used. The structure considered corresponds to a star topology with the module of interest in the center (Yang et al., 2007). This structure can also lend some insight into the usefulness of additional sensors in Chapter 5. In the previous chapter, the model order of all the modules was the same. In this chapter, the model order of the system of interest will be fixed, while the model order of every other module will be allowed to increase. By letting the model order grow large we provide upper bounds on the variance of the parameter estimates. A lower bound can in turn be found by assuming the other modules to be known.

7.2 Problem formulation

We consider two types of networks of linear dynamic systems depicted in Figure 7.1 and Figure 7.2. For both networks, we wish to identify a model for module G. The first network

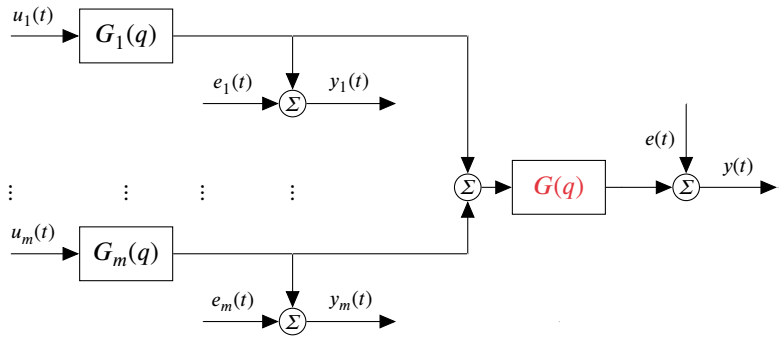

Figure 7.1: Structure 1: Parallel serial structure.

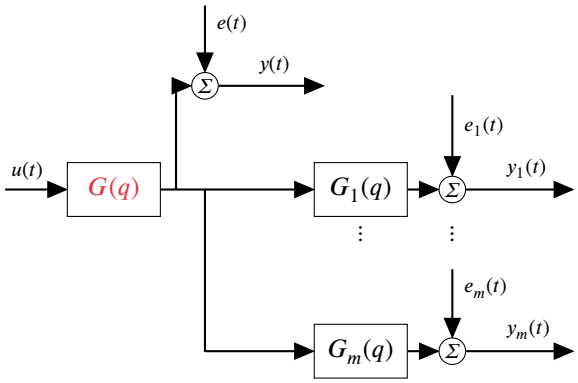

Figure 7.2: Structure 2: Multi-sensor structure.

is the parallel serial (cascade) structure considered in Hägg et al. (2011), see Figure 7.1. For this network, the dynamics are given as

Structure 1:

$$y(t) = \sum_{k=1}^{m} G(q)G_k(q)u_k(t) + e(t), \tag{7.1a}$$

$$y_k(t) = G_k(q)u_k(t) + e_k(t), \quad k = 1, \dots, m, \tag{7.1b}$$

where each input signal $u_k(t)$ is feed to the actuator module $G_k(q)$, the output of which is measured in $y_k(t)$ with additive noise $e_k(t)$. The sum of the outputs of all actuators is fed to the module $G(q)$, which is the one we are interested in. The output of $G(q)$ is measured as $y(t)$ with additive noise $e(t)$. For the second network structure, depicted in Figure 7.2, the dynamics are given as

Structure 2:

$$y_k(t) = G_k(q)G(q)u(t) + e_k(t), \quad k = 1, \dots, m, \tag{7.2a}$$
$$y(t) = G(q)u(t) + e(t), \tag{7.2b}$$

where there is only one input $u(t)$, which is fed to the module of interest $G(q)$ and measured as $y(t)$ with additive noise $e(t)$. The output of $G(q)$ is also fed to additional sensor modules $G_k(q)$ whose outputs are measured with additive noise. We assume that the additive zero mean stationary sequences $\{e_i(t)\}$ are mutually independent, and independent of the input signals $u_k(t), k = 1, \dots, m$ and input signal $u(t)$, with spectra $\Phi_{e_i}(\omega), i = 1, \dots, m$, the same holds for $e(t)$ with spectrum $\Phi_e(\omega)$. We will in the derivations, for improved readability, assume that the noise sequences are white noise with with variances $\lambda_i, i = 1, \dots, m$, the same holds for $e(t)$ with variance λ. The derivations for the general case follows analogously to the white noise case. The input is assumed to be a realization of a weakly stationary stochastic process with spectrum $\Phi_u(\omega)$. The inputs $u_k(t), k = 1, \dots, m$ (input $u(t)$) are assumed to be a realization of a weakly stationary stochastic process with spectra $\Phi_{u_k}(\omega), k = 1, \dots, m$ (spectrum $\Phi_u(\omega)$). The models of the modules are independently parametrized, *i.e.*, $G_k(q) = G_k(q, \theta_k)$, $k = 1, \dots, m$ and $G(q) = G(q, \eta)$. We stack the parameters together in $\theta = \left[\theta_1^\top, \dots, \theta_m^\top, \eta^\top\right]^\top$, where $\theta_i \in \mathbb{R}^{d_i}$, $d_i \in \mathbb{Z}_{\geq 0}$ for all $i = 1, \dots, m+1$, $\eta \in \mathbb{R}^d$.

7.3 Variance bounds for the parallel serial structure

In this section, we study the parallel cascade structure described by (7.1), and visualized in Figure 7.1. The main idea is to express the covariance of η, the parameters of the module of interest, as a sum of two parts, where the second part is a projection onto a space whose size depends on the model structure of the other modules. From this expression it will be possible to determine upper and lower bounds on the covariance of η. If we assume that the other modules are known exactly the projection becomes zero and we get a lower bound on the covariance. On the other hand, if we assume that the space is large, the projection can be removed and we get an upper bound.

The one step ahead predictor of $y(t)$ based on θ is given by

$$\hat{y}(t) = T(\theta)^\top u(t),$$

where

$$T = \begin{bmatrix} G_1(q, \theta_1) & 0 & 0 & G(q, \eta)G_1(q, \theta_1) \\ 0 & \ddots & 0 & \vdots \\ 0 & 0 & G_m(q, \theta_m) & G(q, \eta)G_m(q, \theta_m) \end{bmatrix}.$$

The predictor error gradient is then given by

$$\psi = -\begin{bmatrix} G_1'\big(q,\theta_1\big)u_1(t) & 0 & 0 & G_1'\big(q,\theta_1\big)G(q,\eta)u_1(t) \\ 0 & \ddots & 0 & \vdots \\ 0 & 0 & G_m'\big(q,\theta_m\big)u_m(t) & G_m'\big(q,\theta_m\big)G(q,\eta)u_m(t) \\ 0 & 0 & 0 & G'(q,\eta)\big(\sum_{k=1}^{m} G_k(q,\theta_k)u_k(t)\big) \end{bmatrix}.$$

Utilizing the assumption that the input signals are independent, (2.23) and Parseval's relation, we can express the asymptotic covariance of the parameter estimate as

$$\mathbf{AsCov}\big\{\hat{\theta}\big\} = \langle \Gamma A, \Gamma\rangle^{-1}, \tag{7.3}$$

where

$$\Gamma = \operatorname{diag}\big\{G_1'\big(q,\theta_1^o\big),\dots,G_1'\big(q,\theta_m^o\big),G'(q,\eta^o)\big\},$$

and

$$A = \begin{bmatrix} D & B^* \\ B & S \end{bmatrix},$$

with $D \in \mathcal{L}^{m\times m}$ with elements

$$D_{ij} = \begin{cases} \Phi_{u_i}(\lambda_i^{-1} + |G|^2\lambda^{-1}), & i = j, \\ 0, & \text{otherwise}, \end{cases} \tag{7.4}$$

$B \in \mathcal{L}^{1\times m}$ has elements

$$B_i = \Phi_{u_i}\overline{G_i}G\lambda^{-1}, \quad i = 1,\dots,m,$$

and S is the scalar function

$$S = \sum_{k=1}^{m} \Phi_{u_k}|G_k|^2\lambda^{-1}.$$

We now have an expression for the asymptotic covariance for $\hat{\eta}$ in the lower right corner of (7.3). As our next step, we will apply Lemma 7.3 to reformulate the covariance of $\hat{\eta}$ in (7.3) as the sum of two parts where the second part is a projection onto a space that depends on the model structure of the other modules. Then we will use Lemma 2.3 to derive lower and upper bounds. We are interested in G, so we need make the split to have all quantities related to $G_1,\dots,G_m$ in the first part and the ones related to G in the second part. Thus, we make the split

$$\Gamma_1 = \operatorname{diag}\big\{G_1',\dots,G_m'\big\}, \quad \Gamma_2 = G',$$

and

$$\Psi_2\Psi_1^* = G'B\Gamma_1^*, \quad \Psi_1\Psi_1^* = \Gamma_1 D\Gamma_1^*, \quad \Psi_2\Psi_2^* = G'SG'^*.$$

We assume that $\operatorname{rank}\{D\} = m$, which holds, *e.g.*, when $\Phi_{u_1}(\omega), \dots, \Phi_{u_m}(\omega) > 0$ and furthermore, we assume that also $\Gamma_1 D\Gamma_1^*$ has full rank. From Lemma 7.3 we have that the asymptotic covariance matrix of $\hat{\eta}$ is

$$\mathbf{AsCov}\{\hat{\eta}\} = \left[\left\langle G'S, G'\right\rangle - \left\langle \mathbf{Proj}_{S_{R_1}}\{\gamma\}, \mathbf{Proj}_{S_{R_1}}\{\gamma\}\right\rangle\right]^{-1} \tag{7.5}$$

with $\gamma = G'B\Gamma_1^*[R_1^{\dagger}]^*$, where R_1 is a spectral factor of $\Gamma_1 D\Gamma_1^*$, *i.e.*,

$$\Gamma_1\left(\mathrm{e}^{\mathrm{j}\omega}, \theta^o\right) D\left(\mathrm{e}^{\mathrm{j}\omega}, \theta^o\right) \Gamma_1^*\left(\mathrm{e}^{\mathrm{j}\omega}, \theta^o\right) = R_1\left(\mathrm{e}^{\mathrm{j}\omega}\right) R_1^{\mathsf{T}}\left(\mathrm{e}^{-\mathrm{j}\omega}\right),$$

such that the function $R_1(z)$ is analytic in the unit disc and has full rank on the unit circle. From (7.5) it is still not clear how different quantities affect $\mathbf{AsCov}\{\hat{\eta}\}$. To allow for an interpretation of (7.5), we will consider two extreme cases of the model order of the modules $\left\{G_k\right\}_{k=1}^m$. We first consider the modules $\left\{G_k\right\}_{k=1}^m$ to be known. Then no basis function of $\left\{G_k\right\}_{k=1}^m$ have to be estimated and $\left\langle \mathbf{Proj}_{S_{R_1}}\{\gamma\}, \mathbf{Proj}_{S_{R_1}}\{\gamma\}\right\rangle = 0$, since the projection is made onto the empty set S_{R_1}. This corresponds to a lower bound on $\mathbf{AsCov}\{\hat{\eta}\}$ since the projection is made onto a smaller subspace, cf. Lemma 2.3. The bound is given by

$$\mathbf{AsCov}\{\hat{\eta}\} \geq \left[\left\langle G' \sum_{k=1}^m M_{u_k}^L, G'\right\rangle\right]^{-1}, \tag{7.6}$$

where

$$M_{u_k}^L = \frac{\Phi_{u_k}\left|G_k\right|^2}{\lambda}, \quad k = 1, \dots, m.$$

The second case is when the model order grows large for the models associated with the modules $\left\{G_k\right\}_{k=1}^m$. Formally, if the rows of G_k' span $\mathcal{L}_2$ for all k, we have that $\mathcal{S}_{G_k'} = \mathcal{L}_2$ for all k. This implies that $\mathcal{S}_{\Gamma_1} = \mathcal{L}_2^m$. This is a conservative upper bound since $\mathcal{S}_{G_k'} \subseteq \mathcal{H}_2 \subset \mathcal{L}_2$. In this case, the projection in Lemma 7.4 can be removed (since the projection is made onto $\mathcal{L}_2^m$ and $\tilde{\gamma} \in \mathcal{L}_2^m$), which gives that

$$\mathbf{AsCov}\{\hat{\eta}\} < \left[\left\langle G'(S - \tilde{\gamma}\tilde{\gamma}^*), G'\right\rangle\right]^{-1},$$

where

$$\tilde{\gamma}\tilde{\gamma}^* = BD^{-1}B^* = \sum_{k=1}^m \frac{\Phi_{u_k}|G_kG|^2\lambda^{-2}}{\lambda_k^{-1} + |G|^2\lambda^{-1}}. \tag{7.7}$$

Simplifying the above expression leads to

$$\mathbf{AsCov}\{\hat{\eta}\} < \left[\left\langle G' \sum_{k=1}^m M_{u_k}^U, G'\right\rangle\right]^{-1}, \tag{7.8}$$

where,

$$M_{u_k}^U = \frac{\Phi_{u_k}|G_k|^2}{\lambda + |G|^2\lambda_k}, \quad k = 1, \dots, m. \tag{7.9}$$

We summarize the results in the following theorem for non-white noise spectra.

Theorem 7.1. *Let the system dynamics be described* (7.1)*. We assume that the additive zero mean stationary sequences* $\{e_i(t)\}$ *are mutually independent, and independent of the input signals* $u_k(t), k = 1, \dots, m$*, with spectra* $\Phi_{e_i}(\omega), i = 1, \dots, m$*; the same holds for* $e(t)$ *with spectrum* $\Phi_e(\omega)$*. The inputs* $u_k(t), k = 1, \dots, m$ *are assumed to be a realization of a weakly stationary stochastic process with spectra* $\Phi_{u_k}(\omega), k = 1, \dots, m$*. The models of the modules are independently parametrized,* i.e.*,* $G_k(q) = G_k(q, \theta_k)$*,* $k = 1, \dots, m$ *and* $G(q) = G(q, \eta)$*. We assume that* $\boldsymbol{D}$ *in* (7.4) *is full rank (*$\operatorname{rank}\{\boldsymbol{D}\} = m$*). Then*

$$\left[\left\langle G' \sum_{k=1}^{m} M_{u_k}^L, G' \right\rangle\right]^{-1} \leq \mathbf{AsCov}\{\hat{\eta}\} < \left[\left\langle G' \sum_{k=1}^{m} M_{u_k}^U, G' \right\rangle\right]^{-1}, \tag{7.10}$$

where

$$M_{u_k}^L = \frac{\Phi_{u_k}|G_k|^2}{\Phi_e}, \quad k = 1, \dots, m, \tag{7.11a}$$

$$M_{u_k}^U = \frac{\Phi_{u_k}|G_k|^2}{\Phi_e + |G|^2\Phi_{e_k}}, \quad k = 1, \dots, m. \tag{7.11b}$$

Remark 7.1. Comparing (7.11a) and (7.11b) in (7.10) with open loop SISO identification, we see that $\sum_{k=1}^{m} M_{u_k}$ plays the same role as the signal to noise ratio. For the corresponding open loop SISO case, we have

$$\mathbf{AsCov}\{\hat{\eta}\} = \left[\left\langle G' \frac{\Phi_u}{\Phi_e}, G' \right\rangle\right]^{-1},$$

The lower bound directly corresponds to this case with $\Phi_u = \sum_{k=1}^{m} \Phi_{u_k}|G_k|^2$. When we know the dynamics of the actuators, the measurements of $\{y_k(t)\}_{k=1}^{m}$ are redundant. On the other hand, when the actuator dynamics $\{G_k(q)\}_{k=1}^{m}$ are estimated with high order models, the spectrum of the noise also plays a role. In (7.9), the power spectrum of the input signal fed to the system of interest $G(q)$, is the same as in (7.7). However, the denominator is given by the spectrum of the noise affecting $y(t)$, Φ_e, and by Φ_{e_k}, the spectrum of the noise affecting the input measurement y_k, weighted by the module of interest $|G|^2$. Since Φ_{e_k}, the noise spectrum at the input measurements, is scaled by the system of interest G, high noise variance in the input measurements hurts us the most at frequencies where the gain of the system of interest is high.

The next example illustrates the benefit of knowing a disturbance.

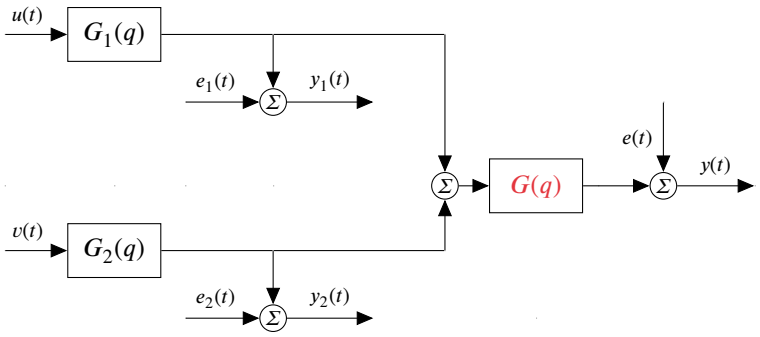

Figure 7.3: Network considered in Example 7.1.

Example 7.1. We consider a system with one input $u(t)$ and a measurable disturbance $v(t)$ with spectrum $\Phi_v(\omega)$. The noise $e(t)$ affecting the output of the system of interest $y(t)$ is white noise with variance λ. The system is shown in Figure 7.3. We will compare the case when the disturbance $v(t)$ is not measured with the case when it is measured and used in the predictor ($v(t)$ known). We assume that we estimate many parameters in G_1 and G_2, and thus we can consider the upper bound given by (7.11b) in (7.10). In the first case, the noise affecting $y(t)$ is given by $e(t) + G(q)G_2(q)v(t)$, which has spectrum $\lambda + \left|G(q)G_2(q)\right|^2\Phi_v(\omega)$. Hence, the upper bound in (7.11b) is given by

$$\mathbf{AsCov}\{\hat{\eta}\} \leq \left[\left\langle G' \frac{\Phi_u|G_1|^2}{\lambda + |GG_2|^2\Phi_v + |G|^2\lambda_1}, G' \right\rangle\right]^{-1}, \tag{7.12}$$

when the disturbance $v(t)$ is not measured. The disturbance thus increases the variance of $\hat{\eta}$, since it increases the denominator in (7.12). If we measure the disturbance, the upper bound on the covariance is instead given by (7.11b) as

$$\mathbf{AsCov}\{\hat{\eta}\} \leq \left[\left\langle G'\left(\frac{\Phi_u|G_1|^2}{\lambda + |G|^2\lambda_1} + \frac{\Phi_v|G_2|^2}{\lambda + |G|^2\lambda_2}\right), G' \right\rangle\right]^{-1}, \tag{7.13}$$

The variance is decreased in (7.13) compared with (7.12) for two reasons: (i) we reduce the noise affecting $y(t)$, and (ii) we provide a new excitation. From the reduced noise (i), the first term inside the parenthesis in (7.13) is larger than the corresponding term in (7.12). The second term inside the parenthesis in (7.13) corresponds to the new excitation (ii).

7.4 Variance bounds for the multi-sensor structure

In this section we study the multi-sensor structure described by (7.2), which is visualized in Figure 7.2. The main idea is to express the covariance of η, the parameters of the module of

interest, as a sum of two parts, where the second part is a projection onto a space whose size depends on the model structure of the other modules. From this expression it will be possible to determine upper and lower bounds on the covariance of η. If we assume that the other modules are known exactly the projection becomes zero and we get a lower bound on the covariance. If, on the other hand, we assume the space is large the projection can be removed and we get an upper bound. The minimum variance one step ahead predictor of $y(t)$ based on θ is given by

$$\hat{y}(t) = T(\theta)^\top u(t), \tag{7.14}$$

where

$$T = \begin{bmatrix} G_1(q,\theta_1)G(q,\eta) & \dots & G_m(q,\theta_m)G(q,\eta) & G(q,\eta) \end{bmatrix}.$$

The predictor error gradient is then given by

$$\psi(t) = -\begin{bmatrix} G_1'(q,\theta_1)G(q,\eta) & 0 & 0 & 0 \\ 0 & \ddots & 0 & 0 \\ 0 & 0 & G_m'(q,\theta_m)G(q,\eta) & 0 \\ G'(q,\eta)G_1(q,\theta_1) & \dots & G'(q,\eta)G_m(q,\theta_1) & G'(q,\eta) \end{bmatrix} u(t).$$

Using (2.23) and Parseval's relation, we can express the asymptotic covariance of the parameter estimate as

$$\mathbf{AsCov}\{\hat{\theta}\} = \langle \Gamma A, \Gamma \rangle^{-1}, \tag{7.15}$$

$$\Gamma = \operatorname{diag}\{G_1'(q,\theta_1^o), \dots, G_1'(q,\theta_m^o), G'(q,\eta^o)\},$$

where Γ should be interpreted as block wise diagonal, and

$$A = \begin{bmatrix} D & B^* \\ B & S \end{bmatrix},$$

with $D \in \mathcal{L}^{m\times m}$ with elements

$$D = \operatorname{diag}\{|G|^2\lambda_1^{-1}, |G|^2\lambda_2^{-1}, \dots, |G|^2\lambda_m^{-1}\}. \tag{7.16}$$

$B \in \mathcal{L}^{1\times m+1}$ has elements

$$B_i = \Phi_u \overline{G} G_i \lambda_i^{-1}$$

and S is the scalar function

$$S = \Phi_u \lambda^{-1} + \sum_{k=1}^{m} \Phi_u |G_k|^2 \lambda_k^{-1}.$$

We now have an expression for the asymptotic covariance for $\hat{\eta}$ in the lower right corner of (7.15). As our next step, we will apply Lemma 7.3 to reformulate the covariance of $\hat{\eta}$ in (7.15) as the sum of two parts where the second part is a projection onto a space that depends on the model structure of the other modules. Then we will use Lemma 2.3 to derive lower and upper bounds.We are interested in G, so we need make the split to have all quantities related to $G_1, \ldots, G_m$ in the first part and the ones related to G in the second part. Thus, we make the split

$$\Psi_2\Psi_1^* = G'B\Gamma_1^*, \quad \Psi_1\Psi_1^* = \Gamma_1 D\Gamma_1^*, \quad \Psi_2\Psi_2^* = G'SG'^*,$$

and

$$\Gamma_1 = \operatorname{diag}\{G_1', \ldots, G_m'\}, \quad \Gamma_2 = G'.$$

We assume that $\tilde{\Psi}_1\tilde{\Psi}_1^*$ has full rank ($\operatorname{rank}\{\tilde{\Psi}_1\tilde{\Psi}_1^*\} = m$), which essentially is an identifiability condition. This holds, *e.g.*, when

$$\Phi_u(\omega) > 0, \qquad \left|G\left(e^{j\omega}\right)\right|^2 > 0, \qquad \omega \in [-\pi, \pi].$$

From Lemma 7.3 we have that the asymptotic covariance matrix for $\hat{\eta}$ is given by (7.5) with $\gamma = G'T\Gamma_1^*[R_1^{\dagger}]^*$, where R_1 is a minimum phase spectral factor of $\Gamma_1 D\Gamma_1^*$, *i.e.*, $\Gamma_1\left(e^{j\omega}, \theta^o\right) D\left(e^{j\omega}, \theta^o\right)\Gamma_1^*\left(e^{j\omega}, \theta^o\right) = R_1\left(e^{j\omega}\right)R_1^{\top}\left(e^{-j\omega}\right)$ such that the function $R_1(z)$ is analytic in the unit disc and has full rank on the unit circle. As in Section 7.3, we consider two extreme cases of the model order of the estimated models of the modules $\left\{G_k(q)\right\}_{k=1}^m$ to give an interpretation of $\mathbf{AsCov}\{\hat{\eta}\}$. The first is to consider the modules $\left\{G_k(q)\right\}_{k=1}^m$ to be known, so no basis functions of $\left\{G_k(q)\right\}_{k=1}^m$ have to be estimated and $\left\langle \mathbf{Proj}_{\mathcal{S}_{R_1}}\{\gamma\}, \mathbf{Proj}_{\mathcal{S}_{R_1}}\{\gamma\}\right\rangle = 0$ (the space $\mathcal{S}_{R_1}$ is empty and hence the projection onto this space is zero). This case corresponds to a lower bound on $\mathbf{AsCov}\{\hat{\eta}\}$. The bound is given by

$$\mathbf{AsCov}\{\hat{\eta}\} \geq \left[\left\langle G'\left(\frac{\Phi_u}{\lambda} + \sum_{k=1}^{m} M_{u_k}^L\right), G'\right\rangle\right]^{-1}, \tag{7.17}$$

where,

$$M_{u_k}^L = \frac{\Phi_u|G_k|^2}{\lambda_k}, \quad k = 1, \ldots, m.$$

The second case is when the model order grows large. Formally, we assume the rows of G_k' span $\mathcal{L}_2$ for all k, *i.e.*, we assume that $\mathcal{S}_{G_k'} = \mathcal{L}_2$ for all k, so then $\mathcal{S}_{\Gamma_1} \to \mathcal{L}_2^m$. The upper bound will be conservative since the space $\mathcal{S}_{G_k'}$ is a subset of $\mathcal{H}_2$, *i.e.*, $\mathcal{S}_{G_k'} \subseteq \mathcal{H}_2 \subset \mathcal{L}_2$. Thus we make the projection onto a larger space and $\tilde{\gamma}$ has a component that is not in $\mathcal{H}_2$. In this case, Lemma 7.4 gives that

$$\mathbf{AsCov}\{\hat{\eta}\} < \left[\left\langle G'(S - \tilde{\gamma}\tilde{\gamma}^*), G'\right\rangle\right]^{-1},$$

where

$$\tilde{\gamma}\tilde{\gamma}^* = BD^{-1}B^* = \sum_{k=1}^{m} \frac{\Phi_u |G_k|^2}{\lambda_k}.$$

Simplifying the above expression leads to

$$\mathbf{AsCov}\{\hat{\eta}\} < \left[\left\langle G' \frac{\Phi_u}{\lambda}, G' \right\rangle \right]^{-1}. \tag{7.18}$$

We summarize the results in the following theorem for non white noise spectra.

Theorem 7.2. *Let the system dynamics be described* (7.2)*. We assume that the additive zero mean stationary sequences* $\{e_i(t)\}$ *are mutually independent, and independent of the input signal* $u(t)$*, with spectra* $\Phi_{e_i}(\omega), i = 1, \dots, m$*; the same holds for* $e(t)$ *with spectrum* $\Phi_e(\omega)$*. The input is assumed to be a realization of a weakly stationary stochastic process with spectrum* $\Phi_u(\omega)$*. The models of the modules are independently parametrized,* i.e.*,* $G_k(q) = G_k(q, \theta_k)$*,* $k = 1, \dots, m$ *and* $G(q) = G(q, \eta)$*. We assume that* D *in* (7.16) *is full rank (*$\operatorname{rank}\{D\} = m$*). Then*

$$\left[\left\langle G' \left(\frac{\Phi_u}{\Phi_e} + \sum_{k=1}^{m} M_{u_k}^L \right), G' \right\rangle \right]^{-1} \leq \mathbf{AsCov}\{\hat{\eta}\} < \left[\left\langle G' \frac{\Phi_u}{\Phi_e}, G' \right\rangle \right]^{-1}, \tag{7.19}$$

where

$$M_{u_k}^L = \frac{\Phi_u |G_k|^2}{\Phi_{e_k}}, \quad k = 1, \dots, m. \tag{7.20}$$

Remark 7.2. Comparing (7.19) with open loop SISO identification of G, we see that the upper bound coincides with the expression for the corresponding SISO case:

$$\mathbf{AsCov}\{\hat{\eta}\} = \left[\left\langle G' \frac{\Phi_u}{\lambda}, G' \right\rangle \right]^{-1}.$$

The lower bound (7.17) indicates that if high model orders are used for the models $\{\hat{G}_k(q)\}_{k=1}^m$, the benefit of including measurements $\{y_k(t)\}_{k=1}^m$ in the predictor (7.14) is limited. If we do not have to estimate the dynamics of the sensor modules $\{G_k\}_{k=1}^m$, each sensor gives a contribution $M_{u_k} = \Phi_u |G_k|^2 / \Phi_{e_k}$. We see that a sensor k adds a term

$$\frac{\Phi_{SNR}^k(\omega)}{\left| G\left(e^{j\omega}\right) \right|^2},$$

where $\Phi_{SNR}^k(\omega)$ is the signal to noise ratio at sensor k. This is the same quantity that determines the variance of the first estimated module of the cascaded systems in Chapter 6, *cf.* Remark 6.1.

7.5 Numerical simulations

In this section, we verify the correctness of the presented results for both parallel cascade systems (Structure 1) and multi-sensor systems (Structure 2) by Monte-Carlo simulations of FIR systems. In all examples $N = 1000$ measurements are used and the sample variances of the frequency function estimate of 500 noise realizations is computed using (1.3). The noise source and input are assumed mutually independent zero mean Gaussian white noise with unit variance. When the input r_2 is not considered it is set to zero. The estimates are computed as the minimizer of

$$V_N(\theta) = \frac{1}{2N}\left\{\sum_{t=1}^{N} \varepsilon(t)^\top \Lambda^{-1} \varepsilon(t)\right\},$$

where $\varepsilon(t) = y(t) - \hat{y}(t)$. We consider examples with $m = 1$ and $m = 2$ input signals ($m = 1$ and $m = 2$ additional sensors) and 3 FIR systems, all with true order $p = 3$, *i.e.*,

$$\begin{aligned} G_1 = G_2 &= 1 + 0.5q^{-1} + 0.25q^{-2}, \\ G &= 1 + 0.2q^{-1} + 0.04q^{-2}. \end{aligned}$$

The systems G_1, G_2 are estimated with 30 parameters and the system of interest in all examples, G, is estimated with 3 parameters:

$$\hat{G}_i = \sum_{k=0}^{29} \hat{g}_{i,k} q^{-k} \quad i = 1, 2, \quad \hat{G} = \sum_{k=0}^{2} \hat{g}_{3,k} q^{-k}.$$

For Structure 1, the parallel serial structure, the sample covariance of the transfer function estimates shows strong similarity to the asymptotic (both in samples and parameters) theoretic expression, see Figure 7.4. In the case of one input signal ($m = 1$), then $r_2 = 0$ and G is estimated. Knowing the first impulse response coefficient of G_1 and G_2 gives a reduction in variance of $\hat{G}$ as seen in Figure 7.5. For Structure 2, the multi-sensor structure, the variance of the transfer function estimate $\hat{G}$ does not improve by using also using y_2, and is the same as what would be achieved by only using y, *cf.* Figure 7.6. When we know the first coefficient of G_1 and G_2, the estimate of the first impulse response coefficient $g_{3,1}$ is improved which results in a lower variance for the estimated transfer function $\hat{G}$, *cf.* Figure 7.7. Knowing some parameters in G_1 and G_2 makes all the difference.

7.6 Summary

In this chapter, we have examined the covariance of the parameter estimates of one module in a parallel cascade structure, as well in a multi-sensor structure. Conservative upper bounds on the asymptotic covariance of the parameter estimates were derived when little assumptions were made on the remaining systems in the network. We derived asymptotic

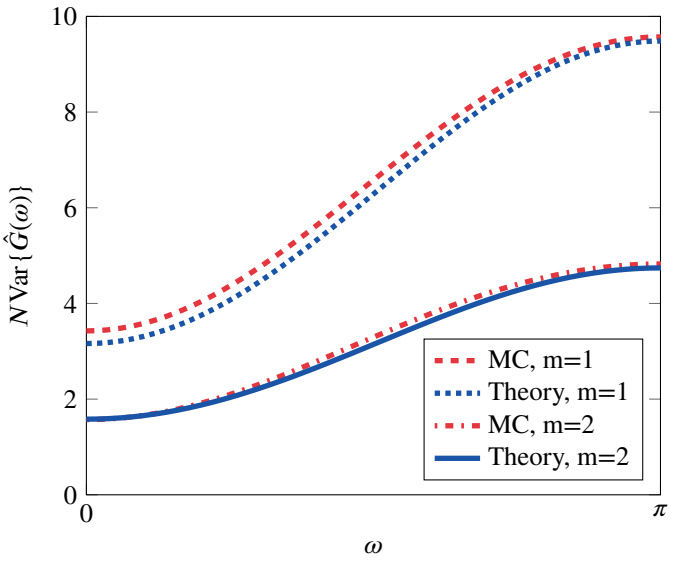

Figure 7.4: Structure 1: Comparison of the variance of $\hat{G}(\omega)$ for Monte-Carlo simulations (MC) and the asymptotic theory for $m = 1, 2$.

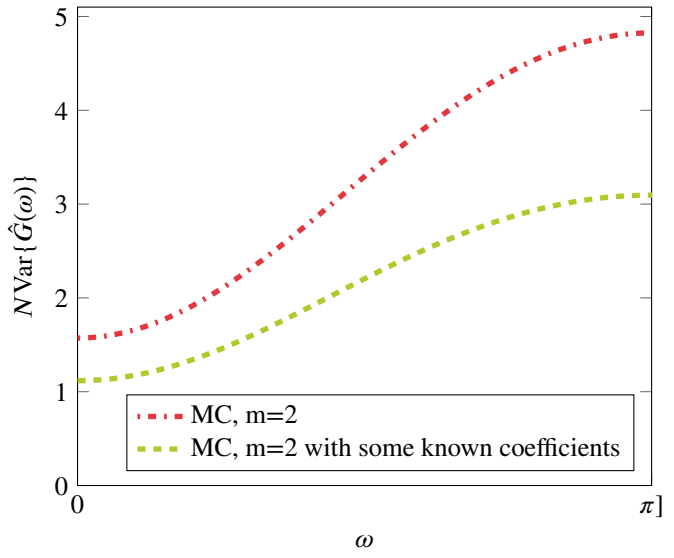

Figure 7.5: Structure 1: Comparison of the variance of $\hat{G}(\omega)$ for Monte-Carlo simulations (MC) and the asymptotic theory for $m = 2$, when the first impulse response coefficients of G_1 and G_2 are known.

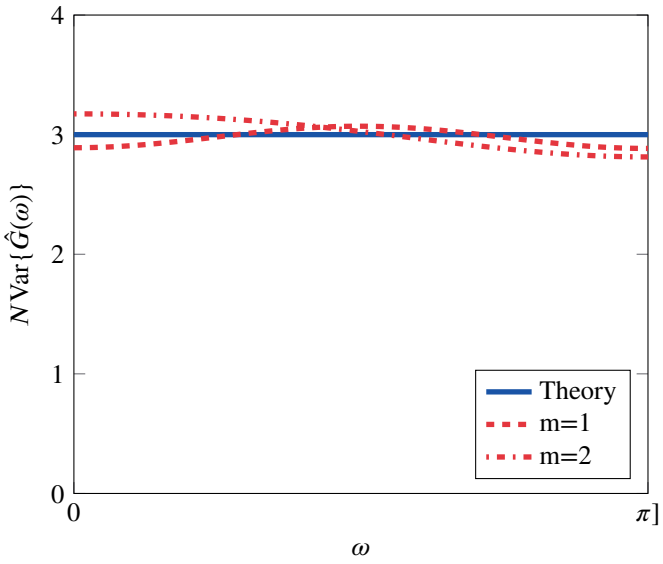

Figure 7.6: Structure 2: Comparison of the variance of $\hat{G}(\omega)$ for Monte-Carlo simulations (MC) and the asymptotic theory for $m = 1, 2$.

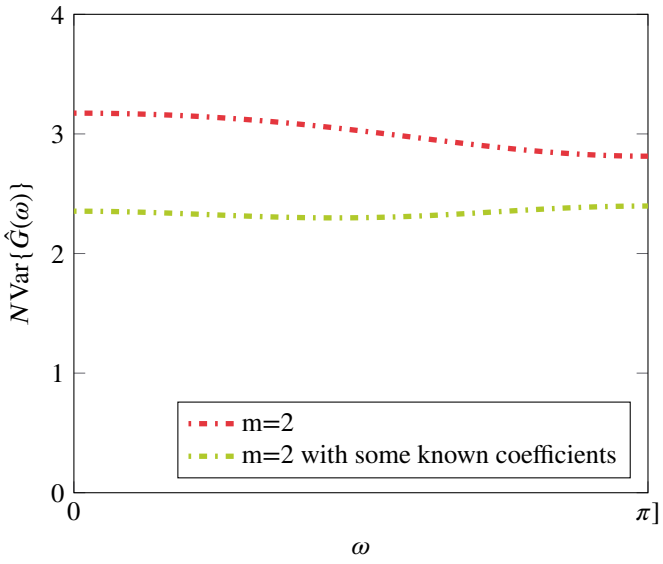

Figure 7.7: Structure 2: Comparison of the variance of $\hat{G}(\omega)$ for Monte-Carlo simulations (MC) and the asymptotic theory for $m = 2$, when the first impulse response coefficients of G_1 and G_2 are known.

variance expressions for two types of structured dynamic systems: parallel cascade systems (Structure 1) and multi-sensor systems (Structure 2). For the parallel cascade structure, when the actuator dynamics $\{G_k\}_{k=1}^m$ are completely unknown, the variance reduction from knowing one input (compared to neglecting it and considering it as noise), was shown to be two-folded. One part corresponded to increased excitation and the other to noise reduction. Previous knowledge about the additional sensors in the multi-sensor structure is imperative for a variance reduction; in fact, without prior knowledge there is no asymptotic variance reduction.

7.A Technical preliminaries

Here we recall some technical preliminaries that reformulate the Schur complement into orthogonal projections.

Lemma 7.3. *Assume that the asymptotic covariance matrix for an estimate of a vector* $\theta = \begin{bmatrix}\theta_1^\top & \theta_2^\top\end{bmatrix}^\top$, $\theta_1 \in \mathbb{R}^{n_1}$, $\theta_2 \in \mathbb{R}^{n_2}$, *can be written as*

$$P_\theta^{-1} = \langle \Psi, \Psi \rangle = \begin{bmatrix}\langle \Psi_1, \Psi_1 \rangle & \langle \Psi_1, \Psi_2 \rangle \\ \langle \Psi_2, \Psi_1 \rangle & \langle \Psi_2, \Psi_2 \rangle\end{bmatrix}$$

where $\Psi = \begin{bmatrix}\Psi_1^\top & \Psi_2^\top\end{bmatrix}^\top$, $\Psi_1 \in \mathcal{L}_2^{n_1 \times m}$, $\Psi_2 \in \mathcal{L}_2^{n_2 \times m}$, *and* $\Psi_1\left(\mathrm{e}^{\mathrm{j}\omega}\right)\Psi_1\left(\mathrm{e}^{-\mathrm{j}\omega}\right)^\top$ *is positive semidefinite and has rank p. Then the asymptotic covariance matrix for* θ_2 *is*

$$P_{\theta_2} = \left[\langle \Psi_2, \Psi_2 \rangle - \left\langle \boldsymbol{Proj}_{S_{R_1}}\{\gamma\}, \boldsymbol{Proj}_{S_{R_1}}\{\gamma\} \right\rangle\right]^\dagger$$

with $\gamma = \Psi_2 \Psi_1^* [{R_1}^\dagger]^*$, *where* R_1 *is a spectral factor of* $\Psi_1\left(\mathrm{e}^{\mathrm{j}\omega}\right)\Psi_1^\top\left(\mathrm{e}^{-\mathrm{j}\omega}\right)$, i.e., $\Psi_1\left(\mathrm{e}^{\mathrm{j}\omega}\right)\Psi_1^\top\left(\mathrm{e}^{-\mathrm{j}\omega}\right) = R_1\left(\mathrm{e}^{\mathrm{j}\omega}\right)R_1^\top\left(\mathrm{e}^{-\mathrm{j}\omega}\right)$ *such that the function* $R_1(z)$ *is analytic in the unit disc and has rank p for all z in this domain.*

Proof. The spectral factor R_1 exists under the given assumptions; see Theorem 10.1 in Rozanov (1967). Rewriting

$$\langle \Psi_2, \Psi_1 \rangle = \left\langle \Psi_2 \Psi_1^* [{R_1}^\dagger]^*, R_1 \right\rangle,$$

and applying the standard inverse of a partitioned matrix (Horn and Johnson, 1990) and Lemma 2.1 proves Lemma 7.3. ■

In the next lemma, we let the number of estimated parameters in the m first modules grow large to make the projection in Lemma 7.3 trivial to calculate.

Lemma 7.4. *Let Ψ be defined as in Lemma 7.3 and assume that $\Psi_1 = \Gamma_1\tilde{\Psi}_1$ and $\Psi_2 = \Gamma_2\tilde{\Psi}_2$ for some $\Gamma_1 \in \mathcal{L}_2^{n_1\times m_1}$, $\Gamma_2 \in \mathcal{L}_2^{n_2\times m_2}$, $\tilde{\Psi}_1 \in \mathcal{L}_2^{m_1\times m}$ and $\tilde{\Psi}_2 \in \mathcal{L}_2^{m_2\times m}$, and that* $\operatorname{rank}\{\tilde{\Psi}_1\tilde{\Psi}_1^*\} = m_1$. *If $\mathcal{S}_{\Gamma_1} = \mathcal{L}_2^{m_1}$, then*

$$P_{\theta_2} = \left[\left\langle \Gamma_2(\tilde{\Psi}_2\tilde{\Psi}_2^* - \tilde{\gamma}\tilde{\gamma}^*), \Gamma_2\right\rangle\right]^{-1},$$

with $\tilde{\gamma} = \tilde{\Psi}_2\tilde{\Psi}_1^*[R_1^{-1}]^*$, where R_1 is a spectral factor of $\Psi_1\left(\mathrm{e}^{\mathrm{j}\omega}\right)\Psi_1^\top\left(\mathrm{e}^{-\mathrm{j}\omega}\right)$, analytic in the unit disc with rank m_1 for all z in this domain.

Proof. R_1 is an invertible mapping, hence $\mathcal{S}_{\Gamma_1 R_1} = \mathcal{S}_{\Gamma_1} = \mathcal{L}_2^{m_1}$, which implies that $\mathbf{Proj}_{\mathcal{S}_{\Gamma_1 R_1}}\{\Gamma_2\tilde{\gamma}\} = \mathbf{Proj}_{\mathcal{L}_2^{m_1}}\{\Gamma_2\tilde{\gamma}\} = \Gamma_2\tilde{\gamma}$ in Lemma 7.3. ■

CHAPTER 8

SIMO MODELS WITH SPATIALLY CORRELATED NOISE

In this chapter, we move from considering cascaded systems to considering parallel systems. We examine how the estimation accuracy of a linear single input multiple output (SIMO) model depends on the correlation structure of the noise, model structure and model order. We derive formulas for the asymptotic covariance of the frequency response function estimate and the model parameters for the case of temporally white, but possibly spatially correlated additive noise. The optimal correlation structure for the noise covariance is also investigated.

8.1 Introduction

SIMO models are interesting in themselves. They find applications in various disciplines, such as signal processing and speech enhancement (Benesty et al., 2005), (Doclo and Moonen, 2002), communications (Bertaux et al., 1999), (R. Schmidt, 1986), (Trudnowski et al., 1998), biomedical sciences (McCombie et al., 2005) and structural engineering (Ulusoy et al., 2011). Some of these applications are concerned with spatio-temporal models, in the sense that the measured output can be strictly related to the location at which the sensor is placed (Stoica et al., 1994), (Viberg et al., 1997), (Viberg and Ottersten, 1991). In these cases, it is reasonable to expect that measurements collected at locations close to each other are affected by disturbances of the same nature. In other words, noise on the outputs can be correlated; understanding how this noise correlation affects the accuracy of the estimated model is a key issue in data-driven modeling of SIMO systems. We characterize the covariance between the estimated parameters of the estimated modules as well as the covariance between the estimated module transfer functions. The results of this chapter are related to the ones found in Ramazi et al. (2014), where multiple input single output (MISO) models are considered, which instead can have correlated inputs. In the MISO case, correlation is detrimental for the accuracy. For white inputs, it was recently shown in Ramazi et al. (2014) that an increment in the model order of one transfer function leads to an increment in the variance of another estimated transfer function only up to a point, after which the variance levels off. For MISO models, the concept of connectedness Gevers et al. (2006) gives conditions on when one input can help reduce the variance of an identified

transfer function. These results were later refined in Mårtensson (2007). Note that variance expressions for the special case of SIMO cascade structures are found in Wahlberg et al. (2009) and in Chapter 6.

As a motivation, consider a system that can be described by the model:

$$y_1(t) = \theta_{1,1}u(t-1) + e_1(t),$$
$$y_2(t) = \theta_{2,2}u(t-2) + e_2(t),$$

where the input $u(t)$ is white noise and $e_k, k = 1, 2$ is measurement noise. We consider two different types of measurement noise (uncorrelated with the input). In the first case, the noise is perfectly correlated; let us for simplicity assume that $e_1(t) = e_2(t)$. For the second case, $e_1(t)$ and $e_2(t)$ are independent. It turns out that in the first case we can perfectly recover the parameters $\theta_{1,1}$ and $\theta_{2,2}$, while, in the second case we do not improve the accuracy of the estimate of $\theta_{1,1}$ by also using the measurement $y_2(t)$. The reason for this difference is that, in the first case, we can construct the noise free equation

$$y_1(t) - y_2(t) = \theta_{1,1}u(t-1) - \theta_{2,2}u(t-2)$$

and we can perfectly recover $\theta_{1,1}$ and $\theta_{2,2}$, while in the second case neither $y_2(t)$ nor $e_2(t)$ contain information about $e_1(t)$.

Also the model structure plays an important role for the benefit of the second sensor. To illustrate the effet of model structure, we consider a third case, where again $e_1(t) = e_2(t)$. This time, the model structure is slightly different:

$$y_1(t) = \theta_{1,1}u(t-1) + e_1(t),$$
$$y_2(t) = \theta_{2,1}u(t-1) + e_2(t).$$

In this case, we can construct the noise free equation

$$y_1(t) - y_2(t) = (\theta_{1,1} - \theta_{2,2})u(t-1).$$

The fundamental difference is that now only the difference $(\theta_{1,1} - \theta_{2,1})$ can be recovered exactly, but not the parameters $\theta_{1,1}$ and $\theta_{2,1}$ themselves. They can be identified from $y_1(t)$ and $y_2(t)$ separately, as long as y_1 and y_2 are measured. A similar consideration is made in Ljung et al. (2011), where SIMO cascade systems are considered.

We will generalize these observations in the following contributions:

- Novel expressions are provided for the variance-error of an estimated frequency response function of a SIMO linear model in orthonormal basis form, or equivalently, in fixed denominator form (Ninness et al., 1999). The expression reveals how the noise correlation structure, model orders and input variance affect the variance-error of the estimated frequency response function;

- For a non-white input spectrum, we show where in the frequency spectrum the benefit of the correlation structure is focused;
- When one module is identified using less parameters, we derive the noise correlation structure under which the mentioned model parametrization gives the lowest total variance.

The chapter is organized as follows: in Section 8.2 we define the SIMO model structure under study and provide an expression for the covariance matrix of the parameter estimates. Section 8.3 contains the main results, namely a novel variance expression for LTI SIMO orthonormal basis function models. The connection with MISO models is explored in Section 8.6. In Section 8.4, the main results are applied to a non–white input spectrum. In section 8.5 we derive the correlation structure that gives the minimum total variance, when one block has less parameters than the other blocks. Numerical experiments illustrating the application of the derived results are presented in Section 8.7. A final discussion ends the chapter in Section 8.8.

8.2 Problem formulation

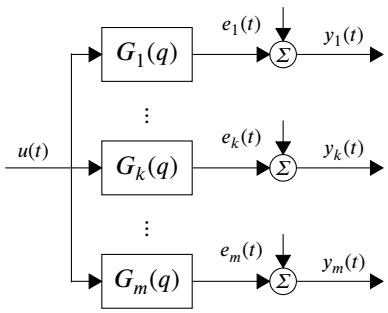

Figure 8.1: *Block scheme of the linear SIMO system.*

We consider linear time-invariant dynamic systems with one input and m outputs (see Figure 8.1). The model is described as follows:

$$\begin{bmatrix} y_1(t) \\ y_2(t) \\ \vdots \\ y_m(t) \end{bmatrix} = \begin{bmatrix} G_1(q) \\ G_2(q) \\ \vdots \\ G_m(q) \end{bmatrix} u(t) + \begin{bmatrix} e_1(t) \\ e_2(t) \\ \vdots \\ e_m(t) \end{bmatrix}, \tag{8.1}$$

where q denotes the forward shift operator, *i.e.*, $qu(t) = u(t+1)$ and the $G_i(q)$ are causal stable rational transfer functions. The G_i are modeled as

$$G_i(q, \theta_i) = \Gamma_i(q)\theta_i, \quad \theta_i \in \mathbb{R}^{n_i}, \tag{8.2}$$

where $n_1 \leq \cdots \leq n_m$ and $\Gamma_i(q) = \begin{bmatrix} \mathcal{B}_1(q) & \dots & \mathcal{B}_{n_i}(q) \end{bmatrix}, i = 1, \dots, m$, for some orthonormal basis functions $\{\mathcal{B}_k(q)\}_{k=1}^{n_m}$. Let us introduce the vector notation

$$y(t) := \begin{bmatrix} y_1(t) \\ y_2(t) \\ \vdots \\ y_m(t) \end{bmatrix}, \quad e(t) := \begin{bmatrix} e_1(t) \\ e_2(t) \\ \vdots \\ e_m(t) \end{bmatrix}.$$

The noise sequence $\{e(t)\}$ is zero mean and temporally white, but may be correlated in the spatial domain:

$$\begin{aligned} \mathbf{E}\{e(t)\} &= 0, \\ \mathbf{E}\left\{e(t)e^\top(s)\right\} &= \delta_{t-s}\Lambda, \end{aligned} \tag{8.3}$$

for some positive definite matrix covariance matrix Λ. We express Λ in terms of its Cholesky factorization

$$\Lambda = \Lambda_{CH}\Lambda_{CH}^\top, \tag{8.4}$$

where $\Lambda_{CH} \in \mathbb{R}^{m \times m}$ is lower triangular, *i.e.*,

$$\Lambda_{CH} = \begin{bmatrix} \gamma_{11} & 0 & \dots & 0 \\ \gamma_{21} & \gamma_{22} & \dots & 0 \\ \vdots & \dots & \ddots & 0 \\ \gamma_{m1} & \gamma_{m2} & \cdots & \gamma_{mm} \end{bmatrix} \tag{8.5}$$

for some $\{\gamma_{ij}\}$. Also notice that since $\Lambda > 0$,

$$\Lambda^{-1} = \Lambda_{CH}^{-\top}\Lambda_{CH}^{-1}. \tag{8.6}$$

The assumption that the modules have the same orthogonal parametrization in (8.2) is less restrictive than it might appear at first glance, and made for clarity and ease of presentation. Some comments on the model structure are listed below:

- A model that consists of a linear combination of non-orthonormal basis functions can be transformed into this format by a linear transformation, which can be computed by the Gram-Schmidt procedure (Trefethen and Bau, 1997).

- Any model structure of the form

$$G_i(q,\theta_i)u_t = Y_t^\top \theta_i, \quad Y_{t+1}^\top = AY_t + Bu_t$$

fits our framework (Ninness et al., 1999), where $A \in \mathbb{R}^{n_i \times n_i}$ and $B \in \mathbb{R}^{n_i \times 1}$ are arbitrary, but A has a specified set of eigenvalues $\{\xi_1, \ldots, \xi_{n_i}\}$. In addition, it is essential for our analysis that the modules share eigenvalues (poles). Notice that fixed denominator models, with the same denominator in all transfer functions, also fit this framework (Ninness et al., 1999). ARX or BJ models do not fit the framework presented here because the poles are not fixed. It may be possible to extend some results of this chapter to such more general models if a similar approach is taken as in Section 7 of (Ninness et al., 1999).

- It is not necessary to restrict the input to be white noise. Section 8.4 will discuss how the results can be generalized and study the case when the input signal is an Autoregression (AR) process.

- Note that the assumption that $n_1 \leq \cdots \leq n_m$ is not restrictive as it only represents an ordering of the modules in the system.

- We can describe quite a few dynamic networks as SIMO systems. Any number of modules connected in cascade can be transformed to this form, however, it is not optimal to do so. For example, if $G_1(q)$ and $G_2(q)$ are connected in cascade, they can be modeled by a SIMO model where the first module is $G_1(q)$ and the second parallel module is $G_1(q)G_2(q)$. Any number of parallel branches fits our SIMO model. The main limitation is that we can not have feedback to $u(t)$ from any of the outputs.

8.2.1 Weighted least-squares estimate

By introducing $\theta = \begin{bmatrix} \theta_1^\top & \cdots & \theta_m^\top \end{bmatrix}^\top \in \mathbb{R}^n$, $n := \sum_{i=1}^m n_i$ and the $n \times m$ transfer function matrix

$$\tilde{\Psi}(q) = \begin{bmatrix} \Gamma_1^\top & 0 & 0 \\ 0 & \ddots & 0 \\ 0 & 0 & \Gamma_m^\top \end{bmatrix},$$

we can write the model (8.1) as a linear regression model

$$y(t) = \varphi^\top(t)\theta + e(t), \tag{8.7}$$

where

$$\varphi^\top(t) = \tilde{\Psi}^\top(q)u(t).$$

An unbiased and consistent estimate of the parameter vector θ can be obtained from weighted least-squares, with weighting matrix Λ^{-1} giving the linear unbiased estimator with lowest

variance (see, *e.g.*, Ljung (1999) or Söderström and Stoica (1989)). The covariance matrix Λ is assumed known, however, this assumption is not restrictive since Λ can be estimated from data and replacing Λ by a consistent estimate does not affect the asymptotic covariance of $\hat{\theta}$ (Cox and Reid, 1987). The estimate of θ is given by

$$\hat{\theta}_N = \left(\sum_{t=1}^{N} \varphi(t) \Lambda^{-1} \varphi^\top(t) \right)^{-1} \sum_{t=1}^{N} \varphi(t) \Lambda^{-1} y(t).$$

Inserting (8.7) in (8.8) gives

$$\hat{\theta}_N = \theta + \left(\sum_{t=1}^{N} \varphi(t) \Lambda^{-1} \varphi^\top(t) \right)^{-1} \sum_{t=1}^{N} \varphi(t) \Lambda^{-1} e(t).$$

Under Assumption 1, the noise sequence is zero mean, hence $\hat{\theta}_N$ is unbiased. It can be noted that this is the same estimate as the one obtained by the prediction error method and, if the noise is Gaussian, by the maximum likelihood method (Ljung, 1999). It also follows that the asymptotic covariance matrix of the parameter estimates is given by

$$\mathbf{AsCov}\{\hat{\theta}_N\} = \left(\mathbf{E}\{\varphi(t) \Lambda^{-1} \varphi^\top(t)\} \right)^{-1}. \tag{8.8}$$

In the problem we consider, using Parseval's formula and (8.6), the asymptotic covariance matrix, (8.8), can be written as[1]

$$\mathbf{AsCov}\{\hat{\theta}_N\} = \langle \Psi, \Psi \rangle^{-1}, \tag{8.9}$$

where

$$\Psi(q) = \frac{1}{\sigma} \tilde{\Psi}(q) \Lambda_{CH}^{-\top}. \tag{8.10}$$

Note that $\Psi(q)$ is block upper triangular since $\tilde{\Psi}(q)$ is block diagonal and $\Lambda_{CH}^{-\top}$ is upper triangular.

With formal assumptions in place, we now consider the introductory example in greater detail.

Example 8.1. Consider the model

$$y_1(t) = \theta_{1,1} q^{-1} u(t) + e_1(t), \tag{8.11}$$

$$y_2(t) = \theta_{2,1} q^{-1} u(t) + \theta_{2,2} q^{-2} u(t) + e_2(t), \tag{8.12}$$

which uses the delays q^{-1} and q^{-2} as orthonormal basis functions. With

$$\theta = \begin{bmatrix} \theta_{1,1} \\ \theta_{2,1} \\ \theta_{2,2} \end{bmatrix} \tag{8.13}$$

[1] Non-singularity of $\langle \Psi, \Psi \rangle$ usually requires parameter identifiability and persistence of excitation (Ljung, 1999).

the corresponding regression matrix is

$$\varphi^\top(t) = \begin{bmatrix} u(t-1) & 0 & 0 \\ 0 & u(t-1) & u(t-2) \end{bmatrix}.$$

The noise vector is generated by

$$\begin{bmatrix} e_1(t) \\ e_2(t) \end{bmatrix} = Lw(t) = \begin{bmatrix} 1 & 0 \\ \sqrt{1-\beta^2} & \beta \end{bmatrix} \begin{bmatrix} w_1(t) \\ w_2(t) \end{bmatrix}, \tag{8.14}$$

where $w_1(t)$ and $w_2(t)$ are uncorrelated white processes with unit variance. The parameter $\beta \in [0,\, 1]$ tunes the correlation between $e_1(t)$ and $e_2(t)$. When $\beta = 0$, the two processes are perfectly correlated (*i.e.*, identical); conversely, when $\beta = 1$, they are completely uncorrelated. Note that, for every $\beta \in [0,\, 1]$, one has $\mathbf{E}\{e_1(t)^2\} = \mathbf{E}\{e_2(t)^2\} = 1$. In fact, the covariance matrix of $e(t)$ becomes

$$\Lambda = LL^\top = \begin{bmatrix} 1 & \sqrt{1-\beta^2} \\ \sqrt{1-\beta^2} & 1 \end{bmatrix}.$$

Then, when computing (8.9) in this specific case gives

$$\mathbf{AsCov}\{\hat{\theta}_N\} = \frac{1}{\sigma^2} \begin{bmatrix} 1 & \sqrt{1-\beta^2} & 0 \\ \sqrt{1-\beta^2} & 1 & 0 \\ 0 & 0 & \beta^2 \end{bmatrix}. \tag{8.15}$$

We note that:

$$\mathbf{AsCov}\left\{ \begin{bmatrix} \hat{\theta}_{1,1} & \hat{\theta}_{2,1} \end{bmatrix}^\top \right\} = \frac{1}{\sigma^2}\Lambda,$$
$$\mathbf{AsCov}\{\hat{\theta}_{2,2}\} = \frac{1}{\sigma^2}\beta^2.$$

The above expressions reveals two interesting facts:

1. The (scalar) variances of $\hat{\theta}_{1,1}$ and $\hat{\theta}_{2,1}$, namely the estimates of parameters of the two modules related to the same time lag, are not affected by possible correlation of the noise processes, *i.e.*, they are independent of the value of β. However, note that the cross correlation between $\hat{\theta}_{1,1}$ and $\hat{\theta}_{2,1}$ in (8.15):

$$\begin{aligned} \mathbf{Var}\left\{ (\hat{\theta}_{1,1} - \sqrt{1-\beta^2}\hat{\theta}_{2,1}) \right\} &= \begin{bmatrix} 1 \\ -\sqrt{1-\beta^2} \end{bmatrix}^\top \frac{1}{\sigma^2}\Lambda \begin{bmatrix} 1 \\ -\sqrt{1-\beta^2} \end{bmatrix} \\ &= \frac{1}{\sigma^2}\beta^2. \end{aligned} \tag{8.16}$$

   This cross correlation will induce a cross correlation in the transfer function estimates as well.

2. As seen in (8.15), the variance of $\hat{\theta}_{1,2}$ strongly depends on β. In particular, when β tends to 0, one is ideally able to estimate $\hat{\theta}_{1,2}$ perfectly. Note that in the limit case $\beta = 0$ one has $e_1(t) = e_2(t)$, so that (8.1) can be rearranged to obtain the noise-free equation

$$y_1(t) - y_2(t) = (\theta_{1,1} - \theta_{2,1})u(t-1) + \theta_{1,2}u(t-2),$$

which shows that both $\theta_{1,2}$ and the difference $\theta_{1,1} - \theta_{2,1}$ can be estimated perfectly. This can of course also be seen from (8.15), *cf.* (8.16).

The example shows that correlated measurements can be favorable for estimating for estimating certain parameters, but not necessarily for all. The main focus of this chapter is to generalize these observations to arbitrary basis functions, number of systems and number of estimated parameters. Additionally, the results are used to derive the optimal correlation structure of the noise. But first, we need some technical preliminaries.

8.2.2 Noise correlation structure

As seen in Example 8.1, strong noise correlation may be helpful in the estimation. In fact, the variance error will depend on the non-estimable part of the noise, i.e., the part that cannot be linearly estimated from other noise sources. To be more specific, define the signal vector $e_{j\setminus i}(t)$ to include the noise sources from module 1 to module j, with the one from module i excluded, *i.e.*,

$$e_{j\setminus i}(t) := \begin{cases} \begin{bmatrix} e_1(t) & \dots & e_j(t) \end{bmatrix}^\top & j < i, \\ \begin{bmatrix} e_1(t) & \dots & e_{i-1}(t) \end{bmatrix}^\top & j = i, \\ \begin{bmatrix} e_1(t) & \dots & e_{i-1}(t) & e_{i+1}(t) & \dots & e_j(t) \end{bmatrix}^\top & j > i. \end{cases}$$

Now, the linear minimum variance estimate of e_i given $e_{j\setminus i}(t)$, is given by

$$\hat{e}_{i|j}(t) := \varrho_{ij}^\top e_{j\setminus i}(t). \tag{8.17}$$

where the vector ϱ_{ij} in (8.17) is given by

$$\varrho_{ij} = \left(\mathbf{Cov}\left\{e_{j\setminus i}(t)\right\}\right)^{-1} \mathbf{E}\left\{e_{j\setminus i}(t)e_i(t)\right\}.$$

We define $e_i(t) - \hat{e}_{i|j}(t)$ as the non-estimable part of $e_i(t)$ given $e_{j\setminus i}(t)$ and introduce the notation

$$\lambda_{i|j} := \mathbf{Var}\left\{e_i(t) - \hat{e}_{i|j}(t)\right\}, \tag{8.18}$$

and we make the convention that $\lambda_{i|0} := \lambda_i$.

Definition 2. When $\hat{e}_{i|j}(t)$ does not depend on $e_k(t)$, where $1 \leq k \leq j$, $k \neq i$, we say that $e_i(t)$ is orthogonal to $e_k(t)$ conditionally to $e_{j\setminus i}(t)$.

The intuition behind Definition 2 is that if we wish to estimate $e_i(t)$ and we already know $e_{j\setminus i}(t)$, then, we do not gain anything from $e_k(t)$, if $e_i(t)$ is orthogonal to $e_k(t)$ conditionally to $e_{j\setminus i}(t)$. The variance of the non-estimable part of the noise is closely related to the Cholesky factor of the covariance matrix Λ. We have the following lemma.

Lemma 8.1. *Let $e(t) \in \mathbb{R}^m$ have zero mean and covariance matrix $\Lambda > 0$. Let Λ_{CH} be the lower triangular Cholesky factor of Λ,* i.e., *Λ_{CH} satisfies* (8.4)*, with $\{\gamma_{ik}\}$ as its entries as defined by* (8.5)*. Then for $j < i$,*

$$\lambda_{i|j} = \sum_{k=j+1}^{i} \gamma_{ik}^2. \tag{8.19}$$

Furthermore, $\gamma_{ij} = 0$ is equivalent to that $e_i(t)$ is orthogonal to $e_j(t)$ conditionallyto $e_{j\setminus i}(t)$.

The proof is given in Appendix 8.A.1. As a small example of why this formulation is useful, we consider the following covariance matrix.

Example 8.2. Let

$$\Lambda = \begin{bmatrix} 1 & 0.6 & 0.9 & 0 \\ 0.6 & 1 & 0.54 & 0.18 \\ 0.9 & 0.54 & 1 & 0 \\ 0 & 0.18 & 0 & 1.09 \end{bmatrix}, \qquad \Lambda_{CH} = \begin{bmatrix} 1 & 0 & 0 & 0 \\ 0.6 & 0.8 & 0 & 0 \\ 0.9 & 0 & 0.44 & 0 \\ 0 & 0.3 & 0 & 1 \end{bmatrix}. \tag{8.20}$$

From Λ (and Λ_{CH}) it is seen that $\mathbf{E}\{e_1(t)e_4(t)\}$ and $\mathbf{E}\{e_3(t)e_4(t)\}$ are zero. Additionally, the Cholesky factorization and Lemma 8.1 gives that $e_3(t)$ is orthogonal to $e_2(t)$ conditionally to $e_{2\setminus 3}(t)$ (since γ_{32} is zero). This means that there is no information about $e_3(t)$ in $e_2(t)$ if we already know $e_1(t)$. This is not apparent from Λ where $\mathbf{E}\{e_2(t)e_3(t)\}$ is non-zero. If we know $e_1(t)$ a considerable part of $e_2(t)$ and $e_3(t)$ can be estimated. Without knowing $e_1(t)$, $\lambda_1 = \lambda_2 = \lambda_3 = 1$, while if we know $e_1(t)$, (8.19) gives that $\lambda_{2|1} = 0.64$ and $\lambda_{3|1} = 0.19$.

Similar to the above, for $i \leq m$, we also define

$$e_{i:m}(t) := \begin{bmatrix} e_i(t) \\ \vdots \\ e_m(t) \end{bmatrix},$$

and for $j < i$ we define $\hat{e}_{i:m|j}(t)$ as the linear minimum variance estimate of $e_{i:m}(t)$ based on the other signals $e_{j\setminus i}(t)$, *i.e.*,

$$\hat{e}_{i:m|j}(t) := \begin{bmatrix} \hat{e}_{i|j}(t) \\ \vdots \\ \hat{e}_{m|j}(t) \end{bmatrix}.$$

Furthermore, we define

$$\Lambda_{i:m|j} := \mathbf{Cov}\left\{ e_{i:m}(t) - \hat{e}_{i:m|j}(t) \right\}. \tag{8.21}$$

8.3 Covariance of frequency response estimates

In this section, we present novel expressions for the variance-error of an estimated frequency response function. The expression reveals how the noise correlation structure, model orders and input variance affect the variance-error of the estimated frequency response function. We will analyze the effect of the correlation structure of the noise on the transfer function estimates. To this end, collect all m transfer functions into

$$G := \begin{bmatrix} G_1 & G_2 & \dots & G_m \end{bmatrix}.$$

For convenience, we will simplify notation according to the following definition:

Definition 3. The asymptotic covariance of $\hat{G}\left(\mathrm{e}^{\mathrm{j}\omega_o}\right) := G\left(\mathrm{e}^{\mathrm{j}\omega_o}, \hat{\theta}^N\right)$ for the fixed frequency ω_0 is denoted by

$$\mathbf{AsCov}\left\{\hat{G}\right\}.$$

In particular, the variance of $\hat{G}_i\left(\mathrm{e}^{\mathrm{j}\omega_o}\right) := G_i\left(\mathrm{e}^{\mathrm{j}\omega_o}, \hat{\theta}_i^N\right)$ for the fixed frequency ω_0 is denoted by

$$\mathbf{AsVar}\left\{\hat{G}_i\right\}.$$

Definition 4. Define χ_k as the index of the first system that contains the basis function $\mathcal{B}_k\left(\mathrm{e}^{\mathrm{j}\omega_o}\right)$.

Notice that $\chi_k - 1$ is the number of systems that do not contain $\mathcal{B}_k$, because of the ordering of the modules. Let the entries of θ be arranged by basis function as follows:

$$\bar{\theta} = \begin{bmatrix} \bar{\theta}_1 \\ \vdots \\ \bar{\theta}_{n_m} \end{bmatrix}, \quad \bar{\theta}_k = \begin{bmatrix} \theta_{\chi_k,k} \\ \vdots \\ \theta_{m,k} \end{bmatrix}, \tag{8.22}$$

for $k = 1, \dots, n_m$, *i.e.*, the parameters $[\, \theta_{1,1} \ \cdots \ \theta_{m,1} \,]^\top$ related to $\mathcal{B}_1$ first and the parameters related to $\mathcal{B}_{n_m}$ last.

Theorem 8.2. *Let Assumption 9.1 hold. Suppose that the parameters $\theta_i \in \mathbb{R}^{n_i}$, $i = 1, \dots, m$, are estimated using weighted least-squares* (8.8)*. Let the parameters $\{\theta_i\}$ be collected in $\bar{\theta}$ according to* (8.22) *and the corresponding weighted least-squares estimate be denoted by $\hat{\bar{\theta}}$. Then, the covariance of $\hat{\bar{\theta}}$ is*

$$\boldsymbol{AsCov}\left\{\hat{\bar{\theta}}\right\} = \frac{1}{\sigma^2}\operatorname{diag}\left\{\Lambda_{1:m}, \Lambda_{\chi_2:m|\chi_2-1}, \dots, \Lambda_{\chi_{n_m}:m|\chi_{n_m}-1}\right\}, \tag{8.23}$$

where $\Lambda_{\chi_{n_m}:m|\chi_{n_m}-1}$ is defined by (8.21)*.*

The proof of Theorem 8.2 will come after the following corollary. In particular, Theorem 8.2 says that the covariance matrix of the parameters related to the k-th basis function is given by

$$\mathbf{AsCov}\left\{\hat{\bar{\theta}}_k\right\} = \frac{1}{\sigma^2}\Lambda_{\chi_k:m|\chi_k-1}, \tag{8.24}$$

where, for $\chi_k \leq i \leq m$,

$$\mathbf{AsVar}\left\{\hat{\theta_{i,k}}\right\} = \frac{\lambda_{i|\chi_k-1}}{\sigma^2}, \tag{8.25}$$

and $\lambda_{i|\chi_k-1}$ is given by (8.18). An interpretation of why this is the case is given in Section 8.3.1

Corollary 8.3. *Under the same assumptions as Theorem 8.2, it holds that*

$$\boldsymbol{AsCov}\left\{\hat{G}\right\} = \sum_{k=1}^{n_m}\begin{bmatrix}\mathbf{0}_{\chi_k-1} & \mathbf{0}\\ \mathbf{0} & \boldsymbol{AsCov}\left\{\hat{\bar{\theta}}_k\right\}\end{bmatrix}\left|\mathcal{B}_k\left(\mathrm{e}^{\mathrm{j}\omega_o}\right)\right|^2, \tag{8.26}$$

where $\boldsymbol{AsCov}\left\{\hat{\bar{\theta}}_k\right\}$ is given by (8.24) *and $\mathbf{0}_{\chi_k-1}$ is a $(\chi_k - 1) \times (\chi_k - 1)$ matrix with all entries equal to zero. For $\chi_k = 1$, $\mathbf{0}_{\chi_k-1}$ is an empty matrix. In* (8.26)*, $\mathbf{0}$ denotes zero matrices of dimensions compatible to the diagonal blocks.*

Corollary 8.3 and Theorem 8.2 are now proven.

Proof. The asymptotic variance is given by (8.9) with $\Psi(q) = \tilde{\Psi}(q)\Lambda_{CH}^{-\top}$. Let $n = n_1 + \cdots + n_m$. From the upper triangular structure of $\Lambda_{CH}^{-\top}$ and $n_1 \leq n_2 \leq \cdots \leq n_m$, an orthonormal basis for $\mathcal{S}_\Psi$, the subspace spanned by the rows of Ψ, is given by

$$\begin{aligned}
\mathcal{B}_k^S\left(\mathrm{e}^{\mathrm{j}\omega}\right) &:= \begin{bmatrix}\mathcal{B}_k & 0 & \dots & 0\end{bmatrix}, && k = 1, \dots, n_1\\
\mathcal{B}_k^S\left(\mathrm{e}^{\mathrm{j}\omega}\right) &:= \begin{bmatrix}0 & \mathcal{B}_{k-n_1} & 0 & \dots\end{bmatrix}, && k = n_1 + 1, \dots, n_2\\
&\vdots &&\\
\mathcal{B}_k^S\left(\mathrm{e}^{\mathrm{j}\omega}\right) &:= \begin{bmatrix}\dots & 0 & \mathcal{B}_{k-n+n_m}\end{bmatrix}, && k = n - n_m + 1, \dots, n.
\end{aligned} \tag{8.27}$$

First note that $\partial G/\partial\theta = \Psi\Lambda_{CH}^{\top}$. Then, using Lemma 2.2,

$$\sigma^2 \operatorname{\mathbf{AsCov}}\{\hat{G}\} = \Lambda_{CH} \sum_{k=1}^{n} \mathcal{B}_k^S\left(e^{j\omega_o}\right)^* \mathcal{B}_k^S\left(e^{j\omega_o}\right)\Lambda_{CH}^{\top}.$$

Sorting the sum with respect to the basis functions $\mathcal{B}_k\left(e^{j\omega_o}\right)$, we get

$$\sigma^2 \operatorname{\mathbf{AsCov}}\{\hat{G}\} = \Lambda_{CH} \sum_{k=1}^{n_m} \left|\mathcal{B}_k\left(e^{j\omega_o}\right)\right|^2 \begin{bmatrix} 0_{\chi_k-1} & 0 \\ 0 & I \end{bmatrix} \Lambda_{CH}^{\top}.$$

Using Lemma 8.11 found in Appendix 8.A.2, we get

$$\operatorname{\mathbf{AsCov}}\{\hat{G}\} = \frac{1}{\sigma^2} \sum_{k=1}^{n_m} \begin{bmatrix} 0_{\chi_k-1} & 0 \\ 0 & \Lambda_{\chi_k:m|\chi_k-1} \end{bmatrix} \left|\mathcal{B}_k\left(e^{j\omega_o}\right)\right|^2.$$

Thus, (8.26) and Corollary 8.3 follows. The covariance of $\hat{G}$ can also be expressed as

$$\operatorname{\mathbf{AsCov}}\{\hat{G}\} = T \operatorname{\mathbf{AsCov}}\left\{\hat{\hat{\theta}}\right\} T^*, \tag{8.28}$$

where

$$T = \begin{bmatrix} \mathcal{B}_1 I(1) & \mathcal{B}_2 I(2) & \dots & \mathcal{B}_{n_m} I(n_m) \end{bmatrix},$$
$$I(k) = \begin{bmatrix} \mathbf{0} \\ I_{m-\chi_k+1} \end{bmatrix} \in \mathbb{R}^{m\times(m-\chi_k+1)}.$$

But, (8.28) equals (8.26) for all ω and thus (8.23) follow. ■

Remark 8.1. The covariance of $\hat{\hat{\theta}}_k$, which contain the parameters related to basis function k, is determined by which other models share the basis function $\mathcal{B}_k$; cf. (8.16) of the introductory example. The asymptotic covariance of $\hat{G}$ can be understood as a sum of the contributions from each of the n_m basis functions. The covariance contribution from a basis function $\mathcal{B}_k$ is weighted by $\left|\mathcal{B}_k\left(e^{j\omega_o}\right)\right|^2$ and only affects the covariance between systems that contain that basis function, as visualized in Figure 8.2.

8.3.1 Interpretation of Theorem 8.2

The orthogonal basis functions correspond to a decomposition of the output signals into orthogonal components and the problem in a sense becomes decoupled.

Example 8.3. Consider the system described by

$$\begin{aligned} y_1(t) &= \theta_{1,1}\mathcal{B}_1(q)u(t) + e_1(t), \\ y_2(t) &= \theta_{2,1}\mathcal{B}_1(q)u(t) + e_2(t), \\ y_3(t) &= \theta_{3,1}\mathcal{B}_1(q)u(t) + \theta_{3,2}\mathcal{B}_2(q)u(t) + e_3(t), \end{aligned} \tag{8.29}$$

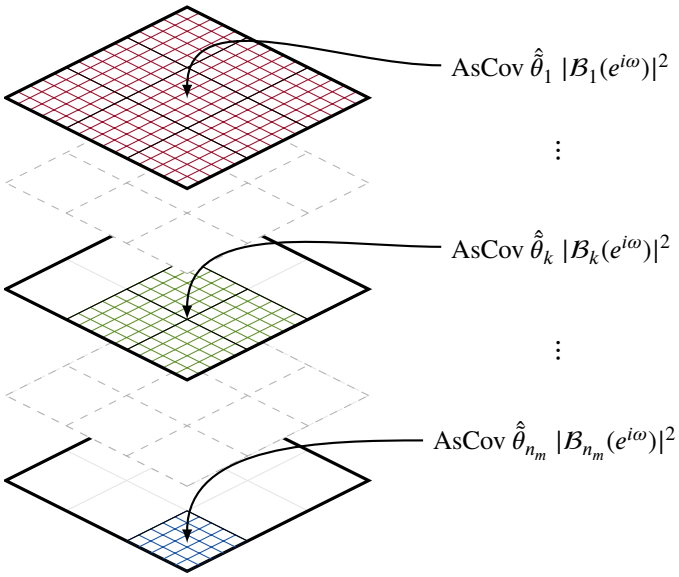

Figure 8.2: A Graphical representation of $\mathbf{AsCov}\{\hat{G}\}$ where each term of the sum in (8.26) is represented by a layer. A basis function only affect the covariance between modules that also contain that basis function. Thus, the first basis function affects the complete covariance matrix while the last basis function n_m only affects modules $\chi_{n_m}, \ldots, m$.

Suppose that we are interested in estimating $\theta_{3,2}$. From (8.25), we can deduce that this parameter has significantly lower variance (depending on the noise correlation)

$$\mathbf{AsVar}\{\hat{\theta}_{3,2}\} = \frac{\lambda_{3|2}}{\sigma^2}$$

compared to $\mathbf{AsVar}\{\hat{\theta}_{3,1}\} = \dfrac{\lambda_3}{\sigma^2}$.

To understand the mechanisms behind this expression, let $u_1(t) = \mathcal{B}_1(q)u(t)$, and $u_2(t) = \mathcal{B}_2(q)u(t)$ so that the system can be visualized as in Figure 8.3, *i.e.*, we can consider u_1 and u_2 as separate inputs.

First we observe that it is only y_3 that contains information about $\theta_{3,2}$, and the term $\theta_{3,1}u_1$ contributing to y_3 is a nuisance from the perspective of estimating $\theta_{3,2}$. This term vanishes when $u_1 = 0$ and we will not be able to achieve better accuracy than the optimal estimate of $\theta_{3,2}$ for this idealized case. So let us study this setting first. Straightforward application of the least-squares method, using u_2 and y_3, gives an estimate of $\theta_{3,2}$ with variance λ_3/σ^2, which is larger than (8.30) when e_3 depends on e_1 and e_2. However, in this idealized case, $y_1 = e_1$ and $y_2 = e_2$, and these signals can thus be used to estimate e_3. This estimate can

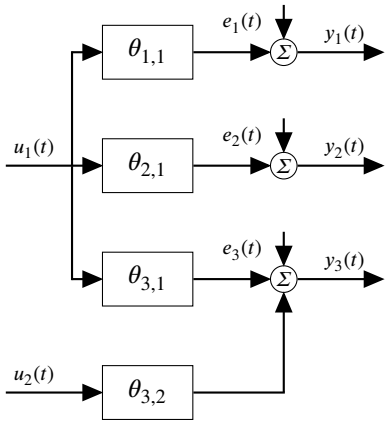

Figure 8.3: The SIMO system of Example 8.3, described by (8.29).

then be subtracted from y_3 before the least-squares method is applied. The remaining noise in y_3 will have variance $\lambda_{3|2}$, if e_3 is optimally estimated (see (8.17)–(8.18)), and hence the least-squares estimate of $\theta_{3,2}$ will now have variance $\lambda_{3|2}/\sigma^2$, *i.e.*, the same as (8.30).

To understand why it is possible to achieve the same accuracy as this idealized case when u_1 is non-zero, we need to observe that our new inputs $u_1(t)$ and $u_2(t)$ are orthogonal (uncorrelated, since $u(t)$ is white and $\mathcal{B}_1$ and $\mathcal{B}_2$ are orthonormal). Returning to the case when only the output y_3 is used for estimating $\theta_{3,2}$, this implies that we pay no price for including the term $\theta_{3,1}u_1$ in our model, and then estimating $\theta_{3,1}$ and $\theta_{3,2}$ jointly, *i.e.*, the variance of $\hat{\theta}_{3,2}$ will still be λ_3/σ^2. With u_1 and u_2 correlated, the variance will be higher, see Section 8.6 for a further discussion. The question now is if we can use y_1 and y_2 as before to estimate e_3. Perhaps surprisingly, we can use the same estimate as when u_1 was zero. The reader may object that this estimate will now, in addition to the previous optimal estimate of e_3, contain a term which is a multiple of u_1. However, due to the orthogonality between u_1 and u_2, this term will only affect the estimate of $\theta_{3,1}$ (which, in this example, we were not interested in), and the accuracy of the estimate of $\theta_{3,2}$ will be $\lambda_{3|2}/\sigma^2$, *i.e.*, (8.30). Figure 8.4 illustrates the setting with $\tilde{y}_3$ denoting y_3 subtracted by the optimal estimate of e_3. In the figure, the new parameter $\tilde{\theta}_{3,1}$ reflects that the relation between u_1 and $\tilde{y}_3$ is different from $\theta_{3,1}$ as discussed above.

Remark 8.2. A key insight from the discussion of Example 8.3 is that for the estimate of a parameter in the path from input i to output j, it is only outputs that are not affected by input i that can be used to estimate the noise in output j; when this particular parameter is estimated, using outputs influenced by input i will introduce a bias, since the noise estimate will then contain a term that is not orthogonal to this input. In (8.25), this manifests itself in that the numerator is $\lambda_{i|\chi_k-1}$; it is only the $\chi_k - 1$ first systems that do not contain u_i.

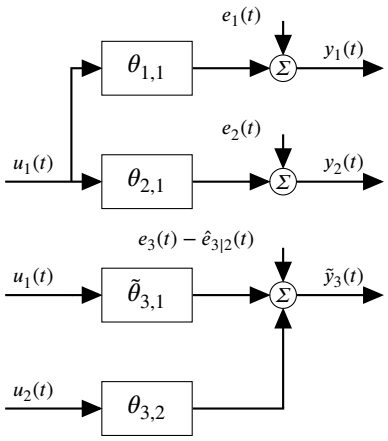

Figure 8.4: The SIMO system of Example 8.3, described by (8.29), but with $\tilde{y}_3$ denoting y_3 subtracted by the optimal estimate of e_3.

8.3.2 Transfer function estimates

We now turn our attention to the variance of the individual transfer function estimates.

Corollary 8.4. *Let the same assumptions as in Theorem 8.2 hold. Then, for any frequency ω_0, it holds that*

$$\boldsymbol{AsVar}\{\hat{G}_i\} = \sum_{k=1}^{n_i} \left|\mathcal{B}_k\left(e^{j\omega_o}\right)\right|^2 \boldsymbol{AsVar}\{\hat{\theta}_{i,k}\}, \tag{8.30}$$

where

$$\boldsymbol{AsVar}\{\hat{\theta}_{i,k}\} = \frac{\lambda_{i|\chi_k - 1}}{\sigma^2}, \tag{8.31}$$

and $\lambda_{i|j}$ is defined in (8.18)*.*

The proof follows directly from Theorem 8.2, since (8.30) is a diagonal element of (8.26). From Corollary 8.4, we can tell when increasing the model order of the l-th transfer function model G_l will increase the asymptotic variance of another transfer function estimate $\hat{G}_i$.

Corollary 8.5. *Under the same conditions as in Theorem 8.2, if we increase the number of estimated parameters of G_j from n_j to $n_j + 1$, the asymptotic variance of G_i will increase, if and only if all the following conditions hold:*

1. $n_j < n_i$,

2. *$e_i(t)$ is not orthogonal to $e_j(t)$ conditioned on $e_{j\setminus i}(t)$,*

3. $\left|\mathcal{B}_{n_{j+1}}\left(\mathrm{e}^{\mathrm{j}\omega_o}\right)\right|^2 \neq 0.$

Proof. See Appendix 8.A.3. ■

Remark 8.3. Corollary 8.5 explicitly tells when an increase in the model order of G_j from n_j to $n_j + 1$ will increase the variance of G_i. Notice that if $n_j \geq n_i$ then there will be no increase in the variance of $\hat{G}_i$, no matter how many additional parameters we introduce to the model G_j. Naturally, if $e_i(t)$ is orthogonal to $e_j(t)$ conditioned on $e_{j\setminus i}(t)$, $\hat{e}_{i|j}(t)$ does not depend on $e_j(t)$ and there is no increase in the variance of $\hat{G}_i$, *cf.* Section 8.3.1.

8.3.3 A graphical representation of Corollary 8.5

Following the notation in Bayesian Networks (Koski and Noble, 2012), Conditions 1) and 2) in Corollary 8.5 can be interpreted graphically. Each module is represented by a vertex in a weighted directed acyclic graph $\mathcal{G}$. Let the vertices be ordered by model order, *i.e.*, let the first vertex correspond to $\hat{G}_1$. Under the additional assumption that module i is the first module with order n_i, let there be an edge, denoted by $j \to i$, from vertex j to i, $j < i$, if $e_i(t)$ is not orthogonal to $e_j(t)$ conditioned on $e_{j\setminus i}(t)$. Notice that this is equivalent to $\gamma_{ij} \neq 0$. Let the weight of the edge be γ_{ij} and define the parents of vertex i to be all nodes with a link to vertex i, *i.e.*, $pa_{\mathcal{G}}(i) := \{j : j \to i\}$. Then, (8.31), together with Lemma 8.1, shows that only outputs corresponding to parents of node i affect the asymptotic variance. Indeed, a vertex without parents has variance

$$\mathbf{AsVar}\left\{\hat{G}_i\right\} = \frac{\lambda_i}{\sigma^2}\sum_{k=1}^{n_i}\left|\mathcal{B}_k\left(\mathrm{e}^{\mathrm{j}\omega_o}\right)\right|^2, \tag{8.32}$$

which corresponds to (8.30) with

$$\lambda_{i|0} = \cdots = \lambda_{i|i-1} = \lambda_i.$$

Thus, $\mathbf{AsVar}\left\{\hat{G}_i\right\}$ is independent of the model order of the other modules.

As an example, consider four systems with the lower Cholesky factor of the covariance of

$e(t)$ given by:

$$\Lambda = \begin{bmatrix} 1 & 0.4 & 0.2 & 0 \\ 0.4 & 1.16 & 0.08 & 0.3 \\ 0.2 & 0.08 & 1.04 & 0 \\ 0 & 0.3 & 0 & 1.09 \end{bmatrix} \tag{8.33}$$

$$= \underbrace{\begin{bmatrix} 1 & 0 & 0 & 0 \\ 0.4 & 1 & 0 & 0 \\ 0.2 & 0 & 1 & 0 \\ 0 & 0.3 & 0 & 1 \end{bmatrix}}_{\Lambda_{CH}} \begin{bmatrix} 1 & 0 & 0 & 0 \\ 0.4 & 1 & 0 & 0 \\ 0.2 & 0 & 1 & 0 \\ 0 & 0.3 & 0 & 1 \end{bmatrix}^{\top} \tag{8.34}$$

If the model orders are distinct, the corresponding graph is given in Figure 8.5, where one can see that $\mathbf{AsVar}\{\hat{G}_4\}$ depends on y_2 (and on y_4 of course), but depends neither on y_3 nor y_1 since $\gamma_{43} = \gamma_{41} = 0$, $\mathbf{AsVar}\{\hat{G}_3\}$ depends on y_1, but not on y_2 since $\gamma_{32} = 0$ and $\mathbf{AsVar}\{\hat{G}_2\}$ depends on y_1, while the variance of $\hat{G}_1$ is given by (8.32). If $n_2 = n_4$, the first condition of Corollary 8.5 is not satisfied and we have to cut the edge between $\hat{G}_4$ and $\hat{G}_2$. Similarly, if $n_1 = n_2$, we have to cut the edge between $\hat{G}_2$ and $\hat{G}_1$, and if additionally $n_1 = n_2 = n_3$, we have to cut the edge between $\hat{G}_3$ and $\hat{G}_1$.

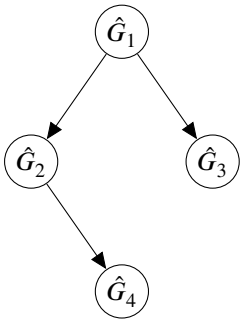

Figure 8.5: Graphical representation of Conditions 1) and 2) in Corollary 8.5 for the Cholesky factor given in (8.33).

8.3.4 Answering the introductory questions

We now revisit the fundamental question posed in the beginning; how much will an added sensor improve the accuracy of an estimate of a certain target transfer function in the network.

We have seen that the crucial factor is what additional dynamics need to be estimated. One of the main messages of Theorem 8.2 is that a sensor (added module) only improves the accuracy of the dynamics not shared by the added module. The best parametrization would then be to parametrize each module by a mutually exclusive subset of the chosen orthogonal basis functions. However, in general, choosing such a parametrization is not possible, since the true modules are assumed to be in the model set. This implies that the true modules must lie in the corresponding subspace, or alternatively, that we have previous knowledge of the dynamics of one module that we wish to estimate in the other. Relaxing the assumption that the true module should be in the model set will introduce a bias error and also lead to an increase in the variance error. The size of the additional variance error is not well understood at this time. How to manage the bias–variance trade–off in identification of dynamic networks is thus a very interesting problem for future research.

8.4 Effect of input spectrum

In this section we will see how a non-white input spectrum changes the results of Section 8.3. A colored input introduces a weighting by its spectrum Φ_u, which means that the basis functions need to be orthogonal with respect to the inner product $\langle f, g\rangle_{\Phi_u} := \langle f\Phi_u, g\rangle$. If $\Phi_u(z) = \sigma^2 R(z)R^*(z)$, where $R(z)$ is a monic stable minimum phase spectral factor; the transformation $\tilde{\Gamma}_i(q) = \sigma^{-1}R(q)^{-1}\Gamma_i(q)$ is a procedure that gives a set of orthogonal basis functions in the weighted space with the weighted inner product $\langle f, g\rangle_{\Phi_u}$. If we use this parametrization, all the main results of the chapter carry over naturally. However, in general, the new parametrization does not contain the same set of models as the original parametrization ($\mathbf{Span}\{\Gamma_i\} \neq \mathbf{Span}\{\tilde{\Gamma}_i\}$).

Example 8.4. If the input is white noise filtered through a first order MA-filter with one zero in $\xi_1 = 0.9$, then the inverse of the spectral factor would be $R(q)^{-1} = (1 - 0.9q^{-1})^{-1}$. If $\Gamma_1 = q^{-1}$, then $\tilde{\Gamma}_1 = \frac{q^{-1}}{1-0.9q^{-1}}$, *i.e.*, Γ_1 has one non-zero impulse response coefficient while $\tilde{\Gamma}_1$ has an infinite number, so they do not span the same space.

Another way to incorporate a non-white input spectrum, is to use the Gram-Schmidt method, which maintains the same model set and the main results are still valid. However, the effect of the input filter is absorbed in the basis functions and it is hard to distinguish the effect of the input filter. If we would like to keep the original parametrization, there is another way to study the effect of the input filter. Using white noise filtered through an AR-filter as input, we may use the developed results to show where in the frequency range the benefit of the correlation structure is focused.

We will use FIR basis functions for the SIMO system, which are not orthogonal with respect to the inner product induced by the input spectrum. We let the input be given by

$$u(t) = \frac{1}{A(q)}w(t) \tag{8.35}$$

where $w(t)$ is a white noise sequence with variance σ_w^2 and the order n_a of A is less than the order of G_1, *i.e.*, $n_a \leq n_1$. In this case, following the derivations of Theorem 8.2, it can be shown that

$$\mathbf{AsVar}\left\{\hat{G}_i\right\} = \sum_{k=1}^{n_i} \mathbf{AsVar}\left\{\hat{\theta}_{i,k}\right\} \left|\mathcal{B}_k\left(\mathrm{e}^{\mathrm{j}\omega_o}\right)\right|^2 \tag{8.36}$$

where

$$\mathbf{AsVar}\left\{\hat{\theta}_{i,k}\right\} = \frac{\lambda_{i|\chi_k - 1}}{\boldsymbol{\Phi}_u(\omega_0)}$$

and the basis functions $\mathcal{B}_k$ have changed due to the input filter. The solutions boil down to finding explicit basis functions $\mathcal{B}_k$ for the case (Ninness and Gustafsson, 1997) when

$$\mathbf{Span}\left\{\frac{\Gamma_n}{A(q)}\right\} = \mathbf{Span}\left\{\frac{q^{-1}}{A(q)}, \frac{q^{-2}}{A(q)}, \ldots, \frac{q^{-n}}{A(q)}\right\}$$

where $A(q) = \prod_{k=1}^{n_a}(1 - \xi_k q^{-1})$, $\left|\xi_k\right| < 1$ for some set of specified poles $\{\xi_1, \ldots, \xi_{n_a}\}$ and where $n \geq n_a$. As discussed in Section 2.6.5, it then holds that

$$\mathbf{Span}\left\{\frac{\Gamma_n}{A(q)}\right\} = \mathbf{Span}\left\{\mathcal{B}_1, \ldots, \mathcal{B}_n\right\}$$

where $\{\mathcal{B}_k\}$ are the Takenaka-Malmquist functions (Ninness and Gustafsson, 1997) given by

$$\begin{aligned}
\mathcal{B}_k(q) &:= \frac{\sqrt{1 - \left|\xi_k\right|^2}}{q - \xi_k}\phi_{k-1}(q), \qquad k = 1, \ldots, n \\
\phi_k(q) &:= \prod_{i=1}^{k} \frac{1 - \overline{\xi}_i q}{q - \xi_i}, \qquad \phi_0(q) := 1
\end{aligned}$$

and with $\xi_k = 0$ for $k = n_a + 1, \ldots, n$. We summarize the result in the following theorem:

Theorem 8.6. *Let the same assumptions as in Theorem 8.2 hold. Additionally the input $u(t)$ is generated by an AR-filter as in* (8.35)*. Then for any frequency ω_0 it holds that*

$$\boldsymbol{AsVar}\left\{\hat{G}_i\right\} = \frac{1}{\boldsymbol{\Phi}_u(\omega_0)}\left(\lambda_i \sum_{k=1}^{n_a} \frac{1 - \left|\xi_k\right|^2}{\left|\mathrm{e}^{\mathrm{j}\omega_o} - \xi_k\right|^2} + \lambda_i(n_1 - n_a) + \sum_{j=2}^{i} \lambda_{i|j-1}(n_j - n_{j-1})\right) \tag{8.37}$$

Proof. The proof follows from (8.36) with the basis functions given by the Takenaka-Malmquist functions and using that $\phi_{k-1}(q)$ is all-pass, and for $k > n_a$, also $\mathcal{B}_k(q)$ is all-pass. This means that $\left|\mathcal{B}_k\left(\mathrm{e}^{\mathrm{j}\omega}\right)\right|^2 = 1$ for all $k > n_a$. ■

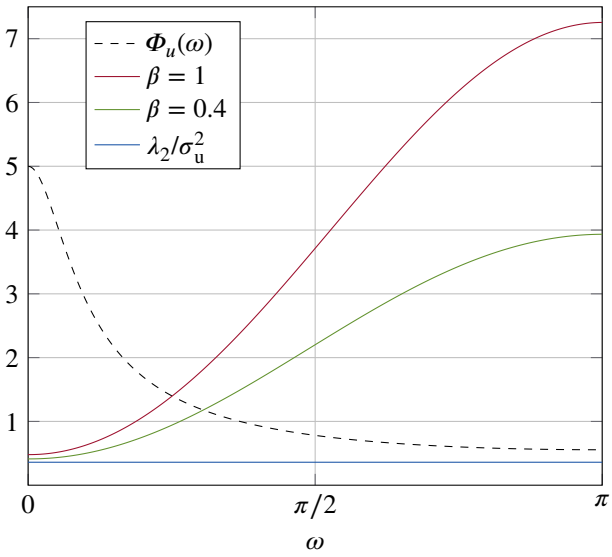

Figure 8.6: Asymptotic variance of $\hat{G}_3\left(e^{j\omega}, \hat{\theta}_2\right)$ for $\beta = 1$ and $\beta = 0.4$. Also shown is λ_2/σ^2, the first term of $\mathbf{AsVar}\left\{\hat{G}_3\left(e^{j\omega}, \hat{\theta}_2\right)\right\}$ in (8.38).

Example 8.5. Consider Example 8.1 again, but now with filtered input when $n_1 = 2$, $n_2 = 3$ and $n_a = 1$. Then, (8.37) simplifies to

$$\mathbf{AsVar}\left\{\hat{G}_2\right\} = \frac{\lambda_2}{\sigma^2} + \frac{\lambda_2}{\Phi_u(\omega_0)} + \frac{\lambda_{2|1}}{\Phi_u(\omega_0)}. \tag{8.38}$$

where $\sigma^2 = \mathbf{E}\left\{u(t)^2\right\}$.

In Figure 8.6 the variance of $\hat{G}_2$ for an input filtered with $A(q) = 1 - 0.8q^{-1}$ is presented for Example 8.5. The filter is of low-pass type and thus gives high input power at low frequencies which results in low variance at those frequencies. Correlation between noise sources decreases the variance mainly where $\Phi_u(\omega)$ is small, *i.e.*, at higher frequencies.

The third term in (8.38) is where the benefit from the correlation structure of the noise at the other sensors enters through $\lambda_{2|1}$. This contribution is weighted by $1/\Phi_u(\omega)$. The benefit thus enters mainly where $\Phi_u(\omega)$ is small. The first term gives a variance contribution that is not focused around frequencies where $\Phi_u(\omega)$ is small. This contribution is not reduced by correlation between noise sources. Thus, the variance is less affected by a non-white input spectrum than what is expected by the asymptotic in model order result (1.4), which in our case is $n_2\lambda_2/\Phi_u(\omega)$ (dashed line) in Figure 8.6. The same reasoning can be made for the general expression (8.37).

8.5 Optimal correlation structure

In this section we characterize the optimal correlation structure, in order to minimize the total variance of $\hat{\theta}$, defined as

$$\operatorname{tvar} \hat{\theta} := \operatorname{Tr}\{\mathbf{AsCov}\{\hat{\theta}\}\},$$

where $\operatorname{Tr}\{\cdot\}$ denotes the trace operator. In most applications, the noise correlation structure can not be manipulated, so why study the optimal correlation structure? One reason is that in some applications we might indirectly affect the noise correlation structure, *e.g.*, when we are allowed to chose the placement of sensor or if we need to decide which sensors to use from a set of sensors. Additionally, in a dynamic network setting, we may choose not to model dynamics related to other input signals (Van den Hof et al., 2013). These inputs signals will give a correlated noise contribution to the output. In general, this contribution will not be temporally white. However, this chapter can be a first step in analyzing also this case. In this section, we will find the optimal correlation structure when the parametrization of the system is such that $n_1 + 1 = n_2 = \ldots = n_m$, *i.e.*, the first module has one parameter less than the others. In Section 8.3, we have seen that if a basis function is not estimated in a module, *e.g.*, the corresponding parameter is known to be zero, parameters related to the same basis function of the other modules are estimated with reduced variance. Assume the SIMO structure of (8.1) and let the input be white noise with unit variance. Recalling Theorem 8.2, only the parameters related to $\mathcal{B}_{n_2}(q)$, $\bar{\theta}_{n_2}$, are estimated with reduced variance. Thus, without loss of generality, we only consider $\operatorname{tvar} \hat{\bar{\theta}}_{n_2}$. The covariance matrix of $\hat{\bar{\theta}}_{n_2}$ is given by $\Lambda_{2:m|1}$. In particular, the variance of the entries of $\hat{\bar{\theta}}_{n_2}$ is

$$\mathbf{AsVar}\left\{\hat{\theta}_{k,n_2}\right\} = \frac{\lambda_{k|1}}{\sigma^2}, \quad k = 2, \ldots, m. \tag{8.39}$$

As before, $\lambda_{k|1}$ is the non-estimable part of $e_k(t)$ given $e_1(t)$. The total variance of $\hat{\bar{\theta}}_{n_2}$ is then

$$\operatorname{tvar} \tilde{\theta} := \sum_{k=2}^{m} \mathbf{AsVar}\left\{\hat{\theta}_{k,n_2}\right\} = \operatorname{Tr}\left\{\frac{1}{\sigma^2}\Lambda_{2:m|1}\right\}.$$

We are interested in understanding how the correlation of $e_1(t)$ with $e_2(t), \ldots, e_m(t)$, *i.e.*, $\Lambda_{12}, \ldots, \Lambda_{1m}$, should be in order to obtain the minimum value of the above total variance. This problem can be expressed as follows:

$$\underset{\Lambda_{12}, \ldots, \Lambda_{1m}}{\text{minimize}} \quad \operatorname{Tr}\{\Lambda_{2:m|1}\} \tag{8.40}$$

$$\text{subject to} \quad \Lambda > 0, \tag{8.41}$$

where the constraint on Λ implies that not all choices of the entries Λ_{1i} are allowed. Directly characterizing the noise structure using this formulation of the problem appears to be hard. Therefore, it turns out convenient to introduce an upper triangular Cholesky factorization of Λ, namely define B *upper triangular* such that $\Lambda = BB^\top$. Note that

1. the rows of B, $b_i^\top$, $i = 1, \dots, m$, are such that $\|b_i\|^2 = \lambda_i$;
2. $\mathbf{E}\{e_1 e_i\} = \Lambda_{1i} = b_1^\top b_i$;
3. there always exists an orthonormal matrix Q such that $B = \Lambda_{CH} Q$, where Λ_{CH} is the previously defined lower triangular Cholesky factor.

Lemma 8.7. *Let*

$$B = \begin{bmatrix} \eta & p^\top \\ 0 & M \end{bmatrix}, \qquad M \in \mathbb{R}^{m-1 \times m-1}, \qquad p \in \mathbb{R}^{m-1 \times 1}, \qquad n \in \mathbb{R};$$

then

$$\Lambda_{2:m|1} = M(I - \frac{1}{\lambda_1}) pp^\top M^\top. \tag{8.42}$$

See Appendix 8.A.4. Note that the constraint $\Lambda > 0$ is satisfied as long as $|\eta| > 0$. Using Lemma 8.7 we reformulate (8.40); keeping η and M fixed, since $MM^\top$ corresponds to the part of Λ which we are not allowed to manipulate, and letting p vary, we have

$$\begin{aligned} \underset{b_1}{\text{maximize}} \quad & \operatorname{Tr}\left\{ \frac{1}{\lambda_1} M pp^\top M^\top \right\} \\ \text{subject to} \quad & \|p\|^2 = \lambda_1 - |\eta|^2 \end{aligned}$$

Let us define $v_1, \dots, v_{m-1}$ as the right singular vectors of M, namely the columns of the matrix V in the singular value decomposition (SVD) $M = USV^\top$. The following result provides the structure of B that solves (8.40).

Theorem 8.8. *Let the input be white noise. Let $n_1 + 1 = n_2 = \dots = n_m$. Then* (8.40) *is solved by an upper triangular Cholesky factor B such that its first row is*

$$b_1^* = \lambda_1 \begin{bmatrix} \eta \\ \sqrt{\lambda_1 - |\eta|^2} v_1 \end{bmatrix}. \tag{8.43}$$

Proof. Observe that $\operatorname{Tr}\left\{ \frac{1}{\lambda_1} M pp^\top M^\top \right\} = \frac{1}{\lambda_1} p^\top M^\top M p = \frac{1}{\lambda_1} \|Mp\|^2$. The minimizer p is (a rescaling of) the first right singular vector of M, namely v_1. Hence $b_1^* = \begin{bmatrix} \eta & \sqrt{\lambda_1 - |\eta|^2} v_1 \end{bmatrix}^\top$. ∎

Theorem 8.8 gives a result that helps understanding when an additional sensor has a positive effect in the identification of the SIMO system. The result may serve as a guideline for decision-making on whether adding a sensor may give an improvement. Suppose that

$G_2(q), \ldots, G_m(q)$ represent the dynamic effect of the input $u(t)$ on a spatial structure at different locations (see, *e.g.*, Kirkegaard and Brincker (1994) and Papadimitriou and Lombaert (2012) for applications to linear structural systems). The output measurements are corrupted by a noise source with a spatial correlation. Assume that, to improve the accuracy of the models at these locations, we have the freedom to add an additional sensor. The optimal location where this sensor should be added is given by Theorem 8.8, that is, it corresponds to the point where the resulting output is affected by a noise source that satisfies the correlation condition (8.43). However, one obtains an advantage in adding this additional sensor only if $G_1(q)$, *i.e.*, the dynamic effect of $u(t)$ on this new output, can be modeled using fewer basis functions than $G_2(q), \ldots, G_m(q)$, which is the essence of Theorem 8.2 and Corollary 8.5.

Remark 8.4. Theorem 8.8 deals with a special case. We note that extension to the case where $n_1 < n_i - 1$, $i = 2, \ldots, m$ is straightforward. However, obtaining a result for the general case where each transfer function is modeled with a different number of basis function is involved and is left for future work. Note that it is possible to iteratively design the covariance matrix by only considering $\lambda_{i+1:m|i}$, in each step, for $i = m-1, \ldots, 1$, *i.e.*, by iteratively adding an additional sensor where it would be of most use. However, this approach is greedy and suboptimal in general.

8.6 Connection between MISO and SIMO models

There is a strong connection between the results presented here and those regarding MISO systems presented in Ramazi et al. (2014). We briefly restate the problem formulation and some results from Ramazi et al. (2014) to show the connection. The MISO data generating system is in some sense the dual of the SIMO case. With m spatially correlated inputs and one output, a MISO system is described by

$$y(t) = \begin{bmatrix} G_1(q) & G_2(q) & \ldots & G_m(q) \end{bmatrix} \begin{bmatrix} u_1(t) \\ u_2(t) \\ \vdots \\ u_m(t) \end{bmatrix} + e(t).$$

The input sequence $\{u(t)\}$ is zero mean and temporally white, but may be correlated in the spatial domain,

$$\begin{aligned} \mathbf{E}\{u(t)\} &= 0 \\ \mathbf{E}\left\{u(t)u^\top(s)\right\} &= \delta_{t-s}\Sigma_u, \end{aligned}$$

for some positive definite matrix covariance matrix $\Sigma_u = \Sigma_{CH}\Sigma_{CH}^\top$, where Σ_{CH} is the lower triangular Cholesky factor of Σ. The noise $e(t)$ is zero mean and has variance λ. The asymptotic covariance of the estimated parameters can be expressed using (8.9) with

$$\Psi = \Psi^{\text{MISO}} := \tilde{\Psi}\Sigma_{CH}. \tag{8.44}$$

We make the convention that $\sum_{k=k_1}^{k_2} x_k = 0$ whenever $k_1 > k_2$.

Theorem 8.9 (Theorem 4 in Ramazi et al. (2014))**.** *With $n_1 \geq n_2 \geq \cdots \geq n_m$, for any frequency ω_0 it holds that*

$$\textit{AsVar}\{\hat{G}_i\} = \sum_{j=i}^{m} \frac{\lambda}{\sigma^2_{i|j}} \sum_{k=n_{j+1}+1}^{n_j} \left|\mathcal{B}_k\left(e^{j\omega_o}\right)\right|^2, \tag{8.45}$$

where $n_{m+1} := 0$ and $\sigma^2_{i|j}$ is the variance of the non-estimable part of $u_i(t)$ given $u_{j\setminus i}(t)$.

Corollary 8.10 (Corollary 6 in Ramazi et al. (2014))**.** *With $n_1 \geq n_2 \geq \cdots \geq n_m$. Suppose that the order of block j is increased from n_j to n_{j+1}. Then there is an increase in the asymptotic variance of $\hat{G}_i$ if and only if all the following conditions hold:*

1. *$n_j < n_i$,*
2. *$u_i(t)$ is not orthogonal to $u_j(t)$ conditioned on $u_{j\setminus i}(t)$,*
3. *$\left|\mathcal{B}_{n_{j+1}}\left(e^{j\omega_o}\right)\right|^2 \neq 0$.*

Remark 8.5. The similarities between Corollary 8.4 and Theorem 8.9, and between Corollary 8.5 and Corollary 8.10 are striking. In both cases it is the non-estimable part of the input and noise, respectively, along with the estimated basis functions that are the key determinants for the resulting accuracy. Just as in Corollary 8.4, Theorem 8.9 can be expressed with respect to the basis functions:

$$\mathbf{AsVar}\{\hat{G}_i\} = \sum_{k=1}^{n_i} \mathbf{AsVar}\{\hat{\theta}_{i,k}\}\left|\mathcal{B}_k\left(e^{j\omega_o}\right)\right|^2. \tag{8.46}$$

However, now

$$\mathbf{AsVar}\{\hat{\theta}_{i,k}\} = \frac{\lambda}{\sigma^2_{i|\chi_k}}, \tag{8.47}$$

where $\sigma^2_{i|l}$ is determined by the correlation structure of the inputs $u_i(t)$ to the systems $G_i(q,\theta_i)$ that *do* share basis function $\mathcal{B}_k(q)$ ($i = 1, \ldots, \chi_k$). Note that in the SIMO case we had

$$\mathbf{AsVar}\{\hat{\theta}_{i,k}\} = \frac{\lambda_{i|\chi_k}}{\sigma^2},$$

where $\lambda_{i|\chi_k}$ is determined by the correlation structure of the noise sources $e_i(t)$ affecting systems $G_i(q,\theta_i)$ that *do not* share basis function $\mathcal{B}_k(q)$ ($i = 1, \ldots, \chi_k$). Note that (8.45) found in Ramazi et al. (2014) does not draw the connection to the variance of the parameters. This is made explicit in the alternate expressions (8.47) and (8.46).

The correlation between parameters related to the same basis functions is not explored in Ramazi et al. (2014). In fact, it is possible to follow the same line of reasoning leading to Theorem 8.2 and arrive at the counter-part for MISO systems. Let the first χ_k systems contain basis function k, so

$$\mathbf{AsVar}\left\{\hat{\theta}_k^{MISO}\right\} = \lambda \Sigma_{1:\chi_k}^{-1},$$

where $\Sigma_{1:\chi_k}$ denotes the covariance matrix of the first χ_k inputs. Hence

$$\mathbf{AsCov}\{\hat{G}\} = \lambda \sum_{k=1}^{n_1} \begin{bmatrix} \Sigma_{1:\chi_k}^{-1} & \mathbf{0} \\ \mathbf{0} & \mathbf{0}_{m-\chi_k} \end{bmatrix} \left|\mathcal{B}_k\left(e^{i\omega_o}\right)\right|^2,$$

and

$$\mathbf{AsCov}\left\{\hat{\theta}^{MISO}\right\} = \lambda \operatorname{diag}\left\{\Sigma_{1:\chi_1}^{-1}, \Sigma_{1:\chi_2}^{-1}, \dots, \Sigma_{1:\chi_{n_m}}^{-1}\right\}. \tag{8.48}$$

Note that, while the correlation between the noise sources is beneficial, the correlation in the input is detrimental for the estimation accuracy. Intuitively, if we use the same input to parallel systems, and only observe the sum of the outputs, there is no way to determine the contribution from the individual systems. On the other hand, as observed in Example 8.1, if the noise is correlated, we can construct equations with reduced noise and improve the accuracy of our estimates.

This difference may also be understood from the structure of Ψ, which through (8.9) determines the variance properties of any estimate. Consider a single SISO system G_1 as the basic case. For the SIMO structure considered in this chapter, as noted before, Ψ^{SIMO} of (8.10) is block upper triangular with m columns (the number of outputs), while Ψ^{MISO} is block lower triangular with as many columns as inputs. Ψ^{MISO} is block lower triangular since $\tilde{\Psi}$ is block diagonal and Σ_{CH} is lower triangular in (8.44). Adding an output y_j to the SIMO structure corresponds to extending Ψ^{SIMO} with one column (and n_j rows):

$$\Psi_e^{\text{SIMO}} = \begin{bmatrix} \Psi^{\text{SIMO}} & \star \\ 0 & \star \end{bmatrix}, \tag{8.49}$$

where the zero comes from that Ψ_e^{SIMO} also is block upper triangular. Since Ψ^{MISO} is block lower triangular, adding an input u_j to the MISO structure extends Ψ^{MISO} with n_j rows (and one column):

$$\Psi_e^{\text{MISO}} = \begin{bmatrix} \Psi^{\text{MISO}} & 0 \\ \star & \star \end{bmatrix}, \tag{8.50}$$

where $\star$ denotes the added column and added row respectively. Addition of columns to Ψ decreases the variance of G_1, while addition of rows increases the variance. First, a short

motivation of this will be given. Second, we will discuss the implication for the variance analysis.

Addition of one more column to Ψ in (8.49) decreases the variance of G_1. With $\Psi = \begin{bmatrix}\psi_1 & \dots & \psi_m\end{bmatrix}$, $\langle \Psi, \Psi \rangle = \sum_k^m \langle \psi_k, \psi_k \rangle$, where $\langle \psi_k, \psi_k \rangle \geq 0$ for every k. The variance of the parameter estimate $\hat{\theta}_N$ decreases with the addition of a column, since

$$\langle \Psi_e, \Psi_e \rangle^{-1} \leq \left(\left\langle \psi_{m+1}, \psi_{m+1} \right\rangle + \langle \Psi, \Psi \rangle \right)^{-1}.$$

On the other hand, addition of rows leads to an increase in variance of $\hat{G}_1$, *e.g.*, consider (2.43) in Lemma 2.2,

$$\mathbf{AsCov}\{G_1(\hat{\theta}_N)\} = L^\top \sum_{k=1}^{r} \mathcal{B}_k^S(z_o)^* \mathcal{B}_k^S(z_o) L,$$

where $L = \Sigma_{CH}^{-\top} \begin{bmatrix}1 & 0 & \dots & 0\end{bmatrix}^\top$ for any number of inputs, and $\{\mathcal{B}_k^S\}_{k=1}^r$ is a basis for the linear span of the rows of Ψ^{MISO}. As can be seen from (8.50), the first rows of Ψ_e^{MISO} are the same as for Ψ^{MISO} and the first r basis functions can therefore be taken the same (with a zero in the last column). To accommodate for the extra rows, n_e extra basis functions $\{\mathcal{B}_k^S\}_{k=r+1}^{r+n_e}$ are needed. Thus, $\{\mathcal{B}_k^S\}_{k=1}^{r+n_e}$ is a basis for the linear span of Ψ_e^{MISO}. We see that the variance of $G_1(\hat{\theta}_N^e)$ is larger than $G_1(\hat{\theta}_N)$ since

$$\mathbf{AsCov}\{G_1(\hat{\theta}_N^e)\} = \mathbf{AsCov}\{G_1(\hat{\theta}_N)\} + L^\top \sum_{k=r+1}^{r+n_e} \mathcal{B}_k^S(z_o)^* \mathcal{B}_k^S(z_o) L,$$

and $L^\top \mathcal{B}_k^S(z_o)^* \mathcal{B}_k^S(z_o) L \geq 0$ is positive semidefinite for every k.

Every additional input of the MISO system corresponds to addition of rows to Ψ. The increase is strictly positive provided that the explicit conditions in Corollary 8.10 hold.

Every additional output of the SIMO system corresponds to the addition of one more column to Ψ. However, the benefit of the additional columns is reduced by the additional rows arising from the additional parameters that need to be estimated, *cf.* Corollary 8.5 and the preceding discussion. When the number of additional parameters has reached n_1 or if $e_1(t)$ is orthogonal to $e_j(t)$ conditioned on $u_{j\setminus 1}(t)$ the benefit vanishes completely. The following examples clarify this point.

Example 8.6. We consider again Example 8.1 for three cases of model orders of the second model, $n_2 = 0, 1, 2$. These cases correspond to Ψ given by the first $n_2 + 1$ rows of

$$\Psi_e^{\mathrm{SIMO}}(q) = \begin{bmatrix} q^{-1} & -\sqrt{1-\beta^2}/\beta q^{-1} \\ 0 & 1/\beta q^{-1} \\ 0 & 1/\beta q^{-2} \end{bmatrix},$$

respectively. When only y_1 is used ($\Psi = q^{-1}$):

$$\mathbf{AsVar}\{\hat{\theta}_{1,1}\} = \langle \Psi, \Psi \rangle^{-1} = 1.$$

When $n_2 = 0$, the second measurement gives a benefit determined by how strong the correlation is between the two noise sources:

$$\mathbf{AsVar}\{\hat{\theta}_{1,1}\} = \langle \Psi, \Psi \rangle^{-1} = (1 + (1 - \beta^2)/\beta^2)^{-1} = \beta^2.$$

However, already if we have to estimate one parameter in G_2 the benefit vanishes completely, *i.e.*, for $n_2 = 1$:

$$\mathbf{AsCov}\{\hat{\theta}\} = \langle \Psi, \Psi \rangle^{-1} = \begin{bmatrix} 1 & \sqrt{1-\beta^2} \\ \sqrt{1-\beta^2} & 1 \end{bmatrix}.$$

The third case, $n_2 = 2$, corresponds to Example 8.1, which shows that the first measurement y_1 improves the estimate of $\theta_{2,2}$ (compared to only estimating $\hat{G}_2$ using y_2):

$$\mathbf{AsVar}\{\hat{\theta}_{2,2}\} = \lambda_{2|1} = \beta^2.$$

Example 8.7. We consider the corresponding MISO system with unit variance noise $e(t)$ and $u(t)$ instead having the same spectral factor

$$\Sigma_{CH} = \begin{bmatrix} 1 & 0 \\ \sqrt{1-\beta^2} & \beta \end{bmatrix}.$$

for $\beta \in (0, 1]$. We now study the impact of the second input $u_2(t)$ when

$$G_1(q) = \theta_{1,1} q^{-1} + \theta_{1,2} q^{-2}, \quad G_2(q) = \sum_{k=1}^{n_2} \theta_{2,k} q^{-k}$$

and $n_2 = 0, 1$. These two cases correspond to Ψ given by the first $n_2 + 2$ rows of

$$\Psi_e^{MISO}(q) = \begin{bmatrix} q^{-1} & 0 \\ q^{-2} & 0 \\ \sqrt{1-\beta^2} q^{-1} & \beta q^{-1} \end{bmatrix},$$

respectively. When only u_1 is used or G_2 is known ($\Psi = \begin{bmatrix} q^{-1} & q^{-2} \end{bmatrix}^\top$):

$$\mathbf{AsCov}\{\hat{\theta}_1\} = \langle \Psi, \Psi \rangle^{-1} = I.$$

When $n_2 = 1$, the variance of $\hat{\theta}_{1,1}$ is increased depending on the correlation between the two inputs:

$$\mathbf{AsVar}\{\hat{\theta}\} = \frac{1}{\beta^2} \begin{bmatrix} 1 & 0 & -\sqrt{1-\beta^2} \\ 0 & \beta^2 & 0 \\ -\sqrt{1-\beta^2} & 0 & 1 \end{bmatrix}.$$

Also notice that the asymptotic covariance of $\begin{bmatrix}\hat{\theta}_{1,1} & \hat{\theta}_{2,1}\end{bmatrix}^\top$ is given by Σ^{-1}, the inverse of the covariance matrix of $u(t)$ and that $\mathbf{AsVar}\{\hat{\theta}_{2,2}\} = \sigma_1^{-1}$. As β goes to zero the variance of $\begin{bmatrix}\hat{\theta}_{1,1} & \hat{\theta}_{2,1}\end{bmatrix}^\top$ increases and at $\beta = 0$ the two inputs are perfectly correlated and we loose identifiability.

8.7 Numerical simulations

In this section, we illustrate the results derived in the previous sections through three sets of numerical Monte Carlo simulations.

8.7.1 Effect of model order

Corollary 8.5 is illustrated in Figure 8.7, where the following systems are identified using $N = 500$ input-output measurements:

$$\begin{aligned} G_i &= \tilde{\Gamma}_i\theta_i, \quad i = 1,2,3 \qquad \tilde{\Gamma}_i(q) = F(q)^{-1}\Gamma_i(q), \\ \Gamma_i(q) &= \begin{bmatrix}\mathcal{B}_1(q), \ldots, \mathcal{B}_{n_i}(q)\end{bmatrix}, \quad \mathcal{B}_k(q) = q^{-k}, \end{aligned} \tag{8.51}$$

with

$$\begin{aligned} F(q) &= \frac{1}{1-0.8q^{-1}}, & \theta_1^0 &= \begin{bmatrix}1 & 0.5 & 0.7\end{bmatrix}^\top, \\ \theta_2^0 &= \begin{bmatrix}1 & -1 & 2\end{bmatrix}^\top, & \theta_3^0 &= \begin{bmatrix}1 & 1 & 2 & 1 & 1\end{bmatrix}^\top. \end{aligned}$$

The input $u(t)$ is drawn from a Gaussian distribution with variance $\sigma^2 = 1$, filtered by $F(q)$. The measurement noise is normally distributed with covariance matrix $\Lambda = \Lambda_{CH}\Lambda_{CH}^\top$, where

$$\Lambda_{CH} = \begin{bmatrix} 1 & 0 & 0 \\ 0.6 & 0.8 & 0 \\ 0.7 & 0.7 & 0.1 \end{bmatrix},$$

thus $\lambda_1 = \lambda_2 = \lambda_3 = 1$. The sample variance is computed using

$$\mathbf{Cov}\{\hat{\theta}_s\} = \frac{1}{MC}\sum_{k=1}^{MC}\left|G_3\left(e^{j\omega_o}, \theta_3^0\right) - G_3\left(e^{j\omega_o}, \hat{\theta}_3\right)\right|^2,$$

where $MC = 2000$ is the number of realizations of the input and noise. The same realizations of the input and noise are used for all model orders.

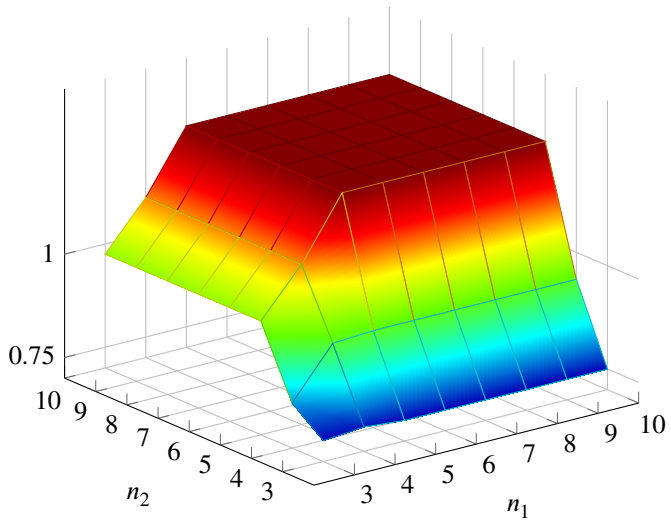

Figure 8.7: Sample variance of $G_3\left(e^{j\omega}, \hat{\theta}_3\right)$ as a function of the number of estimated parameters of G_1 and G_2.

The variance of $G_3\left(e^{j\omega}, \hat{\theta}_3\right)$ increases with increasing n_i, $i = 1, 2$, but only up to the point where $n_i = n_3 = 5$. After that, any increase in n_1 or n_2 does not increase the variance of $G_3\left(e^{j\omega}, \hat{\theta}_3\right)$, as can be seen in Figure 8.7. The behavior can be explained by Corollary 8.5: when $n_3 \geq n_1, n_2$, G_3 is the last block, having the highest number of parameters, and any increase in n_1, n_2 increases the variance of G_3. When for example $n_1 \geq n_3$, the blocks should be reordered so that G_3 comes before G_1. In this case, when n_1 increases the first condition of Corollary 8.5 does not hold and hence the variance of $G_3\left(e^{j\omega}, \hat{\theta}_3\right)$ does not increase further.

8.7.2 Effect of removing one parameter

In the second set of numerical experiments, we simulate the same type of system as in Example 8.1. We let β vary in the interval [0.001, 1]. For each β, we generate $MC = 2000$ Monte Carlo experiments, where in each of them we collect $N = 500$ input-output samples. At the i-th Monte Carlo run, we generate new trajectories for the input and the noise and we compute $\hat{\theta}_i$ as in (8.8). The sample covariance matrix, for each β, is computed as

$$\mathbf{Cov}\left\{\hat{\theta}_s\right\} = \frac{1}{MC}\sum_{i=1}^{MC}\left(\hat{\theta}_i - \theta\right)\left(\hat{\theta}_i - \theta\right)^\top.$$

Figure 8.8 shows that the variance of $\hat{\theta}_{21}$ is always close to one, no matter what the value of β is. It also shows that the variance of the estimate $\hat{\theta}_{22}$ behaves as β^2. In particular, when β

approaches 0 (*i.e.*, almost perfectly correlated noise processes), the variance of such estimate tends to 0. All of the observations are as predicted by Corollary 8.2 and Example 8.1.

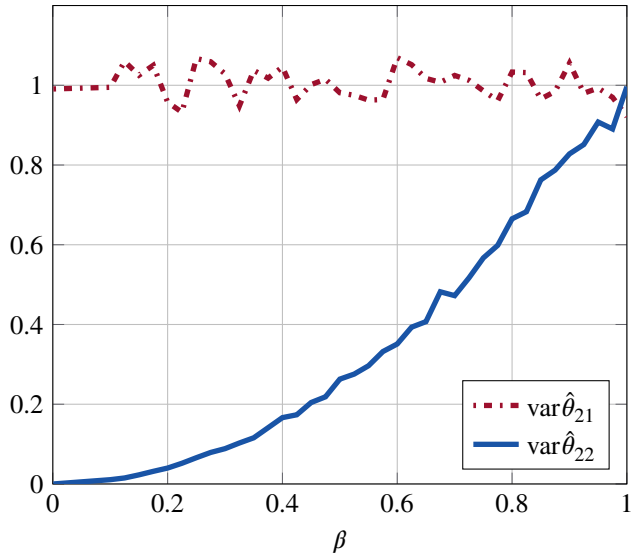

Figure 8.8: Sample variance of the parameters of the first module (as functions of β) when the second module has one parameter.

8.7.3 Optimal correlation structure

A third simulation experiment is performed in order to illustrate Theorem 8.8. We consider a system with $m = 3$ outputs; the modules are

$$G_1(q) = 0.3q^{-1}, \qquad G_2(q) = 0.8q^{-1} - 0.4q^{-2},$$
$$G_3(q) = 0.1q^{-1} + 0.2q^{-2},$$

so that

$$\theta = \begin{bmatrix} \theta_{11} \\ \theta_{21} \\ \theta_{31} \\ \theta_{22} \\ \theta_{32} \end{bmatrix} = \begin{bmatrix} 0.3 \\ 0.8 \\ 0.1 \\ -0.4 \\ 0.2 \end{bmatrix}.$$

The noise process is generated by the following upper triangular Cholesky factor:

$$R = \begin{bmatrix} \beta & \sqrt{1-\beta^2}\cos\alpha & \sqrt{1-\varepsilon^2}\sin\alpha \\ 0 & 0.8 & 0.6 \\ 0 & 0 & 1 \end{bmatrix} = \begin{bmatrix} \varepsilon & p^\top \\ 0 & M \end{bmatrix},$$

where $\beta = 0.1$ and $\alpha \in [0, \pi]$ is a parameter tuning the correlation of $e_1(t)$ with $e_2(t)$ and $e_3(t)$. The purpose of this experiment is to show that, when α is such that $p = \left[\sqrt{1-\beta^2}\cos\alpha \;\; d\sqrt{1-\beta^2}\sin\alpha \right]^\top$ is aligned with the first right-singular vector v_1 of M, then the total variance of the estimate of the sub-vector $\tilde{\theta} = [\, \theta_{12}\, \theta_{22} \,]^\top$ is minimized. In the case under analysis, $v_1 = [\, 0.447\;\; 0.894 \,]^\top = [\, \cos\alpha_0 \;\; \sin\alpha_0 \,]^\top$, with $\alpha_0 = 1.11$. We let α take values in $[0, \pi]$ and for each α we generate $MC = 2000$ Monte Carlo runs of $N = 500$ input-output samples each. We compute the sample total variance of $\tilde{\theta}$ as

$$\mathrm{tvar}\,\hat{\tilde{\theta}}_{\mathrm{S}} = \frac{1}{MC}\sum_{i=1}^{MC}\left((\hat{\theta}_{22,i} - \theta_{22})^2 + (\hat{\theta}_{32,i} - \theta_{32})^2\right),$$

where $\hat{\theta}_{22,i}$ and $\hat{\theta}_{32,i}$ are the estimates obtained at the i-th Monte Carlo run.

The results of the experiment are reported in Figure 8.9. It can be seen that the minimum total variance of the estimate of $\hat{\theta}$ is attained for values close to α_0 (approximations are due to low resolution of the grid of values of α). An interesting observation regards the value of α for which the total variance is maximized: this happens when $\alpha = 2.68$, which yields the second right-singular vector of M, namely $v_2 = [\, -0.894\;\; 0.447 \,]^\top$.

8.8 Summary

In this chapter, we have examined how the estimation accuracy of a linear SIMO model depends on the correlation structure of the noise, model structure and model order. A formula for the asymptotic covariance of the frequency response function estimate and the model parameters has been developed for the case of temporally white, but possibly spatially correlated additive noise. It has been shown that when parts of the noise can be linearly estimated from measurements of other blocks with less estimated parameters, the variance decreases. The expressions reveal how the order of the different blocks and the correlation of the noise affect the variance of one block. In particular, it has been shown that the variance of the block of interest levels off when the number of estimated parameters in another block reaches the number of estimated parameters of the block of interest. The optimal correlation structure for the noise was determined for the case when one block has one parameter less than the other blocks.

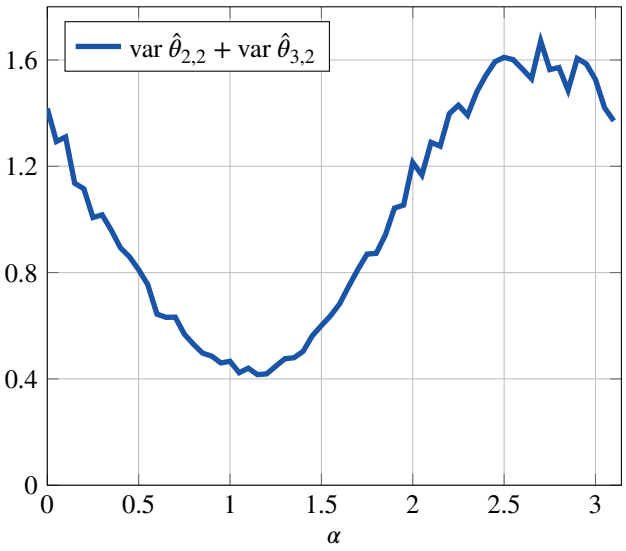

Figure 8.9: Total sample variance of the parameter vector $\tilde{\theta}$ as function of α.

8.A Proofs and auxilliary lemmas

8.A.1 Proof of Lemma 8.1

Let $v(t) = \Lambda_{CH}^{-1} e(t)$ for some real valued random vector $e(t)$ (Λ_{CH}^{-1} exists and is unique for $\Lambda > 0$ (Horn and Johnson, 1990)). Then $\mathbf{Cov}\{v(t)\} = I$. Similarly $e(t) = \Lambda_{CH} v(t)$. The set $\{v_1(t), \ldots, v_j(t)\}$ is a function of $\{e_1(t), \ldots, e_l(t)\}$ only and vice versa, for all $1 \leq l \leq m$. Thus, if $\{e_1(t), \ldots, e_l(t)\}$ are known, then also $\{v_1(t), \ldots, v_l(t)\}$ are known, but nothing is known about $\{v_{l+1}(t), \ldots, v_m(t)\}$. Thus, for $l < i$ the best linear estimator of $e_i(t)$ given $e_1(t), \ldots, e_l(t)$, is

$$\hat{e}_{i|l}(t) = \sum_{k=1}^{l} \gamma_{ik} v_k(t), \tag{8.52}$$

and $e_i(t) - \hat{e}_{i|l}(t)$ has variance $\lambda_{i|l} = \sum_{k=l+1}^{i} \gamma_{ik}^2$. For the last part of the lemma, we realize that the dependence of $\hat{e}_{i|l}(t)$ on $e_l(t)$ in Equation (8.52) is given by γ_{il}/γ_{ll} (since $v_1(t), \ldots, v_{l-1}(t)$ do not depend on $e_l(t)$). Hence $\hat{e}_{i|l}(t)$ depends on $e_l(t)$ if and only if $\gamma_{il} \neq 0$.

8.A.2 Lemma 8.11

Lemma 8.11. *Let $\Lambda > 0$ and its Cholesky factor Λ_{CH} be partitioned according to $e_{1:\chi_k-1}$ and $e_{\chi_k:m}$,*

$$\Lambda = \begin{bmatrix} \Lambda_1 & \Lambda_{12} \\ \Lambda_{21} & \Lambda_2 \end{bmatrix}, \quad \Lambda_{CH} = \begin{bmatrix} (\Lambda_{CH})_1 & 0 \\ (\Lambda_{CH})_{21} & (\Lambda_{CH})_2 \end{bmatrix}.$$

Then $\Lambda_{\chi_k:m|\chi_k-1} = (\Lambda_{CH})_2(\Lambda_{CH})_2^\top$.

Proof. Similar to the derivations of Lemma 8.1, there exists some random vector $v(t)$ with $\mathbf{Cov}\{v(t)\} = I$, such that $e(t) = \Lambda_{CH}v(t)$ and $v_{1:\chi-1}(t)$ are known since $e_{1:\chi-1}(t)$ are known. Furthermore $\hat{e}_{\chi_k:m|\chi_k-1}(t) = (\Lambda_{CH})_{21}v_{1:\chi-1}(t)$, which implies $e_{\chi_k:m|\chi_k-1}(t) - \hat{e}_{\chi_k:m|\chi_k-1}(t) = (\Lambda_{CH})_2 v_{\chi_k:m}(t)$ and the results follows since $\mathbf{Cov}\left\{ v_{\chi_k:m}(t) \right\} = I$. ■

8.A.3 Proof of Corollary 8.5

To prove Corollary 8.5 we will use (8.30). First, we make the assumption that l is the last module that has n_l parameters. This assumption is made for convenience since reordering all modules with n_l estimated parameters does not change (8.30). First of all, we see that if $n_l \geq n_i$, then (8.30) does not increase when n_l increases. If instead $n_l < n_i$, the increase in variance is given by $\gamma_{il}^2 \left| \mathcal{B}_{n_l+1}\left(e^{j\omega_o}\right) \right|^2$, which is non-zero if and only if $\gamma_{il} \neq 0$ and $\left| \mathcal{B}_{n_l+1}\left(e^{j\omega_o}\right) \right|^2 \neq 0$. From Lemma 8.1 the theorem follows.

8.A.4 Proof of Lemma 8.7

The inverse of B is

$$B^{-1} = \begin{bmatrix} \eta^{-1} & -q^\top \\ 0 & M^{-1} \end{bmatrix}, \quad q^\top := \eta^{-1} p^\top M^{-1},$$

so that

$$\Lambda^{-1} = B^{-\top}B^{-1} = \begin{bmatrix} \eta^{-2} & -q^\top \eta^{-1} \\ -q\eta^{-1} & M^{-\top}M^{-1} + qq^\top \end{bmatrix}.$$

Hence, using the Sherman–Morrison formula (Bartlett, 1951) it is straightforward to show (8.42).

CHAPTER 9

MIMO MODELS WITH CORRELATED INPUT AND NOISE

In this chapter, we generalize the covariance results for multi-input single-output (MISO) systems (Ramazi et al., 2014) and single-input multi-output (SIMO) systems discussed in the previous chapter.

9.1 Introduction

Modern control systems for industrial plants are based on mathematical models of the plant dynamics. These control systems need to handle several decision variables (input signals), having access, through sensing devices, to a possibly large number of measured variables (output signals). The whole structure can be modeled as a MIMO model and its identification is a crucial task. In particular, assessing the quality of the identified model by quantifying model uncertainties is an important aspect that must be taken into account when designing model-based and robust control schemes (Barenthin and Hjalmarsson, 2008).

We focus on quantifying these model uncertainties in the identification of MIMO systems, where each system module is expressed as the linear combination of (known) basis functions and where the linear coefficients are unknown. Adopting a stochastic framework, we assume that measurements are corrupted by additive noise, with a given probabilistic description.

We assume the system is in the model set and study the accuracy of the identified model in terms of the parameter error covariance matrix (Ljung, 1999). Our aim is to understand how the experimental conditions and model structure influence this covariance matrix. To this end, we simplify our analysis by assuming that the input signals are temporally white, but may be spatially correlated. We make a similar assumption for the output noise. Under these conditions, we derive an insightful expression for the parameter error covariance matrix. In particular, we characterize the behavior of this covariance matrix in terms of the input and noise correlation matrices and the model orders of the modules composing the MIMO system. Our results show that the combination of suitable input and noise correlation structures and proper model orders of the modules, may significantly improve the accuracy

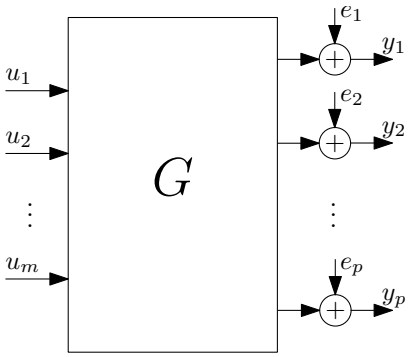

Figure 9.1: Block scheme of the linear MIMO system.

of the estimated model for a specific module. This has important implications in experiment design for MIMO systems (Hjalmarsson, 2009) and fault-detection and diagnosis (Isermann, 2005).

In the literature, there are readily available formulas quantifying the model error of identified MIMO systems. However they provide little insight in what affects the model error. There are other expressions that try to give this insight, however, they are typically valid only asymptotically (in both the number of samples and model orders of the modules). One classic result, valid for large data length N and large model order n, is given by the following expression (Zhu, 2001; Z. D. Yuan and Ljung, 1984)

$$\mathbf{Cov}\left\{\mathrm{vec}\left\{\hat{G}\right\}\right\} \approx \frac{n}{N}\boldsymbol{\Phi}_u^{-1} \otimes \boldsymbol{\Phi}_v,$$

where $\boldsymbol{\Phi}_u$ is the input spectrum and $\boldsymbol{\Phi}_v$ the noise spectrum. This expression was extended in Ninness and Gómez (1996) to a general set of orthonormal basis functions, denoted by $\{\mathcal{B}_k(z)\}$:

$$\mathbf{Cov}\left\{\mathrm{vec}\left\{\hat{G}\right\}\right\} \approx \frac{1}{N}\sum_{k=1}^{n_\mathcal{B}} \left|\mathcal{B}_k(z)\right|^2 \boldsymbol{\Phi}_u^{-1} \otimes \boldsymbol{\Phi}_v.$$

Note that both expressions are valid only for large model orders. Our results, instead, are exact for finite model orders (but still asymptotic in data length).

9.2 Problem formulation

We consider LTI dynamic systems with m inputs and p outputs (see Figure 9.1). The model is described as follows:

$$y(t) = G(q)u(t) + e(t) \tag{9.1}$$

where

$$G(q) = \begin{bmatrix} G_{11}(q) & G_{12}(q) & \dots & G_{1m}(q) \\ G_{21}(q) & G_{22}(q) & \dots & G_{2m}(q) \\ \vdots & \vdots & \ddots & \vdots \\ G_{p1}(q) & G_{p2}(q) & \dots & G_{pm}(q) \end{bmatrix}.$$

Here q denotes the forward shift operator, *i.e.*, $qu(t) = u(t+1)$ and the $G_{ij}(q)$ are causal stable rational transfer functions. The modules G_{ij} are modeled as

$$G_{ij}(q, \theta_{ij}) = \Gamma_{ij}(q)\theta_{ij}, \qquad \theta_{ij} \in \mathbb{R}^{n_{ij}}, \tag{9.2}$$

where $\Gamma_{ij}(q) = \begin{bmatrix} \mathcal{B}_1(q) & \dots & \mathcal{B}_{n_{ij}}(q) \end{bmatrix}$, $i = 1, \dots, p$ and $j = 1, \dots, m$, for some orthonormal basis functions $\{\mathcal{B}_k(q)\}_{k=1}^{n_{\mathcal{B}}}$. The basis functions can be tailored according to a priori knowledge on the system dynamics; for example, Laguerre basis functions can be tailored to the time constant of the system (Wahlberg, 1991). Examples of more general basis functions can be found in P. S. C. Heuberger et al. (1995) and Ninness and Gustafsson (1997). The noise sequence $\{e(t)\}$ is zero mean and temporally white, but may be correlated in the spatial domain:

$$\mathbf{E}\{e(t)\} = 0, \qquad \mathbf{E}\left\{e(t)e(s)^\top\right\} = \delta_{t-s}\Lambda, \tag{9.3}$$

for some positive definite matrix covariance matrix Λ, and where $\mathbf{E}\{\cdot\}$ is the expectation operator. We express Λ in terms of its Cholesky factorization

$$\Lambda = \Lambda_{CH}\Lambda_{CH}^\top, \tag{9.4}$$

where $\Lambda_{CH} \in \mathbb{R}^{p \times p}$ is lower triangular, *i.e.*,

$$\Lambda_{CH} = \begin{bmatrix} \rho_{11} & 0 & \dots & 0 \\ \rho_{21} & \rho_{22} & \dots & 0 \\ \vdots & \vdots & \ddots & \vdots \\ \rho_{p1} & \rho_{p2} & \cdots & \rho_{pp} \end{bmatrix}, \tag{9.5}$$

for some $\{\rho_{ij}\}$. Also notice that since $\Lambda > 0$,

$$\Lambda^{-1} = \Lambda_{CH}^{-\top}\Lambda_{CH}^{-1}. \tag{9.6}$$

The input sequence $\{u(t)\}$ is also zero mean and temporally white, but may be correlated in the spatial domain:

$$\mathbf{E}\{u(t)\} = 0, \qquad \mathbf{E}\left\{u(t)u(s)^\top\right\} = \delta_{t-s}\Sigma, \tag{9.7}$$

for some positive definite matrix covariance matrix Σ. We express Σ in terms of its *upper* triangular Cholesky factorization[1]

$$\Sigma = \Sigma_{CH}\Sigma_{CH}^{\top}, \tag{9.8}$$

where $\Sigma_{CH} \in \mathbb{R}^{m\times m}$ is *upper* triangular. Also Σ_{CH}^{-1} is upper triangular and we denote its elements by $\{\gamma_{ij}\}$ according to

$$\Sigma_{CH}^{-1} = \begin{bmatrix} \gamma_{11} & \gamma_{12} & \cdots & \gamma_{1m} \\ 0 & \gamma_{22} & \cdots & \gamma_{2m} \\ \vdots & \vdots & \ddots & \vdots \\ 0 & 0 & \cdots & \gamma_{mm} \end{bmatrix}. \tag{9.9}$$

We summarize the assumptions on input, noise and model as follows:

Assumption 9.1. The input $\{u(t)\}$ is zero mean temporally white noise with finite moments of all orders, and (9.7) holds with $\Sigma > 0$. The noise $\{e(t)\}$ is zero mean and temporally white, *i.e.*, (9.3) holds with $\Lambda > 0$. It is assumed that $\mathbf{E}\left\{|e(t)|^{4+\rho}\right\} < \infty$ for some $\rho > 0$. The data are generated in open loop, that is, the input $\{u(t)\}$ is independent of the noise $\{e(t)\}$. The true input-output behavior of the data generating system can be captured by our model structure, *i.e.*, the true system can be described by (9.1) and (9.2) for some parameters $\theta_{ij}^{o} \in \mathbb{R}^{n_{ij}}$, $i = 1, \ldots, p$, $j = 1, \ldots, m$. The orthonormal basis functions $\{\mathcal{B}_k(q)\}$ are assumed stable.

9.2.1 Weighted least-squares estimate

We introducing the notation

$$\theta = \begin{bmatrix} \theta_{11}^{\top} & \theta_{21}^{\top} & \ldots & \theta_{p1}^{\top} & \ldots & \theta_{1m}^{\top} & \theta_{2m}^{\top} & \ldots & \theta_{pm}^{\top} \end{bmatrix}^{\top} \in \mathbb{R}^{n},$$

the total number of parameters $n := \sum_{i=1}^{p}\sum_{j=1}^{m} n_{ij}$, the transfer function matrix

$$\underset{(n\times pm)}{\tilde{\Psi}(q)} = \operatorname{diag}\left\{ \Gamma_{11}^{\top}, \Gamma_{21}^{\top}, \ldots, \Gamma_{pm}^{\top} \right\}$$

and the notation

$$\underset{(pm\times 1)}{\operatorname{vec}\{G(q)\}} = \begin{bmatrix} G_{\cdot 1}(q) & G_{\cdot 2}(q) & \ldots & G_{\cdot m}(q) \end{bmatrix}^{\top},$$

where $G_{\cdot j}$ denotes the jth column of G. We can then write

$$\operatorname{vec}\{G(q)\} = \tilde{\Psi}^{\top}(q)\theta$$

[1] The standard Cholesky factorization is defined with a lower triangular factor but for reasons that will be clear in following sections, we need the upper triangular counterpart.

and describe the model (9.1) as a linear regression model

$$y(t) = \varphi^{\top}(t)\theta + e(t), \tag{9.10}$$

where, using Theorem T2.13 in Brewer (1978),

$$\varphi(t) = \tilde{\Psi}(q)\big(u(t) \otimes I_p\big).$$

An unbiased and consistent estimate of the parameter vector θ can be obtained from weighted least-squares, with weighting matrix Λ^{-1} giving the linear unbiased estimator with lowest variance (see, *e.g.*, Ljung (1999) and Söderström and Stoica (1989)). Λ is assumed known; however, this assumption is not restrictive since Λ can be estimated from data and replacing Λ by a consistent estimate does not affect the asymptotic covariance of $\hat{\theta}$ (Cox and Reid, 1987). However, in certain applications, not knowing Λ will increase the covariance of $\hat{\theta}$.

Under Assumption 9.1, the noise sequence is zero mean, hence $\hat{\theta}_N$ is unbiased. It also follows that the asymptotic covariance matrix of the parameter estimates is given by

$$\mathbf{AsCov}\big\{\hat{\theta}_N\big\} = \mathbf{E}\big\{\varphi(t)\Lambda^{-1}\varphi^{\top}(t)\big\}^{-1}, \tag{9.11}$$

where the expectation is over the input sequence. By repeated use of the mixed product rule of Kronecker products (T2.4 in Brewer (1978)) (9.11) can be expressed as

$$\mathbf{AsCov}\big\{\hat{\theta}_N\big\} = \mathbf{E}\big\{\tilde{\Psi}(q)\big(u(t)u^{\top}(t) \otimes \Lambda^{-1}\big)\tilde{\Psi}^{\top}(q)\big\}^{-1}. \tag{9.12}$$

In the problem we consider, using Parseval's formula, (9.4) and (9.6), the asymptotic covariance matrix, (9.12), can be written as[2]

$$\mathbf{AsCov}\big\{\hat{\theta}_N\big\} = \left(\frac{1}{2\pi}\int_{-\pi}^{\pi} \Psi\big(\mathrm{e}^{\mathrm{j}\omega}\big)\Psi^{*}\big(\mathrm{e}^{\mathrm{j}\omega}\big)\, d\omega\right)^{-1} = \langle \Psi, \Psi\rangle^{-1}, \tag{9.13}$$

where

$$\Psi(q) = \tilde{\Psi}(q)(\Sigma_{CH} \otimes \Lambda_{CH}^{-\top}). \tag{9.14}$$

Note that $\Psi(q)$ is block upper triangular since $\tilde{\Psi}(q)$ is block diagonal, $\Lambda_{CH}^{\top}$ is upper triangular and Σ_{CH} is upper triangular[3]. In the following, we will analyze how model structure, input and noise properties affect (9.13).

9.2.2 Characterizing the asymptotic covariance

We notice, using (9.14), that we can write

$$\frac{\partial \operatorname{vec}\{G(q)\}}{\partial \theta} = \tilde{\Psi}(q) = \Psi(q)(\Sigma_{CH}^{-1} \otimes \Lambda_{CH}^{\top}).$$

[2]Non-singularity of $\langle \Psi, \Psi\rangle$ usually requires parameter identifiability and persistence of excitation (Ljung, 1999), both of which are satisfied under Assumption 9.1.

[3]The reason for introducing the upper triangular factorization Σ_{CH} is to obtain this block upper triangular structure.

Introduce

$$L := (\Sigma_{CH}^{-1} \otimes \Lambda_{CH}^{T}). \tag{9.15}$$

Then, using Lemma 2.2,

$$\mathbf{AsCov}\left\{\mathrm{vec}\left\{\hat{G}\left(\mathrm{e}^{\mathrm{j}\omega_o}\right)\right\}\right\} = L^{\top} \sum_{k=1}^{n} \mathcal{B}_k^S\left(\mathrm{e}^{\mathrm{j}\omega_o}\right)^* \mathcal{B}_k^S\left(\mathrm{e}^{\mathrm{j}\omega_o}\right) L. \tag{9.16}$$

To analyze (9.16), we will consider a few special cases. To this end, we need to characterize the basis functions $\{\mathcal{B}_k^S\}$.

9.2.3 Basis functions

We need the following assumption on the model structure:

Assumption 9.2. For each row i, if G_{ij} contains $\mathcal{B}_k$, then $G_{i(j+1)}$ contains $\mathcal{B}_k$.

Assumption 9.2 states that the modules that do not contain $\mathcal{B}_k$ are located in the upper left corner of G, which is somewhat restrictive since this may not be achieved by renaming the modules, in general. We will also need the following definition:

Definition 5. For each basis function $\mathcal{B}_k$, let

$$Q_k := \mathrm{diag}\left\{q_1, \ldots, q_{mp}\right\},$$

where

$$q_i := \begin{cases} 1 & \text{if entry i of vec\{G(q)\} contain } \mathcal{B}_{\mathrm{k}} \\ 0 & \text{if entry i of vec\{G(q)\} does not contain } \mathcal{B}_{\mathrm{k}} \end{cases}$$

The rows of Ψ that contain $\mathcal{B}_k$ are given by

$$\mathcal{B}_k Q_k (\Sigma_{CH} \otimes \Lambda_{CH}^{-\top}). \tag{9.17}$$

Lemma 9.1. *Let Assumption 9.2 hold and let $\mathcal{S}_\Psi$ be the rowspace of Ψ. Let $\{\mathcal{B}_l^S(q)\}_{l=1}^n$ be such that for every basis function $\mathcal{B}_k$ and every row i of* vec$\{G\}$ *that has the basis function $\mathcal{B}_k$, there is a basis function of the form*

$$\mathcal{B}_l^S(q) := \begin{bmatrix} 0 & \ldots & 0 & \mathcal{B}_k(q) & 0 & \ldots & 0 \end{bmatrix},$$

i.e., *the entry in column i of $\mathcal{B}_l^S(q)$ is $\mathcal{B}_k$. Then $\{\mathcal{B}_l^S(q)\}_{l=1}^n$ is a set of basis functions for $\mathcal{S}_\Psi$.*

Proof. See Appendix 9.A.2. ■

Example 9.1. To illustrate Lemma 9.1, we consider a system with 2 inputs and 2 outputs. When all modules contain $\mathcal{B}_k$, Assumption 9.2 is satisfied, and (9.17) gives that the rows of Ψ that contain $\mathcal{B}_k$ are given by

$$\mathcal{B}_k \begin{bmatrix} \gamma_{11}\rho_{11} & \gamma_{11}\rho_{21} & \gamma_{12}\rho_{11} & \gamma_{12}\rho_{21} \\ 0 & \gamma_{11}\rho_{22} & 0 & \gamma_{12}\rho_{22} \\ 0 & 0 & \gamma_{22}\rho_{11} & \gamma_{22}\rho_{21} \\ 0 & 0 & 0 & \gamma_{22}\rho_{22} \end{bmatrix},$$

and since the matrix is full rank, a set of basis functions can be given by Lemma 9.1. We now look at which non-full parametrizations comply with Assumption 9.2. Assumption 9.2 tells us that the modules in G that contain $\mathcal{B}_k$ should be located in the lower right corner. Naturally, if only G_{22} contains $\mathcal{B}_k$, then (9.17) is given by

$$\mathcal{B}_k \begin{bmatrix} 0 & 0 & 0 & 0 \\ 0 & 0 & 0 & 0 \\ 0 & 0 & 0 & 0 \\ 0 & 0 & 0 & \gamma_{22}\rho_{22} \end{bmatrix},$$

and the only basis function is $\mathcal{B}_1^S(q) = [\,0\ 0\ 0\ \mathcal{B}_k(q)\,]$. If Assumption 9.2 still is to hold, we are allowed to add $\mathcal{B}_k$ to either G_{12} or G_{21}. In the first case, (9.17) is given by

$$\mathcal{B}_k \begin{bmatrix} 0 & 0 & 0 & 0 \\ 0 & 0 & 0 & 0 \\ 0 & 0 & \gamma_{22}\rho_{11} & \gamma_{22}\rho_{21} \\ 0 & 0 & 0 & \gamma_{22}\rho_{22} \end{bmatrix},$$

and the second basis function is $\mathcal{B}_2^S(q) = [\,0\ 0\ \mathcal{B}_k(q)\ 0\,]$. If instead $\mathcal{B}_k$ is added to G_{21}, (9.17) is given by

$$\mathcal{B}_k \begin{bmatrix} 0 & 0 & 0 & 0 \\ 0 & \gamma_{11}\rho_{22} & 0 & \gamma_{12}\rho_{22} \\ 0 & 0 & 0 & 0 \\ 0 & 0 & 0 & \gamma_{22}\rho_{22} \end{bmatrix},$$

and the second basis function is $\mathcal{B}_2^S(q) = [\,0\ \mathcal{B}_k(q)\ 0\ 0\,]$. To illustrate what happens when Assumption 9.2 is not satisfied, consider the case when G_{12} does not contain $\mathcal{B}_k$ and the

rest of the modules do. Then, (9.17) is given by

$$\mathcal{B}_k \begin{bmatrix} \gamma_{11}\rho_{11} & \gamma_{11}\rho_{21} & \gamma_{12}\rho_{11} & \gamma_{12}\rho_{21} \\ 0 & 0 & 0 & 0 \\ 0 & 0 & \gamma_{22}\rho_{11} & \gamma_{22}\rho_{21} \\ 0 & 0 & 0 & \gamma_{22}\rho_{22} \end{bmatrix},$$

and the set of basis functions are not on the required form:

$$\begin{aligned} \mathcal{B}_1^S(q) &= \begin{bmatrix} 0 & 0 & 0 & \mathcal{B}_k, \end{bmatrix}, \\ \mathcal{B}_2^S(q) &= \begin{bmatrix} 0 & 0 & \mathcal{B}_k & 0 \end{bmatrix}, \\ \mathcal{B}_3^S(q) &= \mathcal{B}_k(\rho_{11}^2 + \rho_{21}^2)^{-1/2} \begin{bmatrix} \rho_{11} & \rho_{21} & 0 & 0 \end{bmatrix}. \end{aligned}$$

9.3 Covariance of MIMO models

The configuration of basis function prescribed by Lemma 9.1 allows us to derive a neat expression for the asymptotic covariance matrix in (9.16) which in turn will be exemplified for a few special structures.

Theorem 9.2. *Let Assumptions 9.1 and 9.2 hold. Then* (9.16) *is simplified to*

$$\boldsymbol{AsCov}\left\{\operatorname{vec}\left\{\hat{G}\left(e^{j\omega_o}\right)\right\}\right\} = \sum_{k=1}^{n_{\mathcal{B}}} \left|\mathcal{B}_k\left(e^{j\omega_o}\right)\right|^2 L^\top Q_k L. \tag{9.18}$$

where Q_k is given by Definition 5 and

$$L := \Sigma_{CH}^{-1} \otimes \Lambda_{CH}^\top.$$

Proof. Follows from (9.16) using Lemma 9.1. ∎

Remark 9.1. The formula (9.18) is a decomposition of the variance of $\operatorname{vec}\left\{\hat{G}(q)\right\}$ as the sum of the contributions of each module basis function $\mathcal{B}_k$. The weighting factor $L^\top Q_k L$ is determined by which other modules also contain the basis function $\mathcal{B}_k$. In fact, it is possible to associate $L^\top Q_k L$ as the covariance of the parameters related to the basis function $\mathcal{B}_k$ similar to the results found in Chapter 8.

Remark 9.2. If Assumption 9.2 does not hold, (9.18) still holds, but, in this case Q_k in (9.18) must be replaced by $P^\top Q_k P$, where P is an orthogonal matrix such that the rowspace of $\mathcal{B}_k Q_k P$ is the same as the rowspace of $\mathcal{B}_k Q_k L$.

We will now consider a few special cases where we can give some insights into the expression (9.16). We will analyze the weighting factor

$$L^\top Q_k L \tag{9.19}$$

that depends on the other modules that contain $\mathcal{B}_k$.

9.3.1 Full parametrization

We first consider the case when all modules G_{ij} contain the same set of basis functions, *i.e.*, the model orders are identical: $n_{11} = n_{21} = \cdots = n_{pm}$. Naturally, in this case Assumption 9.2 holds and Theorem 9.2 gives that (9.18) holds with $Q_k = I_{mp}$ which, when inserted in in (9.19), gives that

$$L^\top Q_k L = \Sigma^{-1} \otimes \Lambda. \tag{9.20}$$

Hence, we have the following corollary:

Corollary 9.3. *Let Assumption 9.1 hold. Let all modules have the same model order. Then*

$$\boldsymbol{AsCov}\left\{\operatorname{vec}\left\{\hat{G}\right\}\right\} = \sum_{k=1}^{n_\mathcal{B}} \left|\mathcal{B}_k\right|^2 (\Sigma^{-1} \otimes \Lambda). \tag{9.21}$$

Remark 9.3. This is a generalization of (9.1) derived in Ninness and Gómez (1996), to finite model orders, when there is no temporal correlation in neither input nor noise.

9.3.2 Unused input

We consider next the case when we do not estimate parameters related to basis function $\mathcal{B}_k$ for modules with input $\{u_i\}_{i=1}^{\chi_k - 1}$, *i.e.*, modules $G_{11}, G_{21}, \ldots, G_{p(\chi_k - 1)}$ do not contain $\mathcal{B}_k$. Also in this case Assumption 9.2 holds and Theorem 9.2 gives that (9.18) holds with

$$Q_k = \begin{bmatrix} 0_{p(\chi_k - 1)} & 0 \\ 0 & I_{m - \chi_k - 1} \end{bmatrix} \otimes I_p, \tag{9.22}$$

where $0_{p(\chi_k - 1)}$ is a matrix of zeros of dimension $p(\chi_k - 1) \times p(\chi_k - 1)$, and $I_{m - \chi_k - 1}$ is an identity matrix of dimension $(m - \chi_k - 1) \times (m - \chi_k - 1)$. Inserting (9.22) in (9.19) and using Lemma 9.7 gives

$$L^\top Q_k L = \begin{bmatrix} 0_{p(\chi_k - 1)} & 0 \\ 0 & \Sigma^{-1}_{\chi_k : m} \end{bmatrix} \otimes \Lambda, \tag{9.23}$$

where $\Sigma^{-1}_{\chi_k : m}$ is the inverse of the covariance matrix for the inputs $[\, u_\chi(t) \ \cdots \ u_m(t) \,]^\top$. Inserting (9.23) in Theorem 9.2 leads to the following corollary:

Corollary 9.4. *Let Assumption 9.1 hold. Assume that for each basis function $\mathcal{B}_k$, there is a χ_k such that no module with input $\{u_k\}_{k=1}^{\chi_k-1}$ contains the basis function $\mathcal{B}_k$. Then*

$$\boldsymbol{AsCov}\left\{\operatorname{vec}\left\{\hat{G}\right\}\right\} = \sum_{k=1}^{n_B} |\mathcal{B}_k|^2 \begin{bmatrix} 0_{p(\chi_k-1)} & 0 \\ 0 & \Sigma^{-1}_{\chi_k:m} \end{bmatrix} \otimes \Lambda. \tag{9.24}$$

Remark 9.4. If there is only one output, $p = 1$, we recover the MISO case of Theorem 4 of Ramazi et al. (2014), *i.e.*, the main diagonal of (9.24) corresponds to the module variance results of Theorem 4 of Ramazi et al. (2014).

Depending on the input correlation structure, the contribution from a basis function to the variance of a parameter may be greatly reduced, given that the basis function is not present in modules with inputs strongly correlated to the input related to that particular parameter. Define $\sigma^2_{i|l:o}$ as the variance of $u_i(t)$ conditioned on $[\, u_l(t) \;\cdots\; u_o(t) \,]^\top$ (see Ramazi et al. (2014)). From (9.24), Lemma 9.6 in the Appendix and Lemma 9.7, it can be seen that the variance of a module depends on the inverse of the variance of the input to that module, conditioned on the inputs of modules that contain the basis function. To give an example, consider the lower right element of $\Sigma^{-1}_{\chi_k:m}$, which is given by $1/\sigma^2_{m|\chi_k:m-1}$. If there is information about $u_m(t)$ in $\{u_1, \ldots, u_{\chi_{k-1}}\}$ (not found in $\{u_{\chi_k}, \ldots, u_{m-1}\}$), then $\sigma^2_{m|\chi_k:m-1} > \sigma^2_{m|1:m-1}$ and the variance of $\hat{G}_{mp}$ will be lower.

9.3.3 Unused output

We now consider the case when we do not estimate a parameter for basis function $\mathcal{B}_k$ for all modules that affect output $\{y_i(t)\}_{i=1}^{\chi_k-1}$, *i.e.*, modules $G_{11}, G_{12}, \ldots, G_{(\chi_k-1)m}$ do not contain basis function $\mathcal{B}_k$. Also in this case Assumption 9.2 holds and Theorem 9.2 gives that (9.18) holds with

$$Q_k = I_m \otimes \begin{bmatrix} 0_{p(\chi_k-1)} & 0 \\ 0 & I_{p-\chi_k-1} \end{bmatrix}, \tag{9.25}$$

where $0_{p(\chi_k-1)}$ is a matrix of zeros of dimension $p(\chi_k-1) \times p(\chi_k-1)$, and $I_{p-\chi_k-1}$ is an identity matrix of dimension $(p-\chi_k-1)\times(p-\chi_k-1)$. Inserting (9.25) in (9.19) and using Lemma 8.1 we obtain

$$L^\top Q_k L = \Sigma^{-1} \otimes \begin{bmatrix} 0_{p(\chi_k-1)} & 0 \\ 0 & \Lambda_{\chi_k:m|\chi_k-1} \end{bmatrix}, \tag{9.26}$$

where $\Lambda_{\chi_k:m|\chi_k-1}$ is the covariance of $[\, e_\chi(t) \;\cdots\; e_m(t) \,]^\top$ given the other noise sources $[\, e_1(t) \;\cdots\; e_{\chi-1}(t) \,]^\top$. In this case, the following corollary follows from Theorem 9.2:

Corollary 9.5. *Let Assumption 9.1 hold. Assume that for each basis function $\mathcal{B}_k$, there is a χ_k such that no module that affect output $\{y_k(t)\}_{k=1}^{\chi_k-1}$ contains $\mathcal{B}_k$. Then*

$$\boldsymbol{AsCov}\left\{\operatorname{vec}\left\{\hat{G}\right\}\right\} = \sum_{k=1}^{n_{\mathcal{B}}} \left|\mathcal{B}_k\right|^2 \Sigma^{-1} \otimes \begin{bmatrix} 0_{p(\chi_k-1)} & 0 \\ 0 & \Lambda_{\chi_k:m|\chi_k-1} \end{bmatrix}. \tag{9.27}$$

(9.28)

Remark 9.5. Result (9.27) is a generalization of the SIMO result of Corollary 8.3 in the sense that if there is only one input, $m = 1$, we recover Corollary 8.3.

Depending on the noise correlation structure, the parameter variance contribution from a basis function may be greatly reduced, given that the basis function is not present in modules with outputs affected by noise strongly correlated to the noise affecting the output related to the parameter. Define λ_i as the covariance of $e_i(t)$ and $\lambda_{i|\chi_k-1}$ as the covariance of $e_i(t)$ conditioned on the noise sources $[\, e_1(t) \ \cdots \ e_{\chi_k-1}(t) \,]^\top$. Consider the lower right element of $\Lambda_{\chi_k:m|\chi_k-1}$, which is given by $\lambda_{m|\chi_k-1}$. If there is information about $e_m(t)$ in $\{e_1, \ldots, e_{\chi_{k-1}}\}$, then $\lambda_{m|\chi_k-1} < \lambda_m$ and the variance of $\hat{G}_{mp}$ will be lower.

9.4 Numerical simulations

9.4.1 First experiment

In this section we illustrate the developed results on a system with 2 inputs and 2 outputs. To better illustrate the results, the parameter variances will be studied instead of $\mathbf{AsCov}\left\{\operatorname{vec}\left\{\hat{G}\right\}\right\}$. However, the results have a direct link to the parameter variance, *cf.* Remark 9.1. The system is given by

$$G(q) = \begin{bmatrix} q^{-1} & 2q^{-1} + q^{-2} \\ q^{-1} + 4q^{-2} & q^{-1} + 2q^{-2} \end{bmatrix}. \tag{9.29}$$

The model is

$$G(q,\theta) = \begin{bmatrix} \theta_{11}^1 q^{-1} & \theta_{12}^1 q^{-1} + \theta_{12}^2 q^{-2} \\ \theta_{21}^1 q^{-1} + \theta_{21}^2 q^{-2} & \theta_{22}^1 q^{-1} + \theta_{22}^2 q^{-2} \end{bmatrix}, \tag{9.30}$$

where all parameters have been given a superscript that denotes which basis function they correspond to. One parameter, related to the basis function q^{-2}, is not estimated for G_{11}, and this will lead to a decrease in variance for the other parameters related to the basis function q^{-2} when compared to those related to the basis function q^{-1}. We will investigate how the amount of correlation in the input determines the variance reduction. The Cholesky factors

of the noise and input are given by

$$\Lambda_{CH} = \begin{bmatrix} 1 & 0 \\ 0.8 & (1-0.8^2)^{1/2} \end{bmatrix}, \qquad \Sigma_{CH} = \begin{bmatrix} (1-\beta^2)^{1/2} & \beta \\ 0 & 1 \end{bmatrix},$$

respectively. Thus $\sigma_1^2 = \sigma_2^2 = 1$, while the parameter β determines the amount of correlation between the inputs, *i.e.*, $\mathbf{E}\{u_1(t)u_2(t)\} = \beta$. For each β, we generate $MC = 2000$ Monte Carlo experiments, where in each of them we collect $N = 2000$ input-output samples. At the i-th Monte Carlo run, we generate new trajectories for the input and the noise and we estimate $\hat{\theta}^i$ as in (8.8). We will study the sample covariance matrix scaled by the number of samples N for each β

$$\mathbf{AsCov}\{\hat{\theta}\} = \frac{N}{MC}\sum_{i=1}^{MC}\left(\hat{\theta}^i - \theta^o\right)\left(\hat{\theta}^i - \theta^o\right)^\top,$$

It is seen in Figure 9.2 that the variance is reduced for all parameters related to the basis function q^{-2} compared to those related to q^{-1}, as long as there is correlation between the inputs (the variance would have been the same if also G_{11} had a parameter related to q^{-2}). The variance of $\hat{\theta}_{12}^2$ is independent of the input correlation and behaves exactly as the parameters of Corollary 9.4, even though the Corollary is not applicable since θ_{21}^2 is still estimated. This indicates that it should be possible to strengthen Corollary 9.4. The whole input excitation of $q^{-2}u_2(t)$ is used for this estimate, *i.e.*, $\mathbf{AsVar}\{\hat{\theta}_{12}^2\} = \lambda_1/\sigma_2^2 = 1$, since $y_1(t)$ does not depend on $q^{-2}u_1(t)$. The variance of $\hat{\theta}_{21}^2$ is strictly smaller than $\hat{\theta}_{21}^1$, regardless of the input correlation. The variance of this parameter behaves exactly as in Corollary 9.5, even though the assumptions of Corollary 9.5 are not met (θ_{12}^2 is still estimated). This indicates that it should be possible to strengthen Corollary 9.5. The measurement $y_1(t)$ can be used to estimate the noise affecting $y_2(t)$ without corrupting the estimate $\hat{\theta}_{21}^2$, *i.e.*, $\mathbf{AsVar}\{\hat{\theta}_{21}^2\} = \lambda_{2|1}/\sigma_{1|2}^2$, since $y_1(t)$ does not depend on $q^{-2}u_1(t)$. The estimate $\hat{\theta}_{22}^2$ also benefits, from not having to estimate a parameter related to q^{-2} in G_{11}, as long as there is correlation between the inputs.

9.4.2 Second Experiment

Let again the system be given by (9.29) and the model by (9.30). In this experiment we vary the noise correlation instead of the input correlation. Let the Cholesky factors of the noise and input be given by

$$\Lambda_{CH} = \begin{bmatrix} 1 & 0 \\ \beta & (1-\beta^2)^{1/2} \end{bmatrix}, \qquad \Sigma_{CH} = \begin{bmatrix} 0.8 & (1-0.8^2)^{1/2} \\ 0 & 1 \end{bmatrix},$$

respectively. It is seen in Figure 9.3 that the variance is reduced in all parameters related to the basis function q^{-2} compared to those related to q^{-1} as long as there is correlation between the

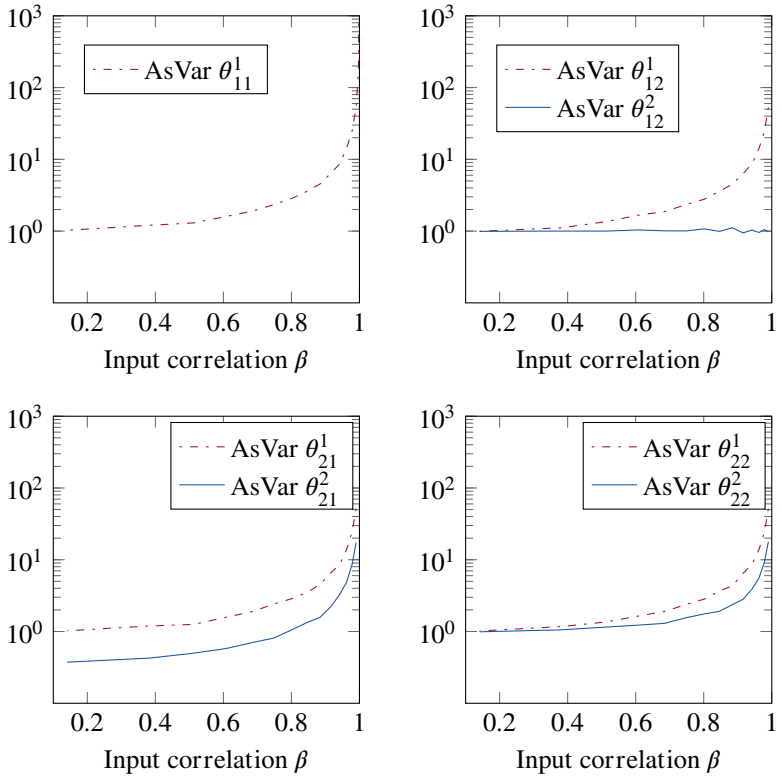

Figure 9.2: Variance of the parameters of G_{11}, G_{12}, G_{21} and G_{22} respectively. The parameters related to the basis function q^{-2}, θ^2_{12}, θ^2_{21} and θ^2_{22}, are estimated with reduced variance compared to those related to the q^{-1}. The variance of θ^2_{12} does not depend on the input correlation.

outputs. The variance of $\hat{\theta}^2_{12}$ behaves as the MISO case, *i.e.*, $\mathbf{AsVar}\{\hat{\theta}^2_{12}\} = \lambda_1/\sigma_2^2 = 1$ and $\mathbf{AsVar}\{\hat{\theta}^2_{12}\}$ does not dependend on the correlation between the outputs. The variance of $\hat{\theta}^2_{21}$ and $\hat{\theta}^2_{22}$ are lower than $\hat{\theta}^1_{21}$ and $\hat{\theta}^1_{22}$ respectively when there is correlation. Furthermore, the variances are the same when there is no correlation. When β goes to one, the non-estimable part of $e_2(t)$ conditioned on $e_1(t)$ goes to zero and we achieve perfect estimation of $\hat{\theta}^2_{21}$.

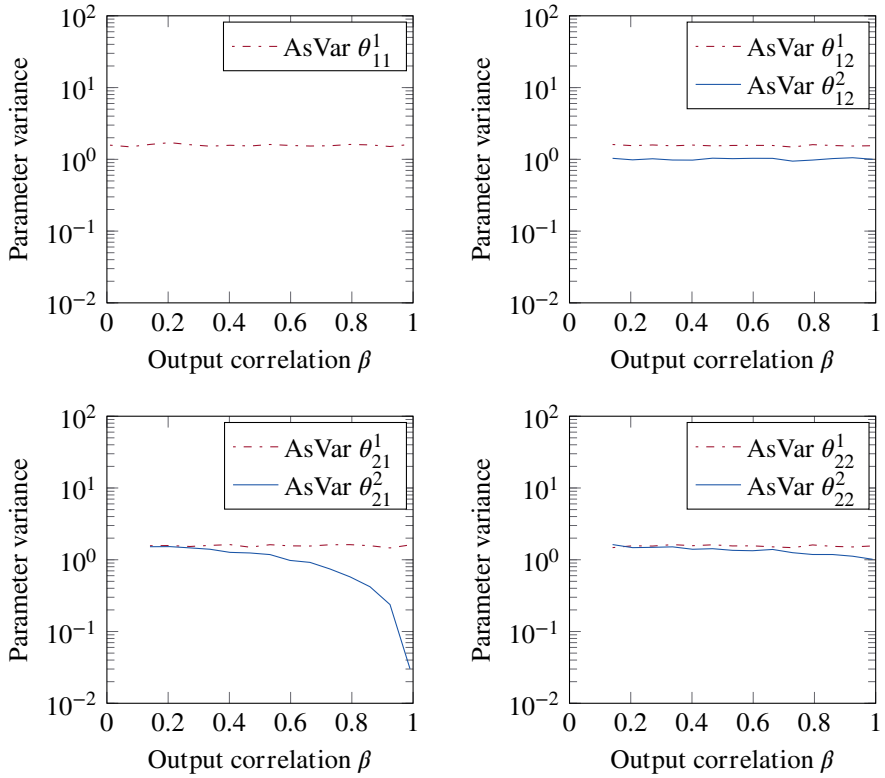

Figure 9.3: Variance of the parameters of G_{11}, G_{12}, G_{21} and G_{22}. The parameters related to the basis function q^{-2}, θ^2_{12}, θ^2_{21} and θ^2_{22}, are estimated with reduced variance compared to those related to the q^{-1}. The variance of θ^2_{12} does not depend on the noise correlation.

9.5 Summary

In this chapter, we have extended existing variance formulas for MIMO systems to finite model orders, assuming temporally uncorrelated input and noise. We have shown that model structure strongly influences the effect spatial correlation in inputs and noise have on the variance of module transfer function estimates. We have highlighted connections with recently developed results for SIMO and MISO models. The interplay of model structure, input correlation and noise correlation has been exemplified by numerical simulations.

9.A Proofs and auxiliary lemmas

9.A.1 Useful lemmas

Lemma 9.6. *Let $u(t) \in \mathbb{R}^m$ have zero mean and covariance matrix $\Sigma > 0$. Let Σ_{CH} be the upper triangular Cholesky factor of Σ so that* (9.8) *holds, and let the elements of its inverse be denoted as in* (9.9)*. Then, for $k \leq i-1$*

$$\sigma^2_{i|k:i-1} = \frac{1}{\sum_{j=k}^{i} \gamma_{ji}^2}.$$

Proof. This Lemma is just the parallel formulation of Lemma 3.1 in Ramazi et al. (2014) for an upper triangular Cholesky decomposition and the proof follows along the same lines. ■

Lemma 9.7. *Let $u(t) \in \mathbb{R}^m$ have zero mean and covariance matrix $\Sigma > 0$. Let Σ_{CH} be the upper triangular Cholesky factor of Σ so that* (9.8) *holds. Let Σ_{CH}^{-1} be partitioned according $[\,[u_1(t) \;\ldots\; u_{i-1}(t)]\,]^\top$ and $[\,u_i(t) \;\ldots\; u_m(t)\,]^\top$ as:*

$$\Sigma_{CH}^{-1} = \begin{bmatrix} \left[\Sigma_{CH}^{-1}\right]_{11} & \left[\Sigma_{CH}^{-1}\right]_{12} \\ 0 & \left[\Sigma_{CH}^{-1}\right]_{22} \end{bmatrix}.$$

Then

$$\Sigma_{i:m}^{-1} = \left(\left[\Sigma_{CH}^{-1}\right]_{22}\right)^\top \left[\Sigma_{CH}^{-1}\right]_{22}$$

Proof. Express

$$\begin{bmatrix} u_i(t) \\ \vdots \\ u_m(t) \end{bmatrix} = \left[\Sigma_{CH}\right]_{22} \begin{bmatrix} r_i(t) \\ \vdots \\ r_m(t) \end{bmatrix},$$

where $\left[\Sigma_{CH}\right]_{22}$ is given by the corresponding partitioning of Σ_{CH} and $r(t)$ is white noise with $\mathbf{E}\left\{r(t)r^\top(s)\right\} = \delta_{t-s} I$.

$$\Sigma_{i:m} = [\Sigma_{CH}]_{22}\left([\Sigma_{CH}]_{22}\right)^\top.$$

The lemma follows by taking the inverse and realizing that $([\Sigma_{CH}]_{22})^{-1} = [\Sigma_{CH}^{-1}]_{22}$. ■

9.A.2 proof of Lemma 9.1

Since Ψ is given by (9.14), each row of Ψ only contains one of the basis functions $\{\mathcal{B}_k\}_{k=1}^n$. This, together with the fact that the basis functions $\{\mathcal{B}_k(q)\}_{k=1}^n$ are orthogonal gives that

the rowspace of Ψ is the direct sum of the rowspaces of the rows of Ψ that contain $\mathcal{B}_k$. In other words, we can look at the rows containing a specific basis function $\mathcal{B}_k$ separately from the rows containing other basis functions, and in the end, join the sets of basis functions together. We can sort the rows of Ψ in (9.14) according to $\{\mathcal{B}_k\}_{k=1}^n$ by sorting the rows of $\tilde{\Psi}$ first:

$$\begin{bmatrix} \mathcal{B}_1 Q_1 \\ \mathcal{B}_2 Q_2 \\ \vdots \\ \mathcal{B}_n Q_n \end{bmatrix},$$

where Q_k is given by Definition 5, and where some rows potentially containing all zeros were added. The rows of Ψ that contain $\mathcal{B}_k$ (potentially with some rows added containing all zeros) are given by

$$\mathcal{B}_k Q_k (\Sigma_{CH} \otimes \Lambda_{CH}^{-\top}). \tag{9.31}$$

Applying the Gram-Smith (orthonormalization) process (Horn and Johnson, 1990), starting from the last rows, it can be shown that the set of basis functions can be chosen according to the lemma, since (9.31) is the Kronecker product of two upper triangular matrices. We will give an inductive proof in the following. Each of the columns of Ψ corresponds to one module G_{ij}. The columns of Ψ are ordered with respect to the inputs, so that for example the last p columns of Ψ correspond to the modules related to the last input u_m, and within each input, the columns are ordered in increasing order of output, *i.e.*, the last column corresponds to output y_p. This ordering will be important in the following. If we start out with zero modules containing the basis function $\mathcal{B}_k$ and consecutively add this basis function to modules, Assumption 9.2 gives a condition on which modules we are allowed to add the basis function to. We are only allowed to add a basis function to a module G_{ij} if module $G_{i(j+1)}$ contains the basis function and if $G_{(i+1)j}$ contains the basis function (for an index outside G, $j \geq p$, $i \geq m$ we are allowed to add the basis function, which is the case for the first module of each input, given that the second condition holds). The basis for the induction is the case when only G_{mp} contains $\mathcal{B}_k$ and in this case the lemma trivially holds. If we now wish to add the basis function $\mathcal{B}_k$ to G_{ij}, looking at the structure of the corresponding row of Ψ, we see that this row has nonzero entries for columns corresponding to inputs $l \geq i$ and outputs $s \geq j$. However, to be allowed to add the basis function to G_{ij} we are required by Assumption 9.2 to already have added the basis functions to those modules corresponding to inputs $l > i$ and outputs $s \geq j$ and the only part not in the span of the previous set of basis functions is the column corresponding to G_{ij}.

CHAPTER 10

CONCLUSIONS AND FUTURE WORK

The first contribution in this thesis is model order reduction Steiglitz-McBride (MORSM), which provides asymptotically efficient estimates for open loop data in a SISO setting. Motivated by maximum likelihood arguments, it is shown to be asymptotically efficient in one least-squares iteration. From simulations, MORSM seems to be a competitive approach to find the global minimum of the PEM cost function. In a dynamic network setting, MORSM resembles standard two-stage methods, but the simulated signals used in MORSM are motivated by asymptotic maximum likelihood (ML) arguments. This should decrease the estimation error compared with two-stage and instrumental variable (IV) methods, which simulations seem to support. In simulation, MORSM proved competitive in terms of performance with the frequency-domain sample maximum likelihood method (SML) method. Although, these methods are different in several aspects, they are both motivated by a ML criterion. Also, from a user perspective, they are attractive because the noise model is of high order.

The second proposed method of this thesis, network empirical Bayes (NEB), was introduced following a Bayesian kernel-based approach, which enables the identification of the target module using empirical Bayes arguments. This method estimates the target module using a ML criterion, whose solution is obtained by a novel iterative scheme designed through the ECM algorithm. The method was also extended to incorporate measurements downstream of the target module, which numerical experiments suggest increases performance. In contrast to the network version of MORSM, NEB in its present form does not handle process noise or non-white measurement noise.

Both MORSM and NEB share the attractive feature that additional reference signals may be added without much trouble. In the case of MORSM, an additional reference signal only increases the complexity of the initial high order ARX, given that the same set of inputs can be used in the second stage. This, of course, requires that the method is generalized to handle more than one input in the second stage. However, the dimension of the initial high order least squares problem will increase. In the case of NEB the additional burden is minor; while an additional reference signal increases the dimensionality of the updates of the sensitivities, it only adds a few extra hyperparameters to estimate.

The second part of the thesis provided some insights into how the interplay between model structure (model order and parametrization) and signal properties (signal spectrums and signal correlations) determines the covariance of the module estimates. Each chapter illustrates some aspect of covariance analysis in dynamic networks and together they provide a starting point for a deeper understanding of the factors that determine the achievable accuracy of module estimates.

In Chapter 7, we noticed that including additional reference signals may have the dual effect of reducing the effective noise affecting the module estimate and providing additional excitation. This lesson carries over directly to the methods presented in this thesis and might be applicable to other prediction error methods as well. Also from Chapter 7, when using additional sensors downstream of the module of interest, the take home message was that the gain of including these sensors diminish, if there was additional dynamics to estimate. The upper bound on the gain in accuracy, which from simulations seemed rather tight, indeed diminished to zero.

In contrast, for finite number of data samples, NEB benefited from including additional sensors downstream of the module of interest. There are two main reasons how this can be explained. First, we expect that as the model order of the additional dynamics grow, the gain diminishes. However, NEB uses regularization to control the growth in parameters or in some sense the effective model order. Therefore, the analysis based on high order models is not valid. Second, the additional measurement provides an additional output that the predictor needs to comply with, which could make it more likely that the optimization finds the global minima and do not end up in a local one.

On the other hand, for cascaded systems in Chapter 6, unit-circle zeros still benefited from additional sensors downstream even though the model orders were allowed to grow. These results are inline with the results found in Mårtensson (2007), where, for example, non-minimum phase zeros of SISO systems are estimated with finite variance even though the model order tends to infinity.

In Chapter 8, correlated noise in SIMO models leads to variance reductions. In a dynamic network, this leads to the possibility to include additional measurements in the predictor when it can be assumed that the noise is correlated. An interesting closely related idea has been pursued in Van den Hof et al. (2017) and Weerts et al. (2017). In these contributions the noise is assumed perfectly correlated, *i.e.*, the noise is of low rank. This is exploited by including this knowledge as a constraint in the estimation, leading to essentially variance free results.

10.1 Future work

The major limitation with the current version of MORSM is that it only works for SISO systems. At first glance, there seem to be major difficulties to generalize the method, since

the implied prefiltering does not work in a MIMO setting. In fact, it may not even be allowed due to inconsistent dimensions. This is because in the SISO case the high order estimate of A has been moved from the left to the right of G in (3.19), which is not possible for MIMO systems, in general. A promising way forward is to keep the estimated A as a weighting factor. The iterations in the second stage would then be weighted least squares instead of least squares iterations. If this is the correct approach, then, MORSM would even more resemble weighted null-space fitting (WNSF), where weighted least squares is used. However, this development is left for future work. In the network setting, the current version is limited to simple networks that only has one external reference and the internal variable at the output of the module of interested is generated only by the module of interest (*i.e.*, the row of the transfer matrix in (5.40) containing the module of interest has no other non-zero entries than the module of interest). If this is not the case, (4.27) will be multivariate. Because multivariate asymptotic ML is covered by (Zhu, 2001), we can use the results therein to generalize the proposed method to cover such cases.

The main limitation with NEB is the noise assumptions and the lack of noise modelling. Without one, NEB may not be applied to the more challenging case when there is process noise in the network leading to noise correlation. One option would be to estimate a noise model of high order in the initialization stage of the method. This noise model would then be kept fixed throughout the iterations of the method.

The noise assumptions in the second part of the thesis also lack both noise modelling and process noise. As seen in the simulation study for network MORSM in Chapter 4, noise correlation affects the performance of all compared methods negatively. Including more realistic assumptions on the noise would improve the applicability of the covariance analysis of the structures examined. This would allow for comparison of direct approaches, such as the direct prediction error method, and indirect approaches such as the ones considered in this thesis. Perhaps, this can change the calculus of how beneficial sensors are to include in the identification procedure. For example in cascade models, downstream sensors would not only carry secondary information about the module of interest, but also information about the process noise affecting the other measurements, which could prove beneficial.

BIBLIOGRAPHY

J. Adebayo, T. Southwick, V. Chetty, E. Yeung, Y. Yuan, J. Goncalves, J. Grose, J. Prince, G. Stan, and S. Warnick (2012). "Dynamical structure function identifiability conditions enabling signal structure reconstruction". In: *Proceedings of the 51st IEEE Conference on Decision and Control*. DOI: 10.1109/cdc.2012.6426183.

J. C. Agüero and G. C. Goodwin (2006). "On the Optimality of Open and Closed Loop Experiments in System Identification". In: *Proceedings of the 45th IEEE Conference on Decision and Control*, 163–168. DOI: 10.1109/cdc.2006.377402.

J. C. Agüero and G. C. Goodwin (2007). "Choosing Between Open- and Closed-Loop Experiments in Linear System Identification". *IEEE Transactions on Automatic Control*. 52 (8): 1475–1480. DOI: 10.1109/tac.2007.902756.

J. C. Agüero, C. R. Rojas, H. Hjalmarsson, and G. C. Goodwin (2012). "Accuracy of linear multiple-input multiple-output (MIMO) models obtained by maximum likelihood estimation". *Automatica*. 48 (4): 632–637. DOI: 10.1016/j.automatica.2012.01.015.

M. Ali, S. S. Chughtai, and H. Werner (2009). "Identification of spatially interconnected systems". In: *Proceedings of the 48th IEEE Conference on Decision and Control, held jointly with the 28th Chinese Control Conference*, 7163–7168. DOI: 10.1109/CDC.2009.5399748.

M. Ali, A. Ali, H. Abbas, and H. Werner (2011). "Identification of Box-Jenkins models for Parameter-Varying Spatially Interconnected systems". In: *Proceedings of the 2011 American Control Conference*. DOI: 10.1109/acc.2011.5991133.

M. Ali, A. Ali, S. S. Chughtai, and H. Werner (2011). "Consistent identification of spatially interconnected systems". In: *Proceedings of the 2011 American Control Conference*. DOI: 10.1109/acc.2011.5991360.

M. Ali, A. P. Popov, H. Werner, and H. S. Abbas (2011). "Identification of Distributed Systems with Identical Subsystems". In: *Proceedings of the 18th IFAC World Congress*, 5633–5638. DOI: 10.3182/20110828-6-it-1002.02543.

P.-O. Amblard and O. J. J. Michel (2010). "On directed information theory and Granger causality graphs". *Journal of Computational Neuroscience*. 30 (1): 7–16. DOI: 10.1007/s10827-010-0231-x.

B. D. O. Anderson and J. B. Moore (1979). *Optimal filtering*. Prentice-Hall. ISBN: 0136381227.

A. Aravkin, J. Burke, A. Chiuso, and G. Pillonetto (2012). "On the estimation of hyperparameters for Empirical Bayes estimators: Maximum Marginal Likelihood vs Minimum MSE". In: *Proceedings of the 16th IFAC Symposium on System Identification*, 125–130. DOI: 10.3182/20120711-3-be-2027.00353.

A. Aravkin, J. V. Burke, A. Chiuso, and G. Pillonetto (2011). "Convex vs nonconvex approaches for sparse estimation: Lasso, Multiple Kernel Learning and Hyperparameter Lasso". In: *Proceedings of the 50th IEEE Conference on Decision and Control and European Control Conference*, 156–161. DOI: 10.1109/cdc.2011.6160997.

N. Aronszajn (1950). "Theory of reproducing kernels". *Transactions of the American Mathematical Society*. 68 (3): 337–337. DOI: 10.1090/s0002-9947-1950-0051437-7.

K. J. Åström and R. M. Murray (2008). *Feedback systems: an introduction for scientists and engineers*. Princeton university press.

J.-S. Bailly, P. Monestiez, and P. Lagacherie (2006). "Modelling Spatial Variability Along Drainage Networks with Geostatistics". *Mathematical Geology*. 38 (5): 515–539. DOI: 10.1007/s11004-006-9033-0.

L. Bakule (2008). "Decentralized control: An overview". *Annual Reviews in Control*. 32 (1): 87–98. DOI: 10.1016/j.arcontrol.2008.03.004.

M. Barenthin and H. Hjalmarsson (2008). "Identification and control: Joint input design and state feedback with ellipsoidal parametric uncertainty via LMIs". *Automatica*. 44 (2): 543–551. DOI: 10.1016/j.automatica.2007.06.025.

M. S. Bartlett (1951). "An Inverse Matrix Adjustment Arising in Discriminant Analysis". *The Annals of Mathematical Statistics*. 22 (1): 107–111.

A. S. Bazanella, M. Gevers, and L. Mišković (2010). "Closed-Loop Identification of MIMO Systems: A New Look at Identifiability and Experiment Design". *European Journal of Control*. 16 (3): 228–239. DOI: https://doi.org/10.3166/ejc.16.228-239.

J. Benesty, S. Makino, and J. Chen (2005). *Speech enhancement*. Springer.

J. O. Berger (1993). *Statistical Decision Theory and Bayesian Analysis*. Springer. ISBN: 0387960988.

N. Bertaux, P. Larzabal, C. Adnet, and E. Chaumette (1999). "A parameterized maximum likelihood method for multipaths channels estimation". In: *Proceedings of the 2nd IEEE Workshop on Signal Processing Advances in Wireless Communications*, 391–394. DOI: 10.1109/SPAWC.1999.783100.

J. Bezanson, A. Edelman, S. Karpinski, and V. B. Shah (2017). "Julia: A Fresh Approach to Numerical Computing". *SIAM Review*. 59 (1): 65–98. DOI: 10.1137/141000671.

C. M. Bishop (2006). *Pattern Recognition and Machine Learning*. Springer-Verlag New York Inc. ISBN: 0387310738.

X. Bombois, A. J. den Dekker, M. Barenthin, and P. M. J. Van den Hof (2009). "Effect of model structure and signal-to-noise ratio on finite-time uncertainty bounding in prediction error identification". In: *Proceedings of the 48th IEEE Conference on Decision and Control, held jointly with the 28th Chinese Control Conference*, 494–499. DOI: 10.1109/cdc.2009.5400852.

X. Bombois, M. Gevers, and G. Scorletti (2005). "Open-loop versus closed-loop identification of Box-Jenkins models: a new variance analysis". In: *Proceedings of the 44th IEEE Conference on Decision and Control*, 3117–3122. DOI: 10.1109/CDC.2005.1582640.

X. Bombois, A. Korniienko, H. Hjalmarsson, and G. Scorletti (2016). "Optimal identification experiment design for the interconnection of locally controlled systems". <hal-01492050>.

G. Bottegal and G. Picci (2014). "Analysis and identification of complex stochastic systems admitting a flocking structure". In: *Proceedings of the 19th IFAC World Congress*. DOI: 10.3182/20140824-6-za-1003.01615.

G. Bottegal, A. Y. Aravkin, H. Hjalmarsson, and G. Pillonetto (2016). "Robust EM kernel-based methods for linear system identification". *Automatica*. 67: 114–126. DOI: 10.1016/j.automatica.2016.01.036.

G. Bottegal and G. Picci (2015). "Modeling Complex Systems by Generalized Factor Analysis". *IEEE Transactions on Automatic Control*. 60 (3): 759–774. DOI: 10.1109/tac.2014.2357913.

G. Bottegal and G. Pillonetto (2013). "Regularized spectrum estimation using stable spline kernels". *Automatica*. 49 (11): 3199–3209. DOI: 10.1016/j.automatica.2013.08.010.

G. Box and G. M. Jenkins (1976). *Time series analysis: forecasting and control*. Holden-Day.

J. Brewer (1978). "Kronecker products and matrix calculus in system theory". *IEEE Transactions on Circuits and Systems*. 25 (9): 772–781. DOI: 10.1109/TCS.1978.1084534.

M. Campi and E. Weyer (2005). "Guaranteed non-asymptotic confidence regions in system identification". *Automatica*. 41 (10): 1751–1764. DOI: 10.1016/j.automatica.2005.05.005.

M. Campi and E. Weyer (2010). "Non-asymptotic confidence sets for the parameters of linear transfer functions". *IEEE Transactions on Automatic Control*. 55 (12): 2708–2720. DOI: 10.1109/TAC.2010.2049416.

G. Casella and R. Berger (2002). *Statistical Inference*. Thomson Learning.

G. Casella (2001). “Empirical bayes gibbs sampling”. *Biostatistics*. 2 (4): 485–500. DOI: 10.1093/biostatistics/2.4.485.

G. Casella and E. L. Lehmann (2003). *Theory of Point Estimation*. Springer. ISBN: 0387985026.

T. Chen, M. S. Andersen, L. Ljung, A. Chiuso, and G. Pillonetto (2014). “System Identification Via Sparse Multiple Kernel-Based Regularization Using Sequential Convex Optimization Techniques”. *IEEE Transactions on Automatic Control*. 59 (11): 2933–2945. DOI: 10.1109/tac.2014.2351851.

T. Chen and L. Ljung (2014). “Constructive state space model induced kernels for regularized system identification”. In: *Proceedings of the 19th IFAC World Congress*, 1047–1052. DOI: 10.3182/20140824-6-za-1003.01254.

T. Chen, H. Ohlsson, and L. Ljung (2012). “On the estimation of transfer functions, regularizations and Gaussian processes—Revisited”. *Automatica*. 48 (8): 1525–1535. DOI: 10.1016/j.automatica.2012.05.026.

A. Chiuso and G. Pillonetto (2010). “Learning sparse dynamic linear systems using stable spline kernels and exponential hyperpriors”. In: *Advances in Neural Information Processing Systems*, 397–405.

A. Chiuso and G. Pillonetto (2012). “A Bayesian approach to sparse dynamic network identification”. *Automatica*. 48 (8): 1553–1565. DOI: 10.1016/j.automatica.2012.05.054.

A. Chiuso, G. Pillonetto, and G. D. Nicolao (2008). “Subspace identification using predictor estimation via Gaussian regression”. In: *Proceedings of the 47th IEEE Conference on Decision and Control*. DOI: 10.1109/cdc.2008.4739144.

J. Chow and P. Kokotovic (1985). “Time scale modeling of sparse dynamic networks”. *IEEE Transactions on Automatic Control*. 30 (8): 714–722. DOI: 10.1109/tac.1985.1104055.

D. R. Cox and N. Reid (1987). “Parameter Orthogonality and Approximate Conditional Inference”. *Journal of the Royal Statistical Society. Series B (Statistical Methodology)*. 49 (1): 1–39.

B. C. Csaji, M. C. Campi, and E. Weyer (2012). “Sign-perturbed sums (SPS): A method for constructing exact finite-sample confidence regions for general linear systems”. In: *Proceedings of the 51st IEEE Conference on Decision and Control*, 7321–7326. DOI: 10.1109/cdc.2012.6425882.

B. C. Csáji, M. C. Campi, and E. Weyer (2012). “Non-Asymptotic Confidence Regions for the Least-Squares Estimate”. In: *Proceedings of the 16th IFAC Symposium on System Identification*, 227–232. DOI: 10.3182/20120711-3-be-2027.00417.

A. G. Dankers (2014). “System identification in dynamic networks”. PhD thesis. Delft University of Technology.

A. G. Dankers and P. M. J. Van den Hof (2015). "Non-parametric identification in dynamic networks". In: *Proceedings of the 54th IEEE Conference on Decision and Control*. DOI: 10.1109/cdc.2015.7402759.

A. G. Dankers, P. M. J. Van den Hof, and X. Bombois (2014). "An Instrumental Variable Method for Continuous-Time Identification in Dynamic Networks". In: *Proceedings of the 53rd IEEE Conference on Decision and Control*.

A. G. Dankers, P. M. J. Van den Hof, X. Bombois, and P. S. C. Heuberger (2014). "Errors-in-Variables Identification in Dynamic Networks by an Instrumental Variable Approach". In: *Proceedings of the 19th IFAC World Congress*. DOI: 10.3182/20140824-6-za-1003.02069.

A. G. Dankers, P. M. J. Van den Hof, X. Bombois, and P. S. C. Heuberger (2015). "Errors-in-variables identification in dynamic networks — Consistency results for an instrumental variable approach". *Automatica*. 62: 39–50. DOI: 10.1016/j.automatica.2015.09.021.

A. G. Dankers, P. M. J. Van den Hof, X. Bombois, and P. S. C. Heuberger (2016). "Identification of Dynamic Models in Complex Networks With Prediction Error Methods: Predictor Input Selection". *IEEE Transactions on Automatic Control*. 61 (4): 937–952. DOI: 10.1109/tac.2015.2450895.

A. G. Dankers, P. M. J. Van den Hof, X. Bombois, and P. S. Heuberger (2013). "Predictor input selection for two stage identification in dynamic networks". In: *Proceedings of the 2013 European Control Conference*, 1422–1427.

A. G. Dankers, P. M. J. Van den Hof, and P. S. C. Heuberger (2013). "Predictor input selection for direct identification in dynamic networks". In: *Proceedings of the 52nd IEEE Conference on Decision and Control*, 4541–4546. DOI: 10.1109/cdc.2013.6760589.

D. del Vecchio, A. J. Ninfa, and E. D. Sontag (2008). "Modular cell biology: retroactivity and insulation". *Molecular Systems Biology*. 4. DOI: 10.1038/msb4100204.

A. P. Dempster, N. M. Laird, and D. B. Rubin (1977). "Maximum Likelihood from Incomplete Data via the EM Algorithm". *Journal of the Royal Statistical Society, Series B (Methodological)*. 39 (1): 1–38.

D. V. Dimarogonas, E. Frazzoli, and K. H. Johansson (2012). "Distributed Event-Triggered Control for Multi-Agent Systems". *IEEE Transactions on Automatic Control*. 57 (5): 1291–1297. DOI: 10.1109/tac.2011.2174666.

F. Dinuzzo (2015). "Kernels for Linear Time Invariant System Identification". *SIAM Journal on Control and Optimization*. 53 (5): 3299–3317. DOI: 10.1137/130920319.

S. Doclo and M. Moonen (2002). "GSVD-based optimal filtering for single and multi-microphone speech enhancement". *IEEE Transactions on Signal Processing*. 50 (9): 2230–2244. DOI: 10.1109/TSP.2002.801937.

S. G. Douma (2006). "Probabilistic Uncertainty Bounding in Output Error Models with Unmodelled Dynamics". In: *Proceedings of the 2006 American Control Conference*, 1677–1682. DOI: 10.1109/ACC.2006.1656460.

J. Etesami and N. Kiyavash (2014). "Directed Information Graphs: A generalization of Linear Dynamical Graphs". In: *Proceedings of the 2014 American Control Conference*. DOI: 10.1109/acc.2014.6859362.

A. Evans and R. Fischl (1973). "Optimal least squares time-domain synthesis of recursive digital filters". *IEEE Transactions on Audio and Electroacoustics*. 21 (1): 61–65. DOI: 10.1109/tau.1973.1162433.

N. Everitt (2015). "Identification of Modules in Acyclic Dynamic Networks A Geometric Analysis of Stochastic Model Errors". Licentiate thesis. KTH Royal Institute of Technology.

N. Everitt, G. Bottegal, and H. Hjalmarsson (2017). "An empirical Bayes approach to identification of modules in dynamic networks". *submitted to Automatica*.

N. Everitt, G. Bottegal, C. R. Rojas, and H. Hjalmarsson (2015a). "On the variance analysis of identified linear MIMO models". In: *Proceedings of the 54th IEEE Conference on Decision and Control*. DOI: 10.1109/cdc.2015.7402414.

N. Everitt, G. Bottegal, C. R. Rojas, and H. Hjalmarsson (2015b). "On the Effect of Noise Correlation in Parameter Identification of SIMO Systems". In: *Proceedings of the 17th IFAC Symposium on System Identification*, 326–331. DOI: 10.1016/j.ifacol.2015.12.148.

N. Everitt, G. Bottegal, C. R. Rojas, and H. Hjalmarsson (2016). "Identification of modules in dynamic networks: An empirical Bayes approach". In: *Proceedings of the 55th IEEE Conference on Decision and Control*. DOI: 10.1109/cdc.2016.7798971.

N. Everitt, G. Bottegal, C. R. Rojas, and H. Hjalmarsson (2017). "Variance analysis of linear SIMO models with spatially correlated noise". *Automatica*. 77: 68–81. DOI: 10.1016/j.automatica.2016.11.017.

N. Everitt, M. Galrinho, and H. Hjalmarsson (2017a). "Incorporating noise modeling in dynamic networks using non-parametric models". In: *Proceedings of the 20th IFAC World Congress*.

N. Everitt, M. Galrinho, and H. Hjalmarsson (2017b). "Optimal model order reduction with the Steiglitz-McBride method for open-loop data". *submitted to Automatica*.

N. Everitt, C. R. Rojas, and H. Hjalmarsson (2013). "A geometric approach to variance analysis of cascaded systems". In: *Proceedings of the 52nd IEEE Conference on Decision and Control*. DOI: 10.1109/cdc.2013.6760917.

N. Everitt, C. R. Rojas, and H. Hjalmarsson (2014). "Variance Results for Parallel Cascade Serial Systems". In: *Proceedings of the 19th IFAC World Congress*, 2317–2322. DOI: 10.3182/20140824-6-za-1003.01262.

U. Forssell and L. Ljung (1999). "Closed-loop identification revisited". *Automatica*. 35 (7): 1215–1241. DOI: 10.1016/s0005-1098(99)00022-9.

A. Friedman (1970). *Foundations of Modern Analysis*. Dover.

M. Galrinho, N. Everitt, and H. Hjalmarsson (2017). "ARX modeling of unstable linear systems". *Automatica*. 75: 167–171. DOI: 10.1016/j.automatica.2016.09.041.

M. Galrinho, C. R. Rojas, and H. Hjalmarsson (2015a). "On estimating initial conditions in unstructured models". In: *Proceedings of the 54th IEEE Conference on Decision and Control*, 2725–2730. DOI: 10.1109/cdc.2015.7402628.

M. Galrinho, C. R. Rojas, and H. Hjalmarsson (2014). "A weighted least-squares method for parameter estimation in structured models". In: *Proceedings of the 53rd IEEE Conference on Decision and Control*. DOI: 10.1109/cdc.2014.7039903.

M. Galrinho, C. R. Rojas, and H. Hjalmarsson (2015b). "A Least Squares Method for Identification of Feedback Cascade Systems". In: *Proceedings of the 17th IFAC Symposium on System Identification*, 98–103. DOI: https://doi.org/10.1016/j.ifacol.2015.12.107.

S. Garatti, M. C. Campi, and S. Bittanti (2004). "Assessing the quality of identified models through the asymptotic theory - when is the result reliable?" *Automatica*. 40 (8): 1319–1332. DOI: https://doi.org/10.1016/j.automatica.2004.03.005.

S. Geman and D. Geman (1984). "Stochastic Relaxation, Gibbs Distributions, and the Bayesian Restoration of Images". *IEEE Transactions on Pattern Analysis and Machine Intelligence*. PAMI-6 (6): 721–741. DOI: 10.1109/tpami.1984.4767596.

M. Gevers, L. Mišković, D. Bonvin, and A. Karimi (2006). "Identification of multi-input systems: variance analysis and input design issues". *Automatica*. 42 (4): 559–572. DOI: https://doi.org/10.1016/j.automatica.2005.12.017.

W. R. Gilks, S. Richardson, and D. Spiegelhalter (1995). *Markov chain Monte Carlo in practice*. CRC press.

M. Gilson and P. M. J. Van den Hof (2005). "Instrumental variable methods for closed-loop system identification". *Automatica*. 41 (2): 241–249. DOI: https://doi.org/10.1016/j.automatica.2004.09.016.

J. Goncalves, R. Howes, and S. Warnick (2007). "Dynamical structure functions for the reverse engineering of LTI networks". In: *Proceedings of the 46th IEEE Conference on Decision and Control*. DOI: 10.1109/cdc.2007.4434406.

J. Goncalves and S. Warnick (2008). "Necessary and Sufficient Conditions for Dynamical Structure Reconstruction of LTI Networks". *IEEE Transactions on Automatic Control*. 53 (7): 1670–1674. DOI: 10.1109/tac.2008.928114.

G. C. Goodwin and R. L. Payne (1977). *Dynamic System Identification: Experiment Design and Data Analysis*. Academic Press.

C. Granger (1963). "Economic processes involving feedback". *Information and Control*. 6 (1): 28–48. DOI: 10.1016/s0019-9958(63)90092-5.

B. Gunes, A. G. Dankers, and P. M. J. Van den Hof (2014). "A variance reduction technique for identification in dynamic networks". In: *Proceedings of the 19th IFAC World Congress*. DOI: 10.3182/20140824-6-za-1003.01495.

I. Gustavsson, L. Ljung, and T. Söderström (1977). "Identification of processes in closed loop - identifiability and accuracy aspects". *Automatica*. 13 (1): 59–75. DOI: https://doi.org/10.1016/0005-1098(77)90009-7.

A. Haber and M. Verhaegen (2014). "Subspace Identification of Large-Scale Interconnected Systems". *IEEE Transactions on Automatic Control*. 59 (10): 2754–2759. DOI: 10.1109/TAC.2014.2310375.

A. Haber and M. Verhaegen (2012). "Identification of spatially distributed discrete-time state-space models". In: *Proceedings of the 16th IFAC Symposium on System Identification*, 410–415. DOI: 10.3182/20120711-3-be-2027.00203.

P. Hägg, B. Wahlberg, and H. Sandberg (2011). "On Identification of Parallel Cascade Serial Systems". In: *Proceedings of the 18th IFAC World Congress*, 9978–9983. DOI: 10.3182/20110828-6-it-1002.02068.

E. J. Hannan and L. Kavalieris (1984). "Multivariate linear time series models". *Advances in Applied Probability*. 16 (3): 492–561. DOI: 10.1017/s0001867800022710.

E. J. Hannan and J. Rissanen (1982). "Recursive estimation of mixed autoregressive-moving average order". *Biometrika*. 69 (1): 81–94. DOI: 10.1093/biomet/69.1.81.

E. Hannan and M. Deistler (1988). *The Statistical Theory of Linear Systems*. SIAM. Vol. 70.

A. Hansson and M. Verhaegen (2014). "Distributed system identification with ADMM". In: *Proceedings of the 53rd IEEE Conference on Decision and Control*. DOI: 10.1109/cdc.2014.7039396.

T. Hastie, R. Tibshirani, and J. Friedman (2009). *Elements of Statistical Learning*. Springer-Verlag New York Inc. ISBN: 0387848576.

D. Hayden, Y. H. Chang, J. Goncalves, and C. J. Tomlin (2016). "Sparse network identifiability via Compressed Sensing". *Automatica*. 68: 9–17. DOI: 10.1016/j.automatica.2016.01.008.

P. S. C. Heuberger, P. Van den Hof, and O. H. Bosgra (1995). "A generalized orthonormal basis for linear dynamical systems". In: *Proceedings of the 32nd IEEE Conference on Decision and Control*, 451–465. DOI: 10.1109/cdc.1993.325715.

R. Hildebrand and M. Gevers (2004). "Quantification of the Variance of Estimated Transfer Functions in the Presence of Undermodeling". *IEEE Transactions on Automatic Control*. 49 (8): 1345–1350. DOI: 10.1109/TAC.2004.832651.

H. Hjalmarsson (2005). "From experiment design to closed loop control". *Automatica*. 41: 393–438. DOI: https://doi.org/10.1016/j.automatica.2004.11.021.

H. Hjalmarsson (2009). "System Identification of Complex and Structured Systems". *European Journal of Control*. 15 (3-4): 275–310. DOI: https://doi.org/10.3166/ejc.15.275-310.

H. Hjalmarsson and J. Mårtensson (2011). "A Geometric Approach to Variance Analysis in System Identification". *IEEE Transactions on Automatic Control*. 56 (5): 983–997. DOI: 10.1109/TAC.2010.2076213.

H. Hjalmarsson, J. Mårtensson, C. R. Rojas, and T. Söderström (2011). "On the accuracy in errors–in–variables identification compared to prediction–error identification". *Automatica*. 47 (12): 2704–2712. DOI: https://doi.org/10.1016/j.automatica.2011.09.002.

H. Hjalmarsson and B. Ninness (2006). "Least-Squares Estimation of a Class of Frequency Functions: A Finite Sample Variance Expression". *Automatica*. 42: 589–600. DOI: https://doi.org/10.1016/j.automatica.2005.12.021.

A. J. Holmgren (2006). "Using Graph Models to Analyze the Vulnerability of Electric Power Networks". *Risk Analysis*. 26 (4): 955–969. DOI: 10.1111/j.1539-6924.2006.00791.x.

R. A. Horn and C. R. Johnson (1990). *Matrix Analysis*. Cambridge University Press.

A. Hyttinen, F. Eberhardt, and P. O. Hoyer (2012). "Learning linear cyclic causal models with latent variables". *Journal of Machine Learning Research*. 13 (Nov): 3387–3439.

G. Innocenti and D. Materassi (2008). "Topological Properties in Identification and Modeling Techniques". In: *Proceedings of the 17th IFAC World Congress*, 15387–15392. DOI: 10.3182/20080706-5-kr-1001.02602.

R. Isermann (2005). "Model-based fault-detection and diagnosis – status and applications". *Annual Reviews in Control*. 29 (1): 71–85. DOI: 10.1016/j.arcontrol.2004.12.002.

A. Julius, M. Zavlanos, G. Pappas, and S. Boyd (2009). "Genetic network identification using convex programming". *IET Systems Biology*. 3 (3): 155–166. DOI: 10.1049/iet-syb.2008.0130.

T. Kailath (1979). *Linear Systems*. Prentice Hall. ISBN: 0135369614.

P. H. Kirkegaard and R. Brincker (1994). "On the optimal location of sensors for parametric identification of linear structural systems". *Mechanical Systems and Signal Processing*. 8 (6): 639–647. DOI: 10.1006/mssp.1994.1045.

S. Kolumbán, I. Vajk, and J. Schoukens (2015). "Perturbed datasets methods for hypothesis testing and structure of corresponding confidence sets". *Automatica*. 51 (0): 326–331. DOI: https://doi.org/10.1016/j.automatica.2014.10.083.

T. J. T. Koski and J. Noble (2012). "A Review of Bayesian Networks and Structure Learning". *Mathematica Applicanda*. 40 (1): 51–103. DOI: 10.14708/ma.v40i1.278.

E. L. Lehmann and G. Casella (1998). *Theory of point estimation*. Springer. New York.

J. Linder (2014). "Graybox Modelling of Ships Using Indirect Input Measurements". Licentiate thesis. Linköping University. DOI: 10.3384/lic.diva-111095.

J. Linder and M. Enqvist (2016). "Identification of systems with unknown inputs using indirect input measurements". *International Journal of Control*. 90 (4): 729–745. DOI: 10.1080/00207179.2016.1222557.

L. Ljung (1985). "Asymptotic variance expressions for identified black-box transfer function models". *IEEE Transactions on Automatic Control*. 30 (9): 834–844. DOI: 10.1109/TAC.1985.1104093.

L. Ljung (1999). *System Identification: Theory for the User*. Prentice Hall. 2nd ed.

L. Ljung, H. Hjalmarsson, and H. Ohlsson (2011). "Four encounters with system identification". *European Journal of Control*. 17 (5): 449–471. DOI: https://doi.org/10.3166/ejc.17.449-471.

L. Ljung and B. Wahlberg (1992). "Asymptotic Properties of the Least-Squares Method for Estimating Transfer Functions and Disturbance Spectra". *Advances in Applied Probability*. 24 (2): 412–440. DOI: 10.2307/1427698.

Y. Majanne (2005). "Model predictive pressure control of steam networks". *Control Engineering Practice*. 13 (12): 1499–1505. DOI: https://doi.org/10.1016/j.conengprac.2005.03.008.

J. S. Maritz and T. Lwin (1989). *Empirical bayes methods*. Chapman and Hall London. Vol. 2.

H. Marko (1973). "The Bidirectional Communication Theory–A Generalization of Information Theory". *IEEE Transactions on Communications*. 21 (12): 1345–1351. DOI: 10.1109/tcom.1973.1091610.

J. Mårtensson (2007). "Geometric analysis of stochastic model errors in system identification". Ph.D. Thesis. KTH Royal Institute of Technology.

J. Mårtensson and H. Hjalmarsson (2009). "Variance-error quantification for identified poles and zeros". *Automatica*. 45 (11): 2512–2525. DOI: https://doi.org/10.1016/j.automatica.2009.08.001.

J. Mårtensson and H. Hjalmarsson (2011). "How to make bias and variance errors insensitive to system and model complexity in identification". *IEEE Transactions on Automatic Control*. 56 (1): 100–112. DOI: 10.1109/TAC.2010.2052294.

J. Mårtensson, N. Everitt, and H. Hjalmarsson (2017). "Covariance analysis in SISO linear systems identification". *Automatica*. 77: 82–92. DOI: 10.1016/j.automatica.2016.11.025.

J. Massey (1990). "Causality, feedback and directed information". In: *Proceedings of the 1990 International Symposium on Information Theory and Its Application*.

P. Massioni and M. Verhaegen (2008). "Subspace identification of circulant systems". *Automatica*. 44 (11): 2825–2833. DOI: 10.1016/j.automatica.2008.04.014.

P. Massioni and M. Verhaegen (2009). "Subspace identification of distributed, decomposable systems". In: *Proceedings of the 48th IEEE Conference on Decision and Control, held jointly with the 28th Chinese Control Conference*. DOI: 10.1109/cdc.2009.5400296.

D. Materassi and G. Innocenti (2010). "Topological Identification in Networks of Dynamical Systems". *IEEE Transactions on Automatic Control*. 55 (8): 1860–1871. DOI: 10.1109/tac.2010.2042347.

D. Materassi, G. Innocenti, L. Giarré, and M. Salapaka (2013). "Model identification of a network as compressing sensing". *Systems & Control Letters*. 62 (8): 664–672. DOI: 10.1016/j.sysconle.2013.04.004.

D. Materassi and G. Innocenti (2009). "Unveiling the connectivity structure of financial networks via high-frequency analysis". *Physica A: Statistical Mechanics and its Applications*. 388 (18): 3866–3878. DOI: 10.1016/j.physa.2009.06.003.

D. Materassi and M. V. Salapaka (2012). "On the Problem of Reconstructing an Unknown Topology via Locality Properties of the Wiener Filter". *IEEE Transactions on Automatic Control*. 57 (7): 1765–1777. DOI: 10.1109/tac.2012.2183170.

D. Materassi and M. V. Salapaka (2015). "Identification of network components in presence of unobserved nodes". In: *Proceedings of the 54th IEEE Conference on Decision and Control*. DOI: 10.1109/cdc.2015.7402433.

D. Materassi, M. V. Salapaka, and L. Giarre (2011). "Relations between structure and estimators in networks of dynamical systems". In: *Proceedings of the 50th IEEE Conference on Decision and Control and European Control Conference*, 162–167. DOI: 10.1109/cdc.2011.6161380.

J. McClellan and D. Lee (1991). "Exact equivalence of the Steiglitz-McBride iteration and IQML". *IEEE Transactions on Signal Processing*. 39 (2): 509–512. DOI: 10.1109/78.80841.

D. B. McCombie, A. T. Reisner, and H. H. Asada (2005). "Laguerre-model blind system identification: Cardiovascular dynamics estimated from multiple peripheral circulatory signals". *IEEE Transactions on Biomedical Engineering*. 52 (11): 1889–1901. DOI: 10.1109/TBME.2005.856260.

X.-L. Meng and D. B. Rubin (1993). "Maximum likelihood estimation via the ECM algorithm: A general framework". *Biometrika*. 80 (2): 267–278. DOI: 10.1093/biomet/80.2.267.

S. Meyn and R. L. Tweedie (2009). *Markov chains and stochastic stability; 2nd ed.* Cambridge Univ. Press. Leiden.

M. Milanese and C. Novara (2011). "Unified Set Membership theory for identification, prediction and filtering of nonlinear systems". *Automatica*. 47 (10): 2141–2151. DOI: https://doi.org/10.1016/j.automatica.2011.03.013.

M. Milanese and A. Vicino (1991). "Optimal estimation theory for dynamic systems with set membership uncertainty: An overview". *Automatica*. 27 (6): 997–1009. DOI: https://doi.org/10.1016/0005-1098(91)90134-N.

L. Mišković, A. Karimi, D. Bonvin, and M. Gevers (2008). "Closed-loop identification of multivariable systems: With or without excitation of all references?" *Automatica*. 44 (8): 2048–2056. DOI: https://doi.org/10.1016/j.automatica.2007.11.016.

J. M. Mooij, D. Janzing, T. Heskes, and B. Schölkopf (2011). "On causal discovery with cyclic additive noise models". In: *Advances in neural information processing systems*, 639–647.

D. Napoletani and T. D. Sauer (2008). "Reconstructing the topology of sparsely connected dynamical networks". *Physical Review E*. 77 (2). DOI: 10.1103/physreve.77.026103.

G. D. Nicolao and G. Pillonetto (2008). "A new kernel-based approach for system identification". In: *Proceedings of the 2008 American Control Conference*. DOI: 10.1109/acc.2008.4587206.

B. Ninness and J. C. Gómez (1996). "Asymptotic Analysis of MIMO System Estimates by the use of Orthonormal Bases". In: *Proceedings of the 13th IFAC World Congress*, 363–368.

B. Ninness and G. C. Goodwin (1995). "Estimation of model quality". *Automatica*. 31 (12): 1771–1797. DOI: https://doi.org/10.1016/0005-1098(95)00108-7.

B. Ninness and F. Gustafsson (1997). "A unifying construction of orthonormal bases for system identification". *IEEE Transactions on Automatic Control*. 42: 515–521. DOI: 10.1109/9.566661.

B. Ninness and H. Hjalmarsson (2004). "Variance Error Quantifications That Are Exact for Finite-Model Order". *IEEE Transactions on Automatic Control*. 49 (8): 1275–1291. DOI: 10.1109/tac.2004.832202.

B. Ninness and H. Hjalmarsson (2005a). "Analysis of the variability of joint input–output estimation methods". *Automatica*. 41 (7): 1123–1132. DOI: https://doi.org/10.1016/j.automatica.2005.03.006.

B. Ninness and H. Hjalmarsson (2005b). "On the Frequency Domain Accuracy of Closed-Loop Estimates". *Automatica*. 41: 1109–1122. DOI: https://doi.org/10.1016/j.automatica.2005.03.005.

B. Ninness, H. Hjalmarsson, and F. Gustafsson (1999). "The fundamental role of general orthonormal bases in system identification". *IEEE Transactions on Automatic Control*. 44 (7): 1384–1406. DOI: 10.1109/9.774110.

R. Olfati-Saber, J. A. Fax, and R. M. Murray (2007). "Consensus and Cooperation in Networked Multi-Agent Systems". In: *IEEE*, 215–233. DOI: 10.1109/jproc.2006.887293.

C. Papadimitriou and G. Lombaert (2012). "The effect of prediction error correlation on optimal sensor placement in structural dynamics". *Mechanical Systems and Signal Processing*. 28: 105–127. DOI: 10.1016/j.ymssp.2011.05.019.

J. Pearl (1988). *Probabilistic reasoning in intelligent systems: networks of plausible inference*. Morgan Kaufmann.

J. Pearl (2000). *Causality*. Cambridge University Press. ISBN: 0-521-74919-0. DOI: 10.1017/cbo9780511803161.

G. Pillonetto, A. Chiuso, and G. D. Nicolao (2010). "Regularized estimation of sums of exponentials in spaces generated by stable spline kernels". In: *Proceedings of the 2010 American Control Conference*. DOI: 10.1109/acc.2010.5530862.

G. Pillonetto and A. Chiuso (2015). "Tuning complexity in regularized kernel-based regression and linear system identification: The robustness of the marginal likelihood estimator". *Automatica*. 58: 106–117. DOI: 10.1016/j.automatica.2015.05.012.

G. Pillonetto, F. Dinuzzo, T. Chen, G. D. Nicolao, and L. Ljung (2014). "Kernel methods in system identification, machine learning and function estimation: A survey". *Automatica*. 50 (3): 657–682. DOI: 10.1016/j.automatica.2014.01.001.

G. Pillonetto and G. D. Nicolao (2010). "A new kernel-based approach for linear system identification". *Automatica*. 46 (1): 81–93. DOI: 10.1016/j.automatica.2009.10.031.

R. Pintelon, J. Schoukens, G. Vandersteen, and K. Barbé (2010a). "Estimation of nonparametric noise and FRF models for multivariable systems—Part I: Theory". *Mechanical Systems and Signal Processing*. 24 (3): 573–595. DOI: 10.1016/j.ymssp.2009.08.009.

R. Pintelon, J. Schoukens, G. Vandersteen, and K. Barbé (2010b). "Estimation of nonparametric noise and FRF models for multivariable systems—Part II: Extensions, applications". *Mechanical Systems and Signal Processing*. 24 (3): 596–616. DOI: 10.1016/j.ymssp.2009.08.010.

R. Pintelon and J. Schoukens (2012). *System Identification: A Frequency Domain Approach*. Wiley-Blackwell. 2nd ed. ISBN: 0470640375. DOI: 10.1002/9781118287422.

G. Prando, A. Chiuso, and G. Pillonetto (2014). "Bayesian and regularization approaches to multivariable linear system identification: The role of rank penalties". In: *Proceedings of the 53rd IEEE Conference on Decision and Control*. DOI: 10.1109/cdc.2014.7039610.

C. J. Quinn, T. P. Coleman, N. Kiyavash, and N. G. Hatsopoulos (2010). "Estimating the directed information to infer causal relationships in ensemble neural spike train

recordings". *Journal of Computational Neuroscience*. 30 (1): 17–44. DOI: 10.1007/s10827-010-0247-2.

C. J. Quinn, N. Kiyavash, and T. P. Coleman (2011). "Equivalence between minimal generative model graphs and directed information graphs". In: *Proceedings of the 2011 IEEE International Symposium on Information Theory Proceedings*. DOI: 10.1109/isit.2011.6034116.

A. Rai and S. Warnick (2013). "A technique for designing stabilizing distributed controllers with arbitrary signal structure constraints". In: *Proceedings of the 2013 European Control Conference*, 3282–3287. ISBN: 978-3-033-03962-9.

P. Ramazi, H. Hjalmarsson, and J. Mårtensson (2014). "Variance analysis of identified linear MISO models having spatially correlated inputs, with application to parallel Hammerstein models". *Automatica*. 50 (6): 1675–1683. DOI: 10.1016/j.automatica.2014.04.014.

C. E. Rasmussen and C. K. I. Williams (2006). *Gaussian processes for machine learning*. Cambridge: MIT Press.

W. Ren and R. W. Beard (2008). *Distributed Consensus in Multi-vehicle Cooperative Control*. Springer. DOI: 10.1007/978-1-84800-015-5.

R. S. Risuleo, G. Bottegal, and H. Hjalmarsson (2016). "Kernel-based system identification from noisy and incomplete input-output data". In: *Proceedings of the 55th IEEE Conference on Decision and Control*. DOI: 10.1109/cdc.2016.7798567.

R. S. Risuleo, G. Bottegal, and H. Hjalmarsson (2015). "A kernel-based approach to Hammerstein system identification". In: *Proceedings of the 17th IFAC Symposium on System Identification*, 1011–1016. DOI: 10.1016/j.ifacol.2015.12.263.

C. R. Rojas, J. S. Welsh, and J. C. Agüero (2009). "Fundamental Limitations on the Variance of Estimated Parametric Models". *IEEE Transactions on Automatic Control*. 54 (5): 1077–1081. DOI: 10.1109/tac.2008.2010981.

Y. A. Rozanov (1967). *Stationary Random Processes*. Holden-Day.

B. M. Sanandaji, T. L. Vincent, and M. Wakin (2012). "A Review of Sufficient Conditions for Structure Identification in Interconnected Systems". In: *Proceedings of the 16th IFAC Symposium on System Identification*, 1623–1628. DOI: 10.3182/20120711-3-be-2027.00254.

B. M. Sanandaji, T. L. Vincent, and M. B. Wakin (2011). "Exact topology identification of large-scale interconnected dynamical systems from compressive observations". In: *Proceedings of the 2011 American Control Conference*, 649–656. DOI: 10.1109/acc.2011.5990982.

M. Schmidt and K. Murphy (2009). "Modeling discrete interventional data using directed cyclic graphical models". In: *Proceedings of the Twenty-Fifth Conference on Uncertainty in Artificial Intelligence*, 487–495. ISBN: 978-0-9749039-5-8.

R. Schmidt (1986). "Multiple emitter location and signal parameter estimation". *IEEE Transactions on Antennas and Propagation*. 34 (3): 276–280. DOI: 10.1109/tap.1986.1143830.

J. Schoukens, Y. Rolain, G. Vandersteen, and R. Pintelon (2011). "User friendly Box-Jenkins identification using nonparametric noise models". In: *Proceedings of the 50th IEEE Conference on Decision and Control and European Control Conference*, 2148–2153. DOI: 10.1109/cdc.2011.6160204.

A. J. Seneviratne and V. Solo (2012a). "Sparse coloured system identification with guaranteed stability". In: *Proceedings of the 51st IEEE Conference on Decision and Control*, 2826–2831. DOI: 10.1109/cdc.2012.6427058.

A. J. Seneviratne and V. Solo (2012b). "Topology identification of a sparse dynamic network". In: *Proceedings of the 51st IEEE Conference on Decision and Control*, 1518–1523. DOI: 10.1109/cdc.2012.6425980.

S. Shahrampour and V. M. Preciado (2015). "Topology Identification of Directed Dynamical Networks via Power Spectral Analysis". *IEEE Transactions on Automatic Control*. 60 (8): 2260–2265. DOI: 10.1109/tac.2014.2374711.

A. Shaw (1994). "Optimal identification of discrete-time systems from impulse response data". *IEEE Transactions on Signal Processing*. 42 (1): 113–120. DOI: 10.1109/78.258126.

D. D. Siljak (2011). *Decentralized control of complex systems*. Courier Corporation.

T. Söderström and P. Stoica (1989). *System identification*. Prentice-Hall. Englewood Cliffs.

T. Söderström and P. Stoica (1983). *Instrumental Variable Methods for System Identification*. Springer-Verlag. New York. DOI: 10.1007/bfb0009019.

K. Steiglitz and L. McBride (1965). "A technique for the identification of linear systems". *IEEE Transactions on Automatic Control*. 10 (4): 461–464. DOI: 10.1109/tac.1965.1098181.

C. M. Stein (1981). "Estimation of the mean of a multivariate normal distribution". *The annals of Statistics*: 1135–1151.

P. Stoica and M. Jansson (2000). "MIMO system identification: state-space and subspace approximations versus transfer function and instrumental variables". *IEEE Transactions on Signal Processing*. 48 (11): 3087–3099. DOI: 10.1109/78.875466.

P. Stoica and T. Söderström (1981). "The Steiglitz-McBride identification algorithm revisited–Convergence analysis and accuracy aspects". *IEEE Transactions on Automatic Control*. 26 (3): 712–717. DOI: 10.1109/tac.1981.1102679.

P. Stoica, M. Viberg, and B. Ottersten (1994). "Instrumental variable approach to array processing in spatially correlated noise fields". *IEEE Transactions on Signal Processing*. 42 (1): 121–133. DOI: 10.1109/78.258127.

S. Thil, M. Gilson, and H. Garnier (2008). "On instrumental variable-based methods for errors-in-variables model identification". *IFAC Proceedings Volumes*. 41 (2): 426–431. DOI: 10.3182/20080706-5-kr-1001.00072.

R. Tibshirani (1996). "Regression Shrinkage and Selection via the Lasso". *Journal of the Royal Statistical Society. Series B (Methodological)*. 58 (1): 267–288.

M. Timme (2007). "Revealing Network Connectivity from Response Dynamics". *Physical Review Letters*. 98 (22). DOI: 10.1103/physrevlett.98.224101.

P. Torres (2014). "Linear State-Space Identification of Interconnected Systems: A structured approach". PhD thesis. TU Delft, Delft University of Technology.

P. Torres, J.-W. van Wingerden, and M. Verhaegen (2014). "Hierarchical subspace identification of directed acyclic graphs". *International Journal of Control*. 88 (1): 123–137. DOI: 10.1080/00207179.2014.942800.

L. N. Trefethen and D. Bau (1997). *Numerical Linear Algebra*. Society for Industrial and Applied Mathematics.

D. Trudnowski, J. Johnson, and J. Hauer (1998). "SIMO system identification from measured ringdowns". In: *Proceedings of the 1998 American Control Conference*, 2968–2972. DOI: 10.1109/acc.1998.688402.

H. S. Ulusoy, M. Q. Feng, and P. J. Fanning (2011). "System identification of a building from multiple seismic records". *Earthquake Engineering & Structural Dynamics*. 40 (6): 661–674. DOI: 10.1002/eqe.1053.

P. M. J. Van den Hof, A. G. Dankers, P. S. C. Heuberger, and X. Bombois (2013). "Identification of dynamic models in complex networks with prediction error methods—Basic methods for consistent module estimates". *Automatica*. 49 (10): 2994–3006. DOI: 10.1016/j.automatica.2013.07.011.

P. M. J. Van den Hof and R. J. Schrama (1993). "An indirect method for transfer function estimation from closed loop data". *Automatica*. 29 (6): 1523–1527. DOI: 10.1016/0005-1098(93)90015-l.

P. M. J. Van den Hof, H. H. M. Weerts, and A. G. Dankers (2017). "Prediction error identification with rank-reduced output noise". In: *Proceedings of the 2017 American Control Conference*.

P. van Overschee and B. de Moor (1996). *Subspace identification for linear systems: theory, implementation, applications*. Kluwer Academic Publishers. Boston.

J.-W. van Wingerden and P. Torres (2012). "Identification of Spatially Interconnected Systems using a Sequentially Semi-Separable Gradient Method." In: *Proceedings of the 16th IFAC Symposium on System Identification*, 173–178. DOI: 10.3182/20120711-3-be-2027.00229.

M. Viberg and B. Ottersten (1991). "Sensor array processing based on subspace fitting". *IEEE Transactions on Signal Processing*. 39 (5): 1110–1121. DOI: 10.1109/78.80966.

M. Viberg, P. Stoica, and B. Ottersten (1997). "Maximum likelihood array processing in spatially correlated noise fields using parameterized signals". *IEEE Transactions on Signal Processing*. 45 (4): 996–1004. DOI: 10.1109/78.564187.

G. Wahba (1990). *Spline Models for Observational Data*. Cambridge University Press. ISBN: 0898712440.

B. Wahlberg (1991). "System identification using Laguerre models". *IEEE Transactions on Automatic Control*. 36 (5): 551–562. DOI: 10.1109/9.76361.

B. Wahlberg, H. Hjalmarsson, and P. Stoica (2012). "On the Performance of Optimal Input Signals for Frequency Response Estimation". *IEEE Transactions on Automatic Control*. 57 (3): 766–771. DOI: 10.1109/tac.2011.2166322.

B. Wahlberg and L. Ljung (1992). "Hard frequency-domain model error bounds from least-squares like identification techniques". *IEEE Transactions on Automatic Control*. 37 (7): 900–912. DOI: 10.1109/9.148343.

B. Wahlberg (1989). "Model reductions of high-order estimated models: the asymptotic ML approach". *International Journal of Control*. 49 (1): 169–192. DOI: 10.1080/00207178908559628.

B. Wahlberg, H. Hjalmarsson, and J. Mårtensson (2009). "Variance results for identification of cascade systems". *Automatica*. 45 (6): 1443–1448. DOI: 10.1016/j.automatica.2009.01.020.

H. H. M. Weerts, A. G. Dankers, and P. M. J. Van den Hof (2015). "Identifiability in dynamic network identification". In: *Proceedings of the 17th IFAC Symposium on System Identification*, 1409–1414. DOI: 10.1016/j.ifacol.2015.12.330.

H. H. M. Weerts, P. M. J. Van den Hof, and A. G. Dankers (2016). "Identifiability of dynamic networks with part of the nodes noise-free". In: *Proceedings of the 12th IFAC Workshop on Adaptation and Learning in Control and Signal Processing*, 19–24. DOI: 10.1016/j.ifacol.2016.07.920.

H. H. M. Weerts, P. M. J. Van den Hof, and A. G. Dankers (2017). "Identification of dynamic networks with rank-reduced process noise". In: *Proceedings of the 20th IFAC World Congress*.

P. Whittle (1951). *Hypothesis testing in time series analysis*. Almqvist & Wiksells. Vol. 4. DOI: 10.2307/2332487.

J. Willems (2007). "The Behavioral Approach to Open and Interconnected Systems". *IEEE Control Systems Magazine*. 27 (6): 46–99. DOI: 10.1109/mcs.2007.4339280.

L.-L. Xie and L. Ljung (2001). "Asymptotic variance expressions for estimated frequency functions". *IEEE Transactions on Automatic Control*. 46 (12): 1887–1899. DOI: 10.1109/9.975472.

L.-L. Xie and L. Ljung (2004). "Variance expressions for spectra estimated using autoregressions". *Journal of econometrics*. 118 (1): 247–256. DOI: 10.1016/s0304-4076(03)00142-8.

Y. Yang, F. Lambert, and D. Divan (2007). "A Survey on Technologies for Implementing Sensor Networks for Power Delivery Systems". In: *Proceedings of the 2007 IEEE Power Engineering Society General Meeting*, 1–8. DOI: 10.1109/PES.2007.386289.

E. Yeung, J. Goncalves, H. Sandberg, and S. Warnick (2010). "Representing structure in linear interconnected dynamical systems". In: *Proceedings of the 49th IEEE Conference on Decision and Control*, 6010–6015. DOI: 10.1109/cdc.2010.5718109.

E. Yeung, J. Goncalves, H. Sandberg, and S. Warnick (2011). "Mathematical relationships between representations of structure in linear interconnected dynamical systems". In: *Proceedings of the 2012 American Control Conference*, 4348–4353.

P. C. Young (2008). "The refined instrumental variable method: Unified estimation of discrete and continuous-time transfer function models". *Journal Europeen des Systemes Automatises*. 42: 149–179.

M. Yuan and Y. Lin (2006). "Model selection and estimation in regression with grouped variables". *Journal of the Royal Statistical Society. Series B (Statistical Methodology)*. 68 (1): 49–67. DOI: 10.1111/j.1467-9868.2005.00532.x.

Y. Yuan, A. Rai, E. Yeung, G.-B. Stan, S. Warnick, and J. Goncalves (2015). "A minimal realization technique for the dynamical structure function of a class of LTI systems". *IEEE Transactions on Control of Network Systems*: 1–1. DOI: 10.1109/tcns.2015.2498468.

Y. Yuan, G.-B. Stan, S. Warnick, and J. Goncalves (2011). "Robust dynamical network structure reconstruction". *Automatica*. 47 (6): 1230–1235. DOI: 10.1016/j.automatica.2011.03.008.

Z. D. Yuan and L. Ljung (1984). "Black-box identification of multivariable transfer functions–asymptotic properties and optimal input design". *International Journal of Control*. 40 (2): 233–256. DOI: 10.1080/00207178408933270.

Y. Zhu (2001). *Multivariable system identification for process control*. Elsevier.

Y. Zhu and H. Hjalmarsson (2016). "The Box–Jenkins Steiglitz–McBride algorithm". *Automatica*. 65: 170–182. DOI: 10.1016/j.automatica.2015.12.001.